

TECHNISCHE UNIVERSITÄT ILMENAU  
Fakultät für Informatik und Automatisierung  
Fachgebiet Regelungstechnik

## Dissertation

### **Applications of Equivalent Representations of Fractional- and Integer-Order Linear Time-Invariant Systems**

zur Erlangung des akademischen Grades Doktoringenieur (Dr.-Ing.)

von

M.Sc. Christoph Weise

geboren am 11. Juni 1989 in Freiberg

- 
- |               |                                 |
|---------------|---------------------------------|
| 1. Gutachter: | Prof. Dr.-Ing. Johann Reger     |
| 2. Gutachter: | Prof. Dr.-Ing. Michael Ruderman |
| 3. Gutachter: | Prof. Dr.-Ing. Paolo Mercorelli |
- 

eingereicht am: 09. April 2020

Wissenschaftliche Aussprache: 16. Juni 2020



## Abstract

Since the seventies, the application of non-integer, so-called fractional-order derivative operators has gained attention in various fields of research like materials science, electrochemistry, signal processing, and control engineering. Thanks to the ability to describe systems with infinite memory these operators are attractive to model various phenomena, for example viscoelastic deformation. In the field of control theory, both the higher degree of freedom in the frequency domain as well as the easy generalization of PID control have been the main motivation to extend various advanced control concepts to the fractional-order domain. Fractional-order approaches in the state-space representation have received less attention.

The long term memory of these operators which help to model real life phenomena, has, however, negative effects regarding the application as controllers or observers. Due to the infinite memory, the transients only decay algebraically and the implementation requires a lot of physical memory.

The main focus of this thesis is the question of how to influence the convergence rates of these fractional-order systems by changing the type of convergence. The first part is concerned with the observer design for different classes of linear time-invariant fractional-order systems. We derive associated system representations with an increased order of differentiation. Based on these systems, the observers are designed to take the unknown memory into account and thus resulting in higher convergence rates.

The second part explores the representation of linear time-invariant systems in terms of fractional-order derivatives. The application of the fractional-order operator introduces an unbounded first-order derivative at the initial time. This accelerates the convergence for a short time interval. With periodic deletion of the memory – a reset of the fractional-order dynamics – the slow algebraic decay is avoided and exponential stability can be achieved despite the fractional-order terms. The periodic reset leads to a reduced demand on physical memory required for the implementation and also induces underlying discrete time dynamics which can be used to prove stability of the hybrid fractional-order system and to give an interpretation of the reset in the frequency domain for the low frequency signals. This concept of memory reset is applied to design an observer and improve fractional-order controllers for integer-order processes. For the controller design this gives us the possibility to design the high-frequency response independently from the behavior at lower frequencies within certain limits. Finally, these approaches have been tested in exemplary experiments.



## Zusammenfassung

Seit den siebziger Jahren ist das Interesse an Ableitungen mit nicht ganzzahliger Ordnung stetig gewachsen. Zu den Anwendungsgebieten zählen unter anderem Werkstoffwissenschaften, Elektrochemie, Signalverarbeitung und Regelungstechnik. Da nicht-ganzzahlige – fraktionale – Ableitungsoperatoren Prozesse mit Gedächtniseffekten beschreiben können, ist es naheliegend, diese Mathematik zur Modellierung verschiedenster Phänomene, z.B. viskoelastischen Verhaltens, zu nutzen. In der Regelungstechnik wird das Konzept hauptsächlich auf Grund des erhöhten Freiheitsgrades im Frequenzbereich verwendet. Deshalb wurden in den vergangenen Jahrzehnten neben einer Verallgemeinerung des PID-Reglers auch fortgeschrittenere Regelungskonzepte auf nicht ganzzahlige Operatoren erweitert. Dabei wurden Ansätze im Zustandsraum seltener verfolgt.

Das Gedächtnis der nicht ganzzahligen Ableitung ist zwar essentiell für die Modellbildung, hat jedoch Nachteile, wenn wir diese verwenden um mit einem Beobachter Zustände zu schätzen oder Regler zu implementieren: Die numerische Approximation des unendlichen Gedächtnisses hat einen erhöhten Speicherbedarf zur Folge und führt zu langsamer algebraischer Konvergenz der Transienten.

Im Zentrum der Arbeit steht die Frage, mit welchen Maßnahmen sich das Konvergenzverhalten dieser nicht ganzzahligen Systeme beeinflussen lässt. Es wird vorgeschlagen, die Ordnung der nicht ganzzahligen Ableitung zu ändern. Im ersten Teil dieser Arbeit werden Beobachter für verschiedene Klassen linearer zeitinvarianter Systeme entworfen. Die Entwurfsmethodik basiert dabei auf einer assoziierten Systemdarstellung, welche einen Differenzialoperator mit höherer Ordnung verwendet. Basierend auf dieser Systembeschreibung können Beobachter entworfen werden, welche das Gedächtnis besser mit einbeziehen und so schneller konvergieren.

Im zweiten Teil werden ganzzahlige lineare zeitinvariante Systeme mit Hilfe nicht-ganzzahliger Operatoren dargestellt. Die Verwendung dieser fraktionalen Ableitungen führt zu einer erhöhten Konvergenz im Zeitintervall direkt nach dem Anfangszeitpunkt, da eine unendliche erste Ableitung auftritt. Die periodische Löschung des so eingeführten Gedächtnisses wird erzielt, indem die nicht ganzzahlige Dynamik periodisch zurückgesetzt wird. Damit kann der algebraischen Konvergenz entgegen gewirkt werden, sodass exponentielle Stabilität erzielt wird. Dies reduziert zum einen den nötigen Speicherbedarf der Implementierung, zum anderen induziert der Reset eine unterlagerte zeitsdiskrete Dynamik. Diese bestimmt die Stabilität des hybriden nicht-ganzzahligen Systems und kann genutzt werden um den Frequenzgang für niedrige Frequenzen zu bestimmen. Dieses Konzept kann benutzt werden um damit Beobachter und Regler für ganzzahlige System zu entwerfen. Im Rahmen des Reglerentwurfs können auf Grund des Resets das Verhalten für niedrige und hohe Frequenzen in gewissen Grenzen getrennt voneinander entworfen werden. Diese Ansätze werden in einfachen Laborexperimenten getestet, welche die Vorteile der vorgestellten Entwurfsmethodik eindeutig belegen.



## Danksagung

An dieser Stelle ist es nun geboten danke zu sagen. Die vorliegende Dissertation entstand während meiner Zeit als wissenschaftlicher Mitarbeiter am Fachgebiet Regelungstechnik der Technischen Universität Ilmenau und wurde durch die Unterstützung zahlreicher Seiten ermöglicht.

Zunächst möchte ich meinen Dank gegenüber meinen Doktorvätern ausdrücken. Prof. Dr.-Ing. Johann Reger fand immer Zeit für meine Fragen und war immer für eine Korrekturschicht in der Frühe zu gewinnen. Dr. Kai Wulff möchte ich für die vielen interessanten Diskussionen danken, in denen meine Ideen mit ein wenig Struktur und Klarheit versehen wurden.

Desweiteren möchte ich meinen Dank an alle Kollegen am Fachgebiet richten. Ich habe mich immer ein Stück zu Hause gefühlt. Ich bedanke mich bei Dr.-Ing. Kai Treichel, Dr.-Ing. Remon Al Azrak, Julian Willkomm, Matti Noack, Oscar Cieza und Daipeng Zhang für die zahlreichen Diskussionen, welche mir auch ihre Themen ein wenig eröffnet haben.

Ein besonderer Dank gilt meinem aktuellen und ehemaligen Gegenüber im Büro: Lars Wattermann und Dr.-Ing. Alexander Barth. Vielen Dank für eure Bemühungen beim Korrekturlesen.

Darüber hinaus bedanke ich mich bei Nora Dempwolf, Nadja Kühler, Jessica Wizowsky, Axel Fink und Volker Pranger für ihre Unterstützung bei Reisekostenabrechnungen und Laboraufbauten.

Meinen Bachelor- und Masterstudenten gebührt ebenfalls ein Dankeschön, da sie mich mit ihren Fragen immer angetrieben haben, mir neue Themen zu erschließen.

Nicht zuletzt gilt mein Dank meiner Familie, welche mir immer den Rücken frei hielt, wenn aus einem Motivationsproblem ein Zeitproblem geworden war. Caro und Line danke ich für ihre Zeit, Beharrlichkeit und Ausdauer mehr als zweihundert Kommata an die richtigen Stellen geschoben zu haben. Meinen Kindern danke ich dafür, dass sie mich immer wieder auf die Erde zurück holen, sodass ich das Staunen über die alltäglichen Dinge nicht verlerne.

Meinen Eltern danke ich für ihre Mühe, die sie auf sich genommen haben um meinen Geschwistern und mir eine solch umfangreiche Bildung zuteil werden zu lassen. Außerdem danke ich meiner Mutter Carola Weise und meinen Schwiegereltern Corinna und Ralf Fliegner, für die Zeit, die sie unseren Söhnen widmen und dass wir immer willkommen sind.





# Contents

<b>1</b>	<b>Introduction</b>	<b>1</b>
1.1	Applications . . . . .	1
1.1.1	Modeling of Partial Differential Equations . . . . .	1
1.1.2	Viscoelasticity . . . . .	2
1.1.3	Abel's Integral . . . . .	3
1.2	Fractional-Order Control and State-Estimation - State of the Art . . . . .	4
1.3	Contribution and Outline of this Thesis . . . . .	5
<b>2</b>	<b>Fractional-Order Integration and Differentiation</b>	<b>7</b>
2.1	Integer-Order Differentiation and Integration . . . . .	8
2.2	Fractional-Order Integration . . . . .	10
2.3	Fractional-Order Differentiation . . . . .	14
2.3.1	Operator Definitions . . . . .	14
2.3.2	Properties . . . . .	17
2.3.3	Right and Left Fractional-Order Derivatives . . . . .	19
2.3.4	Excursus on Further Fractional-Order Operators . . . . .	20
2.4	Laplace Transforms of Fractional-Order Operators . . . . .	20
2.5	Initialization of Fractional-Order Operators . . . . .	22
2.6	Numerical Implementation of Fractional-Order Operators . . . . .	29
2.6.1	Discretization of Grünwald-Letnikov's Operator . . . . .	29
2.6.2	Frequency Domain Approximation . . . . .	31
<b>3</b>	<b>Fundamentals of Fractional-Order LTI Systems</b>	<b>35</b>
3.1	Fractional-Order State-Space LTI Systems with Classical Initial Conditions . . . . .	35
3.1.1	Properties of the Mittag-Leffler Function . . . . .	37
3.1.2	Comparison of Different Fractional-Order LTI Systems . . . . .	40
3.2	Stability of Fractional-Order Systems . . . . .	41
3.2.1	Concepts for Stability and Convergence Characterization . . . . .	42
3.2.2	Stability of Linear Fractional-Order Systems . . . . .	44
3.3	Observability and Controllability . . . . .	48
3.4	Fractional-Order LTI Systems with extended Conditions . . . . .	51
3.4.1	Input-initialized fractional-order systems . . . . .	51
3.4.2	Fractional-Order Luenberger Observer . . . . .	52
3.4.3	Fractional-Order Unknown-Input Observer . . . . .	55
3.5	Fractional-Order LTI Systems in the Frequency Domain . . . . .	57
<b>4</b>	<b>Associated Higher-Order Systems</b>	<b>61</b>
4.1	Associated Integer-Order Systems . . . . .	61
4.2	Low Memory Fractional-Order LTI-System Implementation . . . . .	67
4.3	Indirect Observer Design . . . . .	68
4.3.1	Associated Integer-Order System - Observability Analysis . . . . .	68
4.3.2	Time-Varying Integer-Order Observer . . . . .	71

4.3.3	Impulsive-Observer Design and Implementation . . . . .	74
4.4	Associated Double-Order Systems . . . . .	78
4.4.1	Modification of the Unknown-Input Observer . . . . .	80
4.4.2	Input-initialized FO systems . . . . .	81
<b>5</b>	<b>Associated Fractional-Order Systems</b>	<b>85</b>
5.1	Associated Fractional-Order System . . . . .	85
5.1.1	Fractional-Order Integral Representation . . . . .	86
5.1.2	Fractional-Order Derivative Representation . . . . .	87
5.2	Properties of Associated Fractional-Order Systems . . . . .	93
5.2.1	Observability and Controllability . . . . .	95
5.3	Fractional-Order Observer for Integer-Order LTI System . . . . .	99
5.3.1	Fractional-Order Memory-Reset Luenberger Observer . . . . .	102
5.3.2	Reduced Order Impulsive Observer . . . . .	108
5.4	Fractional-Order Control . . . . .	112
5.4.1	Inter-Order Pole-Placement and Prefilter . . . . .	113
5.4.2	Fractional-Order Control of Integer-Order Systems . . . . .	116
<b>6</b>	<b>Experimental Results</b>	<b>133</b>
6.1	Fractional-Order Memory Reset Observer . . . . .	134
6.2	Extended Fractional-Order Reset Control . . . . .	135
<b>7</b>	<b>Conclusions</b>	<b>141</b>
7.1	Summary . . . . .	141
7.2	Future Work . . . . .	142
<b>A</b>	<b>Miscellaneous</b>	<b>143</b>
A.1	Laplace Transforms . . . . .	143
A.2	Linear-Time-Varying Integer-Order Systems - Observability . . . . .	143
A.3	Strong* Detectability . . . . .	144
	<b>Bibliography</b>	<b>CXLV</b>

*To my father who made me an engineer.  
To CCC and the rest of my family  
who keep me busy being one.*



# 1 Introduction

Since the seventies, fractional-order calculus has become very popular to use in many fields, e.g. materials science [25, 59, 58], electro-chemistry [17, p. 181], geophysics [9] and control theory [60, 82]. However, the concept of a derivative of a non-integer order - so called fractional-order - is much older as it was already mentioned by Leibniz in a letter he wrote to L'Hôpital in 1695 [60, 14, p. 3].

## 1.1 Applications

As the concept of fractional calculus is not very obvious and normally not taught in advanced mathematics classes, we start this introduction with three applications of fractional-order calculus. This motivates why we should take non-integer orders into account to model physical processes.

### 1.1.1 Modeling of Partial Differential Equations

Let us first consider the heat transfer in a semi-infinite rod as depicted in Figure 1.1. The temperature distribution  $u(t, x) = T(t, x) - T_0$  obeys the diffusion equation [63] given by

$$c\rho \frac{\partial u(t, x)}{\partial t} = k \frac{\partial^2 u(t, x)}{\partial x^2}, \quad x > 0. \quad (1.1)$$

We assume zero initial conditions  $u(0, x) = 0$ , such that the heat conductor has the absolute temperature  $T_0$  at  $t = 0$  and transform (1.1) to the Laplace domain

$$c\rho s U(s, x) = k \frac{\partial^2 U(s, x)}{\partial x^2} \quad (1.2)$$

with  $U(s, x) = \mathcal{L}\{u(t, x)\}$ , resulting in a second order differential equation in the variable  $x$ . Its solution contains two parts; for physical reasons, however, we only have to use the stable and decaying mode

$$U(s, x) = U(s, 0) \exp\left(-x \sqrt{s \frac{c\rho}{k}}\right), \quad (1.3)$$

such that the temperature is limited at  $x \rightarrow \infty$  and the energy is conserved. Note that  $U(s, 0)$  has to be zero for  $s \rightarrow \infty$  only, in order to satisfy the initial conditions  $u(0, x) = 0$ . Now, we want to compute the heat flow which enters the rod at  $x = 0$ . Using Fourier's law we have to take the first spatial derivative of the temperature distribution as

$$q(t) = \kappa \left. \frac{\partial u(t, x)}{\partial x} \right|_{x=0}. \quad (1.4)$$

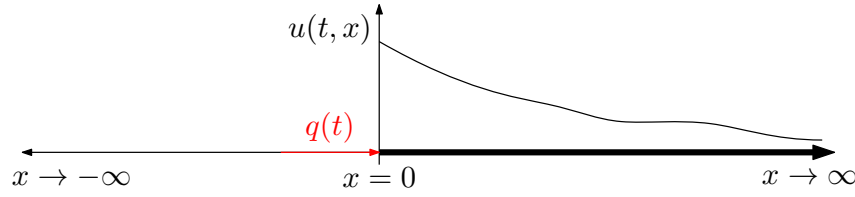


Figure 1.1: Thermal conduction in an infinite one-dimensional media.

Inserting equation (1.3) leads to

$$Q(s) = \kappa \left. \frac{\partial U(s, x)}{\partial x} \right|_{x=0} = s^{\frac{1}{2}} \kappa \sqrt{\frac{cQ}{k}} U(s, 0).$$

The question arises of how to interpret the term  $\sqrt{s}$  in the time domain? The answer can be found in the theory of fractional-order calculus. The heat flux at  $q(t, 0)$  is proportional to the half derivative of the temperature at the same point

$$q(t, 0) \sim \frac{d^{\frac{1}{2}}}{dt^{\frac{1}{2}}} u(t, 0). \quad (1.5)$$

This example already shows a main property of fractional-order operators. The calculation of the heat flow involves the spatial temperature distribution, in (1.5), however, only the temperature at  $x = 0$  is included. The spatial information did not disappear, either. In (1.5) it is included in the fractional-order derivative which is a non-local operator and has a memory.

The concept of this approach can be generalized further. If a system is described by a partial differential equation and we are only interested in the system behavior at the spatial boundaries, we might reshape the system model into a fractional-order differential equation, as shown in [17, p. 54] for semi-infinite transmission lines and in [60, p. 266ff] for a flexible beam.

### 1.1.2 Viscoelasticity

In the first application, the non-integer order of differentiation occur due to a partial (integer-order) differential equation in the background. These orders are usually inverted integers. However, there are also phenomena where the order is not defined by the structure of an underlying partial differential equation. One of these effects is the so-called viscoelastic deformation of "solid" bodies under stress  $\sigma(t)$ . When deformed, the material behaves neither like a pure elastic nor like a viscous one. These two ideal models of the material - the ideal solid body one hand and the ideal Newtonian fluid on the other hand - are the bounds of the viscoelastic behavior.

The deformation  $\epsilon(t)$  of the solid body is described by Hooke's law

$$\sigma(t) = E\epsilon(t), \quad (1.6)$$

with the elastic modulus  $E$  as a material constant. Here the stress  $\sigma(t)$  is proportional to the strain  $\epsilon(t)$ , i.e. the derivative of order zero: In the case of a Newtonian fluid, the stress is

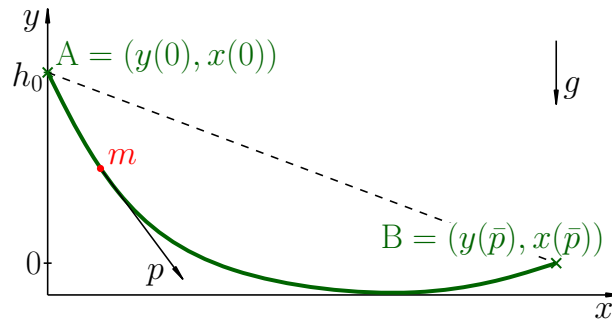


Figure 1.2: Sketch of the tautochrone / baristochrone problem.

proportional to its first derivative, i.e. the local shear velocity

$$\sigma(t) = \eta \dot{\epsilon}(t) \quad (1.7)$$

with the shear modulus  $\eta$ . To model the behavior of real materials where a mixture of energy storage (elastic behavior) and dissipation (viscous behavior) occurs, we either have to combine these models (see [74]) or we change the order of the differentiation. This leads to the fractional-order Hooke's law as given in [76, p. 271]

$$\sigma(t) = E_0 \frac{d^\alpha}{dt^\alpha} \epsilon(t), \quad \alpha \in (0, 1). \quad (1.8)$$

This model is motivated by measurement data as the strain response of a viscoelastic material can only be approximated with reasonable accuracy if the polynomial approximation is extended with roots of the time.

The order of differentiation is a crucial parameter here as it also defines the structure of the model. This arbitrary order allows an accurate modelling with only a few parameters, however, it is also difficult to identify.

In most contributions to fractional-order system identification (e.g. [93, 97, 49, 4]), the basic order is either assumed to be known or identified with non-linear optimization. Due to its direct connection to the system structure, better methods are needed to identify this order  $\alpha$ .

### 1.1.3 Abel's Integral

A first application of fractional-order integration occurs in a classical mechanical problem which is well known in variational calculus. We consider a mass, subjected to gravity, which slides down the track  $(x(p), y(p))$  without friction as illustrated in Figure 1.2 and we want to compute the time  $T$  which the mass  $m$  needs to reach a certain point on the track. We start with the balance of energies

$$m g h_0 = m g y(p) + \frac{m}{2} \left( \frac{dp}{dt} \right)^2,$$

and can reshape this into

$$\frac{dt}{dp} = \frac{1}{\sqrt{2g(h_0 - y(p))}}.$$

Integration leads to the wanted time:

$$T = \frac{1}{\sqrt{2g}} \int_0^{\bar{p}} \frac{dp}{\sqrt{h_0 - y(p)}}$$

with the track's slope  $p'(y) = f(y)$  defined by the spatial derivative of the path variable  $p$  with respect to the height  $y$ . This yields for the time:

$$T = \frac{1}{\sqrt{2g}} \int_{h_0}^0 \frac{p'(y)}{(h_0 - y)^{\frac{1}{2}}} dy = -\frac{1}{\sqrt{2g}} \int_0^{h_0} \frac{f(y)}{(h_0 - y)^{\frac{1}{2}}} dy = -\frac{1}{\sqrt{2g}} \Gamma\left(\frac{1}{2}\right) \mathcal{I}_y^{\frac{1}{2}} f(y).$$

This last convolution integral of the function  $f(y)$  is called Abel's integral [74, p. 262] and it is actually a fractional-order integral  $\mathcal{I}^\alpha$  of the order  $\alpha = \frac{1}{2}$ . In this case, the fractional-order operator contains the information on which path the mass has taken. Note that this problem setup is similar to the brachistochrone or tautochrone problem. But here we are interested in the absolute time  $T$  for an arbitrary path and not the shape of the path for the minimum time.

## 1.2 Fractional-Order Control and State-Estimation - State of the Art

The temptation to put fractional-order calculus to use in the field of control theory is mostly motivated by the frequency domain. The fractional-order  $\text{PI}^\alpha \text{D}^\beta$  (proportional-integral-derivative) controller

$$C(s) = K_P + \frac{K_I}{s^\alpha} + K_D s^\beta$$

introduced by [75] is an easy generalization of the standard PID controller. The additional parameters  $\alpha$  and  $\beta$  allow arbitrary slopes in the frequency domain [44]. Only with the fractional-order integrator we can realize Bode's optimal open loop with phase margins between  $30^\circ$  and  $45^\circ$  [60]. This additional degree of freedom can be used to achieve further requirements, e.g. robustness of the closed loop against parameter variations. For these reasons, numerous papers [98, 18, 62, 87, 61] present different approaches of tuning such controllers.

In addition to that, fractional-order control approaches are well suited to deal with non-minimum phase systems as part of the unstable integer-order dynamics can be compensated in the fractional-order domain [41].

Other control approaches use different fractional-order structures, e.g. the fractional-order lead-lag compensator [79] or the CRONE approach. The different generations of the CRONE controller [71, 72, 43, 73] use a fractional parametrization of an open-loop and the final controller is obtained by rebuilding the theoretical frequency response with a series of integer-order lead-lag compensators.

Generally speaking it seems like every inter-order control concept has been extended to the fractional-order world in the last three decades, e.g.  $\mathcal{H}_\infty$ -control [99, 23], sliding-mode control [3], adaptive control [60], and reset control [36, 12, 31], to mention a few.

Despite the obvious advantages, fractional-order control of integer-order systems leads to two main problems. First, the implementation requires a lot of physical memory which is needed



to approximate the infinite memory of the fractional-order operators. The second disadvantage is less obvious: linear fractional-order systems converge only algebraically which is very slow compared to the exponential convergence which can be achieved with integer-order methods. However, this is not the focus of most papers, as they either use sufficiently high controller gains, control relatively slow processes [24] or focus on the tracking of reference steps, where the effect is less visible.

Regarding the estimation of fractional-order state-space systems, there are considerably fewer approaches listed in the literature as state-space realizations of fractional-order models are difficult to obtain [83]. However, for certain system classes [16, 89], approaches have been published: In [45, 6] a  $\mathcal{H}_\infty$  and a sliding-mode observer are designed to estimate the state of an initialized fractional-order system. The concept of unknown input observers [68, 67] as well as disturbance observers [15] have been investigated.

### 1.3 Contribution and Outline of this Thesis

The first two chapters are dedicated to introduce the reader to the required background. Chapter 2 summarizes and compares the most common definitions of fractional-order operators which are mostly applied in the field of control theory and signal processing. Furthermore, it provides an introduction to the problem of initialization of fractional-order operators which is still an active field of research. The following Chapter 3 is dedicated to introduce the linear time-invariant (LTI) fractional-order system in the state-space representation. Preliminary results regarding the stability, controllability and observability are given. The focus is set on the state estimation of fractional-order systems with different initializations.

The main contribution of this work is contained in Chapter 4 and 5. The two main questions answered in these parts are

1. How can we represent fractional-order systems in terms of integer-order derivatives and vice versa?
2. How can we apply these connections between the different system classes to design controllers and observers with an increased convergence?

The first chapter recaptures the results presented in [102] and [104], it focuses on the state estimation of different classes of fractional-order systems. We derive alternative representations of the fractional-order dynamics and apply these to increase the convergence of the estimation error. The associated integer-order systems can also be applied to implement fractional-order systems more efficiently.

In Chapter 5, the fractional-order representation of integer-order LTI systems is investigated. We make use of the connection of both system classes and change the control perspective such that a controlled fractional-order system behaves like an integer-order system in the closed loop [101].

Furthermore, we derive an observer as shown in [103] with increased initial convergence or lower observer gains. Applying similar approaches, we improve the fractional-order control of an integer-order system by introducing the memory reset [105]. This idea is further extended to include the reset of the controller state as presented in [106].

In the penultimate Chapter 6, the observer and reset control approaches are verified on a simple laboratory test bench. Conclusions are drawn in Chapter 7 which also presents ideas for the continuation of this research.

## 2 Fractional-Order Integration and Differentiation

A generalization of the concept of differentiation and integration to arbitrary non-integer orders is difficult to understand because of the graphical intuition we connect with these operations. The first order derivative gives us the slope of the function at a certain time instant, whereas we connect the first order integral with the area under the function as illustrated in Figure 2.1. With these illustrations in mind, it is difficult to imagine how the concept changes when the operator's order is not limited to integer numbers any more.

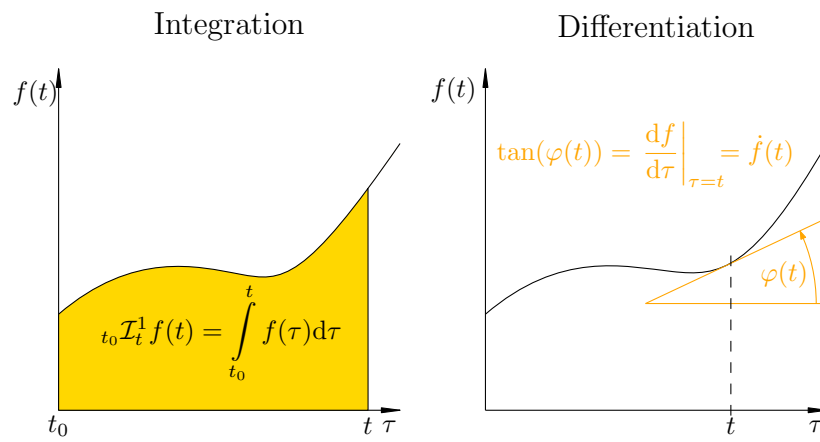


Figure 2.1: Graphical illustration of the concepts of integration and differentiation.

However, the rules to differentiate and integrate certain functions might be extended more directly, as they unify both operations. Let us first consider the harmonic functions  $\sin(\cdot)$  and  $\cos(\cdot)$ . Each first-order derivative results in a phase shift of  $+90^\circ$ . For the integration only the sign of this phase shift changes

$$\begin{aligned} \frac{d^n}{dt^n} \sin(t) &= \sin\left(t - n\frac{\pi}{2}\right), \quad n \in \mathbb{Z} \\ \frac{d^n}{dt^n} \cos(t) &= \cos\left(t - n\frac{\pi}{2}\right), \quad n \in \mathbb{Z}, \end{aligned}$$

hence negative  $n$  represent the integration here. In this formula we can change the integer  $n$  to a real-valued  $\alpha \in \mathbb{R}$ .

$$\begin{aligned} \frac{d^\alpha}{dt^\alpha} \sin(t) &= \sin\left(t - \alpha\frac{\pi}{2}\right), \quad \alpha \in \mathbb{R} \\ \frac{d^\alpha}{dt^\alpha} \cos(t) &= \cos\left(t - \alpha\frac{\pi}{2}\right), \quad \alpha \in \mathbb{R}. \end{aligned}$$

Let us continue with the exponential function  $\exp(\cdot)$ , which does not change applying either operation. The generalization to an arbitrary order  $\alpha$  keeps this property

$$\frac{d^\alpha}{dt^\alpha} \exp(t) = \exp(t), \quad \alpha \in \mathbb{R}. \quad (2.1)$$

Finally, we consider polynomials. In this case the transition to  $\alpha \in \mathbb{R}$  is less straight forward because the factorial is only defined for natural numbers

$$\frac{d^n}{dt^n} t^k = \frac{k!}{(k-n)!} t^{k-n}, \quad k \in \mathbb{N} \setminus \{0\}, \quad n \in \mathbb{Z}. \quad (2.2)$$

We restrict this formula here to integer-order powers of  $t$ , although it can be extended to the arbitrary  $k \in \mathbb{R} \setminus \{0\}$ . We have to apply Euler's gamma function  $\Gamma(\cdot)$  (see Section 2.2), which generalizes the factorial to real and complex numbers  $\Gamma(n+1) = n!$  with  $n \in \mathbb{N}$ , i.e.

$$\frac{d^\alpha}{dt^\alpha} t^k = \frac{\Gamma(k+1)}{\Gamma(k+1-\alpha)} t^{k-\alpha}, \quad k \in \mathbb{N} \setminus \{0\}, \quad \alpha \in \mathbb{R}. \quad (2.3)$$

So far all these extensions have been obvious; however, they are inconsistent. Let us consider the Taylor series representation of the exponential function around the time instant  $t^* = 0$  and apply equation (2.3)

$$\frac{d^\alpha}{dt^\alpha} \exp(t) = \frac{d^\alpha}{dt^\alpha} \left( \sum_{k=0}^{\infty} \frac{t^k}{k!} \right) = \left( \sum_{k=0}^{\infty} \frac{t^{k-\alpha}}{\Gamma(k+1-\alpha)} \right) \neq \exp(t) \quad (2.4)$$

This inequality is the so called Leibniz' Paradox [42, p. 17]. There is obviously a slight difference between the terms. Some insights gives us the special case  $\alpha = -1$  where the integration results in

$$\frac{d^{-1}}{dt^{-1}} \exp(t) = \frac{d^{-1}}{dt^{-1}} \left( \sum_{k=0}^{\infty} \frac{t^k}{k!} \right) = \left( \sum_{k=0}^{\infty} \frac{t^{k+1}}{\Gamma(k+2)} \right) = \exp(t) - 1 = \int_0^t \exp(\tau) d\tau \quad (2.5)$$

whereas the direct application of (2.1) leads to

$$\frac{d^{-1}}{dt^{-1}} \exp(t) = \exp(t) = \int_{-\infty}^t \exp(\tau) d\tau. \quad (2.6)$$

We see that while both expressions are integrals of the exponential function, the lower limit of the integration is different. The time instant  $t^* = 0$  to develop the Taylor series comes into play here. The fractional-order derivative unifying the operations of differentiation and integration needs to consider some kind of limits.

## 2.1 Integer-Order Differentiation and Integration

Before we introduce different definitions of fractional-order derivatives we want to have a closer look at the properties of the integer-order derivatives. We use the basic definition of the classical derivative based on the limes [74, p. 43]

$$\mathcal{D}^n f(t) = \frac{d^n}{dt^n} f(t) = \lim_{h \rightarrow 0} \frac{1}{h^n} \sum_{k=0}^n (-1)^k \binom{n}{k} f(t - kh). \quad (2.7)$$

with

$$\binom{n}{k} = \frac{n(n-1)(n-2)\dots(n-k+1)}{k!}. \quad (2.8)$$

The definition of the inverse operation, the integration in the sense of Riemann, is slightly more complicated, see [7, p. 496f], and therefore omitted here. We will denote the operation of integration with the lower limit at  $t_0$  by

$${}_{t_0}\mathcal{I}^1 f(t) = {}_{t_0}\mathcal{D}^{-1} f(t) = \int_{t_0}^t f(\tau) d\tau. \quad (2.9)$$

**Properties** We list the most relevant properties of the integer-order operators in order to point out differences to fractional-order calculus later on:

1. Identity:

$$\mathcal{D}^0 f(t) = f(t) \quad (2.10)$$

2. Linearity:

$$\mathcal{D}^n (\alpha f(t) + \beta g(t)) = \alpha \mathcal{D}^n f(t) + \beta \mathcal{D}^n g(t) \quad (2.11)$$

3. Derivatives of constants  $f(t) \equiv c$  with  $n > 0$  vanish:

$$\mathcal{D}^n f(t) = 0. \quad (2.12)$$

4. The integration is a right inverse, but no left inverse of the differentiation:

$$\mathcal{D}^{-n} \mathcal{D}^n f(t) = \mathcal{I}^n \mathcal{D}^n f(t) \neq f(t), \quad (2.13)$$

$$\mathcal{D}^n \mathcal{D}^{-n} f(t) = \mathcal{D}^n \mathcal{I}^n f(t) = f(t). \quad (2.14)$$

5. Leibniz' rule (product rule) [7, p. 441]:

$$\mathcal{D}^n (f(t)g(t)) = \sum_{k=0}^n \binom{n}{k} \mathcal{D}^k f(t) \mathcal{D}^{n-k} g(t). \quad (2.15)$$

6. The derivative of a composite function can be evaluated using the (well known) chain rule

$$\mathcal{D}^1 [f(g(t))] = \frac{\partial f}{\partial g} \mathcal{D}^1 g(t). \quad (2.16)$$

A first generalization of the chain rule is the Theorem of FAÀ DI BRUNO [80].

7. Time scaling is a special case of the chain rule as the scalar multiplication with a scaling factor  $\lambda$  is combined with the outer function  $f(\cdot)$ ;

$$\mathcal{D}^n f(\lambda t) = \lambda^n \mathcal{D}^n f(\tau) \Big|_{\tau=\lambda t}. \quad (2.17)$$

Note that for the time scale  $\lambda = -1$  we invert the time to investigate the history of a system.

8. The composition of integer-order derivatives (semi-group property) leads to the index law

$$\mathcal{D}^n (\mathcal{D}^m f(t)) = \mathcal{D}^m (\mathcal{D}^n f(t)) = \mathcal{D}^{n+m} f(t). \quad (2.18)$$

9. Analyticity: If  $f(t)$  is an analytic function, i.e. the function can be represented locally by a Taylor series, then its derivatives are all also analytic.

Generalizing the operators to an arbitrary real order  $\alpha \in \mathbb{R}$ , we lose some of these properties (refer to Section 2.3).

## 2.2 Fractional-Order Integration

The generalization of the  $n$ -th integral  ${}_{t_0}\mathcal{I}_t^n f(t)$  of an arbitrary real order  $\alpha \in \mathbb{R}$  is a direct consequence of the  $n$ -folded integral given by Cauchy's formula [60, p. 10]

$${}_{t_0}\mathcal{I}_t^n f(t) = \underbrace{\int_{t_0}^t \int_{t_0}^{\tau_1} \dots \int_{t_0}^{\tau_{n-1}}}_{n} f(\tau_1) d\tau_1 d\tau_2 \dots d\tau_n = \frac{1}{(n-1)!} \int_{t_0}^t (t-\tau)^{n-1} f(\tau) d\tau, \quad \begin{array}{l} t > t_0, \\ n \in \mathbb{N} \setminus \{0\}. \end{array} \quad (2.19)$$

A simple proof of this formula can be derived in terms of the Laplace transform. We shift the initial time to  $t_0 = 0$  and the  $n$ -th order integral in the original domain is reduced to the multiplication with  $s^{-n}$  in the Laplace domain. Equation (2.19) is then given by the inverse Laplace transform where we interpret the product in the Laplace domain as a convolution of the function  $f(t)$  with  $\mathcal{L}^{-1}\{s^{-n}\} = t^{n-1}/(n-1)!$  in the time domain.

In Equation (2.19) the integer order  $n$  can be easily extended to an arbitrary non-integer order  $\alpha \in \mathbb{R}^+$  by applying Euler's gamma function

$$\Gamma(z) = \int_0^{\infty} x^{(z-1)} e^{-x} dx. \quad (2.20)$$

The gamma function for real arguments is shown in Figure 2.2 illustrating its property  $\Gamma(n) = (n-1)!$ . This yields the generalization of the integral to an arbitrary real order.

**Definition 2.1** (Riemann-Liouville Integral [20]). *Let  $\alpha \in \mathbb{R}^+$ . The operator  ${}_{t_0}\mathcal{I}_t^\alpha$  defined on  $L_1([t_0, t_1])$*

$${}_{t_0}\mathcal{I}_t^\alpha f(t) = \frac{1}{\Gamma(\alpha)} \int_{t_0}^t (t-\tau)^{\alpha-1} f(\tau) d\tau, \quad t > t_0, \alpha \in \mathbb{R}^+ \quad (2.21)$$

for  $t_0 \leq t \leq t_1$  is called the Riemann-Liouville fractional-order integral operator of the order  $\alpha$ .

Note that this definition is only valid for  $\alpha > 0$ , as the gamma function is infinite for  $\alpha = 0$ . Hence the operator is extended with the identity to also cover this case [20, p. 13]:

$${}_{t_0}\mathcal{I}_t^0 f(t) = f(t). \quad (2.22)$$

The Riemann-Liouville Integral can be written as a convolution of the function  $f(t)$  with the convolution kernel  $Y_{t_0}^\alpha(t)$

$${}_{t_0}\mathcal{I}_t^\alpha f(t) = Y_{t_0}^\alpha(t) \star f(t) \quad (2.23)$$

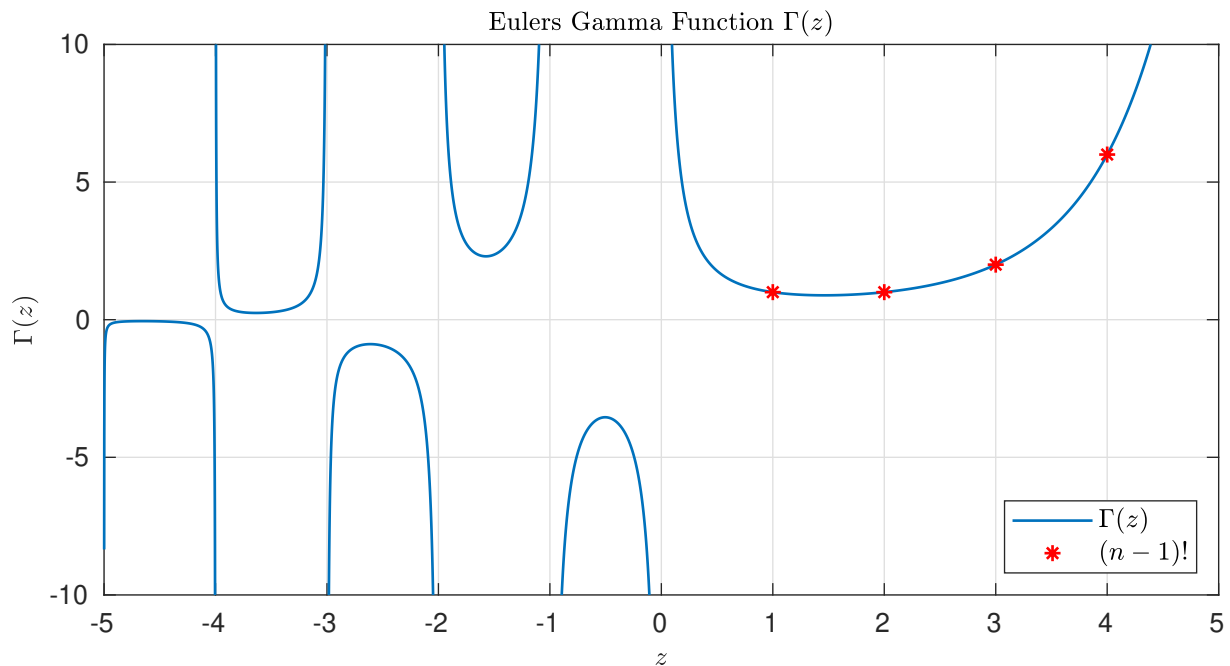


Figure 2.2: Euler's gamma function for real arguments.

with the causal kernel [56]

$$Y_{t_0}^\alpha(t) = \frac{(t-t_0)_+^{\alpha-1}}{\Gamma(\alpha)} = \begin{cases} 0, & t < t_0 \\ \frac{(t-t_0)^{\alpha-1}}{\Gamma(\alpha)}, & t \geq t_0. \end{cases} \quad (2.24)$$

This convolution kernel exhibits a singularity at the lower limit  $t_0$  which leads to difficulties regarding the numerical evaluation. If  $f(t)$  has  $m+1$  continuous derivatives, however, this singularity can be reduced by integration by parts [74, p. 52]

$${}_{t_0}\mathcal{I}_t^\alpha f(t) = \sum_{k=0}^m \frac{f^{(k)}(t_0)(t-t_0)^{\alpha+k}}{\Gamma(\alpha+k+1)} + \frac{1}{\Gamma(\alpha+k+1)} \int_{t_0}^t (t-\tau)^{\alpha+m} f^{(m+1)}(\tau) d\tau. \quad (2.25)$$

Note that the fractional-order integral is a linear operator and satisfies the semigroup property:

$${}_{t_0}\mathcal{I}_t^\alpha \left( {}_{t_0}\mathcal{I}_t^\beta f(t) \right) = {}_{t_0}\mathcal{I}_t^\beta \left( {}_{t_0}\mathcal{I}_t^\alpha f(t) \right) = {}_{t_0}\mathcal{I}_t^{\alpha+\beta} f(t). \quad (2.26)$$

**Behavior at the lower limit** Let us investigate the result of the fractional-order integral of the order  $\alpha \in (0,1)$  for  $t \rightarrow t_0$ . From integer-order calculus the integral of a continuous function is always zero if the lower limit equals the upper limit. The convolution integral defining the fractional-order integral however contains a singularity which might lead to unexpected behavior. Using equation (2.25), we see that  ${}_{t_0}\mathcal{I}_{t_0}^\alpha f(t) = 0$  if the function is differentiable  $f(\cdot) \in \mathcal{C}^1$ . We can relax these conditions further.

**Theorem 2.1** ([20]). Let  $f(t)$  be Hölder continuous of the order  $\mu \in [0, 1]$  in the interval  $t \in [t_0, t_f]$ , i.e.  $f(\cdot) \in \mathcal{H}^\mu[t_0, t_f]$  and  $\alpha \in (0, 1)$ , then

$${}_{t_0}\mathcal{I}_t^\alpha f(t) = \frac{f(t_0)}{\Gamma(\alpha + 1)}(t - t_0)^\alpha + \Theta(t). \quad (2.27)$$

With some function  $\Theta(\cdot)$  satisfying

$$\Theta(t) = O\left((x - t_0)^{\mu+\alpha}\right) \quad \text{for } t \rightarrow t_0, \quad (2.28)$$

using the Landau symbol  $O(\cdot)$  here.

This is a part of the results in Theorem 2.5 given in [20, p. 15].

*Proof.* First of all we introduce a zero into the definition of the fractional order integral to derive the function  $\Theta(t)$

$${}_{t_0}\mathcal{I}_t^\alpha f(t) = \frac{1}{\Gamma(\alpha)} \int_{t_0}^t \frac{f(\tau) - f(t_0) + f(t_0)}{(t - \tau)^{1-\alpha}} d\tau \quad (2.29)$$

$$= \frac{1}{\Gamma(\alpha)} \int_{t_0}^t \frac{f(t_0)}{(t - \tau)^{1-\alpha}} d\tau + \frac{1}{\Gamma(\alpha)} \int_{t_0}^t \frac{f(\tau) - f(t_0)}{(t - \tau)^{1-\alpha}} d\tau \quad (2.30)$$

$$= \frac{f(t_0)}{\Gamma(\alpha + 1)}(t - t_0)^\alpha + \Theta(t). \quad (2.31)$$

It remains to show how  $\Theta(t)$  is bounded. For that, we use the Hölder continuity

$$|\Theta(t)| \leq \frac{1}{\Gamma(\alpha)} \int_{t_0}^t \frac{L|\tau - t_0|^\mu}{(t - \tau)^{1-\alpha}} d\tau = \frac{L}{\Gamma(\alpha)} \int_{t_0}^t (\tau - t_0)^\mu (t - \tau)^{\alpha-1} d\tau. \quad (2.32)$$

To solve this convolution integral we use the Laplace transform of the two pseudo polynomials (2.64)

$$\int_{t_0}^t (\tau - t_0)^\mu (t - \tau)^{\alpha-1} d\tau = \mathcal{L}^{-1} \left\{ \frac{e^{-t_0 s} \Gamma(\mu + 1) \Gamma(\alpha)}{s^{\mu+1} s^\alpha} \right\} = \frac{\Gamma(\mu + 1) \Gamma(\alpha)}{\Gamma(\mu + \alpha + 1)} (t - t_0)^{\alpha+\mu}. \quad (2.33)$$

Finally, the bound is given by

$$|\Theta(t)| \leq \frac{L\Gamma(\mu + 1)}{\Gamma(\mu + \alpha + 1)} (t - t_0)^{\alpha+\mu} = O((t - t_0)^{\alpha+\mu}). \quad (2.34)$$

□

The consequences of this theorem are that the fractional-order integral at the lower limit is zero if the function is at least continuous, as  $f(\cdot) \in \mathcal{C}^0[t_0, t_f]$  equals  $f(\cdot) \in \mathcal{H}^0[t_0, t_f]$ . For functions which are not continuous at the lower limit, e.g.  $f(t) = (t - t_0)^{\alpha-1}$  with  $\alpha \in (0, 1)$ , this is not the case, we will give an example in Section 2.4.



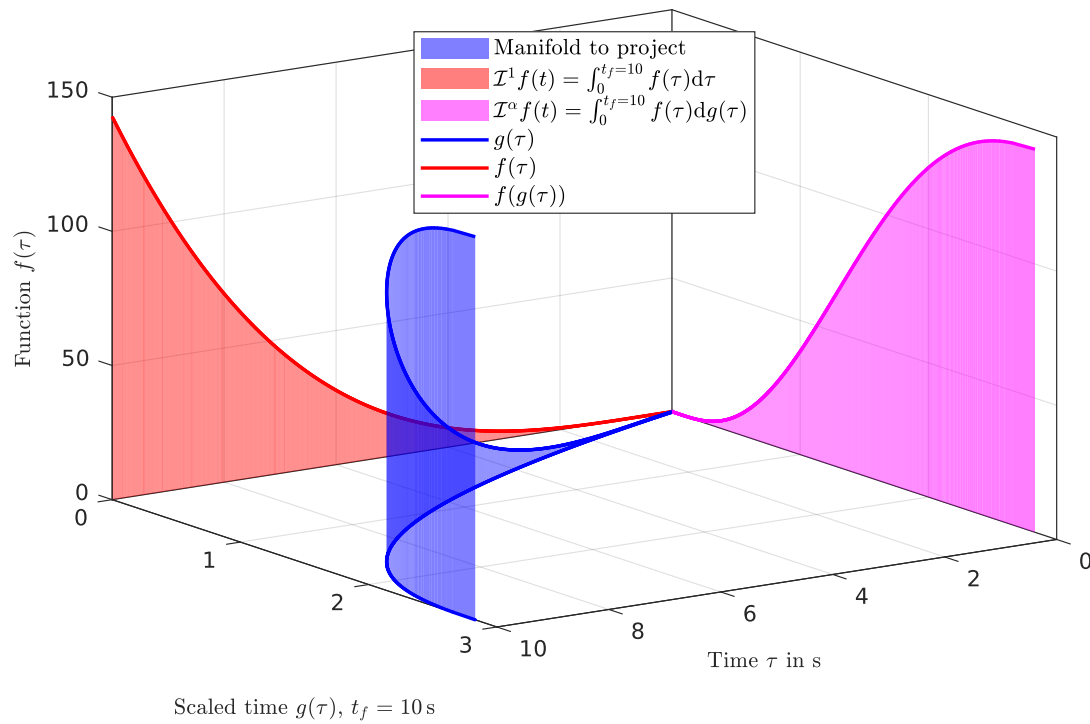


Figure 2.3: Three-dimensional representation of fractional-order integration.

**Heterogeneous Time Interpretation [76]** We consider the function  $g(\tau)$  given by [17, p. 82]

$$g(\tau) = \frac{1}{\Gamma(\alpha + 1)} (t^\alpha - (t - \tau)^\alpha) \quad (2.35)$$

with the total differential depending on  $d\tau$

$$dg(\tau) = \frac{(t - \tau)^{\alpha-1}}{\Gamma(\alpha)} d\tau. \quad (2.36)$$

The fractional-order integral can be written as

$$\mathcal{I}^\alpha f(t) = \int_0^t f(\tau) dg(\tau). \quad (2.37)$$

With this change of coordinates we can restate our interpretation of the fractional-order integral. The fractional-order integral represents the area under the curve  $f(g(t))$ . This is illustrated in Figure 2.3. The function  $f(t)$  is plotted over the evaluation of  $g(\tau)$ . The area defined by this curve  $(\tau, g(\tau), f(\tau))$  and its baseline  $(\tau, g(\tau), 0)$  is highlighted in blue. The projection of this area onto the  $\tau - f(\tau)$ -plane results in the integer-order integral (red) and the projection towards the  $g(\tau) - f(\tau)$ -plane gives us the fractional-order integral. As the function  $g(\tau)$  also depends on the actual time  $t$ , it changes its shape with increasing time  $t$ , and the time  $g(\tau)$  evolves heterogeneously.

## 2.3 Fractional-Order Differentiation

There are different approaches to generalize the integer-order derivative to non-integer orders. A first approach is a direct extension of the difference quotient defining the derivative of the integer-order  $n \in \mathbb{N}$

$$\mathcal{D}^n f(t) = \lim_{h \rightarrow 0} \frac{1}{h^n} \sum_{k=0}^n (-1)^k \binom{n}{k} f(t - kh), \quad (2.38)$$

with

$$\binom{n}{k} = \frac{n(n-1)(n-2)\dots(n-k+1)}{k!}. \quad (2.39)$$

The generalization here is not that obvious compared to the extension of Cauchy's formula in the previous section. Again, the binomial coefficient can be generalized applying the gamma function. The main part to consider here is the sum itself, because the integer-order  $n$  does not only define the coefficient weighting the past function values - it also defines the number of summands. In order to also cover integration by this formula, we have to take an infinite number of summands into account:

$$\mathcal{D}^n f(t) = \lim_{h \rightarrow 0} \frac{1}{h^n} \sum_{k=0}^{\infty} (-1)^k \binom{n}{k} f(t - kh). \quad (2.40)$$

Note, that this does not change the results for  $n < 0$  because  $\binom{n}{k} = 0$  for  $k \geq n + 1$ .

### 2.3.1 Operator Definitions

The final generalization to an arbitrary order  $\alpha \in \mathbb{R}$  needs to take the limits into account:

**Definition 2.2** (Grünwald-Letnikov Fractional Derivative [20, 74]). *Let  $\alpha > 0$ ,  $f(\cdot) \in \mathcal{C}^{[\alpha]}([t_0, t_f])$  and  $t \in (t_0, t_f]$ . Then*

$${}_{t_0}^{\text{GL}}\mathcal{D}_t^\alpha f(t) = \lim_{\substack{h \rightarrow 0 \\ nh = t - t_0}} \frac{1}{h^\alpha} \sum_{k=0}^n (-1)^k \binom{\alpha}{k} f(t - kh) \quad (2.41)$$

*is called the Grünwald-Letnikov fractional-order derivative of the function  $f$  of the order  $\alpha$ .*

For negative  $n \in \mathbb{Z}^-$  this formula results in Cauchy's  $n$ -folded integral, as shown in [74, p. 46ff]. The definition unifies the operations of integration and differentiation. Although this definition is hard to work with, it is useful for the digital implementation (see Section 2.6).

Another approach to generalize the classical derivative operator to an arbitrary order is given by the combination of integer-order derivatives  $\mathcal{D}^m$  with the fractional-order integral  $\mathcal{I}^{m-\alpha}$  (2.21). The order of application, however, leads to different definitions. The generally most frequently used operators are the so called Riemann-Liouville fractional-order derivative [60, p. 11] and the definition given by Caputo [60, p. 11].

**Definition 2.3** (Riemann-Liouville Fractional Derivative [20, 74]). Let  $\alpha \in \mathbb{R}^+$  and  $f(\cdot) \in \mathcal{L}_{\text{loc}}^1([t_0, t_f])$ . The operator  ${}^{\text{R}}\mathcal{D}_t^\alpha$ , defined by

$${}^{\text{R}}\mathcal{D}_t^\alpha f(t) = \mathcal{D}^m \mathcal{I}^{m-\alpha} f(t) = \frac{1}{\Gamma(m-\alpha)} \frac{d^m}{dt^m} \int_{t_0}^t \frac{f(\tau)}{(t-\tau)^{\alpha-m+1}} d\tau, \quad m-1 < \alpha < m, m \in \mathbb{N}, \quad (2.42)$$

with  $t_0 \leq t \leq t_f$  is called the Riemann-Liouville fractional-order derivative of the order  $\alpha$ .

**Definition 2.4** (Caputo Fractional Derivative [20, 74]). Let  $\alpha \in \mathbb{R}^+$  and  $f^{(m)} \in \mathcal{L}_{\text{loc}}^1([t_0, t_f])$ . The operator  ${}^{\text{C}}\mathcal{D}_t^\alpha$ , defined by

$${}^{\text{C}}\mathcal{D}_t^\alpha f(t) = \mathcal{I}^{m-\alpha} \mathcal{D}^m f(t) = \frac{1}{\Gamma(m-\alpha)} \int_{t_0}^t \frac{f^{(m)}(\tau)}{(t-\tau)^{\alpha-m+1}} d\tau, \quad m-1 < \alpha < m, m \in \mathbb{N} \quad (2.43)$$

with  $t_0 \leq t \leq t_f$  is called the Caputo fractional-order derivative of the order  $\alpha$ .

Note that in these definitions of both operators the integer-order case is excluded by the inequality defining the integer floor and ceiling of  $m-1 < \alpha < m$ . To include the integer-order case  $\alpha \in \mathbb{N}$  we can only allow the floor to be integer  $m-1 \leq \alpha < m$  such that the singularity in the prefactor  $(\Gamma(m-\alpha))^{-1}$  does not occur with  $\alpha = m-1$ . For the Riemann-Liouville derivative, this leads to  $\alpha = m-1$

$${}^{\text{R}}\mathcal{D}_t^{m-1} f(t) = \frac{1}{\Gamma(1)} \frac{d^m}{dt^m} \int_{t_0}^t \frac{f(\tau)}{(t-\tau)^0} d\tau = \frac{d^{m-1}}{dt^{m-1}} f(t) \quad (2.44)$$

In contrast, Caputo's derivative cannot be generalized in the same manner with  $\alpha = m-1$ . This would lead to

$${}^{\text{C}}\mathcal{D}_t^{m-1} f(t) = \frac{1}{\Gamma(1)} \int_{t_0}^t \frac{f^{(m)}(\tau)}{(t-\tau)^0} = f^{(m-1)}(t) - f^{(m-1)}(t_0), \quad (2.45)$$

however, the limit  $\alpha \rightarrow m$  does approach the integer-order derivative without bias (see [74, p. 79]). Therefore, the definition of Caputo's operator is extended in [20, p. 49] to be backwards compatible with the classical integer derivatives. This abrupt change of the behavior for orders close to integers is another reason, why Riemann's approach is preferred in modelling physical processes, as the effect of a slightly disturbed system order is less grave.

Referring to [74, p. 62] the Grünwald-Letnikov definition is equivalent to the Riemann's approach (2.42) if the function  $f(t)$  is sufficiently smooth, i.e.  $f(\cdot) \in \mathcal{C}^{m+1}$ . The proof uses integration by parts sequentially.

Note that these formulas define the fractional-order derivative with a limited past  $t \geq t_0$ , however, we might also set  $t_0 \rightarrow -\infty$  to use an unlimited past.

The difference of both operators is shown in Figure 2.4. This graphic shows the analytical fractional-order derivative of a third order polynomial. To evaluate the Riemann-operator the results listed in [74, p. 72] are used, whereas the Caputo's fractional-order derivative of a polynomial is given in [20, p. 193]. The difference is clearly visible at the initial value of

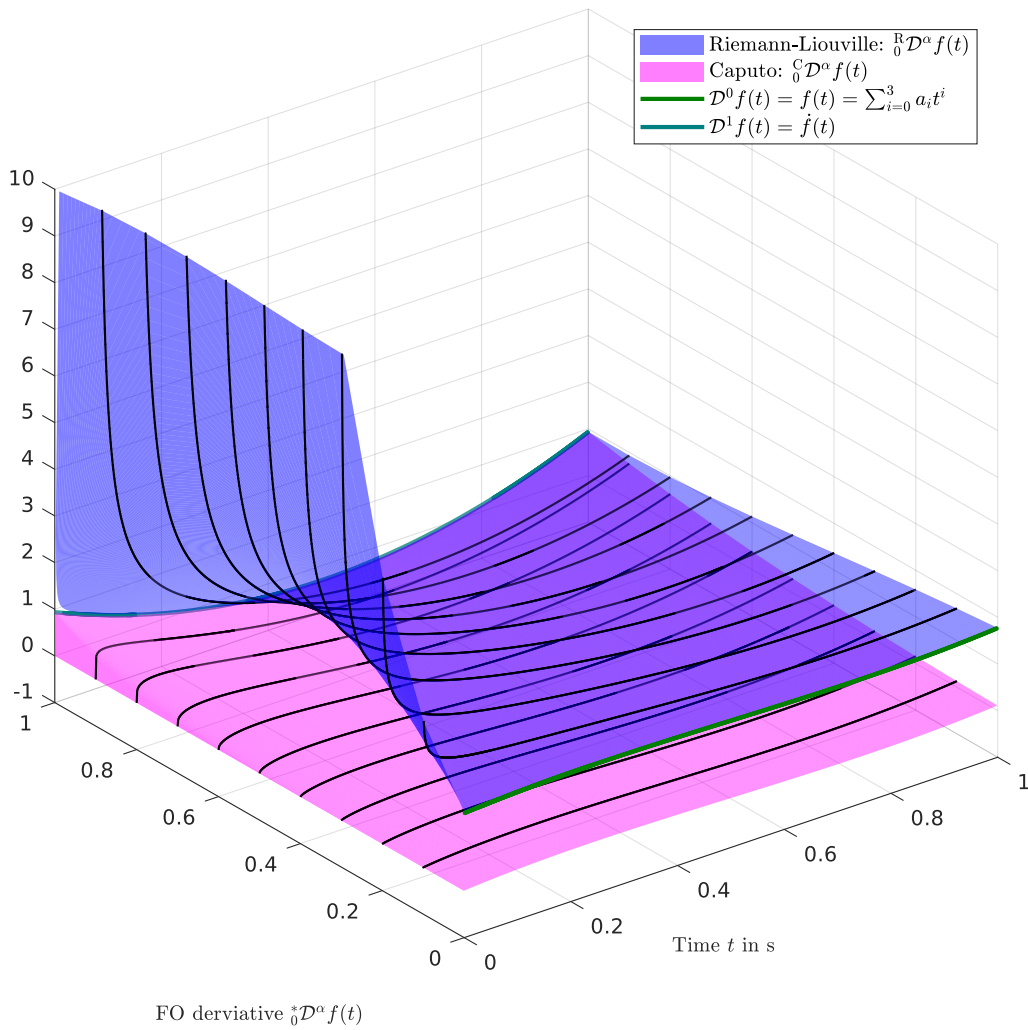


Figure 2.4: Comparison of Caputo's and Riemann's fractional-order derivative of a third-order polynomial:  $f(t) = \frac{5}{3}t^3 + \frac{5}{2}t^2 + \frac{15}{16}t + \frac{1}{3}$ .

the function,  $f(0) = \frac{1}{3} \neq 0$ . This constant part is also causing the singularity at  $t = 0$ s when Riemann's operator is applied, whereas the initial value of Caputo's derivative of a polynomial is always zero for non-integer  $\alpha$ . For  $\alpha \rightarrow 1$  both operators approach the first derivative  $\dot{f}(t)$ . For  $\alpha \rightarrow 0$ , only Riemann's operator results in the function itself (Caputo's derivative approaches the function only for  $\alpha \rightarrow 0^-$ ).

The different operators defined by Caputo and Riemann-Liouville are connected with respect to their initial conditions [60, p. 11]:

$${}_t^R \mathcal{D}_t^\alpha f(t) = {}_t^C \mathcal{D}_t^\alpha f(t) + \sum_{k=0}^{m-1} \frac{(t-t_0)^{k-\alpha}}{\Gamma(k-\alpha+1)} f^{(k)}(0^+). \quad (2.46)$$

We will proof this formula for the case  $\alpha < 1$ . First, we apply Leibniz' rule of differentiating parameter integrals to equation (2.42) yielding

$${}^R_{t_0}\mathcal{D}_t^\alpha f(t) = \frac{1}{\Gamma(1-\alpha)} \left( \frac{d}{dt} \int_{t_0}^t f(\tau)(t-\tau)^{-\alpha} d\tau \right) \quad (2.47)$$

$$= \frac{1}{\Gamma(1-\alpha)} \left( -\alpha \int_{t_0}^t f(\tau)(t-\tau)^{-\alpha-1} d\tau + \frac{f(\tau)}{(t-\tau)^\alpha} \Big|_{\tau=t} \frac{d}{dt} t \right). \quad (2.48)$$

This reformulation shows the unbounded term at the lower limit. However, when we partially integrate Caputo's definition (2.43)

$$\begin{aligned} {}^C_{t_0}\mathcal{D}_t^\alpha f(t) &= \frac{1}{\Gamma(1-\alpha)} \int_{t_0}^t \frac{f^{(1)}(\tau)}{(t-\tau)^\alpha} d\tau = \frac{1}{\Gamma(1-\alpha)} \left( \frac{f(\tau)}{(t-\tau)^\alpha} \Big|_{t_0}^t - \int_{t_0}^t \alpha \frac{f(\tau)}{(t-\tau)^{\alpha+1}} d\tau \right) \\ &= \frac{1}{\Gamma(1-\alpha)} \left( \frac{f(\tau)}{(t-\tau)^\alpha} \Big|_{\tau=t} - \frac{f(t_0)}{(t-t_0)^\alpha} - \alpha \int_{t_0}^t (t-\tau)^{-\alpha-1} f(\tau) d\tau \right) \end{aligned}$$

we end up with the identical term. In the comparison of both operators, this term cancels out and equation (2.46) holds.

Throughout this thesis the following abbreviations are used:

$$\begin{aligned} {}^R_{t_0}\mathcal{D}^\alpha f(t) &= {}^R_{t_0}\mathcal{D}_t^\alpha f(t) & {}^R\mathcal{D}^\alpha f(t) &= {}^R_0\mathcal{D}_t^\alpha f(t) \\ {}^{GL}_{t_0}\mathcal{D}^\alpha f(t) &= {}^{GL}_{t_0}\mathcal{D}_t^\alpha f(t) & {}^{GL}\mathcal{D}^\alpha f(t) &= {}^{GL}_0\mathcal{D}_t^\alpha f(t) \\ {}_{t_0}\mathcal{D}^\alpha f(t) &= {}^C_{t_0}\mathcal{D}_t^\alpha f(t) & \mathcal{D}^\alpha f(t) &= {}^C_0\mathcal{D}_t^\alpha f(t) \\ \mathcal{I}^\alpha f(t) &= {}_0\mathcal{I}_t^\alpha f(t). \end{aligned}$$

### 2.3.2 Properties

Let us circle back to the introduction of this chapter. Having defined different possibilities to extend the operation of differentiating to an arbitrary fractional order, we should have a look at the remaining properties.

1. Backwards compatibility: As shown before, Riemann's derivative is directly backwards compatible by allowing integer orders such that

$$m-1 \leq \alpha < m. \quad (2.49)$$

Caputo's derivative leads to an offset given by the initial conditions, if we apply (2.49) to the Definition 2.4. However, in [74, p. 79] it is shown, that Caputo's operator is also backwards compatible by means of the upper limit  $\alpha \rightarrow m$ .

2. Fractional-order differentiation is a linear operation for  $\mu, \beta \in \mathbb{R}$  and  $\alpha \in \mathbb{R}^+$ :

$${}^* \mathcal{D}_{t_0}^\alpha (\mu f(t) + \beta g(t)) = \mu {}^* \mathcal{D}_{t_0}^\alpha f(t) + \beta {}^* \mathcal{D}_{t_0}^\alpha g(t), \quad (2.50)$$

where  ${}^* \mathcal{D}_{t_0}^\alpha$  is any of the previously defined operators. The linearity follows directly from each definition.

3. Only the Caputo derivative of a constant function vanishes. The Riemann-Liouville derivative of a constant function  $f(t) = c$  is given by [74, p. 72]

$${}^R \mathcal{D}_t^\alpha c = \frac{ct^{-\alpha}}{\Gamma(1-\alpha)}. \quad (2.51)$$

For this reason Riemann's operator is preferred in modelling applications, e.g. in viscoelastic materials creep occurs even under constant stress.

4. Although the fractional-order derivative of the constant does not vanish, the time scaling property holds [70, p. 76] for Riemann-Liouville also:

$${}^* \mathcal{D}_t^\alpha f(\lambda t) = \lambda^\alpha {}^* \mathcal{D}_\tau^\alpha f(\tau) \Big|_{\tau=\lambda t} \quad (2.52)$$

5. In [74, p. 96] the generalization of Leibniz's formula is derived for  $f, g \in \mathcal{C}^\infty$  on the interval  $t \in [t_0, t_1]$ .

$${}^R \mathcal{D}_t^\alpha (f(t)g(t)) = \sum_{k=0}^{\infty} \binom{\alpha}{k} f^{(k)}(t) {}^R \mathcal{D}_t^{\alpha-k} g(t). \quad (2.53)$$

This formula is especially useful if one function is a polynomial, such that only a finite number of summands needs to be taken into account.

6. The fractional-order derivative of a composite function  $F(\cdot) = f(g(\cdot))$  can be computed by applying (2.53) to the product  $F(t) \cdot \sigma(t - t_0)$ , where  $\sigma(\cdot)$  represents the Heaviside function. This reduces the fractional differentiation to the integer-order differentiation of the original composite function  $F(\cdot)$  and FAÀ DI BURNO'S formula can be applied resulting in [74, p. 98]:

$$\begin{aligned} {}^R \mathcal{D}_{t_0}^\alpha f(g(t)) &= \frac{(t-t_0)^\alpha}{\Gamma(1-\alpha)} f(g(t)) + \\ &\sum_{k=1}^{\infty} \binom{\alpha}{k} \frac{k!(t-t_0)^{k-\alpha}}{\Gamma(k-\alpha+1)} \sum_{m=1}^k f^{(m)}(g(t)) \sum_{a_r \in T_m} \prod_{r=1}^k \frac{1}{a_r!} \left( \frac{g^{(r)}(t)}{r!} \right)^{a_r} \end{aligned} \quad (2.54)$$

with the set  $T_m$  given by

$$T_m = \left\{ a \in \mathbb{N}^m \mid \sum_{r=1}^k r a_r = k, \quad \sum_r a_r = m \right\}. \quad (2.55)$$

Despite its complexity, this equation still might be useful if the outer function  $f(t)$  is a polynomial, meaning that only a finite number of summands appears.

7. Composition of fractional-order integrals: The semigroup property holds for fractional-order integrals, i.e.

$$\mathcal{I}^\alpha \left( \mathcal{I}^\beta f(t) \right) = \mathcal{I}^\beta \left( \mathcal{I}^\alpha f(t) \right) = \mathcal{I}^{\alpha+\beta} f(t). \quad (2.56)$$

8. For fractional-order derivatives, the semigroup property does not hold in general:

$${}^*_{t_0} \mathcal{D}^\alpha \left( {}^*_{t_0} \mathcal{D}^\beta f(t) \right) \neq {}^*_{t_0} \mathcal{D}^\beta \left( {}^*_{t_0} \mathcal{D}^\alpha f(t) \right) \neq {}^*_{t_0} \mathcal{D}^{\alpha+\beta} f(t). \quad (2.57)$$

Only for zero initial conditions we can apply the standard composition [74, p. 75]. For non-zero initialization, we have [74, p. 74]

$${}^R_{t_0} \mathcal{D}^\alpha \left( {}^R_{t_0} \mathcal{D}^\beta f(t) \right) = {}^R_{t_0} \mathcal{D}^{\alpha+\beta} f(t) - \sum_{k=1}^m \frac{(t-t_0)^{-\alpha-k}}{\Gamma(1-\alpha-k)} \left[ {}^R_{t_0} \mathcal{D}^{\beta-k} f(t) \right]_{t=t_0}. \quad (2.58)$$

A special case is the combination with integer-order derivatives, a detailed perspective is given in Podlubny's book [74, p. 73f]. A summary is given in [70, p. 82f]. As the fractional-order derivative does not fulfill the semigroup property for arbitrary initial conditions, it is a non-local operator [20, p. 37]. Compared to integer-order derivatives, it is not sufficient to know the function  $f(t)$  in an arbitrary small neighborhood of  $t$ , as the definition of each fractional-order derivative requires the complete history of the considered interval  $[t_0, t]$ .

### 2.3.3 Right and Left Fractional-Order Derivatives

So far the fractional-order differentiation was only considered with a fixed lower limit  $t_0$  and an increasing upper limit  $t > t_0$ . However, it is also possible to fix the upper limit of the fractional-order integral and move backwards in time with the integer-order differentiation. This leads to the so called "right derivatives" [74, p. 89]. For example the right Riemann-Liouville derivative is given by

$${}^R_t \mathcal{D}_{t_f}^\alpha f(t) = \frac{1}{\Gamma(m-\alpha)} \left( -\frac{d}{dt} \right)^m \int_t^{t_f} (t-\tau)^{m-\alpha-1} f(\tau) d\tau, \quad m-1 \leq \alpha < m, m \in \mathbb{Z}. \quad (2.59)$$

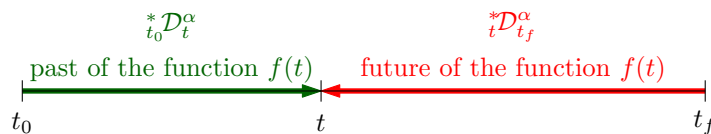


Figure 2.5: The left and right fractional-order derivatives depend on the past and future of the function  $f(t)$  [74, p. 89].

As these operators contain the future of the function  $f(t)$  (as illustrated in Figure 2.5), they are not causal and therefore not useful to model physical processes. If the fractional-order derivative is applied with respect to a spatial variable and not to time, these operators are essential to solve boundary value problems. In the field of fractional-order control theory, we have to apply the right fractional-order derivatives to solve optimal control problems [2, 1].

### 2.3.4 Excursus on Further Fractional-Order Operators

A generalization of Caputo's and Riemann-Liouville's operator is given by the so called sequential fractional-order derivatives defined by Miller and Ross [74, p. 87]. The derivative of the order  $\alpha$  is constructed by applying lower-order operators sequentially to the function

$${}^{\text{MR}}\mathcal{D}_t^\alpha f(t) = {}^*\mathcal{D}_t^{\alpha_1} {}^*\mathcal{D}_t^{\alpha_2} \cdots {}^*\mathcal{D}_t^{\alpha_n} f(t), \quad \sum_{k=1}^n \alpha_k = \alpha \quad (2.60)$$

where the operator  ${}^*\mathcal{D}_t^{\alpha_k}$  can be interpreted as any of the previously shown derivative operators. This notation is not to be confused with the composition rule of the sequential use of a fractional-order derivative (composition rule). This approach has the advantage that it unifies the operators of Riemann-Liouville and Caputo since both are special cases for  $m - 1 < \alpha < m, m \in \mathbb{N}$

$${}^{\text{R}}\mathcal{D}_t^\alpha = {}^{\text{MR}}\mathcal{D}_t^\alpha f(t), \quad \alpha_n = \alpha - m, \quad \alpha_1 = \alpha_2 = \dots = \alpha_{n-1} = 1 \quad (2.61)$$

$${}^{\text{C}}\mathcal{D}_t^\alpha = {}^{\text{MR}}\mathcal{D}_t^\alpha f(t), \quad \alpha_1 = \alpha - m, \quad \alpha_2 = \alpha_3 = \dots = \alpha_n = 1 \quad (2.62)$$

with  $n = m + 1$ . Note that in [74] the proofs to show the existence and uniqueness of solutions to fractional-order initial value problems are given within the framework of sequential derivatives.

In addition to this concept there is a huge variety of approaches to generalize the integer-order derivative. An extensive overview is given in [19], wherein more than 20 different operators are defined. Some of these operators are more suited to investigate the fractional-order behavior with respect to space rather than time, e.g. the Caputo-Riesz derivative [91]. Even a local fractional-order derivative for  $\alpha \in (0, 1)$  is defined by Kolwankar and Gangal [17, p. 9].

In general, we can state that each operator has its use for special applications. For the application in the field of control theory, the previously presented operators defined by Caputo, Grünwald-Letnikov and Riemann-Liouville are most suited, as numerical tools are available [21, 92] and a clear connection to integer-order systems can be established.

## 2.4 Laplace Transforms of Fractional-Order Operators

The function  $F(s)$  depending on the complex variable  $s \in \mathbb{C}$  defined by

$$F(s) = \mathcal{L}\{f(t); s\} = \int_0^\infty f(t)e^{-st} dt \quad (2.63)$$

is called Laplace transform of the function  $f(t)$ . Note, that we set the lower limit to zero and not  $0^+$  or  $0^-$ .

The fractional-order integral is the convolution of the function  $f(t)$  with the kernel  $\tilde{Y}_+$ . Hence the Laplace transform to this operator results in the multiplication with the Laplace transform of the kernel [22, p. 137]:

$$\mathcal{L}\{t^\alpha; s\} = \frac{\Gamma(\alpha + 1)}{s^{\alpha+1}}, \quad \alpha > -1, \text{Re}\{s\} > 0. \quad (2.64)$$



The Laplace transform of the fractional-order integral with respect to a time scale with zero initial time  $t_0 = 0$  results in

$$\mathcal{L} \{ {}_0\mathcal{I}_t^\alpha f(t); s \} = s^{-\alpha} F(s). \quad (2.65)$$

**Remark 2.1.** Let us compute the fractional order integral of the order  $1 - \beta$  at the starting point  $t = 0$  of the function  $f(t) = t^{\beta-1}$  with  $\beta \in (0, 1)$ . Applying equations (2.64) and (2.65) results in

$$\mathcal{I}^{1-\beta} \left( \frac{1}{t^{1-\beta}} \right) = \mathcal{L}^{-1} \left\{ \frac{1}{s^{1-\beta}} \frac{\Gamma(\beta)}{s^\beta} \right\}. \quad (2.66)$$

The appropriate initial value theorem of the Laplace transform [96, p. 59] yields

$$\mathcal{I}^{1-\beta} \left( \frac{1}{t^{1-\beta}} \right) \Big|_{t=0} = \lim_{s \rightarrow \infty} s \frac{\Gamma(\beta)}{s} = \Gamma(\beta). \quad (2.67)$$

This is a surprising result, as it does not correspond with our intuition, as the classical improper integral of this function is zero for  $t = 0$ .

Applying this result and the differentiation identity of the Laplace transform [74, p. 104]

$$\mathcal{L} \{ f^{(n)}(t); s \} = s^n F(s) - \sum_{k=0}^{n-1} s^k f^{(n-k-1)}(0) \quad (2.68)$$

the computation of the Laplace transforms connected to each fractional operator of differentiation is more or less straight forward. Note that a change of the initial condition from  $f^{(n-k-1)}(0)$  to  $f^{(n-k-1)}(0^+)$  leads to the similar change in the Laplace transforms of the fractional-order derivatives. Again, the Laplace transform shows the difference of the operators defined previously as the initial conditions are weighted differently

$$\mathcal{L} \left\{ {}_0^R \mathcal{D}_t^\alpha f(t); s \right\} = s^\alpha F(s) - \sum_{k=0}^{m-1} \left[ {}_0^R \mathcal{D}_t^{\alpha-k-1} f(t) \right]_{t=0} \quad (2.69)$$

$$\mathcal{L} \left\{ {}_0^C \mathcal{D}_t^\alpha f(t); s \right\} = s^\alpha F(s) - \sum_{k=0}^{m-1} s^{\alpha-k-1} f^{(k)}(0). \quad (2.70)$$

Note that for Caputo's operator all fractional-order derivatives of the order  $\alpha \in (m-1, m)$  have the same initial conditions. Furthermore, we see that both operators generalize the integer-order case in a different way. Riemann's operator keeps the order of the polynomial in  $s$  weighing the initial conditions, whereas Caputo's operator changes this polynomial to a pseudo polynomial but keeps the integer-order initial conditions.

In contrast to these operators, the Laplace transform of the Grünwald-Letnikov operator only exists for  $0 \leq \alpha < 1$  [74, p. 106] with  $f(0)$  bounded in the classical sense. Here, the initial conditions disappear:

$$\mathcal{L} \left\{ {}_0^{\text{GL}} \mathcal{D}_t^\alpha f(t); s \right\} = s^\alpha F(s). \quad (2.71)$$

For  $\alpha > 1$  this derivative and the Laplace transform only hold in the sense of generalized functions (distributions). This result is remarkable as it differs from the Laplace transform of Riemann's operator (2.69), although these operators are identical for  $\alpha \in [0, 1)$  and  $f(t) \in \mathcal{C}^1$ . The reason for this are the special fractional-order initial conditions, which turn into fractional-order integrals in this case:

$$\left[ {}_{t_0}^R \mathcal{D}_t^{\alpha-1} f(t) \right]_{t=0} = \mathcal{I}^{(1-\alpha)} f(t) \Big|_{t=0} = 0. \quad (2.72)$$

As the function is continuous at zero, this integral vanishes for  $t = 0$  (see Theorem 2.1).

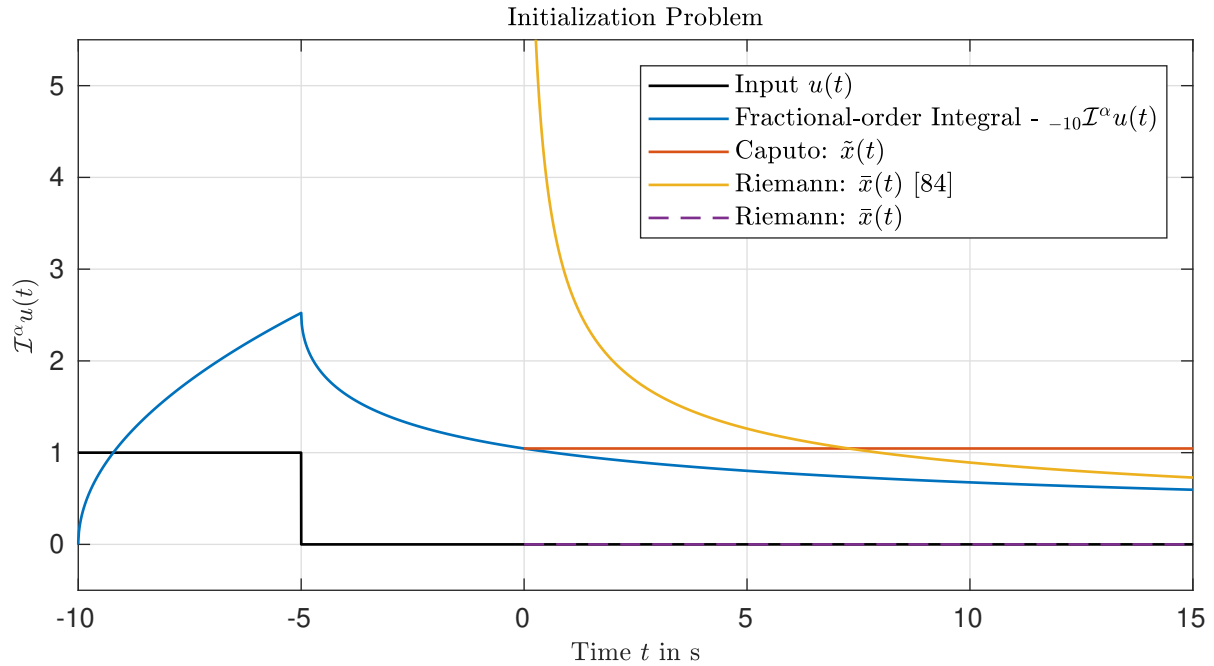


Figure 2.6: The ignored history of the input function  $u(t)$  has a huge influence on the system state. Neither Riemann's nor Caputo's operator give the exact solution if the history is ignored by starting at a later time instant ( $t_0 = 0$ ). Note that Riemann's response uses the wrong initial conditions here.

## 2.5 Initialization of Fractional-Order Operators

The previously shown fractional-order differential operators only consider causal functions with  $f(t) = 0, \forall t < 0$ . However, in real physical systems we cannot ignore the history of a system as it might have an effect on the future. If we neglect this past, the system representation might lead to wrong results. To illustrate this issue further, we rework an example presented in [85]. It establishes a connection of the operators to the scalar fractional-order system.

**Example 2.1.** We consider the fractional-order integration of the function  $f(t)$  being a rectangular impulse:

$$f(t) = \sigma(t) - \sigma(t - t_0), \quad (2.73)$$

where  $\sigma(\cdot)$  represents the Heaviside function. The fractional-order integral  $\mathcal{I}^\alpha f(t)$  reads:

$$x(t) = \mathcal{I}^\alpha f(t) = \frac{t^\alpha}{\Gamma(\alpha + 1)}\sigma(t) - \frac{(t - t_0)^\alpha}{\Gamma(\alpha + 1)}\sigma(t - t_0). \quad (2.74)$$

This integral is shown in Figure 2.6. Let us now change the initial time to the new time scale  $\tau = t - t_1$  with  $t_1 > t_0$ , such that we have a non-zero history of the function to take into account and the function  $x(\tau)$  is not at rest at  $\tau = 0$ .

In order to show the differences of the shown operators, we convert the integration back to a fractional-order differential equation. We start with Riemann's operator.

$${}^R_0\mathcal{D}_\tau^\alpha x(\tau) = f(\tau). \quad (2.75)$$

Applying the Laplace transform (2.69) with  $\mathcal{L}\{x(t), s\} = X(s)$  yields:

$$s^\alpha X(s) - s^0 \left[ {}^R\mathcal{D}_\tau^{\alpha-1} x(\tau) \right]_{\tau=0} = s^\alpha X(s) - \left[ \mathcal{I}^{1-\alpha} x(\tau) \right]_{\tau=0} = 0. \quad (2.76)$$

In the case  $\alpha < 1$  the fractional initial condition is reduced to the fractional-order integral at the initial time. Furthermore, the right side of equation (2.76) is zero due to  $f(\tau) = 0, \forall \tau \geq 0$ . The difficulty here is to evaluate the initial conditions. As shown in [85] we make use of the Laplace transform and apply the time shift law of the Laplace transform. In [85] the authors obtain

$$\begin{aligned} \left[ \mathcal{I}^{1-\alpha} x(\tau) \right]_{\tau=0} &= \mathcal{L}^{-1} \left\{ \left( \frac{1}{s^{1-\alpha}} \left( \frac{1}{s^{\alpha+1}} - \frac{e^{-t_0 s}}{s^{\alpha+1}} \right) \right) e^{t_1} \right\} \Bigg|_{\tau=0} \\ &= \mathcal{L}^{-1} \left\{ \frac{e^{t_1 s} - e^{(t_1-t_0)s}}{s^2} \right\} \Bigg|_{\tau=0} \\ &= (\tau + t_1)\sigma(\tau + t_1) - (\tau + (t_1 - t_0))\sigma(\tau + (t_1 - t_0)) \Big|_{\tau=0} = t_0. \end{aligned}$$

Finally, the solution to (2.75) arises to be [85]:

$$x(\tau) = \frac{\tau^{\alpha-1}}{\Gamma(\alpha)} t_0, \quad \tau \geq 0. \quad (2.77)$$

However, this conflicts with the results of Theorem 2.1, which states, that the fractional-order integral is zero at  $\tau = 0$  as  $x(\cdot) \in \mathcal{C}^0([0, \infty))$ . The error occurs as the right time shift law has an additional term [7, p. 776] and we have

$$\left[ \mathcal{I}^{1-\alpha} x(\tau) \right]_{\tau=0} = \mathcal{L}^{-1} \left\{ \left( \frac{1}{s^{1-\alpha}} \left( \frac{1}{s^{\alpha+1}} - \frac{e^{-t_0 s}}{s^{\alpha+1}} \right) - \int_0^{t_1} x(\tau) e^{-s\tau} d\tau \right) e^{t_1} \right\} \Bigg|_{\tau=0} = 0$$

and the solution to (2.75) is actually  $x(\tau) = 0$ .

With the initial conditions from [85] this result is a decaying pseudo polynomial of an exponent  $\alpha - 1$ . We should also note that the state  $x(t)$  is unbounded at the new initial time  $\tau = 0$ .

Now we want to apply Caputo's operator to solve the same integration problem using the shifted time scale for  $\tau \geq 0$ .

$${}_0^C\mathcal{D}_\tau^\alpha \tilde{x}(\tau) = 0. \quad (2.78)$$

Again, we apply the Laplace transform to solve for  $\tilde{x}(\tau)$

$$s^\alpha \tilde{X}(s) - s^{\alpha-1} \tilde{x}(0) = 0 \quad (2.79)$$

$$\tilde{x}(\tau) = \mathcal{L}^{-1} \left\{ \frac{s^{\alpha-1}}{s^\alpha} \right\} \tilde{x}(0) = \mathcal{L}^{-1} \left\{ \frac{1}{s} \right\} \tilde{x}(0). \quad (2.80)$$

In contrast to Riemann's operator, we have to use the initial function value here to set the initial conditions

$$\tilde{x}(0) = \frac{(\tau + t_1)^\alpha}{\Gamma(\alpha + 1)} \sigma(\tau + t_1) - \frac{(\tau + t_1 - t_0)^\alpha}{\Gamma(\alpha + 1)} \sigma(\tau + t_1 - t_0) \Bigg|_{\tau=0} = \frac{t_1^\alpha - (t_1 - t_0)^\alpha}{\Gamma(\alpha + 1)}. \quad (2.81)$$

Hence, the time response of the system (2.78) is a scaled Heaviside function

$$\tilde{x}(t) = \frac{t_1^\alpha - (t_1 - t_0)^\alpha}{\Gamma(\alpha + 1)} \sigma(\tau), \quad \tau \geq 0. \quad (2.82)$$

To sum up the results, we see that both operators are unable to reproduce the original time response of the system (2.74). Therefore, we have to extend the definitions of the fractional-order operators to describe physical systems with a non-negligible history.

The discussion of how to incorporate the history of the function before  $t = t_0$  is still a field of research. A first approach is proposed in [51, 26]. The basic idea is to compute the difference between an operator starting in the past at  $t = c$  and another one with the lower limit at  $t = t_0$ .

**Definition 2.5** (Generalized Fractional Integral, [51]). Let  $\alpha > 0$ . The operator

$${}_t \mathcal{I}_t^\alpha f(t) = {}_t \mathcal{I}_t^\alpha f(t) + \Psi(\alpha, f(\cdot), t_0, c, t) \quad (2.83)$$

with  $t \geq t_0 \geq c$  acting on the function  $f(\cdot) \in \mathcal{L}_1([c, b])$  with  $f(t) = 0$  for  $t \leq c$  is called generalized fractional-order integral.

The initialization function  $\Psi(\alpha, f(\cdot), t_0, c, t)$  can be computed by splitting and comparing the fractional-order integral with the lower limit  $c$  with the fractional-order integral starting at  $t_0$

$$\begin{aligned} \Psi(\alpha, f(\cdot), t_0, c, t) &= {}_c \mathcal{I}_t^\alpha f(t) - {}_{t_0} \mathcal{I}_t^\alpha f(t) \\ &= \frac{1}{\Gamma(\alpha)} \int_c^t (t - \tau)^{\alpha-1} f(\tau) d\tau - \frac{1}{\Gamma(\alpha)} \int_{t_0}^t (t - \tau)^{\alpha-1} f(\tau) d\tau \\ &= \frac{1}{\Gamma(\alpha)} \int_c^{t_0} (t - \tau)^{\alpha-1} f(\tau) d\tau = {}_c \mathcal{I}_{t_0}^\alpha f(t) \end{aligned} \quad (2.84)$$

For  $\alpha = 1$  we have

$$\Psi(1, f(\cdot), t_0, c, t) = \int_c^{t_0} f(\tau) d\tau = a_0, \quad (2.85)$$

representing the constant initial conditions  $a_0$ , which do not depend on future time instants  $t > t_0$ . In the integer-order case  $\alpha \in \mathbb{N}$ , this initialization function is reduced to Cauchy's  $n$ -folded integral within the initialization limits  $c$  and  $t_0$  such that

$$\Psi(n, f(\cdot), t_0, c, t) = \sum_{k=0}^n a_k t^k. \quad (2.86)$$

Although this integral is defined within the limits  $[c, t_0]$ , the initialization function is still influencing the dynamics for  $t > t_0$  and non-integer  $\alpha$ . This is caused by the convolution kernel  $Y_\alpha(t)$  which does not vanish for  $t \geq t_0$ . To further clarify this, we define the function

$$\bar{f}(t) = \begin{cases} f(t), & t \in [c, t_0) \\ 0, & t \geq t_0. \end{cases} \quad (2.87)$$

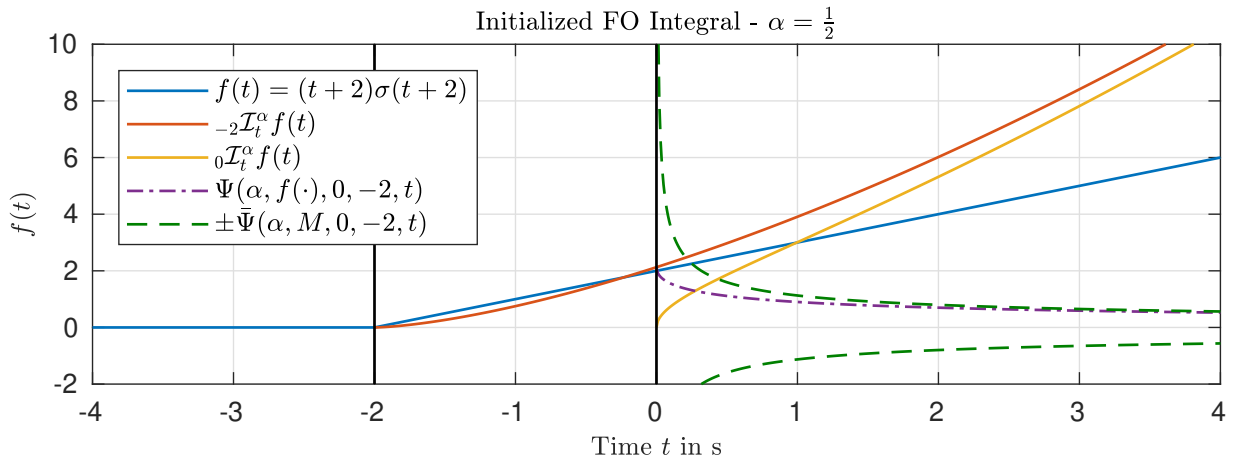


Figure 2.7: Comparison of the fractional-order integral starting at different initial conditions (see [51]). In the case  $\alpha \in (0, 1)$ , the initialization function  $\Psi(\cdot)$  decays to zero.

This allows us to change the upper limit in (2.84) to  $t$  and we have

$${}_c\mathcal{I}_{t_0}^\alpha f(t) = \frac{1}{\Gamma(\alpha)} \int_c^{t_0} (t-\tau)^{\alpha-1} f(\tau) d\tau = \frac{1}{\Gamma(\alpha)} \int_c^t (t-\tau)^{\alpha-1} \bar{f}(\tau) d\tau = {}_c\mathcal{I}_t^\alpha \bar{f}(t). \quad (2.88)$$

We set  $t_0 = 0$  without loss of generality. Assuming the function  $f(t)$  is bounded by  $M$  such that  $|f(t)| \leq M$  in the interval  $t \in [c, 0)$ , we see that this initialization function decays for  $t > 0$  if  $\alpha < 1$

$$|\Psi(\alpha, f(\cdot), 0, c, t)| \leq \frac{M}{\Gamma(\alpha)} \int_c^0 (t-\tau)^{\alpha-1} d\tau = - \frac{M(t-\tau)^\alpha}{\Gamma(\alpha+1)} \Big|_{\tau=c}^{\tau=0} = \frac{M((t-c)^\alpha - t^\alpha)}{\Gamma(\alpha+1)}. \quad (2.89)$$

Applying the generalized binomial formula [7, p. 1066] with  $\tilde{c} = -c$  yields

$$|\Psi(\alpha, f(\cdot), 0, c, t)| \leq \frac{M}{\Gamma(\alpha+1)} \left( \sum_{k=0}^{\infty} \binom{\alpha}{k} t^{\alpha-k} \tilde{c}^k - t^\alpha \right) = \frac{M}{\Gamma(\alpha+1)} \left( \sum_{k=1}^{\infty} \binom{\alpha}{k} t^{\alpha-k} \tilde{c}^k \right) \leq \frac{M\tilde{c}}{\Gamma(\alpha)} t^{\alpha-1}. \quad (2.90)$$

This is illustrated in Figure 2.7 for the semi-integral ( $\alpha = \frac{1}{2}$ ).

Proceeding with the ideas presented in [51], we can extend this technique to the fractional-order derivative operators.

**Definition 2.6** (Generalized Fractional Caputo Derivative [52]). *Let  $\alpha > 0$ . The operator*

$${}^C_t\mathcal{D}_t^\alpha f(t) = {}^C_{t_0}\mathcal{D}_t^\alpha f(t) + {}^C\Psi(f(\cdot), \alpha, t_0, c, t) = {}^C_c\mathcal{D}_t^\alpha f(t) \quad (2.91)$$

with  $c \leq t_0 \leq t \leq t_f$  acting on the function  $f(\cdot) \in \mathcal{L}_{\text{loc}}^1([c, t_f])$  with  $f(t) = 0$  for  $t \leq c$  is called generalized fractional-order Caputo derivative.

**Definition 2.7** (Generalized Fractional Riemann-Liouville Derivative, [51]). Let  $\alpha > 0$ . The operator

$${}^R_{t_0}\mathcal{D}_t^\alpha f(t) = {}^R_{t_0}\mathcal{D}_t^\alpha f(t) + {}^R\Psi(\alpha, f(\cdot), t_0, c, t) = {}^R_c\mathcal{D}_t^\alpha f(t) \quad (2.92)$$

with  $c \leq t_0 \leq t \leq t_f$  acting on the function  $f(\cdot) \in \mathcal{L}_1([c, t_f])$  with  $f(t) = 0$  for  $t \leq c$  is called generalized fractional-order Riemann-Liouville derivative.

The corresponding initialization functions can be derived by splitting the integral from  $c$  to  $t$  at the time  $t_0$ . Hence, the initialization function corresponding to Caputo's operator is given by:

$$\begin{aligned} {}^C\Psi(\alpha, f(\cdot), t_0, a, t) &= {}_c\mathcal{D}_t^\alpha f(t) - {}_{t_0}\mathcal{D}_t^\alpha f(t) \\ &= \frac{1}{\Gamma(m-\alpha)} \left( \int_c^t \frac{f^{(m)}(\tau)}{(t-\tau)^{\alpha-m+1}} d\tau - \int_{t_0}^t \frac{f^{(m)}(\tau)}{(t-\tau)^{\alpha-m+1}} d\tau \right) \\ &= \frac{1}{\Gamma(m-\alpha)} \int_c^{t_0} \frac{f^{(m)}(\tau)}{(t-\tau)^{\alpha-m+1}} d\tau = {}_c\mathcal{D}_{t_0}^\alpha f(t). \end{aligned} \quad (2.93)$$

Similarly for Riemann's operator we have

$$\begin{aligned} {}^R\Psi(\alpha, f(\cdot), t_0, a, t) &= {}^R_c\mathcal{D}_t^\alpha f(t) - {}^R_{t_0}\mathcal{D}_t^\alpha f(t) \\ &= \frac{d^m}{dt^m} \frac{1}{\Gamma(m-\alpha)} \left( \int_c^t \frac{f(\tau)}{(t-\tau)^{\alpha-m+1}} d\tau - \int_{t_0}^t \frac{f(\tau)}{(t-\tau)^{\alpha-m+1}} d\tau \right) \\ &= \frac{1}{\Gamma(m-\alpha)} \frac{d^m}{dt^m} \int_c^{t_0} \frac{f(\tau)}{(t-\tau)^{\alpha-m+1}} d\tau = {}^R_c\mathcal{D}_{t_0}^\alpha f(t). \end{aligned} \quad (2.94)$$

In the literature [50] the term  ${}_{t_0}\mathcal{D}_t^\alpha f(t)$  is referred to as the uninitialized fractional-order derivative, because the initial conditions of this operator are set to zero. Therefore, it is usually written in minor letters  ${}_{t_0}d_t^\alpha f(t) = {}_{t_0}\mathcal{D}_t^\alpha f(t)$ , if  $f(0) = 0$ .

With this extension, we have two methods to initialize the fractional-order operators. On the one hand, we might set an arbitrary initialization at the time instant  $t = t_0$ , which is called "side initialization" [50]. On the other hand, we have the "terminal initialization", where it is assumed that the operator can only be initialized or charged by considering the non-zero past of the function [50]. This will be discussed in more detail in Section 3.4.1.

Note that with  ${}^R\Psi(\cdot) = \delta(t-t_0)\bar{f}(t_0)$  (where  $\delta(\cdot)$  represents the Dirac impulse) the memoryless initial conditions (side initialization) are reproduced for Riemann's operator. For Caputo's operator, the special initialization function  ${}^C\Psi(\cdot) = \frac{t-t_0}{\Gamma(1-\alpha)}f(t_0)$  restores the side initialization.

Assuming the boundedness of  $f^{(m)}(t)$  in the past time interval  $|f^{(m)}(t)| \leq M$  for  $t \in [c, t_0]$ , we can derive bounds for the initialization functions  ${}^C\Psi(\cdot)$  for  $t > t_0$  similar to the initialized

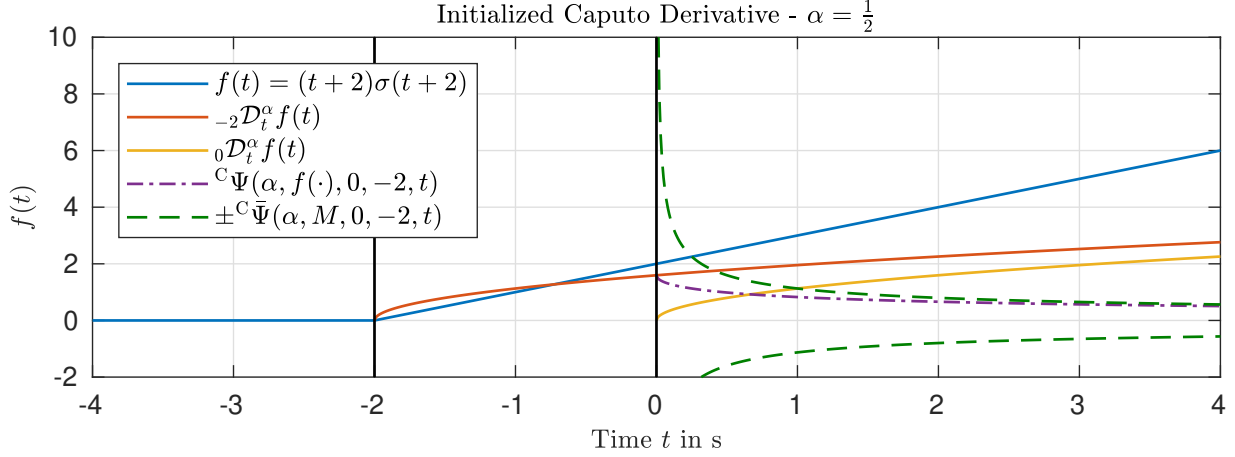


Figure 2.8: The initialization function corresponding to Caputo's operator only decays for  $\alpha \in (0, 1)$ . This is caused by the order of operations defining the operator, the fractional-order integral causes an increasing initialization function for  $\alpha > 1$ .

fractional-order integral. We set  $t_0 = 0$  without loss of generality and have  $\tilde{c} = -c$ . As  $m - \alpha \in (0, 1)$  we apply the generalized binomial formula [7, p. 1066]

$$\begin{aligned}
 \left| {}^C\Psi(\alpha, f(\cdot), 0, c, t) \right| &\leq \frac{1}{\Gamma(m - \alpha)} \int_c^0 \frac{M}{(t - \tau)^{\alpha - m + 1}} d\tau = - \frac{M(t - \tau)^{m - \alpha}}{\Gamma(m - \alpha + 1)} \Bigg|_{\tau=c}^{\tau=0} \\
 &= \frac{M}{\Gamma(m - \alpha + 1)} \left( (t - c)^{m - \alpha} - t^{m - \alpha} \right) \\
 &= \frac{M}{\Gamma(m - \alpha + 1)} \left( \sum_{k=0}^{\infty} \binom{m - \alpha}{k} t^{m - \alpha - k} \tilde{c}^k - t^{m - \alpha} \right) \\
 &= \frac{M}{\Gamma(m - \alpha + 1)} \left( t^{m - \alpha} + \sum_{k=1}^{\infty} \binom{m - \alpha}{k} t^{m - \alpha - k} \tilde{c}^k - t^{m - \alpha} \right) \\
 &\leq \frac{M\tilde{c}}{\Gamma(m - \alpha)} t^{m - \alpha - 1}.
 \end{aligned} \tag{2.95}$$

We find that the initialization always decays as  $m - \alpha = [\alpha] - \alpha < 1$  as illustrated in Figure 2.8.

The bounds limiting the initialization function of the Riemann-Operator are calculated in a similar way with the assumption that  $f(t)$  is bounded in the initialization interval  $|f(t)| \leq M$  for  $t \in [c, 0]$ . However, as the derivative does not conserve the sign, slight adjustments are made

$$\begin{aligned}
 \left| {}^R\Psi(\alpha, f(\cdot), t_0, c, t) \right| &\leq \left| \frac{1}{\Gamma(m - \alpha)} \frac{d^m}{dt^m} \int_c^0 \frac{M}{(t - \tau)^{\alpha - m + 1}} d\tau \right| = \left| \frac{d^m}{dt^m} \left[ - \frac{M(t - \tau)^{m - \alpha}}{\Gamma(m - \alpha + 1)} \Bigg|_{\tau=c}^{\tau=t_0} \right] \right| \\
 &= \left| \frac{M}{\Gamma(1 - \alpha)} \left( (t - c)^{-\alpha} - t^{-\alpha} \right) \right| = \frac{M}{\Gamma(1 - \alpha)} \left( t^{-\alpha} - (t - c)^{-\alpha} \right) \\
 &\leq \frac{M\tilde{c}\alpha}{\Gamma(1 - \alpha)} t^{-\alpha - 1}.
 \end{aligned}$$

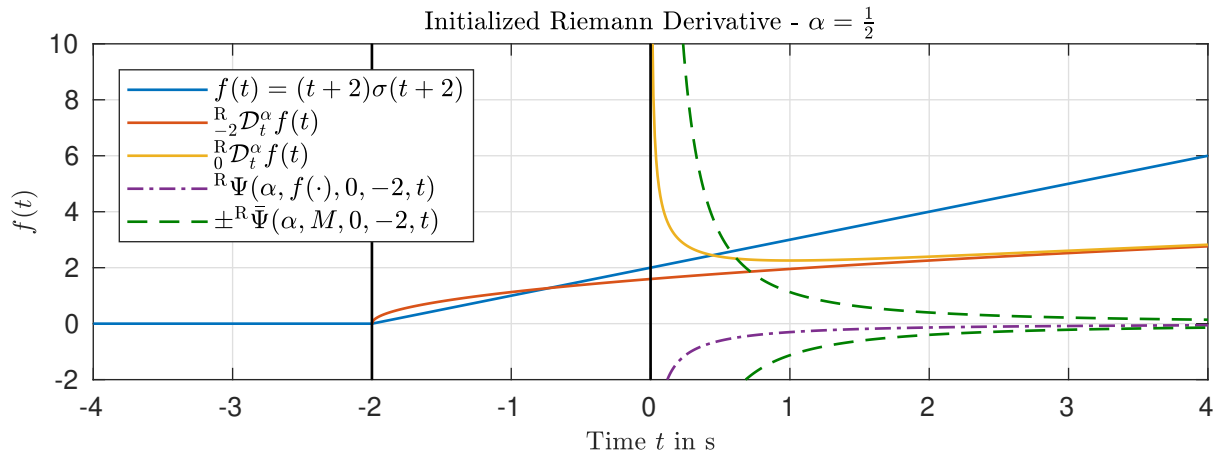


Figure 2.9: Initialization function and its bounds for the Riemann-Liouville derivative.

Compared to Caputo's approach, the initialization function always decays. The decay is algebraic and of higher order  $t^{-1-\alpha}$  compared to the previous cases where the initialization function decays with  $t^{-\alpha}$ . This is illustrated in Figure 2.9.

**Distributed-State Representation** Another approach to specify an arbitrary memory is given in [95]. This approach is motivated by the frequency domain approximation of the fractional-order operator. The frequency distributed model makes use of an improper integral [7, p. 1108] and the fractional-order integral can be derived by considering ordinary first-order differential equation

$$\dot{z}(t, w) = -wz(t, w) + f(t) \quad (2.96)$$

with

$$\mu_\alpha(w) = \frac{\sin(\alpha\pi)}{\pi} w^{-\alpha}. \quad (2.97)$$

Finally, the fractional-order integral is given by:

$${}_0\mathcal{I}_t^\alpha f(t) = \int_0^\infty \mu_\alpha(w) z(t, w) dw \quad (2.98)$$

The proof uses the solution of (2.96) and the improper integral given in [7, p. 1108].

This definition can easily be extended to Caputo's operator by changing the input of the distributed state ordinary differential equation (2.96) from  $f(t)$  to  $\dot{f}(t)$  or higher derivatives of  $f(t)$ .

This representation has some advantages:

- With this reformulation we can simulate fractional-order systems with an arbitrary past as illustrated in [28].
- Due to the connection to integer-order systems it allows the construction of Lyapunov-functions without the need to take time-varying terms into account [29].



## 2.6 Numerical Implementation of Fractional-Order Operators

The purpose of this section is to illustrate the effort which is needed to implement fractional-order operators, especially in real-time systems. The techniques to be presented are the most applied within the field of control theory. However, we do not aim for completeness here.

As all fractional-order operators depend on the complete history of the function  $f(t)$ , the implementation requires a lot of physical memory, as the past function values need to be stored. However, this memory fades out over time, i.e., function values far from the actual time instant  $t$  have less influence on the fractional-order derivative than the more recent past of the function. Therefore, we can introduce a fixed horizon  $L$  which defines the past we are taking into account. The error  $e(t) = {}^*_{t-L}\mathcal{D}_t^\alpha f(t) - {}^*_{t_0}\mathcal{D}_t^\alpha f(t)$  is bounded if the function is bounded  $|f(t)| \leq M$  in the relevant time interval  $t \in [t_0, t_f]$  [74, p. 203].

$$|e(t)| = \left| {}^*_{t-L}\mathcal{D}_t^\alpha f(t) - {}^*_{t_0}\mathcal{D}_t^\alpha f(t) \right| \leq \frac{ML^{-\alpha}}{|\gamma(1-\alpha)|}, \quad t_0 + L \leq t \leq t_f. \quad (2.99)$$

This first approximation of the fractional-order operators is called the *short-memory-principle* [74, p. 203]. and we can use this formula to compute the required memory length  $L$  to achieve a predefined accuracy.

### 2.6.1 Discretization of Grünwald-Letnikov's Operator

We can also illustrate this principle by discretizing the operator defined by Grünwald-Letnikov with a finite sampling time  $T_s$  such that:

$${}_0\mathcal{D}_t^\alpha f(kT_s) \approx \frac{1}{T_s^\alpha} \sum_{k=0}^N w_k^{(\alpha)} f(t - kT_s) =: {}_0\tilde{\mathcal{D}}_t^\alpha f(t) \quad \text{with} \quad N = \min\left(k, \frac{L}{T_s}\right) \quad (2.100)$$

and the recursive computation of the signed binomial coefficients  $w_k^{(\alpha)}$  given by

$$w_0^{(\alpha)} = 1 \quad \text{and} \quad w_k^{(\alpha)} = \left(1 - \frac{\alpha + 1}{k}\right) w_{k-1}^{(\alpha)}, \quad k = 1, 2, \dots \quad (2.101)$$

The plot of these coefficients  $w_k^{(\alpha)}$  is shown in Figure 2.10 and Figure 2.11. For  $\alpha = 1$  only, the past has no influence on the approximation. In contrast, for non-integer  $\alpha$  the coefficients only tend towards zero and therefore the complete history is required to compute the approximation of the fractional-order derivative.

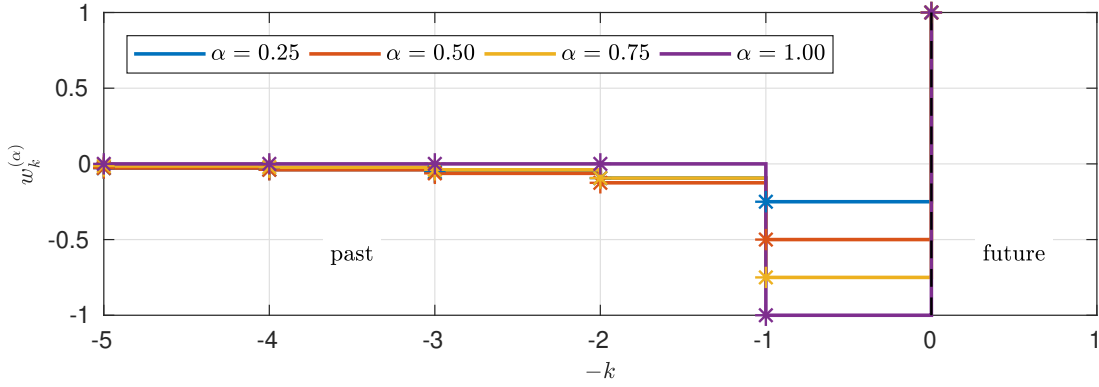


Figure 2.10: The coefficients of the discretized Grünwald-Letnikov operator represent the operator's memory. For  $\alpha > 0$  these weights decay relatively fast towards past time instants.

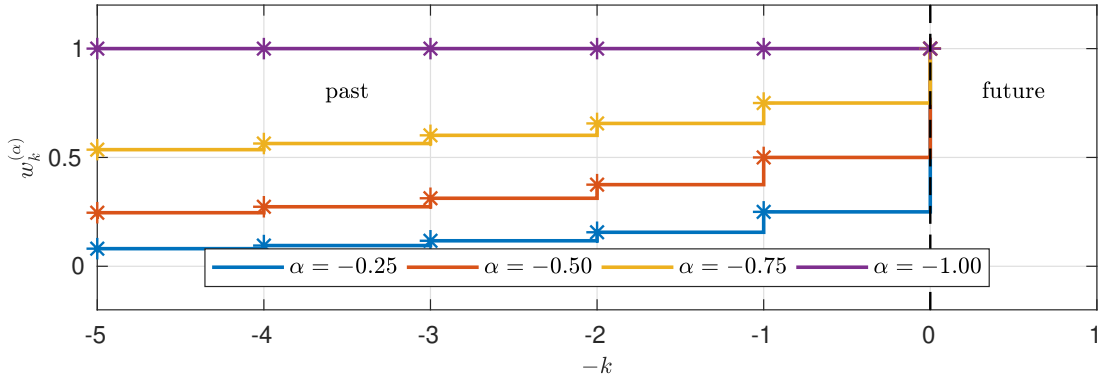


Figure 2.11: The coefficients of the discretized Grünwald-Letnikov operator represent the operator's memory. For  $\alpha < 0$  these weights decay slowly towards the past time instants compared to the differentiation case with  $\alpha > 0$ .

If we apply this technique directly to the fractional-order integration, i.e.  $\alpha < 0$  the weights  $w_k^{(\alpha)}$  decay slower towards zero (see Figure 2.11). For  $\alpha = 1$  we have a constant weight which leads to an upper sum approximating the integer-order integral. With this slow decay it is therefore advisable to separate the integer-order integrator first

$$\frac{1}{s^\alpha} = \frac{1}{s} s^{1-\alpha}. \quad (2.102)$$

Although we have to distinguish the cases  $\alpha > 0$  and  $\alpha < 0$ , the simplicity of this approximation in the discrete time framework is advantageous, as the fractional-order derivative is reduced to a multiplication of the offline computed weights  $w_k^{(\alpha)}$  with the stored past of the function. This allows for the evaluation of fractional-order operators without increasing the required physical memory – only the past of one function needs to be stored online.

A drawback of this implementation is a rather erroneous approximation of the fractional-order operators in the frequency domain. This is illustrated in Figure 2.12. It shows the theoretical and approximated frequency response of the semi-integrator.

In order to derive the frequency response of the approximated Grünwald-Letnikov operator, we introduce the linear discrete time system given by:

$$x(k+1) = \underbrace{\begin{pmatrix} 0 & 1 & \cdots & 0 \\ \vdots & \vdots & \ddots & \vdots \\ 0 & 0 & \cdots & 1 \\ 0 & 0 & 0 & 0 \end{pmatrix}}_{\tilde{A} \in \mathbb{R}^{(N-1) \times (N-1)}} x(k) + \underbrace{\begin{pmatrix} 0 \\ \vdots \\ 0 \\ 1 \end{pmatrix}}_{\tilde{B} \in \mathbb{R}^{(N-1) \times 1}} f(kT_s) \quad (2.103)$$

$${}_0\tilde{D}^\alpha f(kT_s) = y(k) = \underbrace{\begin{pmatrix} \frac{w_N^{(\alpha)}}{T_s^\alpha} & \frac{w_{N-1}^{(\alpha)}}{T_s^\alpha} & \cdots & \frac{w_1^{(\alpha)}}{T_s^\alpha} \end{pmatrix}}_{\tilde{C} \in \mathbb{R}^{1 \times (N-1)}} x(k) + \underbrace{\frac{w_0^{(\alpha)}}{T_s^\alpha}}_{\tilde{D} \in \mathbb{R}} f(kT_s). \quad (2.104)$$

The state  $x(k) \in \mathbb{R}^{N-1}$  is needed here, as it stores the past of the function  $f(kh)$ . The frequency response is given by the evaluation of the z-transform [96, p. 143]:

$$G_{\text{app}}(j\omega) = G_{\text{app}}(z) \Big|_{z=\exp(j\omega)} = \tilde{C} (zI - \tilde{A})^{-1} \tilde{B} + \tilde{D} \Big|_{z=\exp(j\omega)}. \quad (2.105)$$

The valid region within the frequency domain is clearly given by the memory length  $\tilde{\omega}_{\text{low}} = \frac{2\pi}{LT_s}$  on the one hand and the sampling frequency on the other hand  $\tilde{\omega}_{\text{high}} = \frac{\pi}{T_s}$ . As illustrated in Figure 2.12 we can see that the approximation can be improved with a longer memory in the lower frequency domain. Approaches to achieve this in a memory efficient way are presented in [53, 101].

### 2.6.2 Frequency Domain Approximation

The second approach is the direct approximation of the frequency response in a continuous time framework. We use an integer-order LTI system and set its poles and zeros relatively close to each other such that we can reproduce the slope of the amplitude response  $20\alpha$  dB/dec in a desired frequency range  $\omega \in (\omega_{\text{low}}, \omega_{\text{high}})$ . The best known approximations of this type are the Oustaloup filter [92] given by:

$$s^\alpha \approx H_\alpha(s) = \omega_{\text{high}}^\alpha \prod_{k=-N}^N \frac{s + \omega_k^-}{s + \omega_k^+}, \quad \omega_k^\pm = \omega_{\text{low}} \left( \frac{\omega_{\text{high}}}{\omega_{\text{low}}} \right)^{\frac{k + N + (1 \pm \alpha)/2}{2N + 1}} \quad (2.106)$$

and its modified version [60, p. 195]

$$s^\alpha \approx \tilde{H}_\alpha(s) = \left( \frac{d\omega_{\text{high}}}{b} \right)^\alpha \left( \frac{ds^2 + b\omega_{\text{high}}s}{d(1-\alpha)s^2 + b\omega_{\text{high}}s + d\alpha} \right) \prod_{k=-N}^N \frac{s + \omega_k^-}{s + \omega_k^+}, \quad (2.107)$$

with

$$\omega_k^\pm = \omega_{\text{low}} \left( \frac{\omega_{\text{high}}}{\omega_{\text{low}}} \right)^{\frac{2k-1 \pm \alpha}{N}}, \quad b = 10 \quad \text{and} \quad d = 9. \quad (2.108)$$

The capability to approximate the frequency response is demonstrated in Figure 2.13 for different orders of approximation. In contrast to the Grünwald-Letnikov approach, the lower frequency range can be approximated better with a lower order of approximation.

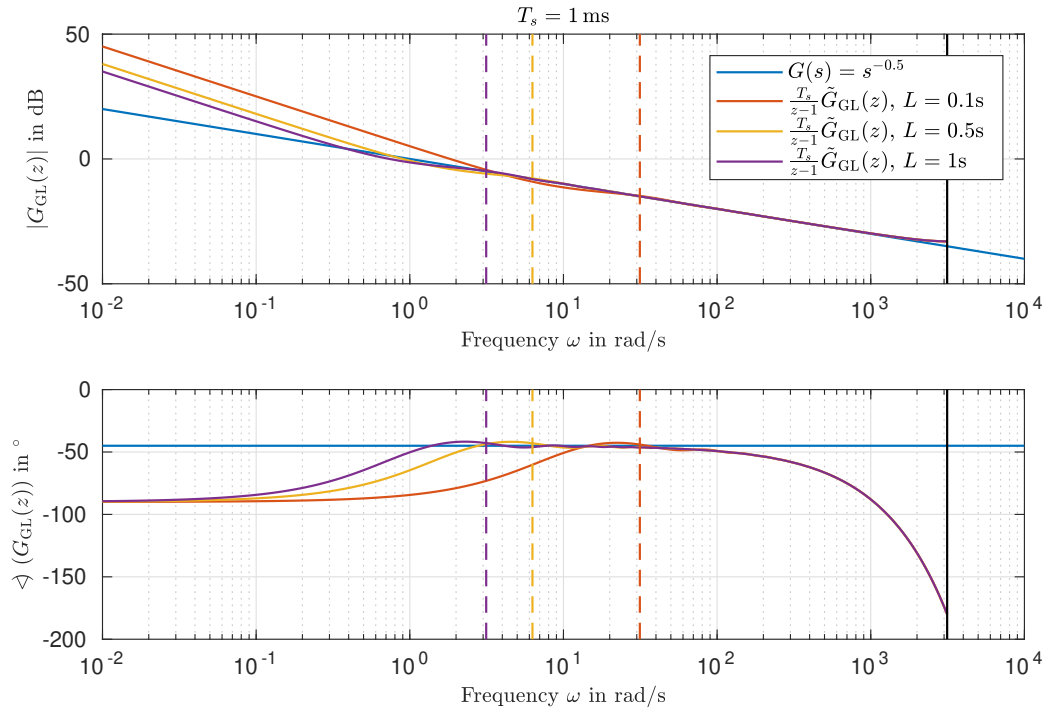


Figure 2.12: Frequency response of the discrete approximation of the Grünwald-Letnikov derivative for different memory lengths  $L$ .

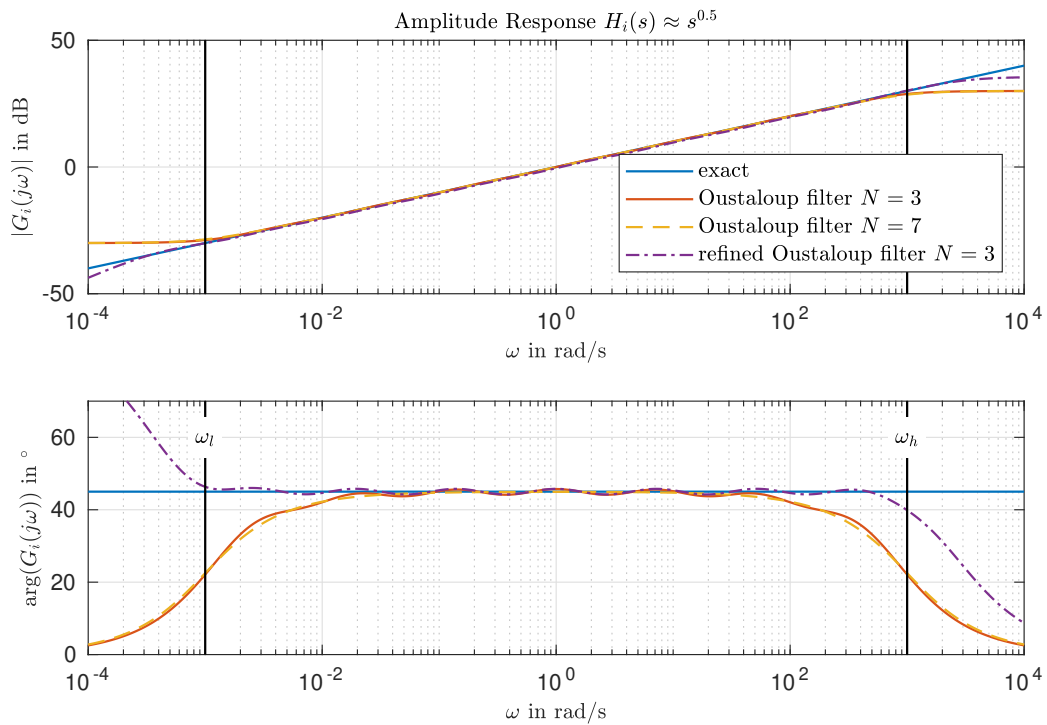


Figure 2.13: Oustaloup filters of different order to approximate the semi-derivative.

Note that the relative degree of all shown approximations is zero. This is one reason why a lot of controllers in the literature contain improper terms like  $s^\alpha$  with  $\alpha > 0$ , which still can be approximated in a causal way.

**Remark 2.2.** *Fractional-order integrators can be implemented by applying the split of Equation (2.102) together with the classical Oustaloup filter or by inverting the modified Oustaloup filter, i.e.  $s^{-\alpha} \approx \tilde{H}^{-1}(s)$ . Keeping the integrating behavior for the low frequency range is required to approximate the stationary gain of the fractional-order transfer function  $G(s)$  correctly [106].*



### 3 Fundamentals of Fractional-Order LTI Systems

Having established the fractional-order derivative operators, we can now study dynamical systems containing such derivatives. The usual form of such systems is given by fractional-order differential equations containing the fractional-order derivatives of the input  $u(t) \in \mathbb{R}$  and an output  $y(t) \in \mathbb{R}$ , i.e.

$$H(D^{\alpha_0}y(t), D^{\alpha_1}y(t), \dots, D^{\alpha_n}y(t)) = G(D^{\beta_0}u(t), D^{\beta_1}u(t), \dots, D^{\beta_m}u(t)) \quad (3.1)$$

with the possible non-linear functions  $H(\cdot) : \mathbb{R}^{n+1} \rightarrow \mathbb{R}$  and  $G(\cdot) : \mathbb{R}^{m+1} \rightarrow \mathbb{R}$  combining the fractional-order derivatives. This form is often motivated by physics, e.g. (3.1) could represent a sum of forces.

With linear combination functions  $\tilde{H}(\cdot)$  and  $\tilde{G}(\cdot)$  we have

$$\sum_{k=0}^n a_k \mathcal{D}^{\alpha_k} y(t) = \sum_{k=0}^m b_k \mathcal{D}^{\beta_k} u(t). \quad (3.2)$$

For integer-order systems a typical way of analysing such systems is either the frequency domain or the state-space representation. With fractional-order systems we have to take care here. First of all, we have to restrict the systems to have a commensurate order  $\gamma$ , such that  $\alpha_k = q_k \gamma$  and  $\beta_k = p_k \gamma$  with  $q_k, p_k \in \mathbb{N}$ . If the system is not commensurate, e.g.  $\alpha_1 = 2$  and  $\alpha_2 = \sqrt{\pi}$ , there is no state-space representation. Furthermore, we have to keep in mind that the semigroup property for fractional-order derivatives does only hold except for certain additional assumptions, therefore, it might also be difficult to derive the state-space representation if the system is of commensurate order.

#### 3.1 Fractional-Order State-Space LTI Systems with Classical Initial Conditions

The fractional-order linear time-invariant system applying Caputo's operator is given by

$$\Sigma_{\text{FO}} : \begin{cases} {}_{t_0} \mathcal{D}^{\alpha} x(t) = Ax(t) + Bu(t) & (3.3a) \\ y(t) = Cx(t) + Du(t), & (3.3b) \end{cases}$$

with the (pseudo) state  $x(t) \in \mathbb{R}^n$ , the input  $u(t) \in \mathbb{R}^p$ , the output  $y(t) \in \mathbb{R}^q$ , the order of differentiation  $\alpha \in (0, 1]$  and matrices of appropriate dimensions, namely the system matrix  $A \in \mathbb{R}^{n \times n}$ , the input matrix  $B \in \mathbb{R}^{n \times p}$ , the output matrix  $C \in \mathbb{R}^{q \times n}$  and the feedthrough matrix  $D \in \mathbb{R}^{q \times p}$ . Note that the variable  $x(t)$  is called pseudo state in the literature [84], as the complete history of the state is needed to predict its future evolution, in contrast to integer-order systems ( $\alpha = 1$ ) where the state  $x(t)$  contains the complete required information. As we use Caputo's operator here, the initial conditions are set to

$$x(t_0) = x_0. \quad (3.4)$$

We can also consider a wider range of the order of differentiation such that  $\alpha \in (0, 2)$ . However, for  $\alpha > 1$  we need additional initial conditions,  $\dot{x}(t_0)$  in this case. This is evident by considering the Laplace transform (2.70). If not further specified we set these additional initial conditions to zero  $\dot{x}(t_0) = 0$  such that the following solution still holds.

Note that we have to consider two system orders here. First we have the order of differentiation  $\alpha$  and second we have the number of states  $n$ . A generalized system order is given by their product:  $N = \alpha n$ .

The solution to this initial value problem defined by Equation (3.3a) and (3.4) is given by [60, p. 43]:

$$x(t) = \mathcal{E}_{\alpha,1}(A(t-t_0)^\alpha)x_0 + \int_{t_0}^t (t-\tau)^{\alpha-1} \mathcal{E}_{\alpha,\alpha}(A(t-\tau)^\alpha)u(\tau)d\tau \quad (3.5)$$

with the two-parameter matrix Mittag-Leffler function given by [74, p. 17]:

$$\mathcal{E}_{\alpha,\beta}(z) = \sum_{k=0}^{\infty} \frac{z^k}{\Gamma(\alpha k + \beta)}, \quad z \in \mathbb{C}. \quad (3.6)$$

This series representation converges for  $\alpha > 0$  and  $\beta > 0$ . However, it can be relaxed to complex values with  $\text{Re}\{\alpha\} > 0$  and  $\text{Re}\{\beta\} \in \mathbb{C}$  [20, p. 68]. In addition to that the derivative for some functions involving Mittag-Leffler functions can also include  $\beta = 0$  [74, p. 21].

Note that the Mittag Leffler-Function acts as a transition matrix here. However, it is only a pseudo transition, due to the memory of the operator itself.

*Proof.* We will prove equation (3.5) by applying the Laplace-transform to (3.3a) with respect to the time  $\tau = t - t_0$ :

$$\begin{aligned} s^\alpha X(s) - s^{\alpha-1}x(0) &= AX(s) + BU(s) & (3.7) \\ X(s) &= \underbrace{(s^\alpha I - A)^{-1}s^{\alpha-1}x(0)}_{\mathcal{L}\{\Phi_\alpha(t,t_0);s\}} + \underbrace{(s^\alpha I - A)^{-1}BU(s)}_{\mathcal{L}\{\tilde{\Phi}_\alpha(t,t_0);s\}} \end{aligned}$$

with the Laplace transforms of the state  $X(s) = \mathcal{L}\{x(t);s\}$  and input  $U(s) = \mathcal{L}\{u(t);s\}$ . The inverse Laplace transforms of  $\Phi_\alpha(t, 0)$  and  $\tilde{\Phi}_\alpha(t, 0)$  are given by [60, p. 391ff]

$$\mathcal{L}^{-1}\{(s^\alpha I - A)^{-1}s^{\alpha-1};s\} = \mathcal{E}_{\alpha,1}(A\tau^\alpha) = \mathcal{E}_{\alpha,1}(A(t-t_0)^\alpha) \quad (3.8)$$

$$\mathcal{L}^{-1}\{(s^\alpha I - A)^{-1};s\} = \tau^{\alpha-1}\mathcal{E}_{\alpha,\alpha}(A\tau^\alpha) = (t-t_0)^{\alpha-1}\mathcal{E}_{\alpha,\alpha}(A(t-t_0)^\alpha). \quad (3.9)$$

The Laplace transforms can be determined by performing the Laplace transform on each summand of the infinite sum defining the Mittag-Leffler function in (3.6) and using the geometric series.  $\square$

Note that compared to integer-order systems the transition matrix  $\Phi_\alpha(t, t_0)$  only acts on the initial state, while the input  $u(t)$  is convoluted with a slightly different transition  $\tilde{\Phi}_\alpha(t, t_0)$ . Only for  $\alpha = 1$  the integer-order formulas (see e.g. [81, p. 48ff]) are recovered

$$\mathcal{E}_{1,1}(A(t-t_0)^1) = (t-t_0)^0 \mathcal{E}_{1,1}(A(t-t_0)^1) = \exp(A(t-t_0)). \quad (3.10)$$



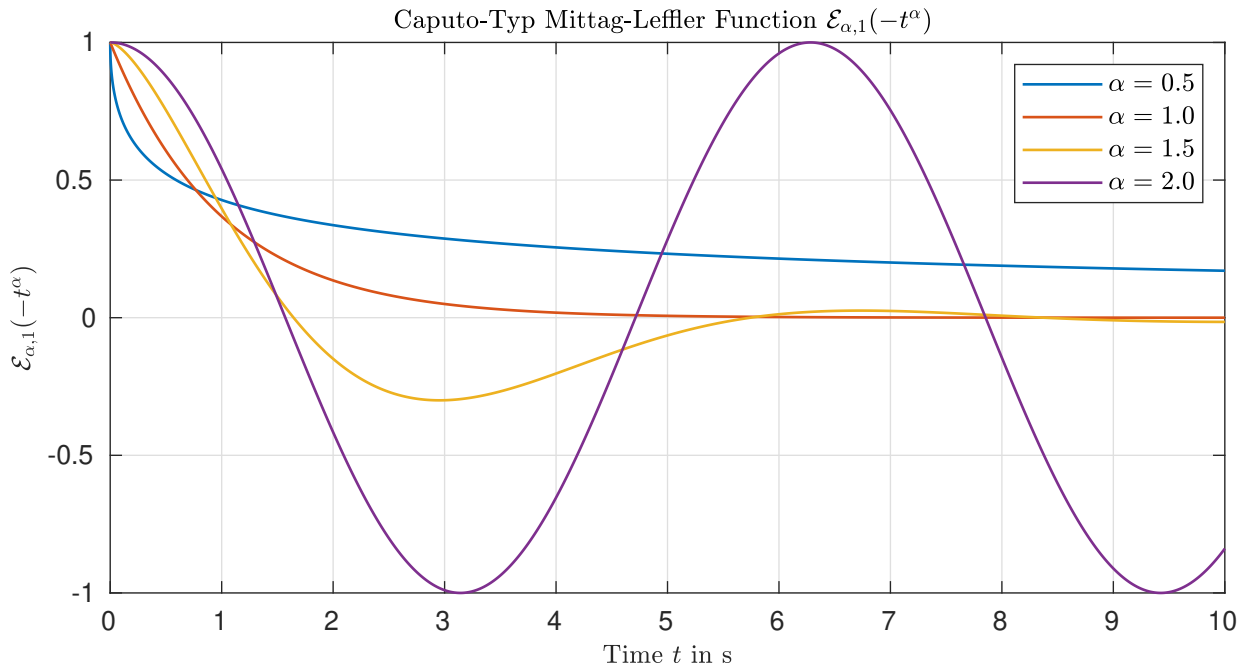


Figure 3.1: The scalar Mittag-Leffler functions show different decays depending on the order  $\alpha$ .

**Remark 3.1** (Fractional-order LTI system with Riemann-Liouville's Operator). *If Riemann's operator is applied to define the system dynamics*

$$\Sigma_{\text{FO-R}} : \begin{cases} {}^R\mathcal{D}_{t_0}^\alpha \bar{x}(t) = A\bar{x}(t) + Bu(t) & (3.11a) \\ y(t) = Cx(t) + Du(t), & (3.11b) \end{cases}$$

the initial conditions change to

$$\left[ {}^R\mathcal{D}_\tau^{\alpha-1} \bar{x}(\tau) \right]_{\tau=t_0} = \left[ \mathcal{I}_\tau^{1-\alpha} \bar{x}(\tau) \right]_{\tau=t_0} = \bar{x}_0. \quad (3.12)$$

The solution to the initial value problem changes to:

$$\begin{aligned} \bar{x}(t) &= (t-t_0)^{\alpha-1} \mathcal{E}_{\alpha,\alpha}(A(t-t_0)^\alpha) \bar{x}_0 + \int_{t_0}^t (t-\tau)^{\alpha-1} \mathcal{E}_{\alpha,\alpha}(A(t-\tau)^\alpha) u(\tau) d\tau & (3.13) \\ &= \tilde{\Phi}(t, t_0) \bar{x}_0 + \int_{t_0}^t \tilde{\Phi}(t, \tau) u(\tau) d\tau \end{aligned}$$

As shown for the previous case, this can be easily proven by applying the Laplace transform. We can see that the homogeneous solution shows a singularity at the initial time  $t = t_0$ .

### 3.1.1 Properties of the Mittag-Leffler Function

At this point it is interesting to look at the main properties of the scalar Mittag-Leffler function for different orders  $\alpha$  and compare it to its integer-order counterpart. Figure 3.1 shows the scalar Mittag-Leffler function for different values of  $\alpha$ . For orders smaller than one two main properties can be seen:

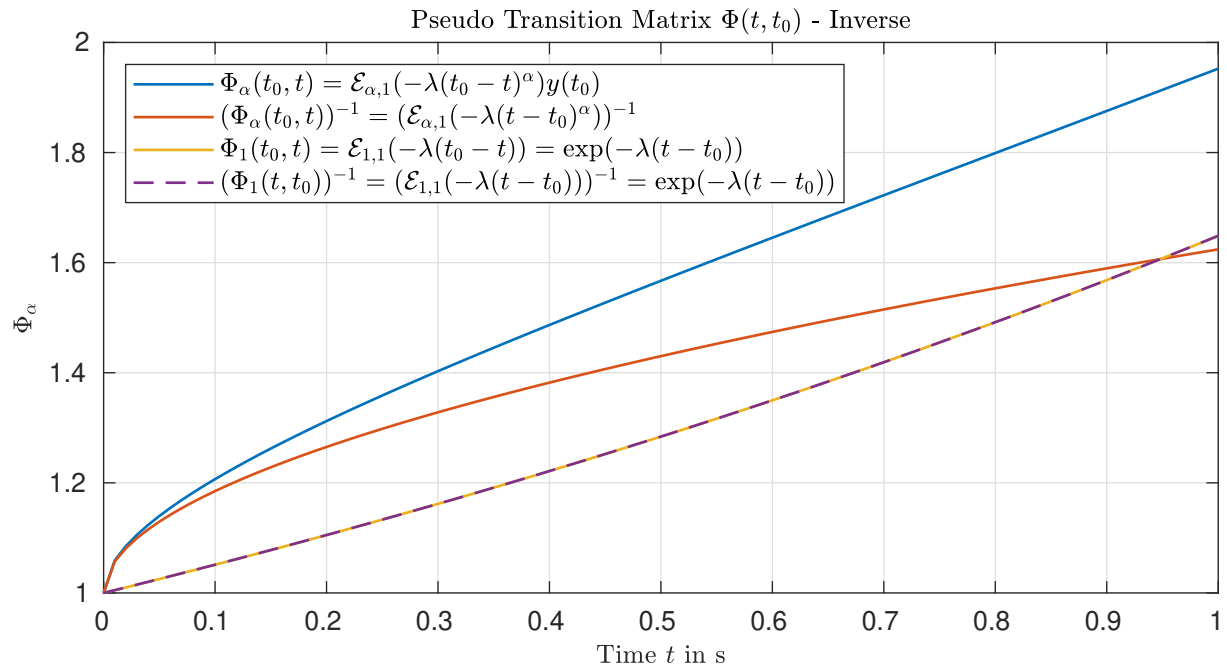


Figure 3.2: Inverses of different scalar pseudo-transitions  $\Phi_\alpha(t, t_0)$ . Only for  $\alpha = 1$  the inverse is given by swapping the time arguments.

1. The derivative of the Mittag-Leffler function at the initial time  $t = 0$  is unbounded:

$$\frac{d}{dt} (\mathcal{E}_{\alpha,1}(-\lambda t^\alpha)) = t^{-1} \sum_{k=1}^{\infty} \frac{\alpha k (-\lambda t^\alpha)^k}{\Gamma(\alpha k + 1)} = t^{-1} \mathcal{E}_{\alpha,0}(-\lambda t^\alpha). \quad (3.14)$$

2. For  $\alpha \in (0, 1)$  the Mittag-Leffler function decays algebraically [54]:

$$\mathcal{E}_{\alpha,1}(-\lambda t^\alpha) \sim \frac{\lambda t^{-\alpha}}{\Gamma(1 - \alpha)}, \quad \alpha \in (0, 1), \quad \text{for } t \rightarrow \infty. \quad (3.15)$$

In contrast to integer-order systems this pseudo transition matrix does not show the typical properties as listed in [81]: The inversion of the transition matrix is not given by the exchange of time arguments

$$\Phi_\alpha(t, t_0)^{-1} = (\mathcal{E}_{\alpha,1}(A(t - t_0)^\alpha))^{-1} \neq \mathcal{E}_{\alpha,1}(A(t_0 - t)^\alpha) = \Phi_\alpha(t_0, t), \quad (3.16)$$

as shown in Figure 3.2. Furthermore, the pseudo transition matrix does not satisfy the semi-group property

$$\Phi_\alpha(t, t_0) \neq \Phi_\alpha(t, \tau) \Phi_\alpha(\tau, t_0). \quad (3.17)$$

this is illustrated in Figure 3.3. In order to derive the correct evolution of the state from its state  $x(t_1)$  we have to take the history into account

$$\Phi_\alpha(t, t_1) = \Phi_\alpha(t, t_0) (\Phi_\alpha(t_1, t_0))^{-1} \quad (3.18)$$

such that we move backwards in time until we reach the initial state and after that we make use of the known transition starting at  $t_0$ .

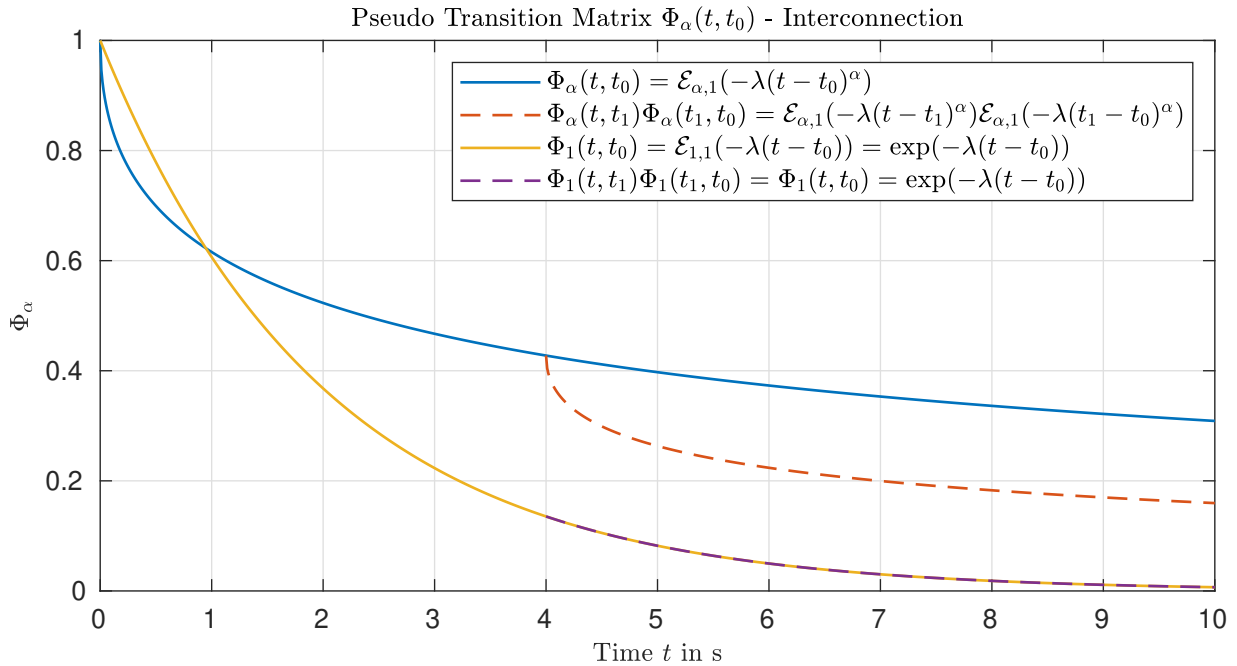


Figure 3.3: Due to the memory of the operator, the interconnection of two pseudo transitions leads to different results than a single transition to the final time  $t$ . The reason here is that the second transition is computed based on the memory-free initial-conditions at  $t = t_1$ .

The asymptotes of the scalar Mittag-Leffler function for  $t \rightarrow \infty$  are given in [74, p. 32ff] with respect to the argument of  $z$ .

**Lemma 3.1** ([74]). *Given an  $\alpha \in (0, 2)$ , an arbitrary real  $\beta \in \mathbb{R}$  and an arbitrary real  $\mu \in \mathbb{R}$  such that*

$$\alpha \frac{\pi}{2} < \mu < \min\{\pi, \alpha\pi\}, \quad (3.19)$$

*then for an arbitrary integer  $p \geq 1$  the following expansion holds:*

$$\mathcal{E}_{\alpha,\beta}(z) = - \sum_{k=1}^p \frac{z^{-k}}{\Gamma(\beta - \alpha k)} + O(|z|^{-1-p}), \quad |z| \rightarrow \infty, \quad \mu \leq |\arg(z)| \leq \pi. \quad (3.20)$$

**Lemma 3.2** ([74]). *Given an  $\alpha \in (0, 2)$ , an arbitrary real  $\beta \in \mathbb{R}$  and an arbitrary real  $\mu \in \mathbb{R}$  such that*

$$\alpha \frac{\pi}{2} < \mu < \min\{\pi, \alpha\pi\}, \quad (3.21)$$

*then for an arbitrary integer  $p \geq 1$  the following expansion holds:*

$$\mathcal{E}_{\alpha,\beta}(z) = \frac{1}{\alpha} z^{(1-\beta)/\alpha} \exp\left(z^{1/\alpha}\right) - \sum_{k=1}^p \frac{z^{-k}}{\Gamma(\beta - \alpha k)} + O(|z|^{-1-p}), \quad \begin{array}{l} |z| \rightarrow \infty, \\ |\arg(z)| \leq \mu \end{array}. \quad (3.22)$$

The possible location of  $z$  in the complex plane is different for each lemma. This is illustrated in Figure 3.4.

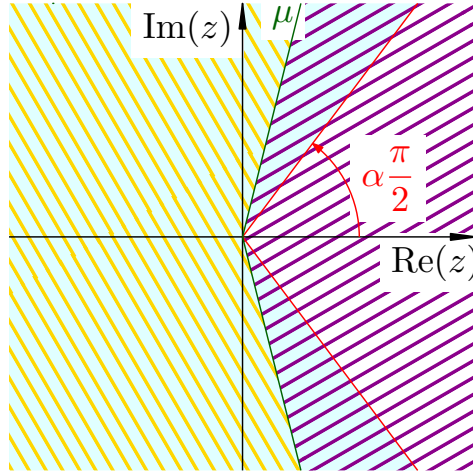


Figure 3.4: Illustration of the possible location of the argument  $z$  of the Mittag-Leffler function. Lemma 3.1 leads to the yellow colored sector and Lemma 3.2 is represented by the purple colored area. The angle defining  $\mu$  may vary according to  $\alpha \frac{\pi}{2} < \mu < \min\{\pi, \alpha\pi\}$ .

### 3.1.2 Comparison of Different Fractional-Order LTI Systems

**Example 3.1.** To illustrate the difference between both operators, as well as between fractional- and integer-order operators, we consider the three systems:

$$\dot{x}(t) = Ax + Bu, \quad x(0) = x_0 \quad (3.23)$$

$$\mathcal{D}^\alpha \tilde{x}(t) = A\tilde{x} + Bu, \quad \tilde{x}(0) = \tilde{x}_0 \quad (3.24)$$

$${}^R\mathcal{D}^\alpha \bar{x}(t) = A\bar{x} + Bu, \quad \left[ {}^R\mathcal{D}_\tau^{\alpha-1} \bar{x}(\tau) \right]_{\tau=0} = \left[ \mathcal{I}_\tau^{1-\alpha} \bar{x}(\tau) \right]_{\tau=0} = \bar{x}_0 \quad (3.25)$$

with the parameters

$$A = \begin{pmatrix} -2 & 1 \\ 0 & -2 \end{pmatrix}, \quad B = \begin{pmatrix} 2 \\ -1 \end{pmatrix}, \quad \alpha = \frac{1}{3}, \quad x_0 = \tilde{x}_0 = \bar{x}_0 = \begin{pmatrix} 2 \\ -2 \end{pmatrix} \quad (3.26)$$

As the matrix  $A$  is already in the Jordan canonical form, the homogeneous solutions are hence given by (see Section 3.2):

$$x(t) = \exp(At)x_0 = \begin{pmatrix} e^{-2t} & e^{-2t}t \\ 0 & e^{-2t} \end{pmatrix} x_0 \quad (3.27)$$

$$\tilde{x}(t) = \mathcal{E}_{\alpha,1}(At^\alpha) \tilde{x}_0 = \begin{pmatrix} \mathcal{E}_{\alpha,1}(-2t^\alpha) & \sum_{k=0}^{\infty} \frac{\lambda^{k-1} k t^{\alpha k}}{\Gamma(\alpha k + 1)} \\ 0 & \mathcal{E}_{\alpha,1}(-2t^\alpha) \end{pmatrix} \tilde{x}_0 \quad (3.28)$$

$$\bar{x}(t) = t^{\alpha-1} \mathcal{E}_{\alpha,\alpha}(At^\alpha) \bar{x}_0 = t^{\alpha-1} \begin{pmatrix} \mathcal{E}_{\alpha,\alpha}(-2t^\alpha) & \sum_{k=0}^{\infty} \frac{\lambda^{k-1} k t^{\alpha k}}{\Gamma(\alpha k + \alpha)} \\ 0 & \mathcal{E}_{\alpha,\alpha}(-2t^\alpha) \end{pmatrix} \bar{x}_0 \quad (3.29)$$

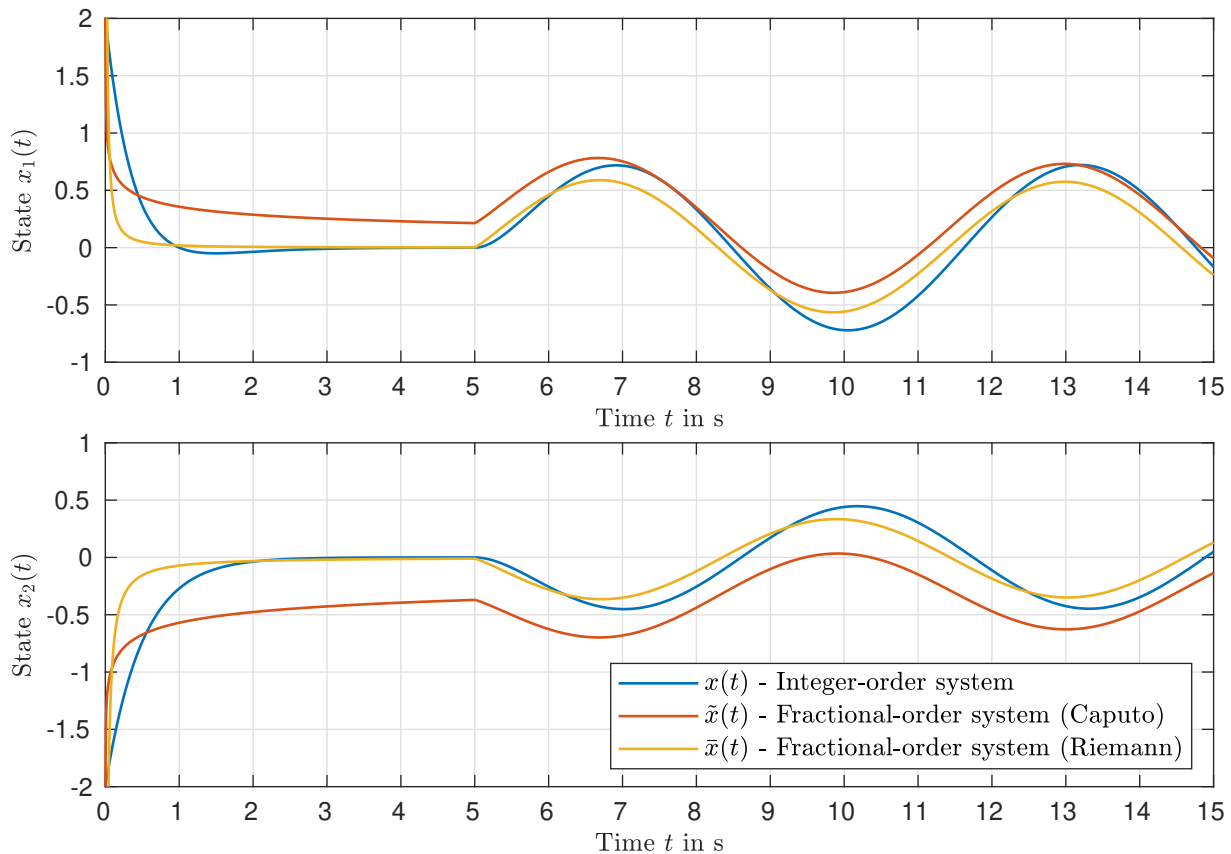


Figure 3.5: Comparison of an integer-order system with two fractional-order systems defined by different operators.

For the piecewise defined input

$$u(t) = \begin{cases} 0, & t \leq T = 2\text{ s} \\ \sin(t - T), & t > T \end{cases} \quad (3.30)$$

the state trajectories are depicted in Figure 3.5. First of all, we see that the state trajectories of the system (3.25) are unbounded at the time instant  $t_0$ . The second aspect to point out here is the convergence of all systems for larger times. The integer-order system converges exponentially, therefore, the effect of the initial conditions is barely visible after  $t = 5 \cdot \frac{2\pi}{\lambda} = 5\tau$ . In both fractional-order systems this is not the case. Here the convergence is algebraic and therefore the homogeneous part of the solution has still a huge influence on the state, even for large times  $t \gg 5\tau$ . Note that the system states defined by Riemann's operator converge faster compared to Caputo's operator.

## 3.2 Stability of Fractional-Order Systems

In this section we are recalling the major stability concepts and theorems of linear time invariant fractional-order system.

### 3.2.1 Concepts for Stability and Convergence Characterization

As shown in Example 3.1, the state trajectories of Riemann systems show a singularity at the initial time  $t_0$ . This is caused by the fractional-order initial conditions which might be bounded but do not belong to the state itself. For these reasons we have to define stability for Riemann systems differently than for integer-order systems. With the connection to Caputo's operator, however, it is possible to reformulate each fractional-order system defined with Caputo's operator as a time-varying Riemann-Liouville system.

First of all, let us discuss how to define the concept of equilibrium points and stability of nonlinear fractional-order systems applying Riemann's derivative. We consider the system:

$${}^R_{t_0}\mathcal{D}^\alpha x(t) = f(t, x), \quad {}^R_{t_0}\mathcal{D}^{\alpha-1}x(\tau)\Big|_{\tau=0} = \bar{x}_0. \quad (3.31)$$

As the Riemann derivative of a constant function does not vanish, the concept of equilibria is slightly different.

**Definition 3.1 (Equilibrium).** *The constant point  $x_e$  satisfying the equation*

$${}^R_{t_0}\mathcal{D}^\alpha x_e = f(t, x_e) \quad (3.32)$$

*is called equilibrium of system (3.31).*

We define the stability of the equilibrium  $x_e$  with the concepts presented in [3, p. 65].

**Definition 3.2 (Stability).** *The zero solution of the nonlinear Riemann system (3.31) given by*

$$x(t) = \frac{(t-t_0)^{\alpha-1}}{\Gamma(\alpha)}\bar{x}_0 + \frac{1}{\Gamma(\alpha)}\int_{t_0}^t (t-\tau)^{\alpha-1}f(\tau, x(\tau))d\tau \quad (3.33)$$

*respectively, the equilibrium point  $x_e = 0$  is*

- *stable if for each  $\epsilon > 0$ , there is  $\delta = \delta(\epsilon, t_0, t_\epsilon)$  such that*

$$\|\bar{x}(t_0)\| < \delta(\epsilon) \implies \|\bar{x}(t)\| < \epsilon, \quad \forall t \geq t_\epsilon \geq t_0, \quad (3.34)$$

- *asymptotically stable if in addition to being stable*

$$\|x(t)\| \xrightarrow{t \rightarrow \infty} 0, \quad (3.35)$$

- *and unstable if it is not stable.*

In this definition, we can move arbitrarily close to the initial time  $t_0$  to keep the state bounded. The zero solution (3.33) shows a singularity at the initial time due to the singular kernel of the fractional-order integral.

Note that this zero solution here only exists on the open interval  $t \in (t_0, \infty)$ .

For Caputo systems this singularity might be cancelled and if we restrict the stability analysis to systems with a unique solution on the semi open interval  $t \in [t_0, \infty)$ , we can apply a more common definition of stability (see [20, p. 157] and [40, p. 112]).

Compared to integer-order systems, we have to use slightly different approaches to further characterize the asymptotically stable case. For integer-order systems the trajectories are bounded by an exponential envelope.

**Definition 3.3** (Exponential Stability [40]). *The equilibrium point  $x = 0$  of the system (3.31) with  $\alpha = 1$  is exponentially stable if there exist constants  $c > 0$ ,  $b > 0$  and  $\lambda > 0$ , such that*

$$\|x(t)\| \leq b\|\bar{x}_0\| \exp(-\lambda(t - t_0)), \quad \forall \|\bar{x}_0\| < c, \quad \forall t \geq t_0. \quad (3.36)$$

If Equation (3.36) holds for any  $\bar{x}_0 \in \mathbb{R}^n$ , then the system is globally exponentially stable.

As the eigenfunctions for linear fractional-order systems contain terms like  $t^{-\alpha}$  with  $\alpha \in \mathbb{R}$  this concept is extended to the so called  $t^{-\alpha}$ -stability [86].

**Definition 3.4** ( $t^{-\bar{\alpha}}$ -Stability [65]). *The trajectory  $x(t)$  of the system  ${}^*D^\alpha x(t) = f(t, x)$  is  $t^{-\bar{\alpha}}$  asymptotically stable if the system is asymptotically stable and if there exists an  $\bar{\alpha} > 0$  such that:*

$$\forall \|x(t_0)\| \leq c, \quad \exists N(x(t_0)) \quad \text{such that} \quad \forall t > t_0 \quad \|x(t)\| \leq N(t - t_0)^{-\bar{\alpha}}. \quad (3.37)$$

Let us break down this definition. The definition states that we can find the order  $\bar{\alpha}$  of an envelope  $N(t - t_0)^{-\bar{\alpha}}$ , which is parametrized with an amplitude  $N$  and the initial time  $t_0$ . In [86] and [3] this definition looks slightly different, the initial state is replaced with by an initialization interval.

In contrast to integer-order systems the state  $x(t)$  is bounded by  $t^{-\bar{\alpha}}$ . Only for linear systems the order of differentiation  $\alpha$  and the chosen operator are directly connected to the decay rate  $\bar{\alpha}$ . Note that this bound is not limiting the initial singularity, which occurs if Riemann's operator is applied.

**Definition 3.5** (Mittag-Leffler-Stability [48]). *The solution of  ${}^*D^\alpha x(t) = f(t, x)$  with  $\bar{x}(0) = x_0$  is called Mittag-Leffler stable if*

$$\|x(t)\| \leq \left[ m(x_0) \mathcal{E}_{\alpha,1}(-\lambda t^\alpha) \right]^b$$

with  $\alpha \in (0, 1)$ ,  $\lambda > 0$ ,  $b > 0$ ,  $m(x) \geq 0$ ,  $m(0) = 0$  and  $m(x)$  locally Lipschitz on  $x \in \mathcal{B} \subset \mathbb{R}^n$  with the Lipschitz constant  $m_0$ , where  $\mathcal{B}$  is domain containing the origin.

Linear fractional-order systems are Mittag-Leffler stable, as the Lipschitz constant is given by  $\|A\|$  and we can apply the following theorem given in [47].

**Theorem 3.1.** *If  $x = 0$  is an equilibrium point of the system  ${}^C_{t_0}D^\alpha x(t) = f(t, x)$ ,  $f$  is Lipschitz with on  $x$  with the Lipschitz constant  $l$  and piecewise continuous with respect to  $t$ , then the solution  $x(t)$  satisfies*

$$\|x(t)\| \leq \|x(t_0)\| \mathcal{E}_{\alpha,1}(l(t - t_0)^\alpha) \quad (3.38)$$

with  $\alpha \in (0, 1)$ .

**Lyapunov Theory for Fractional-Order Systems** The stability theory based on Lyapunov functions has also been expanded to access the stability of fractional-order systems.

**Theorem 3.2** (Lyapunov's Direct Method [47]). *Let  $x = 0$  be an equilibrium point of  ${}_{t_0}^* \mathcal{D}^\alpha x(t) = f(t, x)$  and  $\mathbb{D} \subset \mathbb{R}^n$  be a domain containing the origin. Let the function  $V(t, x(t)) : [0, \infty) \times \mathbb{D} \rightarrow \mathbb{R}$  be a continuously differentiable function wrt.  $t$  and locally Lipschitz with respect to  $x$  such that*

$$\gamma_1 \|x(\cdot)\|^a \leq V(t, x(\cdot)) \leq \gamma_2 \|x(\cdot)\|^{ab}, \quad (3.39)$$

$${}_{t_0}^C \mathcal{D}^\alpha V(t, x(\cdot)) \leq -\gamma_3 \|x(\cdot)\|^{ab}, \quad (3.40)$$

with  $t \geq t_0$ ,  $x \in \mathbb{D}$ ,  $\alpha \in (0, 1)$ ,  $a > 0$ ,  $b > 0$  and  $\gamma_i > 0$ ,  $i = 1, 2, 3$ . Then  $x = 0$  is locally Mittag-Leffler stable on  $\mathbb{D}$ .

Note that this theorem holds for Riemann or Caputo systems. If all assumptions are satisfied in  $\mathbb{R}^n$ , then the equilibrium  $x = 0$  is globally Mittag-Leffler stable. The proof is given in [47] as well as a different version of this theorem which can be used to test only for asymptotic stability. An extension including comparison functions can be found in [48].

Compared to integer-order systems the application of this theorems is more difficult. Even for simple quadratic approaches the fractional-order derivative has to be evaluated using the Leibniz' rule (2.53), which leads to an infinite sum representation.

### 3.2.2 Stability of Linear Fractional-Order Systems

Let us now consider linear systems defined by Equation (3.3) using Caputo's operator. The best known stability theorem for these systems was introduced by Matignon in [55].

**Theorem 3.3** (Stability Conditions - Linear Systems [55]). *The system  $\mathcal{D}^\alpha x(t) = Ax(t)$  with the initial state  $x(0) = x_0 \in \mathbb{R}^n$ ,  $\text{rank}(A) = n$  and the order of differentiation  $\alpha \in (0, 1)$  is*

- asymptotically stable if and only if all eigenvalues  $\lambda_i$  of  $A$  satisfy

$$|\arg(\lambda_i)| > \alpha \frac{\pi}{2}, \quad i = 1, 2, \dots, n. \quad (3.41)$$

In this case the system is  $t^{-\alpha}$  stable.

- stable if and only if either it is asymptotically stable or the critical eigenvalues  $\lambda_i$  with  $|\arg(\lambda_i)| = \alpha \frac{\pi}{2}$  have the same algebraic and geometric multiplicity and for the others (3.41) holds.

Note that this theorem does not cover the most relevant case of a fractional-order integrator contained in the system dynamics, i.e.  $\text{rank}(A) < n$ , because the argument of zero in the complex plane cannot be defined.

An extension is to include the multiple eigenvalues at zero, such that an arbitrary real matrix  $A \in \mathbb{R}^{n \times n}$  is introduced in [77] for the Riemann-Liouville operator which is then modified to the case of Caputo's operator.

**Theorem 3.4** (Stability Conditions - Linear Systems). *The system  $\mathcal{D}^\alpha x(t) = Ax(t)$  with the initial state  $x(0) = x_0 \in \mathbb{R}^n$  and the order of differentiation  $\alpha \in (0, 1)$  is*



- asymptotically stable if and only if all eigenvalues  $\lambda_i$  of  $A$  satisfy

$$|\arg(\lambda_i)| > \alpha \frac{\pi}{2}, \quad i = 1, 2, \dots, n. \quad (3.42)$$

In this case the system is  $t^{-\alpha}$  stable.

- stable if and only if either it is asymptotically stable or all non-zero eigenvalues  $\lambda_i$  with  $|\arg(\lambda_i)| = \alpha \frac{\pi}{2}$  as well as all the critical eigenvalues with  $\lambda_i = 0$  have the same algebraic and geometric multiplicity and for the others (3.41) holds.

*Proof.* In order to proof this theorem in detail we use the Jordan canonical decomposition of the matrix  $A$  and apply Lemma 3.4. We follow the ideas presented in [77] for the linear Riemann system. Let us first consider the trivial case with a diagonalizable matrix  $A$ . Due to the definition of the matrix Mittag-Leffer function we have

$$\mathcal{E}_{\alpha,1}(At^\alpha) = T \mathcal{E}_{\alpha,1}(At^\alpha) T^{-1} = T \operatorname{diag}(\mathcal{E}_{\alpha,1}(\lambda_1 t^\alpha), \mathcal{E}_{\alpha,1}(\lambda_2 t^\alpha), \dots, \mathcal{E}_{\alpha,1}(\lambda_n t^\alpha)) T^{-1}. \quad (3.43)$$

In the case  $|\arg(\lambda_i)| > \alpha\pi/2$  we apply Lemma 3.1 and hence have for each eigenvalue

$$\|\mathcal{E}_{\alpha,1}(\lambda_i t^\alpha)\|_{t \rightarrow \infty} = \left\| -\sum_{k=1}^p \frac{(\lambda_i t^\alpha)^{-k}}{\Gamma(1-\alpha k)} + O(|\lambda_i t^\alpha|^{-1-p}) \right\|_{t \rightarrow \infty} = 0 \quad (3.44)$$

with  $p \in \mathbb{N}$  and  $p \geq 1$ . Here we also see, that the linear asymptotically stable fractional-order system decays with  $t^{-\alpha}$ . Therefore it is  $t^{-\alpha}$  stable.

If the eigenvalues are on the edge of the stability region, i.e.  $|\arg(\lambda_i)| = \alpha \frac{\pi}{2} = \varphi_i$ , we can also apply Lemma 3.2. With  $\lambda_i = r_i \exp(\varphi_i)$ , this yields

$$\begin{aligned} \|\mathcal{E}_{\alpha,1}(\lambda_i t^\alpha)\|_{t \rightarrow \infty} &= \left\| \frac{1}{\alpha} \exp\left(\left(r_i e^{\varphi_i j} t^\alpha\right)^{1/\alpha}\right) - \sum_{k=1}^p \frac{(\lambda_i t^\alpha)^{-k}}{\Gamma(1-\alpha k)} + O(|\lambda_i t^\alpha|^{-1-p}) \right\|_{t \rightarrow \infty} \\ &= \left\| \frac{1}{\alpha} \exp\left(r_i^{1/\alpha} t \exp\left(\frac{\pi}{2} j\right)\right) - \sum_{k=1}^p \frac{(\lambda_i t^\alpha)^{-k}}{\Gamma(1-\alpha k)} + O(|\lambda_i t^\alpha|^{-1-p}) \right\|_{t \rightarrow \infty} \\ &= \left\| \frac{1}{\alpha} \exp\left(r_i^{1/\alpha} t j\right) - \sum_{k=1}^p \frac{(\lambda_i t^\alpha)^{-k}}{\Gamma(1-\alpha k)} + O(|\lambda_i t^\alpha|^{-1-p}) \right\|_{t \rightarrow \infty} < \frac{1}{\alpha}. \end{aligned} \quad (3.45)$$

The Mittag-Leffler function hence tends to a bounded oscillation with the frequency  $\sqrt[\alpha]{r_i}$  and the amplitude  $\alpha^{-1}$  for  $t \rightarrow \infty$ .

In the unstable case with at least one eigenvalue  $\lambda_i = r_i \exp(j\varphi_i)$  with  $|\varphi| < \alpha \frac{\pi}{2}$ , we also apply Lemma 3.2 with  $p \in \mathbb{N}$  and  $p \geq 1$  leading to

$$\begin{aligned} \|\mathcal{E}_{\alpha,1}(\lambda_i t^\alpha)\|_{t \rightarrow \infty} &= \left\| \frac{1}{\alpha} \exp\left(\left(r_i e^{\varphi_i j} t^\alpha\right)^{1/\alpha}\right) - \sum_{k=1}^p \frac{(\lambda_i t^\alpha)^{-k}}{\Gamma(1-\alpha k)} + O(|\lambda_i t^\alpha|^{-1-p}) \right\|_{t \rightarrow \infty} \\ &= \left\| \frac{1}{\alpha} \exp\left(r_i^{1/\alpha} t \exp\left(\frac{\varphi_i}{\alpha} j\right)\right) - \sum_{k=1}^p \frac{(\lambda_i t^\alpha)^{-k}}{\Gamma(1-\alpha k)} + O(|\lambda_i t^\alpha|^{-1-p}) \right\|_{t \rightarrow \infty}. \end{aligned} \quad (3.46)$$

With  $\frac{|\varphi_i|}{\alpha} < \frac{\pi}{2}$ , we have  $\cos(\alpha\varphi_i) > 0$  and the Mittag-Leffler function is unbounded:

$$\|\mathcal{E}_{\alpha,1}(\lambda_i t^\alpha)\|_{t \rightarrow \infty} = \infty. \quad (3.47)$$

Now we will discuss the case of  $A$  not being diagonalizable. We use the Jordan canonical form, with the Jordan block  $J_i \in \mathbb{C}^{n_i \times n_i}$

$$J_i = \begin{pmatrix} \lambda_i & 1 & \cdots & 0 \\ 0 & \lambda_i & \ddots & \vdots \\ \vdots & \ddots & \ddots & 1 \\ 0 & 0 & \cdots & \lambda_i \end{pmatrix} = \lambda_i I + N. \quad (3.48)$$

Hence we have

$$\begin{aligned} \mathcal{E}_{\alpha,1}(J_i t^\alpha) &= \sum_{k=0}^{\infty} \frac{(J_i t^\alpha)^k}{\Gamma(\alpha k + 1)} = \sum_{k=0}^{\infty} \frac{(t^\alpha)^k}{\Gamma(\alpha k + 1)} J_i^k = \sum_{k=0}^{\infty} \frac{(t^\alpha)^k}{\Gamma(\alpha k + 1)} (\lambda_i I + N)^k \\ &= \sum_{k=0}^{\infty} \frac{(t^\alpha)^k}{\Gamma(\alpha k + 1)} \left( \lambda_i^k I + \binom{k}{1} \lambda_i^{k-1} N + \binom{k}{2} \lambda_i^{k-2} N^2 + \cdots + \binom{k}{n_i-1} \lambda_i^{k-n_i+1} N^{n_i-1} \right) \\ &= \begin{pmatrix} \sum_{k=0}^{\infty} \frac{(\lambda_i t^\alpha)^k}{\Gamma(\alpha k + 1)} & \sum_{k=0}^{\infty} \frac{(t^\alpha)^k}{\Gamma(\alpha k + 1)} \binom{k}{1} \lambda_i^{k-1} & \cdots & \sum_{k=0}^{\infty} \frac{(t^\alpha)^k}{\Gamma(\alpha k + 1)} \binom{k}{n_i-1} \lambda_i^{k-n_i+1} \\ 0 & \sum_{k=0}^{\infty} \frac{(\lambda_i t^\alpha)^k}{\Gamma(\alpha k + 1)} & \cdots & \sum_{k=0}^{\infty} \frac{(t^\alpha)^k}{\Gamma(\alpha k + 1)} \binom{k}{n_i-2} \lambda_i^{k-n_i+2} \\ \vdots & \ddots & \ddots & \vdots \\ 0 & 0 & \cdots & \sum_{k=0}^{\infty} \frac{(\lambda_i t^\alpha)^k}{\Gamma(\alpha k + 1)} \end{pmatrix} \\ &= \begin{pmatrix} \mathcal{E}_{\alpha,1}(\lambda_i t^\alpha) & \frac{1}{1!} \frac{\partial}{\partial \lambda_i} \mathcal{E}_{\alpha,1}(\lambda_i t^\alpha) & \cdots & \frac{1}{(n_i-1)!} \left( \frac{\partial}{\partial \lambda_i} \right)^{n_i-1} \mathcal{E}_{\alpha,1}(\lambda_i t^\alpha) \\ 0 & \mathcal{E}_{\alpha,1}(\lambda_i t^\alpha) & \cdots & \frac{1}{(n_i-2)!} \left( \frac{\partial}{\partial \lambda_i} \right)^{n_i-2} \mathcal{E}_{\alpha,1}(\lambda_i t^\alpha) \\ \vdots & \ddots & \ddots & \vdots \\ 0 & 0 & \cdots & \mathcal{E}_{\alpha,1}(\lambda_i t^\alpha) \end{pmatrix}. \end{aligned}$$

**Remark 3.2.** In the case of  $n_i = 2$  we can write the off-diagonal element directly in terms of a Mittag-Leffler function:

$$\mathcal{E}_{\alpha,1}(J_i t^\alpha) = \begin{pmatrix} \mathcal{E}_{\alpha,1}(\lambda_i t^\alpha) & \frac{t^\alpha}{\alpha} \mathcal{E}_{\alpha,\alpha}(\lambda_i t^\alpha) \\ 0 & \mathcal{E}_{\alpha,1}(\lambda_i t^\alpha) \end{pmatrix}. \quad (3.49)$$

Now, we can apply both Lemmas 3.1 and 3.2 again to the off-diagonal elements of the Jordan block  $J_i$  and see their influence on the stability. For the stable case with  $|\arg(\lambda_i)| > \alpha \frac{\pi}{2}$  for  $\kappa = 1, 2, \dots, n_i$  this leads to

$$\frac{1}{\kappa!} \left( \frac{\partial}{\partial \lambda_i} \right)^\kappa \mathcal{E}_{\alpha,1}(\lambda_i t^\alpha) = -\frac{1}{\kappa!} \sum_{k=2}^p \frac{(-1)^\kappa t^{-\alpha k} (k + \kappa - 1)!}{\Gamma(1 - \alpha k) (k - 1)!} \lambda_i^{-k-\kappa} + O\left(\frac{|\lambda_i|^{-1-p-\kappa}}{t^{(1+p)\alpha}}\right), \quad t \rightarrow \infty.$$

The norm of this term decays with  $t^{-\alpha}$  and we have

$$\left\| \frac{1}{\kappa!} \left( \frac{\partial}{\partial \lambda_i} \right)^\kappa \mathcal{E}_{\alpha,1}(\lambda_i t^\alpha) \right\|_{t \rightarrow \infty} = 0. \quad (3.50)$$

In the critical case of  $\arg(\lambda_i) < \alpha \frac{\pi}{2}$ , we apply Lemma 3.2 and it is sufficient to investigate the first off-diagonal element. Setting  $\kappa = 1$  yields for  $t \rightarrow \infty$

$$\begin{aligned} \frac{1}{1!} \left( \frac{\partial}{\partial \lambda_i} \right) \mathcal{E}_{\alpha,1}(\lambda_i t^\alpha) &= \frac{\partial}{\partial \lambda_i} \left( \frac{1}{\alpha} \exp(\lambda_i^{1/\alpha} t) - \sum_{k=1}^p \frac{\lambda_i^k t^{-\alpha k}}{\Gamma(1 - \alpha k)} + O(|\lambda_i t^\alpha|^{-1-p}) \right) \\ &= \frac{\lambda_i^{1/\alpha-1}}{\alpha^2} \exp(\lambda_i^{1/\alpha} t) t + \sum_{k=2}^p \frac{k \lambda_i^{-k-1} t^{-\alpha k}}{\Gamma(1 - \alpha k)} + O\left(\frac{|\lambda_i|^{-2-p}}{t^{(1+p)\alpha}}\right). \end{aligned} \quad (3.51)$$

The first term obviously grows with  $t$  and is not suppressed by the exponential function in the critical case  $\arg(\lambda_i) = \alpha \frac{\pi}{2}$  as shown in Equation (3.46) and 3.45.

Finally, we have to address the case of  $\lambda_i = 0$ . In this case the Mittag-Leffler function of the Jordan block becomes

$$\mathcal{E}_{\alpha,1}(J_i t^\alpha) = \begin{pmatrix} 1 & \frac{t^\alpha}{\Gamma(\alpha+1)} & \cdots & \frac{t^{(n_i-1)\alpha}}{\Gamma((n_i-1)\alpha+1)} \\ 0 & 1 & \cdots & \frac{t^{(n_i-2)\alpha}}{\Gamma((n_i-2)\alpha+1)} \\ \vdots & \ddots & \ddots & \vdots \\ 0 & 0 & \cdots & 1 \end{pmatrix} \quad (3.52)$$

which is only bounded for  $n_i = 1$ . Therefore the geometric and algebraic multiplicities of the critical eigenvalues have to be equal to maintain a stable behavior.  $\square$

In contrast to that the linear Riemann system is stable for a larger class of matrices.

**Theorem 3.5** (Stability of Riemann Systems). *The system  ${}^R\mathcal{D}^\alpha x(t) = Ax(t)$  with the initial state  ${}^R\mathcal{D}^{\alpha-1}x(t)|_{t=0} = \bar{x}_0 \in \mathbb{R}^n$  and the order of differentiation  $\alpha \in (0, 1)$  is*

- asymptotically stable if and only if all eigenvalues  $\lambda_i$  of  $A$  satisfy

$$|\arg(\lambda_i)| > \alpha \frac{\pi}{2}, \quad i = 1, 2, \dots, n. \quad (3.53)$$

*In this case the system is  $t^{-\alpha-1}$  stable.*

- stable if and only if either it is asymptotically stable or all non-zero eigenvalues  $\lambda_i$  with  $|\arg(\lambda_i)| = \alpha \frac{\pi}{2}$  have the same algebraic and geometric multiplicity and the  $k$  zero eigenvalues corresponding to a Jordan block matrix  $\text{diag}(J_1, J_2, \dots, J_{n_i})$  with the Jordan blocks  $J_l \in \mathbb{C}^{l \times l}$  such that  $\sum_{i=1}^i n_i = k$ , satisfy

$$n_l \alpha \leq 1, \quad 1 \leq l \leq i \quad (3.54)$$

*and for the other eigenvalues Equation (3.41) holds. In this case the equilibrium is stable but not asymptotically stable.*

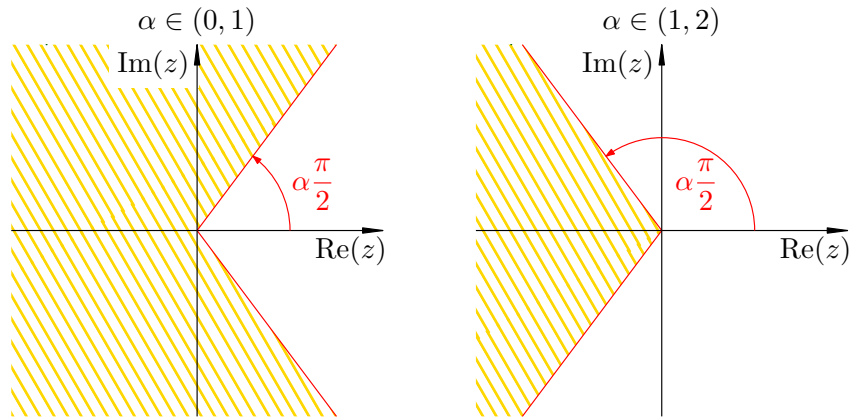


Figure 3.6: For  $\alpha \in (0, 1)$  the region of stability is a non-convex set.

The complete proof is given in [77]. Compared to the previously shown approach, we have to take into account the stabilizing singularity  $(t - t_0)^{\alpha-1}$  of the Riemann transition matrix  $\tilde{\Phi}_\alpha(t, t_0) = (t - t_0)^{\alpha-1} \mathcal{E}_{\alpha, \alpha}(A(t - t_0)^\alpha)$ , which leads to slightly larger Jordan blocks corresponding to the eigenvalue at zero. This also leads to the faster algebraic convergence of the order  $t^{-\alpha-1}$ .

Note that this major stability theorem also holds for the case  $\alpha \in (0, 2)$  [86] which leads to the well known illustration shown in Figure 3.6.

A good overview on the various formulations of this main stability criteria is given in [46] or [100]. The main reformulations in terms of linear matrix inequalities are given in [86, 66].

### 3.3 Observability and Controllability

We consider the linear time invariant fractional-order system given by equation (3.3). First of all, we define the properties of observability and controllability following [57] analogous to integer-order systems.

**Definition 3.6** (Observability). *The system (3.3) is called observable on the interval  $[t_0, t_1]$  if the initial state  $x(t_0)$  can be uniquely determined from the knowledge of the output  $y(t)$  and the input  $u(t)$  on the interval  $t \in [t_0, t_1]$ .*

**Definition 3.7** (Observability Gramian). *The observability Gramian of the order  $\alpha$  is a positive symmetric matrix given by:*

$$\mathcal{M}_\alpha(t_0, t_1) := \int_{t_0}^{t_1} \mathcal{E}_{\alpha, 1}(A^\top \tau^\alpha) C^\top C \mathcal{E}_{\alpha, 1}(A \tau^\alpha) d\tau. \quad (3.55)$$

**Theorem 3.6** (Observability). *The system (3.3) is completely observable on the interval  $[t_0, t_1]$  if and only if*

1. *its observability Gramian is positive definite:  $\mathcal{M}_\alpha(t_0, t_1) > 0$  or*

2. the observability matrix  $\mathcal{O}$  is regular, i.e.

$$\text{rank}(\mathcal{O}) = n, \quad \text{with} \quad \mathcal{O} = \begin{pmatrix} C \\ CA \\ \vdots \\ CA^{n-1} \end{pmatrix}. \quad (3.56)$$

If the system (3.3) is observable, it is also possible to reconstruct the actual state  $x(t_1)$  by applying the transition matrix defining the solution to the initial value problem (3.5).

Due to the linearity of the system, we can introduce the dual concept of controllability like in the integer-order case.

**Definition 3.8** (Controllability). *The system (3.3) is controllable on the interval  $[t_0, t_1]$  if for any pair  $(x_0, x_1)$  there exists a bounded control signal  $u(t) \in \mathbb{R}^p$  for  $t \in [t_0, t_1]$  which drives the initial state  $x(t_0) = x_0$  to the final state  $x(t_1) = x_1$ .*

In order to compare the forced part of the solution (3.5) to the integer-order case, we have to use the different transition  $\tilde{\Phi}_\alpha(t, t_0)$  to define the controllability Gramian.

**Definition 3.9** (Controllability Gramian [57]). *The controllability Gramian of the order  $\alpha$  is a positive symmetric matrix given by:*

$$\mathcal{W}_\alpha(t_0, t_1) := \int_{t_0}^{t_1} \mathcal{E}_{\alpha, \alpha}(A(t_1 - \tau)^\alpha) B B^\top \mathcal{E}_{\alpha, \alpha}(A^\top(t_1 - \tau)^\alpha) d\tau. \quad (3.57)$$

**Theorem 3.7** (Controllability). *The system (3.3) is completely controllable on the interval  $[t_0, t_1]$  if and only if*

1. its controllability Gramian is positive definite:  $\mathcal{W}_\alpha(t_0, t_1) > 0$  or
2. the controllability matrix  $\mathcal{C}$  is regular, i.e.

$$\text{rank}(\mathcal{C}) = n, \quad \text{with} \quad \mathcal{C} = \begin{pmatrix} B & AB & \dots & A^{n-1}B \end{pmatrix}. \quad (3.58)$$

**Remark 3.3.** *If we consider the Riemann-Liouville operator instead of Caputo's derivative*

$$\Sigma_{\text{FO}} : \begin{cases} {}^R\mathcal{D}^\alpha \bar{x}(t) = A\bar{x}(t) + Bu(t) & (3.59a) \\ y(t) = C\bar{x}(t) + Du(t) & (3.59b) \end{cases}$$

*we have to change the definitions of the introduced Gramians as shown in [5]*

$$\bar{\mathcal{W}}_\alpha(t_0, t_1) := \int_{t_0}^{t_1} \mathcal{E}_{\alpha, 1}(A(t_1 - \tau)^\alpha) B B^\top \mathcal{E}_{\alpha, 1}(A^\top(t_1 - \tau)^\alpha) d\tau. \quad (3.60)$$

*However, the observability and controllability matrices  $\mathcal{O}$  and  $\mathcal{C}$  do not change.*

**Remark 3.4.** Due to the different transitions contained in the solution, the control signal to steer the current state  $x(t_0) = x_0$  to the desired state  $x(t_1) = x_1$  is constructed differently compared to the integer-order case:

$$u^*(t) = -B^\top (t_1 - t)^{1-\alpha} \mathcal{E}_{\alpha,\alpha} \left( A^\top (t_1 - t)^\alpha \right) \mathcal{W}_\alpha^{-1}(t_0, t_1) \left( \mathcal{E}_{\alpha,1} (A(t_1 - t_0)^\alpha) x_0 - x_1 \right). \quad (3.61)$$

Of course we can further detail these properties with respect to the eigenvalue location of the system matrix, leading to the well established concepts of stabilizability [81, p. 351] and detectability [81, p. 352].

**Definition 3.10 (Stabilizability).** The linear fractional-order system  $\Sigma_{\text{FO}}$  given by (3.3) is called stabilizable if there exists a feedback gain  $K \in \mathbb{R}^{p \times n}$ , such that the closed-loop dynamics

$$\mathcal{D}^\alpha x(t) = (A + BK)x(t) \quad (3.62)$$

are asymptotically stable, i.e.  $|\arg(\lambda_i)| > \alpha \frac{\pi}{2}$  with the eigenvalues  $\lambda_i$  of the closed-loop system matrix  $A + BK$ .

**Definition 3.11 (Detectability).** The linear fractional-order system  $\Sigma_{\text{FO}}$  given by (3.3) is called detectable if there exists an observer gain  $L \in \mathbb{R}^{n \times q}$ , such that the estimation error dynamics

$$\mathcal{D}^\alpha e(t) = (A + LC)e(t) \quad (3.63)$$

are asymptotically stable, i.e.  $|\arg(\lambda_i)| > \alpha \frac{\pi}{2}$  with the eigenvalues  $\lambda_i$  of the system matrix  $A + LC$ .

These definitions state, that there should not be any unstable modes which are also not controllable or not observable. This leads to the following generalization of the Hautus criterion [67] to the fractional-order case.

**Theorem 3.8 (Detectability [67]).** The system  $\Sigma_{\text{FO}}$  given by (3.3) is detectable if and only if

$$\text{rank} \begin{pmatrix} \lambda I - A \\ C \end{pmatrix} = n \quad (3.64)$$

for all  $\lambda \in \mathbb{C}$  such that  $|\arg(\lambda)| \leq \alpha \frac{\pi}{2}$ .

Using the duality of detectability and stabilizability, we can rewrite this theorem to check for non-controllable, unstable modes.

**Theorem 3.9 (Stabilizability).** The system  $\Sigma_{\text{FO}}$  given by (3.3) is stabilizable if and only if

$$\text{rank} \begin{pmatrix} \lambda I - A & B \end{pmatrix} = n \quad (3.65)$$

for all  $\lambda \in \mathbb{C}$  such that  $|\arg(\lambda)| \leq \alpha \frac{\pi}{2}$ .

### 3.4 Fractional-Order LTI Systems with extended Conditions

Initialized fractional-order systems are defined using the initialized fractional-order derivatives. The resulting state equations are

$$\Sigma_{\text{FO-INI}} : \begin{cases} {}^C\mathcal{D}^\alpha x(t) = Ax(t) + Bu(t) - {}^C\Psi(x, \alpha, t_0, c, t) & (3.66a) \\ y(t) = Cx(t) + Du(t), & (3.66b) \end{cases}$$

with the (pseudo) state  $x(t) \in \mathbb{R}^n$ , the input  $u(t) \in \mathbb{R}^p$ , the output  $y(t) \in \mathbb{R}^q$ , order of differentiation  $\alpha \in (0, 1)$  and matrices of suitable dimensions. The function  ${}^C\Psi(x, \alpha, t_0, c, t) \in \mathbb{R}^n$  represents the memory of the fractional-order operator. On the one hand, we can charge this memory in the time-interval  $t \in [c, t_0]$  as shown in Section 2.5. On the other hand, this system description also allows to incorporate the side initialization by using Dirac impulses. Note that before  $t = c$  all the system states are assumed to be zero - the system is at rest. Only an input can drive the system to a non-zero state at the initial time  $x(t_0) \neq 0$ .

For  $t \geq t_0$  we can interpret this initialization function as an additional input, which decays over time. Hence the solution to the fractional-order differential equation is given by:

$$x(t) = - \int_{t_0}^t (t-\tau)^{\alpha-1} \mathcal{E}_{\alpha, \alpha}(A(t-\tau)^\alpha) {}^C\Psi(x, \alpha, t_0, c, \tau) d\tau + \int_{t_0}^t (t-\tau)^{\alpha-1} \mathcal{E}_{\alpha, \alpha}(A(t-\tau)^\alpha) Bu(\tau) d\tau. \quad (3.67)$$

**Remark 3.5.** Note that we cannot properly reformulate the initialized fractional-order dynamics in terms of a fractional-order system with standard initial conditions. The required input will be non-causal and depend on the future. A method for the proper initialization of these fractional-order operators is described in [85].

#### 3.4.1 Input-initialized fractional-order systems

If an input  $u(t)$  is used to initialize the fractional-order system, and this input channel is still available after  $t = 0$ , we can restrict the system class to the input-initialized fractional-order systems. We assume that the memory was accumulated by an unknown input acting on the system before  $t_0 = 0$  in the past. Therefore, we split the input into the unknown part  $\bar{u}(t)$  acting in the past and the known part  $\underline{u}(t)$ , which influences the dynamics for  $t > t_0$

$$\left. \begin{aligned} \bar{u}(t) &= (\sigma(t-a) - \sigma(t)) u(t) \\ \underline{u}(t) &= \sigma(t) u(t) \end{aligned} \right\} u(t) = \bar{u}(t) + \underline{u}(t). \quad (3.68)$$

We assume that no input acts before  $t = a$  such that  $u(t) = 0, \forall t < a < 0$ . Before  $t = a < 0$  we assume an energy free system  $x(t) = 0$  for all  $t \leq a$ . During the time interval  $t \in [a, 0]$  the input  $\bar{u}(t)$  acts on the system and moves the state to a non-zero value at  $t = 0$ , i.e.  $x(0) = x_0 \neq 0$ . Due to the memory of the fractional-order operator, this input still influences the evolution of the state trajectories for  $t > 0$ . As we are considering linear systems and operators, we can

apply superposition. The initialization part is covered by the fractional-order system starting at the time  $t = a$

$${}_a\mathcal{D}_t^\alpha \bar{x}(t) = A\bar{x}(t) + B\bar{u}(t), \quad \bar{x}(a) = 0. \quad (3.69)$$

The remaining part of the state  $\underline{x}(t)$  satisfies

$${}_0\mathcal{D}_t^\alpha \underline{x}(t) = A\underline{x}(t) + B\underline{u}(t), \quad \underline{x}(0) = 0. \quad (3.70)$$

Superposition of  $\bar{x}(t)$  and  $\underline{x}(t)$  yields the overall state

$$x(t) = \bar{x}(t) + \underline{x}(t), \quad t > 0. \quad (3.71)$$

This is illustrated in Figure 3.7 for a scalar system. The system description starting at  $t = 0$  can be derived in terms of the initialization function  ${}^C\Psi(\cdot)$ . We compute Caputo's derivative with the lower limit  $t_0 = 0$ , i.e.

$${}_0\mathcal{D}_t^\alpha x(t) = {}_0\mathcal{D}_t^\alpha \underline{x}(t) + {}_0\mathcal{D}_t^\alpha \bar{x}(t) = A\underline{x}(t) + B\underline{u}(t) + {}_0\mathcal{D}_t^\alpha \bar{x}(t)$$

and use (2.91) to move the lower limit of the differentiation from  $t_0 = 0$  to  $t_0 = a$

$$\begin{aligned} {}_0\mathcal{D}_t^\alpha x(t) &= A\underline{x}(t) + B\underline{u}(t) + \left( {}_a\mathcal{D}_t^\alpha \bar{x}(t) - {}^C\Psi(\bar{x}, \alpha, 0, a, t) \right) \\ &= A(\underline{x}(t) + \bar{x}(t)) + B(\underline{u}(t) + \bar{u}(t)) - {}^C\Psi(\bar{x}, \alpha, 0, a, t) \\ &= Ax(t) + Bu(t) - {}^C\Psi(x, \alpha, 0, a, t). \end{aligned} \quad (3.72)$$

Note that we can change one argument of the initialization function  ${}^C\Psi(\cdot)$  from  $\bar{x}$  to  $x$  as  ${}^C\Psi(\cdot)$  only considers the state before  $t = 0$ , which is only defined by  $\bar{x}(t)$ .

We see that the input-initialization is a special case of the terminal initialization. We can also interpret the  $n$ -dimensional initialization function  ${}^C\Psi(x, \alpha, 0, a, t)$  as additional  $n$  unknown inputs. The special case of the side initialization cannot be achieved with a bounded past input.

### 3.4.2 Fractional-Order Luenberger Observer

With this kind of system definition, we cannot apply the usual concept of observability. We might be able to compute the state at the beginning of the observation interval  $x(t_0)$ . However, this information is not sufficient to predict the future evolution of the state. In order to compute the future state, we have to know either the initialization function  ${}^C\Psi(x, \alpha, t_0, c, t)$  or the charging input  $\bar{u}(t)$  acting during the past. The actual time horizon  $a$  of this input is also unknown. The concept of observability needs to be modified and the question arises whether we can reconstruct the unknown input  $\bar{u}(t)$  and the charging interval  $[a, t_0]$  based on measurements  $y(t)$  and the known input  $\underline{u}(t)$  on a certain time interval  $t \in [t_0, t_f]$ .

For practical applications the reconstruction of the system's initial state is not of much use. Normally, the actual state  $x(t)$  is more relevant, e.g. for control purposes or fault diagnostics. We can still apply some of the concepts presented before as we are interested in the estimation of the current state  $x(t)$ . We need to stabilize the error dynamics of an observer and hence be able to move the eigenvalues of  $A$  with an observer gain  $L$  (ignoring the initialization function for now). This is still only possible if the system is observable (detectable) and we can still apply the results of Theorem 3.6 to design a Luenberger observer.



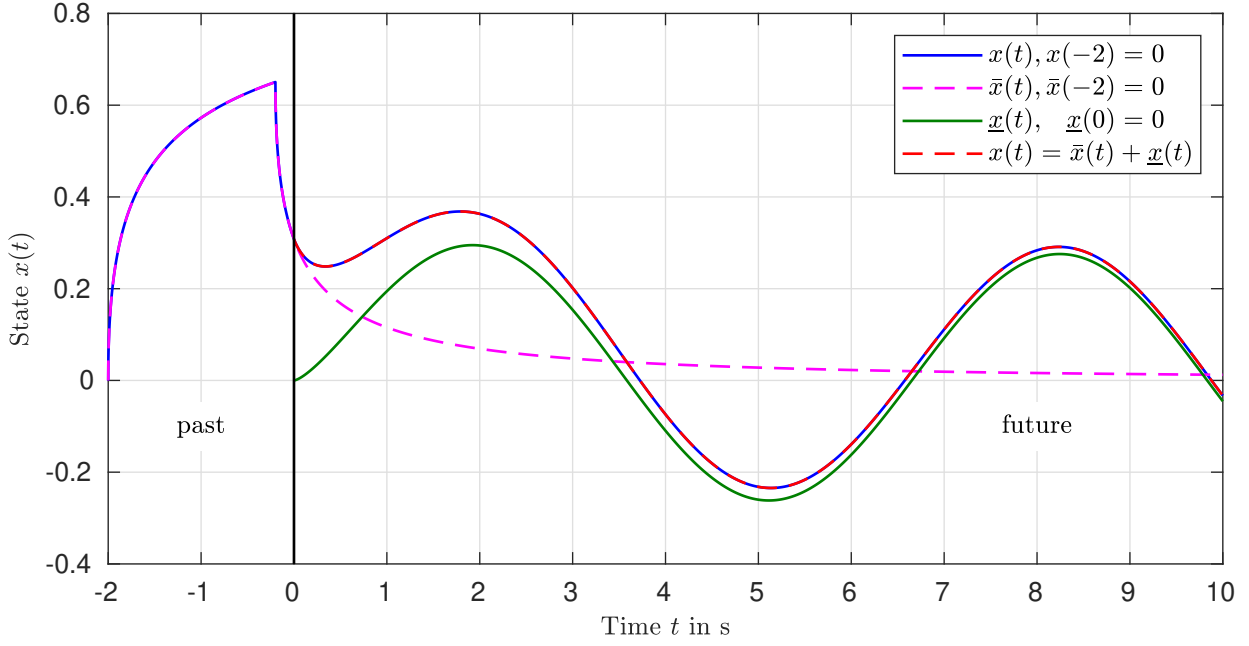


Figure 3.7: The correct state is the result of superposing the known state  $\underline{x}(t)$  and the state  $\bar{x}(t)$  driven by the unknown past input. The unknown past input is  $\bar{u}(t) = 2\sigma(t+2) - 2\sigma\left(t + \frac{1}{10}\right)$  and the known input for  $t \geq 0$  is  $\underline{u}(t) = \sin(t)$ .

Similar to integer-order systems, we can use an observer to estimate the states which are not measured if the system is observable. The observer reads

$$\hat{\Sigma}: \quad \mathcal{D}^\alpha \hat{x}(t) = A\hat{x}(t) + Bu(t) - {}^C\hat{\Psi}(\hat{x}, \alpha, 0, \hat{a}, t) + L(\hat{y}(t) - y(t)) \quad (3.73)$$

$$\hat{y}(t) = C\hat{x}(t) + Du(t). \quad (3.74)$$

As an initial guess of the initialization function  ${}^C\hat{\Psi}(\hat{x}, \alpha, 0, \hat{a}, t)$ , we can use either the trivial approach  ${}^C\hat{\Psi}(\hat{x}, \alpha, 0, \hat{a}, t) = 0$  or a decaying function which is compatible with the system structure to be observed. This means that the ansatz of  ${}^C\hat{\Psi}(\hat{x}, \alpha, 0, \hat{a}, t) \neq 0$  has to be bounded by an algebraic envelope (2.95). The estimation error  $e(t) = \hat{x}(t) - x(t)$  shows fractional-order dynamics

$$\begin{aligned} \mathcal{D}^\alpha e(t) &= \mathcal{D}^\alpha \hat{x}(t) - \mathcal{D}^\alpha x(t) \\ &= A\hat{x}(t) + Bu(t) - {}^C\hat{\Psi}(\hat{x}, \alpha, 0, \hat{a}, t) + L(C\hat{x}(t) - Cx(t)) - \\ &\quad \left( Ax(t) + Bu(t) - {}^C\Psi(x, \alpha, 0, a, t) \right) \\ &= (A + LC)e(t) - \left( {}^C\hat{\Psi}(\hat{x}, \alpha, 0, \hat{a}, t) - {}^C\Psi(x, \alpha, 0, a, t) \right) \\ &= (A + LC)e(t) - e_\Psi(t). \end{aligned} \quad (3.75)$$

If the pair  $(A, C)$  is observable, we can set the eigenvalues such that Theorem 3.41 is satisfied

$$|\arg(\lambda_i(A + LC))| > \alpha \frac{\pi}{2}. \quad (3.76)$$

The error dynamics (3.75) are then asymptotically stable but driven by  $e_\Psi(t)$ , the error caused by the deviation of the different initialization functions. However, this input decays to zero

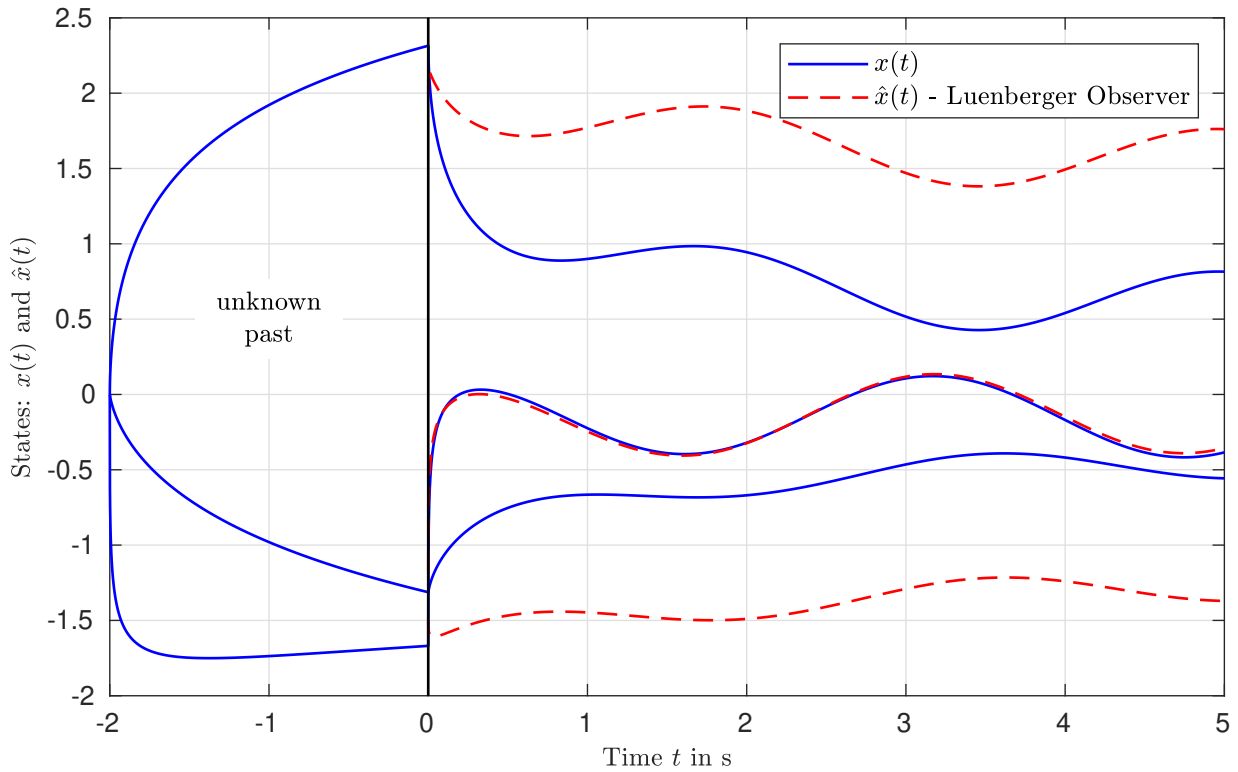


Figure 3.8: Simulation results of a Luenberger-observer applied to an initialized fractional-order system.

as the bound (2.95) of both initialization functions is zero for  $t \rightarrow \infty$  and the estimation error converges to zero, i.e.

$$\lim_{t \rightarrow \infty} e(t) = 0. \quad (3.77)$$

The rate of convergence of the estimation error is limited because of two main reasons. First of all, the homogeneous part of (3.75) decays algebraically and second the unknown initialization function slows the convergence further.

**Example 3.2.** To illustrate the poor convergence of this approach, we consider an example system motivated by an integer-order example presented in [11, p. 88]

$$\mathcal{D}^\alpha x(t) = \begin{pmatrix} -1 & 1 & 0 \\ -1 & 0 & 0 \\ 0 & -1 & -1 \end{pmatrix} x(t) + \begin{pmatrix} -1 \\ 0 \\ 0 \end{pmatrix} u(t) \quad (3.78a)$$

$$y(t) = \begin{pmatrix} 1 & 0 & 0 \\ 0 & 0 & 1 \end{pmatrix} x(t) \quad (3.78b)$$

with  $\alpha \in (0, 1)$ . In order to avoid computing the initialization function, we use  $a = -2$  s and set the state to  $x(-2) = 0$ . Using this setup we can apply the solver FDE12 provided in [21]. The system is excited with the constant input  $\bar{u}(t) = 5$  for  $t \in [-2, 0]$ . After this charging period, the known input is  $u(t) = 1.5 \sin^2(t)$  for  $t > 0$ . The transient behavior for  $\alpha = 0.3$  is depicted in Figure 3.8.

The observer gain  $L \in \mathbb{R}^{3 \times 2}$  is chosen such that it places the eigenvalues close to one, i.e.  $\lambda_i \in \{-0.9, -1.0, -1.1\}$ . The observer uses the side initialization  $\hat{x}(0) = \hat{x}_0$  (and  $\hat{x}(t) = 0$  for  $t < 0$ ).

Note that even the correct initialization of the observer with  $\hat{x}_0 = x(0)$  leads to erroneous estimates for  $t > 0$ . Due to the infinite initial derivative in the transients, the correct initialization is not visible in Figure 3.8. The estimation error increases in the first two seconds because the actual memory is not known.

For this reason we also cannot apply these observers as filters to smooth the measurement signals, if the memory is unknown.

### 3.4.3 Fractional-Order Unknown-Input Observer

Motivated by the theory of unknown input observer for integer order systems [11], we apply these methods to increase observer performance. The basic idea is that we consider the initialization function  ${}^C\Psi(\cdot)$  as an unknown input to the system dynamics, such that we rewrite the dynamics introducing the unknown input  $d(t)$

$$\Sigma_{\text{FOD}} : \begin{cases} \mathcal{D}^\alpha x(t) = Ax(t) + Bu(t) + Ed(t) & (3.79a) \\ y(t) = Cx(t) & (3.79b) \end{cases}$$

This unknown input is now considered in the observer design. A structure for an unknown input observer (UIO) is given in [11] for integer-order systems. We extend this approach to a fractional-order processes described by (3.79)

$$\mathcal{D}^\alpha z(t) = Fz(t) + TBu(t) + (L_1 + L_2)y(t), \quad (3.80a)$$

$$\hat{x}(t) = z(t) + Hy(t), \quad (3.80b)$$

with the tuning parameters  $T \in \mathbb{R}^{n \times p}$ ,  $L_1 \in \mathbb{R}^{n \times q}$ ,  $L_2 \in \mathbb{R}^{n \times q}$  and  $H \in \mathbb{R}^{n \times q}$ . In the nominal case with  $Ed(t) = 0$ , this structure resembles a standard Luenberger observer with  $T = I$  and  $H = 0$ . The estimation error  $e(t) = \hat{x}(t) - x(t)$  shows the following dynamics:

$$\begin{aligned} \mathcal{D}^\alpha e(t) = & (A - HCA - L_1C)e(t) + (F - (A - HCA - L_1C))z(t) + & (3.81) \\ & (L_2 - (A - HCA - L_1C)H)y(t) + (T - (I - HC))Bu(t) + (HC - I)Ed(t). \end{aligned}$$

In order to exclude the influences of  $z(t)$ ,  $y(t)$  and the unknown input  $d(t)$ , the observer parameters have to satisfy

$$0 = (HC - I)E \quad (3.82a)$$

$$0 = (T - (I - HC))B \quad (3.82b)$$

$$0 = (L_2 - (A - HCA - L_1C)H) \quad (3.82c)$$

$$0 = (F - (A - HCA - L_1C)). \quad (3.82d)$$

This reduces the error dynamics (3.81) to

$$\mathcal{D}^\alpha e(t) = (A - HCA - L_1C)e(t) = Fe(t). \quad (3.83)$$

The first critical parameter here is the matrix  $H$ , as it also defines  $T$  and  $L_2$ . Furthermore,  $L_1$  should be able to move the eigenvalues of  $F$  to the stable domain, hence we require the detectability of the pair  $(C, A - HCA)$  here. These considerations lead to the following theorem.

**Theorem 3.10** (Existence of a Fractional-Order Unknown Input Observer). *There exists an unknown-input observer of the form (3.80) with respect to system  $\Sigma_{\text{FOD}}$  from (3.79) if and only if*

$$\text{rank}(CE) = \text{rank}(E). \quad (3.84a)$$

and the pair  $(C, A_1)$  is detectable with

$$A_1 = \left( I - E \left( (CE)^\top CE \right)^{-1} (CE)^\top C \right) A. \quad (3.84b)$$

*Proof.* The proof is given in [11, p. 83ff.] for integer-order systems. As only algebraic considerations are involved, the extension to the fractional-order case is straightforward.  $\square$

Note that in the integer-order case ( $\alpha = 1$ ) the existence of an unknown input observer is equivalent to the system property called strong\* detectability [27].

If condition (3.84a) is satisfied, we can compute  $H$  by a right pseudo-inverse

$$H = E \left( (CE)^\top CE \right)^{-1} (CE)^\top. \quad (3.85)$$

Hence we have  $T = I - HC$  and have to place the eigenvalues of the matrix  $A_1$  with the gain  $L_1$  such that

$$|\arg(\lambda_i(F))| > \alpha \frac{\pi}{2}, \quad i = 1, 2, \dots, n \quad \text{and} \quad F = TA - L_1C. \quad (3.86)$$

The second gain  $L_2$  is given by

$$L_2 = (A - HCA - L_1C)H. \quad (3.87)$$

We can now apply this unknown input observer to the initialized fractional-order system (3.72) resulting in the estimation error dynamics given by

$$\begin{aligned} {}_0\mathcal{D}^\alpha e(t) = & (A - HCA - L_1C) e(t) + (F - (A - HCA - L_1C)) z(t) + \\ & (L_2 - (A - HCA - L_1C)H) y(t) + (T - (I - HC)) Bu(t) - \\ & (HC - I)^C \Psi(x, \alpha, 0, a, t). \end{aligned} \quad (3.88)$$

As the unknown initialization function  $\Psi(\cdot) \in \mathbb{R}^n$  is different on each line (channel), it can only be completely compensated if  $\text{rank}(C) = n$ . As we cannot measure the complete state, some parts of the unknown initialization function will excite the remaining error dynamics. However, we may design  $H$  such that the effect of the unknown history is reduced. To this end, we introduce the matrices  $E$  and  $\bar{E}$  with diagonal elements  $e_i, \bar{e}_i \in \{0, 1\}$  for  $i = 1, 2, \dots, n$  such that  $E + \bar{E} = I$ . We can set as many elements of  $E$  to one as long as the rank condition (3.84a) is satisfied. In the remaining error dynamics

$${}_0\mathcal{D}^\alpha e(t) = Fe(t) + \bar{E}\Psi(x, \alpha, 0, a, t). \quad (3.89)$$

only a part of the unknown initialization function still influences the convergence. The basic fractional-order Luenberger observer is disturbed in each channel.

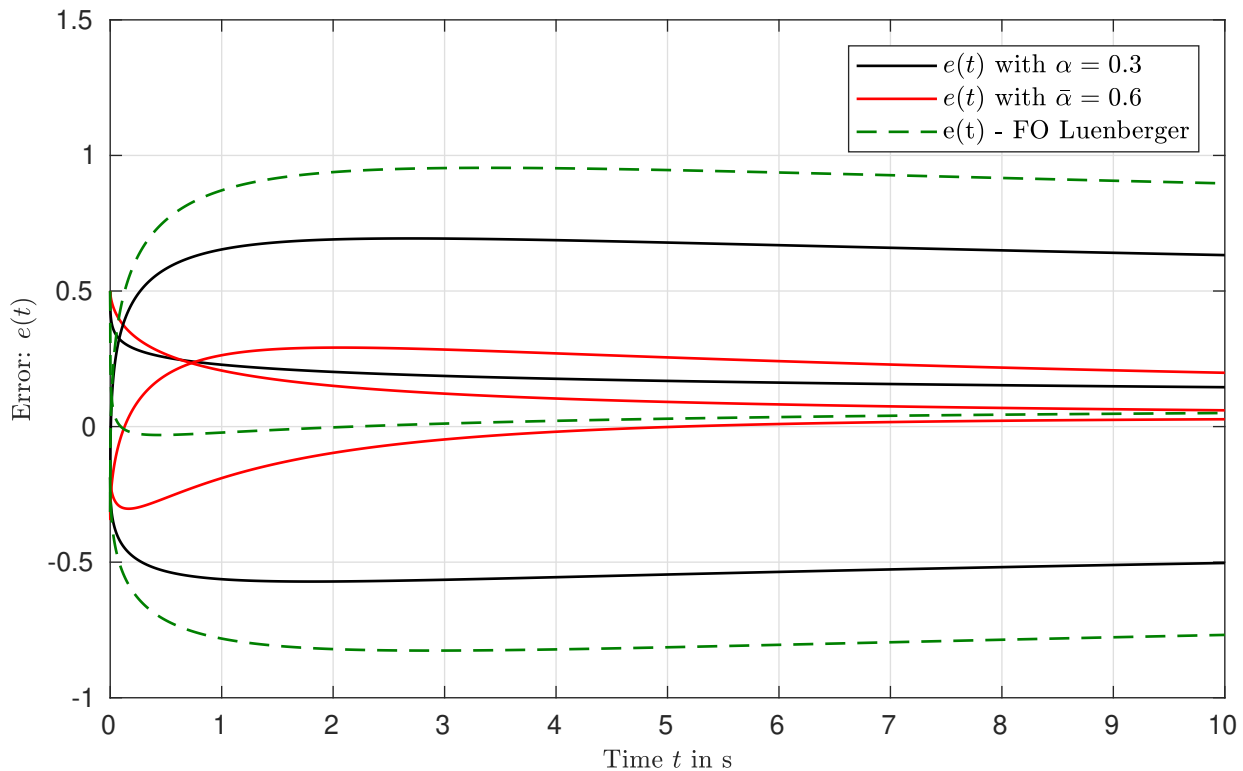


Figure 3.9: Estimation error of an unknown input observer and a fractional-order observer without additional compensation of the unknown history.

**Example 3.2** (continued). For the system described by (3.78) the relative-degree one condition (3.84a) holds and we can compute  $H$ ,  $T$  and  $A_1$  as

$$H = \begin{pmatrix} 1 & 0 \\ 0 & 0 \\ 0 & 0 \end{pmatrix}, \quad T = \begin{pmatrix} 0 & 0 & 0 \\ -1 & 0 & 0 \\ 0 & -1 & -1 \end{pmatrix}, \quad A_1 = \begin{pmatrix} 0 & 0 & 0 \\ -1 & 0 & 0 \\ 0 & -1 & -1 \end{pmatrix}. \quad (3.90)$$

The pair  $(C, A_1)$  is observable and the poles are placed at  $\lambda_i \in \{-0.9, -1, -1.1\}$ . We initialize both observers with  $\hat{x}(0) = (0.5 \ 2 \ -1.5)^\top$ . The simulation results are shown in Figure 3.9.

Note that the initial estimation error is close to zero at  $t = 0$ , however, due to the unknown past of the system, the observer is still not able to maintain this good initial guess. In contrast to the Luenberger observer, the convergence increases as the unknown initialization function no longer influences the error dynamics.

### 3.5 Fractional-Order LTI Systems in the Frequency Domain

Let us consider the SISO case with  $y(t) \in \mathbb{R}$  and  $u(t) \in \mathbb{R}$ . With zero initial conditions for  $t \leq t_0$  the fractional-order transfer function defining the input-output-relation of system (3.3) and (3.11), in the single-input single-output case is given by:

$$G(s) = \frac{Y(s)}{U(s)} = C(s^\alpha I - A)^{-1} B + D = \frac{A(s^\alpha)}{B(s^\alpha)} \quad (3.91)$$

where  $A(\cdot)$  and  $B(\cdot)$  are the pseudo-polynomials defined by:

$$A(s^\alpha) = a_n s^{n\alpha} + a_{n-1} s^{(n-1)\alpha} + \dots + a_1 s^\alpha + a_0 = \sum_{i=0}^n a_i s^{i\alpha} \quad (3.92a)$$

$$B(s^\alpha) = b_m s^{m\alpha} + b_{m-1} s^{(m-1)\alpha} + \dots + b_1 s^\alpha + b_0 = \sum_{i=0}^m b_i s^{i\alpha}. \quad (3.92b)$$

As all the exponents of  $A$  and  $B$  are multiples of the order  $\alpha$ , the transfer function  $G(s)$  is called commensurate and we can use the substitution  $p = s^\alpha$  in order to reduce the pseudo-polynomials in  $s$  to polynomials in  $p$ .

In order to factorize the pseudo polynomials  $A(s^\alpha)$  and  $B(s^\alpha)$  and to establish a connection to integer-order systems, we also need the concepts of pseudo poles and zeros.

**Definition 3.12** (Pseudo pole). *A complex number  $p_0 \in \mathbb{C}$  is called a pseudo pole of the transfer function  $G(s)$  if*

$$A(p_0) = 0 \quad \text{with} \quad p = s^\alpha. \quad (3.93)$$

Note that the pseudo poles of  $G(s)$  correspond to the eigenvalues of  $A$ , the system matrix of its state-space representation (3.3) or (3.11).

**Definition 3.13** (Pseudo zero). *A complex number  $p_z \in \mathbb{C}$  is called a pseudo zero of the transfer function  $G(s)$  if*

$$B(p_z) = 0 \quad \text{with} \quad p_z = s^\alpha. \quad (3.94)$$

The system poles and zeros are hence given by

$$s_0 = p_0^\alpha \quad \text{and} \quad s_z = p_z^\alpha. \quad (3.95)$$

These system zeros and poles give the corner frequencies [39] to approximate the amplitude and phase responses as shown in the Bode plot (see Figure 3.10 for example). Compared to integer-order systems, the direct interpretation of the Bode plot is of minor use, due to the algebraic decay of the homogeneous solution. For integer-order systems, the response to the initial conditions is approximately zero after the slowest time constant has passed five times. With the algebraic decay this empirical formula does not hold any more. With a sinusoidal input of frequency  $\omega$  and a unit amplitude, only for very large times  $t \gg t_0$  the amplitude response  $|G(j\omega)|$  becomes the amplitude of the output. The same holds for the phase shift of the output signal defined by the phase response. For stability analysis of simple processes, however, we can still use the simplified Nyquist criterion [94].

In contrast to the state-space description, in the frequency domain we are interested in bounded-input bounded-output stability, which is defined by the location of the pseudo poles.

**Theorem 3.11** (BIBO Stability [56]). *The commensurate fractional-order transfer function  $G(s) = A(s^\alpha)B^{-1}(s^\alpha)$  with two coprime polynomials  $A(p)$  and  $B(p)$  with  $p = s^\alpha$ ,  $\alpha \in (0, 1)$  for  $\text{Re}(s) > a \geq 0$  is bounded-input bounded-output stable if and only if*

$$|\arg(p_i)| > \alpha \frac{\pi}{2}, \quad \forall p_i \in \mathbb{C}, A(p_i) = 0. \quad (3.96)$$

If the transfer function is BIBO stable, the impulse response  $g(\cdot)$  shows the following asymptotics

$$g(t) \approx Kt^{-1-\alpha} \quad \text{for } t \rightarrow \infty. \quad (3.97)$$

Note that the impulse response decays faster than the homogeneous solution of the state equation. This is a result of the different pseudo transition matrices in equation (3.5). The convolution

$$C\tilde{\Phi}_\alpha(t, t_0)B \star \delta(t) \quad (3.98)$$

decays with  $t^{-1-\alpha}$  as we can interpret it as the homogeneous solutions of a Riemann system with initial conditions  $\bar{x}_0 = B$  and apply Theorem 3.5.

## Extensions

To design controllers in the frequency domain, this seems to be a too rigid structure. A more general (non-commensurate) form is hence given by:

$$\tilde{G}(s) = \frac{Y(s)}{U(s)} = \frac{b_m s^{\beta_m} + b_{m-1} s^{\beta_{m-1}} + \dots + b_1 s^{\beta_1} + b_0}{a_n s^{\alpha_n} + a_{n-1} s^{\alpha_{n-1}} + \dots + a_1 s^{\alpha_1} + a_0} \quad (3.99)$$

with arbitrary real orders  $\alpha_n > \alpha_{n-1} > \alpha_1 > 0$  and  $\alpha_n \geq \beta_m > \beta_{m-1} > \beta_1 > 0$ . In this case the orders  $\alpha_i$  and  $\beta_i$  do not have to share a common order. From a numerical point of view, however, we can approximate each system with a reasonable accuracy to be of commensurate order. The main disadvantage of this method is the necessity to have a high system order  $\tilde{n}$  while the majority of the coefficients is zero.

A further generalization of fractional-order structures in the frequency domain are the so-called implicit fractional-order structures, e.g. fractional-order lead-lag compensators [79].

$$G_{\text{imp}}(s) = \frac{Y(s)}{U(s)} = \left( \frac{s + \omega_0}{s + \omega_p} \right)^\gamma, \quad \gamma \in \mathbb{R}. \quad (3.100)$$

The state-space realization of such structures is derived in [79]. It is infinite and exponential convergence is achieved in theory, although the graphics in [79] suggest a slower convergence if only a finite state-space approximation is used in the implementation.

The exponential convergence of terms like (3.100) can also be illustrated by looking at the Laplace transform of a slightly simpler structure [60, p. 393]

$$\mathcal{L}^{-1} \left\{ \frac{1}{(s+a)^\alpha} \right\} = \frac{t^{\alpha-1}}{\Gamma(\alpha)} e^{-at}. \quad (3.101)$$

In this structure, the slowly decaying algebraic part  $t^{\alpha-1}$  for  $\alpha \in (0, 1)$  is dominated by the exponential term.

Figure 3.10 shows the amplitude and phase responses of an explicit and implicit fractional-order structure. The explicit fractional-order transfer function  $G_\alpha(s)$  is given by

$$G_\alpha(s) = \frac{Y(s)}{U(s)} = \frac{s^\alpha + \omega_0}{s^\alpha + \omega_p}, \quad (3.102)$$

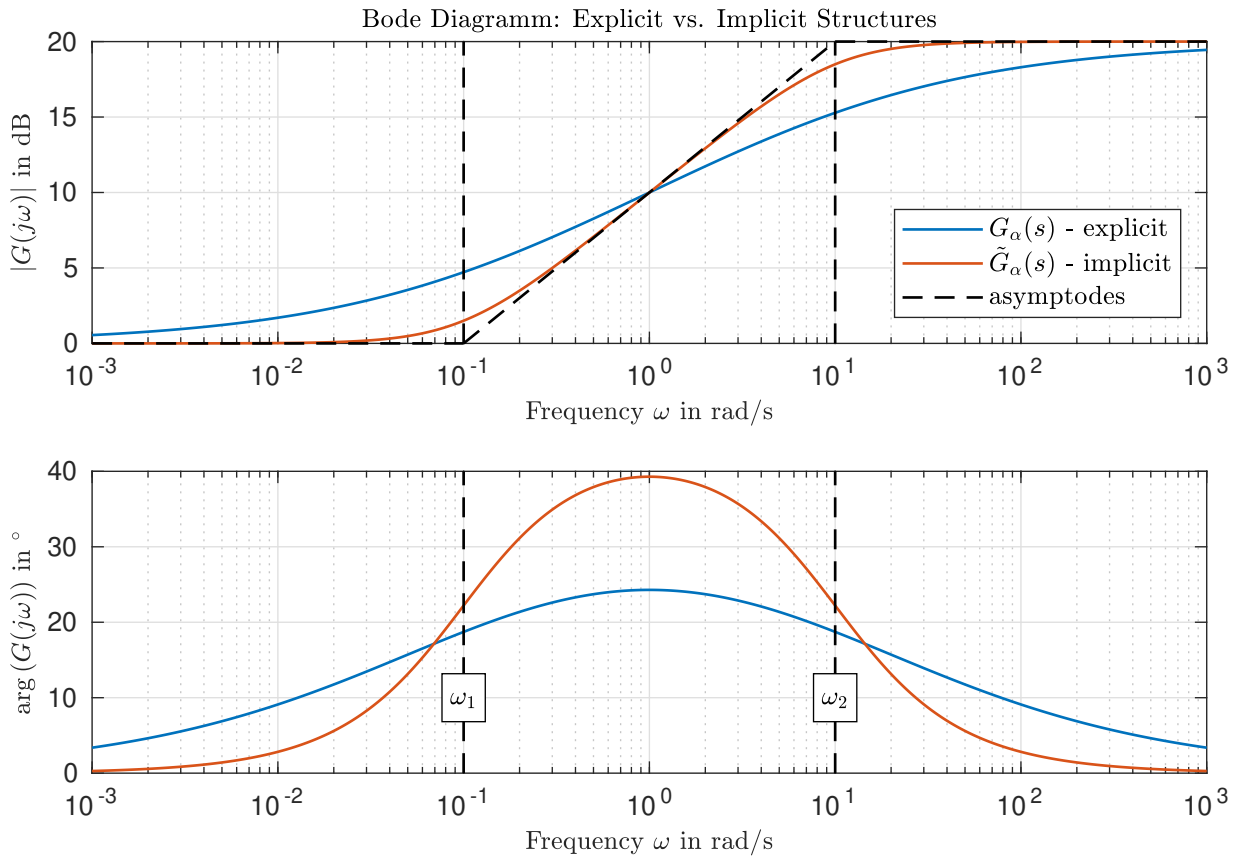


Figure 3.10: Frequency responses of the explicit and implicit fractional-order lead-lag compensator

whereas the implicit structure is a fractional-order lead-lag-compensator defined by (3.100) with  $\gamma = \alpha$ . In the amplitude response the asymptotes (black dashed) with the slope  $\pm\alpha$  20 dB/dec fit the actual amplitude response better than the explicit structure. The amplitude response of  $G_\alpha(s)$  can be approximated better if the distance between corner frequencies is increased.



## 4 Associated Higher-Order Systems

In this chapter, we investigate how to express the solutions of a fractional-order system of the order  $\alpha$  as trajectories of another system defined with a different order, e.g. an integer order. The obtained results are then used to design faster converging observers with a reduced requirement of physical memory.

### 4.1 Associated Integer-Order Systems

In this section, we show how a fractional-order LTI system can be rewritten as an integer-order system. We therefore have to restrict the order of differentiation to be rational:

$$\alpha = \frac{d_\alpha}{n_\alpha}, \quad \text{with: } d_\alpha, n_\alpha \in \mathbb{N} \quad \text{and} \quad d_\alpha, n_\alpha \text{ coprime.} \quad (4.1)$$

We first consider the homogeneous system given by:

$$\Sigma : \quad \mathcal{D}^\alpha x(t) = Ax(t), \quad x(0) = x_0 \quad (4.2)$$

with  $\alpha^{-1} = n_\alpha \in \mathbb{N}$ . Note that this is no restriction, if  $d_\alpha \neq 1$ , the original state-space can be extended in order to reduce the order of differentiation such that  $\tilde{d}_\alpha = 1$ .

Consider the system  $\Sigma^*$  given by

$$\Sigma^* : \dot{\tilde{x}}(t) = \tilde{A}\tilde{x}(t) + \tilde{u}(t, u(\cdot), x_0). \quad (4.3)$$

**Definition 4.1** (Associated Integer-Order System). *The system  $\Sigma^*$  is called associated integer-order system to the fractional-order system  $\Sigma$  if for every  $x_0, u(\cdot)$  there exists a function  $\tilde{u}(t, u(\cdot), x_0)$ , and a matrix  $\tilde{A} \in \mathbb{R}^{n_\alpha \times n_\alpha}$  such that*

$$\tilde{x}(t) = x(t) \quad \forall t \geq 0. \quad (4.4)$$

The first case to look at with  $n_\alpha = 2$  is investigated in [3, p. 14ff], using differential equations leading to solutions in terms of Mittag-Leffler functions [74, p. 21].

**Theorem 4.1.** *An integer-order system associated to the system (4.2) is given by:*

$$\dot{\tilde{x}}(t) = A^{n_\alpha} \tilde{x}(t) + t^{-1} \sum_{k=1}^{n_\alpha-1} \frac{(At^\alpha)^k}{\Gamma(\alpha k)} x_0, \quad \tilde{x}(0) = x_0. \quad (4.5)$$

With this equivalent representation of the original dynamics, the memory effect of the fractional-order operator becomes clear again. The initial state  $x_0$  influences the state evolution at each time as it is weighted with the nonzero memory function

$$f(t) = t^{-1} \sum_{k=1}^{n_\alpha-1} \frac{(At^\alpha)^k}{\Gamma(\alpha k)}. \quad (4.6)$$

Due to the decay of the weighing function  $f(t)$  the effect is reduced over time.

*Proof.* We compute the derivative of the Mittag-Leffler function and compare it to the homogeneous part  $A^{n_\alpha} x(t)$  such that we can determine the additional function weighing the initial state  $x_0$

$$\begin{aligned}\dot{\mathcal{E}}_{\alpha,1}(At^\alpha)x_0 &= \frac{d}{dt} \left( \sum_{k=0}^{\infty} \frac{(At^\alpha)^k}{\Gamma(\alpha k + 1)} x_0 \right) = \sum_{k=1}^{\infty} \frac{A^k (\alpha k) t^{\alpha k - 1}}{\Gamma(\alpha k + 1)} x_0 \\ &= \sum_{k=1}^{n_\alpha - 1} \frac{A^k (\alpha k) t^{\alpha k - 1}}{\Gamma(\alpha k + 1)} x_0 + \sum_{k=n_\alpha}^{\infty} \frac{A^k (\alpha k) t^{\alpha k - 1}}{\Gamma(\alpha k + 1)} x_0.\end{aligned}\quad (4.7)$$

We apply the property of the gamma function  $\Gamma(z+1) = z\Gamma(z)$  and shift the index of the second sum to  $\bar{k} = k - n_\alpha$ , i.e.

$$\begin{aligned}\dot{\mathcal{E}}_{\alpha,1}(At^\alpha)x_0 &= \sum_{k=1}^{n_\alpha - 1} \frac{A^k t^{\alpha k - 1}}{\Gamma(\alpha k)} x_0 + \sum_{\bar{k}=0}^{\infty} \frac{A^{n_\alpha + \bar{k}} t^{\alpha(\bar{k} + n_\alpha) - 1}}{\Gamma(\alpha(\bar{k} + n_\alpha))} x_0 \\ &= t^{-1} \sum_{k=1}^{n_\alpha - 1} \frac{(At^\alpha)^k}{\Gamma(\alpha k)} x_0 + A^{n_\alpha} \sum_{\bar{k}=0}^{\infty} \frac{A^{\bar{k}} t^{\alpha \bar{k}}}{\Gamma(\alpha \bar{k} + 1)} x_0 \\ &= f(t)x_0 + A^{n_\alpha} \mathcal{E}_{\alpha,1}(At^\alpha)x_0 = f(t)x_0 + A^{n_\alpha} x(t).\end{aligned}\quad (4.8)$$

This completes the proof.  $\square$

**Remark 4.1.** The derivative at the initial time  $t = 0$  is unbounded due to the pole contained in the function  $f(t)$ . However, the solution to (4.5) is unique because the right side of (4.5) is Lipschitz [7, p. 544] in  $x$  with the Lipschitz constant given by any norm of  $\|A^{n_\alpha}\|$ . As the right side is integrable with respect to  $t$ , we can use a time-varying state transformation to remove this initial singularity [102]. The transformed state  $z(t)$  reads

$$z(t) = x(t) - \int_0^t f(\tau) d\tau x_0 = x(t) - \sum_{k=1}^{n_\alpha} \frac{(At^\alpha)^k}{\Gamma(\alpha k + 1)} x_0. \quad (4.9)$$

This leads to an initial value problem defined in the new coordinates with a bounded initial derivative

$$\begin{aligned}\dot{z}(t) = \dot{x}(t) - f(t)x_0 &= A^{n_\alpha} \left( z(t) + \sum_{k=1}^{n_\alpha} \frac{(At^\alpha)^k}{\Gamma(\alpha k + 1)} x_0 \right) + f(t)x_0 - f(t)x_0 \\ &= A^{n_\alpha} z(t) + A^{n_\alpha} \sum_{k=1}^{n_\alpha} \frac{(At^\alpha)^k}{\Gamma(\alpha k + 1)} x_0.\end{aligned}\quad (4.10)$$

With this reformulation of the problem standard solvers can be applied to simulate such fractional-order systems. However, the state transformation is only bounded for a finite time interval  $t \in [0, T]$ ,  $T < \infty$ . The state  $z(t)$  thus increases with time. After a time  $\Delta t$  has passed, we can use the original coordinates again as the singularity only occurs at  $t = t_0$ .

**Remark 4.2** (Numerical stability). Note that the eigenvalues  $\lambda$  of the matrices  $A$  and the eigenvalues  $\tilde{\lambda}$  of  $\tilde{A} = A^{n_\alpha}$  are connected via:

$$\lambda^{n_\alpha} = \tilde{\lambda}, \quad (4.11)$$

meaning the homogeneous part of the associated description (4.5) might be unstable since the eigenvalues of  $A^{n_\alpha}$  are not restricted to the negative open complex half-plane. The stability is the consequence of the additional function  $f(t)$  weighing the initial state. The reason for this is investigated in [82, p. 426ff.].

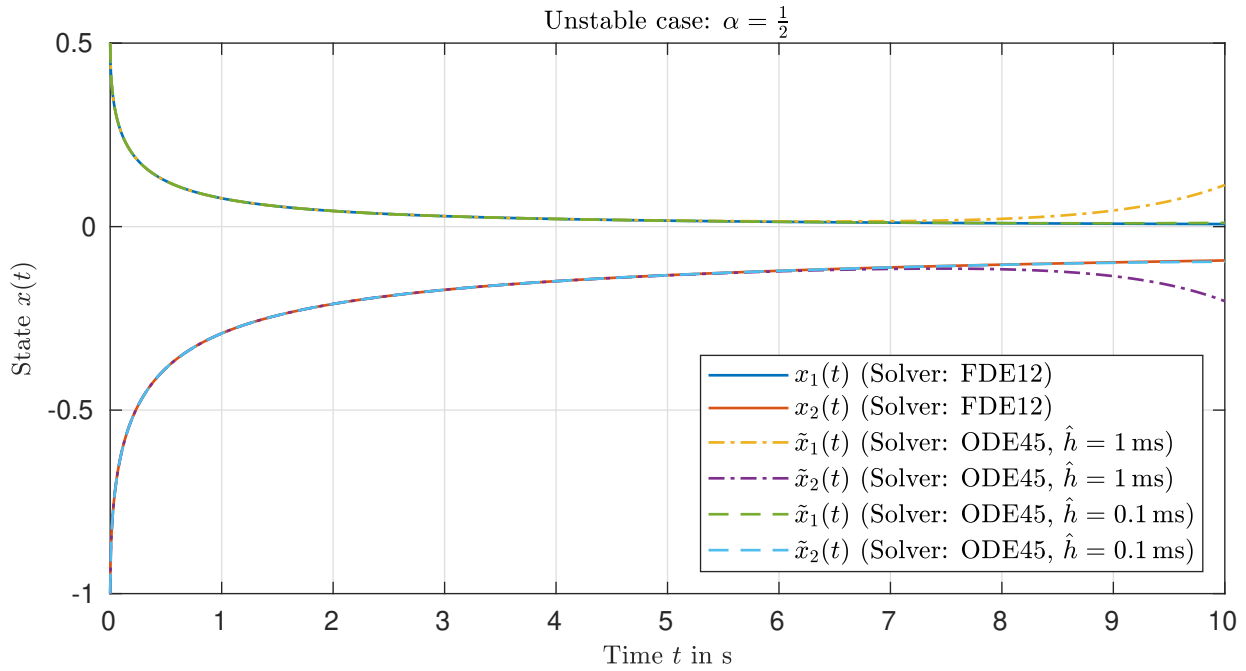


Figure 4.1: Comparison of the numerical solutions applying the associated integer-order system. Due to the unstable homogeneous dynamics, the integer-order solution deviates.

The authors use the fractional-order integral representation of the memory function  $f(t)$  and show that the unstable pseudo poles in  $A^{n_\alpha}$  are canceled by a corresponding pseudo zero.

Regarding the numerical solution of the initial value problem (4.5), this is problematic. For large times  $t \gg 0$ , the memory function is close to zero and therefore the homogeneous part  $A^{n_\alpha} \tilde{x}(t)$  dominates the evolution of the states towards unstable behavior. This is illustrated in Figure 4.1. It compares the solution of the system

$$\mathcal{D}^\alpha x(t) = \begin{pmatrix} 0 & 1 \\ -1 & -2 \end{pmatrix} x(t) = Ax(t), \quad \alpha = \frac{1}{2} \quad (4.12)$$

computed with a fractional-order solver *FDE12.m* [21] with simulations of the associated integer-order system with different step sizes using the solver *ODE45.m*. At the end of the time interval, the error increases. However, the error can be reduced by decreasing the step size, which is a clear hint towards a numerical error. It is caused by the unstable eigenvalues  $\tilde{\lambda}_{1,2} = 1$  of the integer-order system matrix  $\tilde{A} = A^2$  in contrast to the Hurwitz matrix  $A$  with  $\lambda_{1,2} = -1$ . If the system matrix of the associated integer-order system, however, is also Hurwitz, these numerical errors are less severe, as illustrated in Figure 4.2 for the system (4.12) with  $\alpha = \frac{1}{3}$ .

The stability analysis of the homogeneous part therefore only leads to a sufficient but not to a necessary condition.

**Theorem 4.2** (Stability (sufficient condition)). *The fractional-order LTI system  $\Sigma_{\text{FO}}$  with the order of differentiation  $\alpha^{-1} = n_\alpha \in \mathbb{N}$  is asymptotically stable if*

$$\text{Re}(\tilde{\lambda}_i) < 0, \quad i = 1, 2, \dots, n, \quad (4.13)$$

where  $\tilde{\lambda}_i$  are the eigenvalues of the associated system matrix  $A^{n_\alpha}$ .

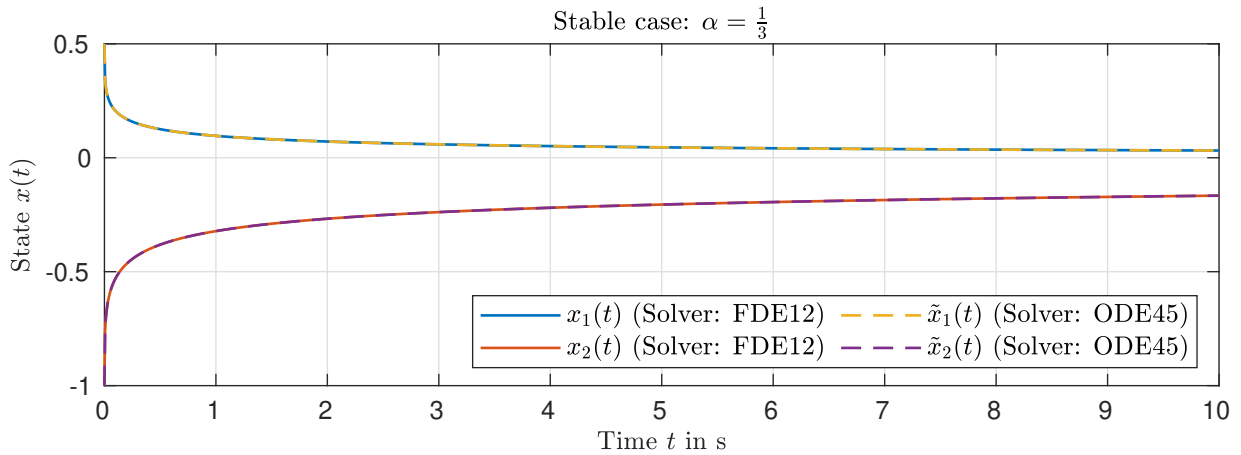


Figure 4.2: Comparison of the numerical solutions applying the associated integer-order system. As the matrix  $A^3$  is Hurwitz, the simulation of the integer-order system leads to the correct (stable) solution.

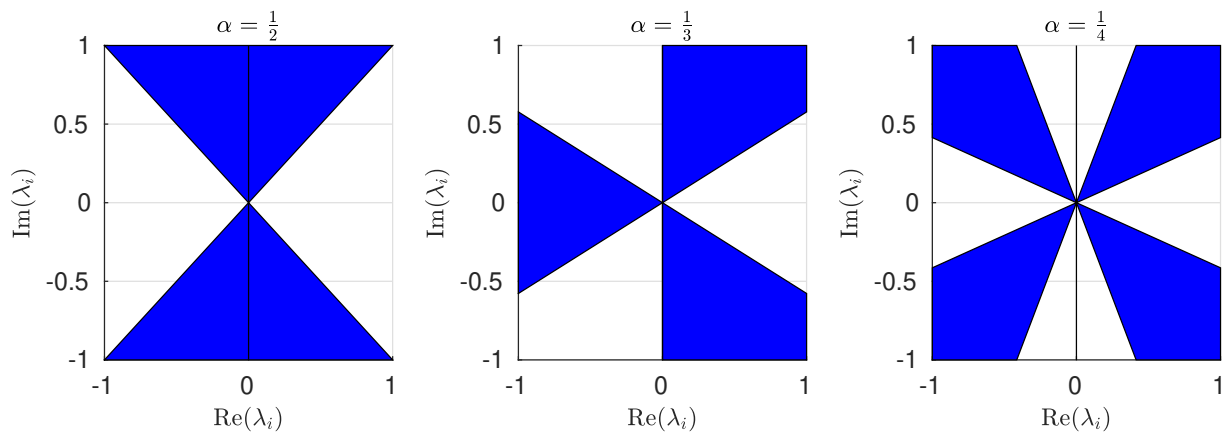


Figure 4.3: Reduced stability domains for Theorem 4.2 (colored in blue).

This sufficient condition corresponds to a linear matrix inequality condition given in [82, 86].

The application of this stability theorem to the controller design restricts the domain to place the poles significantly. This is illustrated in Figure 4.3 for three different values of  $\alpha$ . We have to guarantee that

$$\left| n_\alpha \arg(\lambda_i) - \left\lfloor \frac{n_\alpha \arg(\lambda_i)}{2\pi} \right\rfloor 2\pi \right| = |n_\alpha \arg(\lambda_i) \bmod 2\pi| > \frac{\pi}{2}. \quad (4.14)$$

This leads to the shapes depicted in Figure 4.3.

Having defined an associated integer-order system for the homogeneous fractional-order system, we now extend this idea to the non-homogeneous case with a nonzero input.

**Theorem 4.3** (Associated Integer-order system). *Considering the fractional-order linear time-invariant system given by (3.3) with the rational order of differentiation  $\alpha^{-1} = n_\alpha \in \mathbb{N}$ , an associated*

integer-order system is given by:

$$\dot{\tilde{x}}(t) = A^{n_\alpha} \tilde{x}(t) + t^{-1} \sum_{k=1}^{n_\alpha-1} \frac{(At^\alpha)^k}{\Gamma(\alpha k)} x_0 + \sum_{k=0}^{n_\alpha-1} A^{n_\alpha-1-k} B \left[ \mathcal{D}^{k\alpha} u(t) \right] + t^{-1} \sum_{k=1}^{n_\alpha-1} \frac{A^{k-1} t^{\alpha k}}{\Gamma(\alpha k)} B u(0). \quad (4.15)$$

*Proof.* The proof follows the ideas presented in [3, p. 15]. With  $x(0) = x_0$  the Laplace transform of (3.3a) reads

$$s^\alpha X(s) - s^{\alpha-1} x_0 = AX(s) + BU(s). \quad (4.16)$$

We want to change the order of derivation on the left side, hence we have to multiply the Laplace transform with powers of  $s$ . Let us first construct the integer-order case by multiplying (4.16) with  $s^{1-\alpha}$

$$sX(s) - x_0 = As^{1-\alpha} X(s) + Bs^{1-\alpha} U(s). \quad (4.17)$$

We have to introduce the initial conditions  $x_0$  and  $u_0 = u(0)$  in order to transform the terms  $s^{1-\alpha} X(s)$  and  $s^{1-\alpha} U(s)$  back to the time domain:

$$sX(s) - x_0 = A(s^{1-\alpha} X(s) - s^{-\alpha} x_0) + As^{-\alpha} x_0 + B(s^{1-\alpha} U(s) - s^{-\alpha} u_0) + Bs^{-\alpha} u_0. \quad (4.18)$$

With the Laplace transform of Caputo's operator (2.70) and  $\mathcal{L}\{t^{\alpha-1}; s\} = \Gamma(\alpha)s^{-\alpha}$  the time domain equivalent reads

$$\dot{x}(t) = A\mathcal{D}^{1-\alpha} x(t) + \frac{t^{\alpha-1}}{\Gamma(\alpha)} Ax_0 + B\mathcal{D}^{1-\alpha} u(t) + \frac{t^{\alpha-1}}{\Gamma(\alpha)} Bu_0. \quad (4.19)$$

An alternative representation contains the fractional-order integrals of the constant initial conditions

$$\dot{x}(t) = A\mathcal{D}^{1-\alpha} x(t) + \mathcal{I}^{\alpha-1} Ax_0 + B\mathcal{D}^{1-\alpha} u(t) + \mathcal{I}^{\alpha-1} Bu_0. \quad (4.20)$$

A similar approach is used to compute the fractional-order derivatives of the orders  $i\alpha$  with  $i = 2, \dots, n_\alpha - 1$ . The fractional-order derivative  $\mathcal{D}^{i\alpha} x(t)$  contains the fractional-order derivatives of  $x(t)$  of a lower order. The final step is reached, when the original system Equation (3.3a) is inserted. The recursive substitution of the derivatives in (4.19) leads to Equation (4.15) which completes the proof. □

**Remark 4.3** (Memory Shift). *Note that the fractional-order derivatives of the system also contain memory due to the operator. In the representation of the associated integer-order system, the memory of the original fractional-order description is shifted to the inputs and the memory function  $f(t)$  weighing the initial state  $x_0$ .*

**Remark 4.4** (Integer-order representations for Riemann systems). *We can apply the same techniques to construct an integer-order system associated to a Riemann system. As these systems contain a singularity at the initial time  $t_0$ , this yields a representation of minor usability, e.g. consider the system*

$${}^R\mathcal{D}^\alpha x(t) = Ax(t), \quad \alpha = \frac{1}{2}, \quad \mathcal{I}^{1-\alpha} x(\tau) \Big|_{\tau=0} = \bar{x}_0. \quad (4.21)$$

*Multiplying the Laplace transform of this system with  $s^{1-\alpha}$  yields*

$$s^\alpha X(s) - \bar{x}_0 = AX(s) \quad | \cdot s^{1-\alpha} \quad (4.22)$$

$$sX(s) - s^{1-\alpha} \bar{x}_0 = As^{1-\alpha} X(s). \quad (4.23)$$

Here, this multiplication does not lead to the integer-order derivative on the left hand side. Introducing artificial initial conditions  $x_0$  leads to

$$s^\alpha X(s) - x_0 - s^{1-\alpha} \bar{x}_0 = A(s^\alpha X(s) - \bar{x}_0) + A\bar{x}_0 - x_0 \quad (4.24)$$

Inserting (4.22) and transforming the results back to the time domain shows the difficulties

$$\dot{x}(t) = A^2 x(t) + (A\bar{x}_0 - x_0)\delta(t) + \bar{x}_0 {}^R\mathcal{D}^\alpha \delta(t). \quad (4.25)$$

This equation contains Dirac impulses  $\delta(t)$  as inputs in order to capture the singularity at  $t = 0$ . Furthermore, the initial state  $x_0 = x(0) = \infty$  is actually unbounded and we have not defined the concept of fractional-order differentiation for distributions. Therefore, an associated integer-order description of a linear fractional-order Riemann system is only useful if the initial conditions are zero.

**Remark 4.5.** The associated integer-order system contains the fractional-order derivatives of the input. Since the input  $u(\cdot) \in \mathcal{L}_{\text{loc}}^1[0, T]$  is only locally continuous and might jump, its fractional-order derivatives  $\mathcal{D}^{i n_\alpha}$  are infinite at each discontinuity. However, we do not lose the uniqueness of the solution because the fractional-order derivatives of the input are still integrable with respect to time and do not depend on the state. We show this by extending the previously introduced state transformation (4.9) by the fractional-order integrals of the input:

$$z(t) = \tilde{x}(t) - \sum_{k=1}^{n_\alpha-1} \frac{(At^\alpha)^k}{\Gamma(\alpha k + 1)} x_0 - \sum_{k=1}^{n_\alpha-1} A^{n_\alpha-1-k} B \left[ \mathcal{I}^{1-k\alpha} u(t) \right]. \quad (4.26)$$

Each integral is initialized with zero which leads to equal initial conditions

$$z(0) = \tilde{x}(0) = x_0. \quad (4.27)$$

The first derivative of the new state  $z(t)$  is given by

$$\begin{aligned} \dot{z}(t) &= \dot{\tilde{x}}(t) - \sum_{k=1}^{n_\alpha-1} \frac{\alpha k (At^\alpha)^k}{\Gamma(\alpha k + 1)} z_0 - \sum_{k=1}^{n_\alpha-1} A^{n_\alpha-1-k} B \frac{d}{dt} \left[ \mathcal{I}^{1-k\alpha} u(t) \right] \\ &= \dot{\tilde{x}}(t) - \sum_{k=1}^{n_\alpha-1} \frac{(At^\alpha)^k}{\Gamma(\alpha k)} x_0 - \sum_{k=1}^{n_\alpha-1} A^{n_\alpha-1-k} B {}^R\mathcal{D}^{k\alpha} u(t). \end{aligned} \quad (4.28)$$

This equation contains the first order derivative of a fractional-order integral; the order of operations corresponds to the Riemann-Liouville derivative (2.42). We apply equation (2.46) leading to the needed fractional-order derivatives of the input

$$\dot{z}(t) = \dot{\tilde{x}}(t) + A^{n_\alpha} \sum_{k=1}^{n_\alpha-1} \frac{(At^\alpha)^k}{\Gamma(\alpha k)} x_0 - \sum_{k=1}^{n_\alpha-1} A^{n_\alpha-1-k} B \left( \mathcal{D}^{k\alpha} u(t) + \frac{t^{-k\alpha} u(0^+)}{\Gamma(1-k\alpha)} \right). \quad (4.29)$$

Substituting  $\dot{x}(t)$  with (4.15) we see that all fractional-order derivatives as well as the initial singularity are canceled in the dynamics of the new state, i.e.

$$\begin{aligned} \dot{z}(t) &= \underbrace{A^{n_\alpha} \tilde{x}(t) + t^{-1} \sum_{k=0}^{n_\alpha-1} \frac{(At^\alpha)^k}{\Gamma(\alpha k)} x_0 + \sum_{k=0}^{n_\alpha-1} A^{n_\alpha-1-k} B \left[ \mathcal{D}^{k\alpha} u(t) \right] + t^{-1} \sum_{k=1}^{n_\alpha-1} \frac{A^{k-1} t^{\alpha k}}{\Gamma(\alpha k)} B u(0^+)}_{\dot{\tilde{x}}(t)} \\ &\quad - \sum_{k=1}^{n_\alpha-1} \frac{(At^\alpha)^k}{\Gamma(\alpha k)} x_0 - \sum_{k=1}^{n_\alpha-1} A^{n_\alpha-1-k} B \mathcal{D}^{k\alpha} u(t) - \sum_{k=1}^{n_\alpha-1} A^{n_\alpha-1-k} B \frac{t^{-k\alpha} u(0^+)}{\Gamma(1-k\alpha)} \\ &= A^{n_\alpha} \tilde{x}(t) + A^{n_\alpha-1} B u(t). \end{aligned} \quad (4.30)$$

Finally, we have to replace  $\tilde{x}(t)$  with equation (4.26) leading to

$$\dot{z}(t) = A^{n_\alpha} z(t) + A^{n_\alpha} \int_0^t f(\tau) d\tau x_0 + A^{n_\alpha} \sum_{k=1}^{n_\alpha-1} A^{n_\alpha-1-k} B \left[ \mathcal{I}^{1-k\alpha} u(t) \right] + A^{n_\alpha-1} B u(t). \quad (4.31)$$

Note that the norm of the state  $z(t)$  increases with time as the integral of the memory function  $f(t)$  is increasing. In addition to that the fractional-order integrals are not bounded. As the fractional-order integral depends on the past of the input, we can only remove the increasing influence of the integrated memory function after the time interval  $\Delta t$ . If the input  $u(t)$  is not converging to zero for  $t \rightarrow \infty$  we hence have to restrict any implementation using (4.31) to a finite time interval.

## 4.2 Low Memory Fractional-Order LTI-System Implementation

As shown in Section 2.6, the implementation of fractional-order systems requires a lot of memory, as each fractional-order integrator needs its own memory. If we apply an integer-order approximation of the order  $N$ , the direct implementation of a controller which can be parameterized by (3.3) requires

$$N_{\text{IO-States,FO}} = n N \quad (4.32)$$

states. Compared to that, the associated integer-order system only requires the fractional-order integrals of the input. With the same order of approximation, we can reduce the required implementation states to

$$N_{\text{IO-States,IO-LTV}} = n + p (n_\alpha - 1) N, \quad (4.33)$$

as we have to implement  $n$  states of the associated integer-order system and  $p \cdot (n_\alpha - 1)$  approximations of the fractional-order integrals of the input  $u(t) \in \mathbb{R}^p$ . The required memory can be reduced further as only the past of the input needs to be stored in order to compute fractional-order integrals of various orders.

Obviously, this strategy is especially applicable for systems with a higher number of states  $n$  and a small inverted order  $n_\alpha$ . However, we have to take additional considerations into account:

1. In order to reduce the numerical error, the matrix  $A^{n_\alpha}$  has to be Hurwitz. In case of a pole-placement controller (using an observer) this restricts the possible pole locations.
2. In order to maintain a bounded transformed state  $z(t)$ , the controller application has to be either
  - a) limited to a finite time horizon (see Remark 4.5) or
  - b) can only be used to stabilize the origin, such that the controller input and its fractional-order integrals remain bounded.

### 4.3 Indirect Observer Design

Having defined the integer-order dynamics we can use this description to design an observer. In order to keep the notation short, we combine the fractional-order derivatives of the input to a generalized input

$$\dot{x}(t) = A^{n_\alpha}x(t) + f(t)x_0 + \bar{B}\bar{u}(t) \quad (4.34)$$

with

$$\bar{B} = \begin{pmatrix} A^{n_\alpha-1}B \\ A^{n_\alpha-2}B \\ \vdots \\ B \end{pmatrix}, \quad \bar{u}(t) = \begin{pmatrix} u(t) \\ \mathcal{D}^\alpha u(t) \\ \vdots \\ \mathcal{D}^{(n_\alpha-1)\alpha}u(t) \end{pmatrix}. \quad (4.35)$$

The aim here is to achieve exponential convergence of the estimation error and overcome the algebraic nature of the fractional-order system.

#### 4.3.1 Associated Integer-Order System - Observability Analysis

However, the observability properties of the original system (3.3) and the time-varying description (4.34) do vary.

**Theorem 4.4.** *The complete observability of the fractional-order LTI system (3.3), i.e. of the pair  $(C, A)$  does not imply the complete observability of the associated time varying integer-order system (4.34).*

*Proof.* First, we consider  $x_0 = 0$ . With zero initial conditions, the associated integer-order system is reduced to the time invariant part

$$\dot{x}(t) = A^{n_\alpha}x(t) + \bar{B}\bar{u}(t) \quad (4.36)$$

which is observable if the pair  $(C, A^{n_\alpha})$  is observable. We construct a counterexample with  $A \in \mathbb{R}^{3 \times 3}$  with the characteristic polynomial:

$$\lambda^3 + a_2\lambda^2 + a_1\lambda + a_0 = 0. \quad (4.37)$$

The order of differentiation be  $\alpha = \frac{1}{2}$  which leads to the observability matrix given by:

$$\bar{O} = \begin{pmatrix} C \\ CA^2 \\ CA^4 \end{pmatrix}. \quad (4.38)$$

Applying the theorem of Cayley-Hamilton twice leads to

$$\begin{aligned} A^3 &= -a_2A^2 - a_1A - a_0I \\ A^4 &= -a_2A^3 - a_1A^2 - a_0A \\ &= -a_2(-a_2A^2 - a_1A - a_0I) - a_1A^2 - a_0A \\ &= (a_2^2 - a_1)A^2 + (a_1a_2 - a_0)A + a_2a_0I \end{aligned}$$



and the changed observability matrix is given by

$$\tilde{\mathcal{O}} = \begin{pmatrix} C \\ CA^2 \\ C \left( (a_2^2 - a_1)A^2 + (a_1a_2 - a_0)A + a_2a_0I \right) \end{pmatrix}. \quad (4.39)$$

Clearly, for  $(a_1a_2 - a_0) = 0$  the rank of the observability matrix  $\tilde{\mathcal{O}}$  drops, i.e.

$$\text{rank}(\tilde{\mathcal{O}}) = 2. \quad (4.40)$$

If  $x_0 \neq 0$  the situation is even more complicated, because the dynamics depend on the initial conditions  $x_0$ . The integer-order system is time varying, therefore we cannot apply Theorem 3.6.  $\square$

There are different approaches for taking the time variation into account for the observer design. As a first approach, we can consider the term  $f(t)x_0$  as a disturbance which we include in the state reconstruction. Within the integer-order framework, however, this is only possible by using a polynomial approximation because integer-order systems can only produce exponential, harmonic, and polynomial functions.

Another approach is to use a time varying observer gain  $L(t)$ . In order to keep the analysis within a linear framework, we extend the state by the constant state  $\xi \in \mathbb{R}^n$  representing the initial conditions. This gives us the augmented system

$$\begin{pmatrix} \dot{x}(t) \\ \dot{\xi}(t) \end{pmatrix} = \begin{pmatrix} A^{n_\alpha} & f(t) \\ 0 & 0 \end{pmatrix} \begin{pmatrix} x(t) \\ \xi(t) \end{pmatrix} + \begin{pmatrix} \bar{B} \\ 0 \end{pmatrix} \bar{u}(t) \quad (4.41)$$

with the initial conditions  $x(0) = \xi(0) = x_0$ . With this representation and the extended output equation

$$y(t) = \begin{pmatrix} C & 0 \end{pmatrix} \begin{pmatrix} x(t) \\ \xi(t) \end{pmatrix} = \bar{C} \begin{pmatrix} x(t) \\ \xi(t) \end{pmatrix} \quad (4.42)$$

we can now apply the observability theorems for linear time-varying integer-order system [90] (see Appendix A.2).

The application of Theorem A.1 leads to the following observability matrix with the abbreviation  $\tilde{A} = A^{n_\alpha}$ :

$$\mathcal{O}(t) = \begin{pmatrix} \bar{C} \\ \bar{C} \tilde{A}(t) \\ \bar{C} \left( \tilde{A}^2(t) + \frac{d}{dt} \tilde{A}(t) \right) \\ \vdots \\ \bar{C} \sum_{k=0}^{2n-1} \left( \tilde{A}^k(t) \right)^{(2n-1-k)} \end{pmatrix} = \underbrace{\begin{pmatrix} C \\ C\tilde{A} \\ C\tilde{A}^2 \\ \vdots \\ C\tilde{A}^{2n-1} \end{pmatrix}}_{\mathcal{O}_1 \in \mathbb{R}^{2nq \times n}} \underbrace{\begin{pmatrix} 0 \\ Cf(t) \\ C \left( \tilde{A}f(t) + \dot{f}(t) \right) \\ \vdots \\ C \sum_{k=1}^{2n-1} \tilde{A}^{2n-1-k} f^{(k-1)}(t) \end{pmatrix}}_{\mathcal{O}_2(t) \in \mathbb{R}^{2nq \times n}}. \quad (4.43)$$

**Corollary 4.1.** *The extended state representation (4.41)-(4.42) is completely observable on  $[t_0, t_f]$  if and only if there exists a time instant  $t_a \in [t_0, t_f]$  such that the observability matrix  $\mathcal{O}(t)$  given in (4.43) has full rank*

$$\text{rank}(\mathcal{O}(t_a)) = 2n. \quad (4.44)$$

A typical approach to check the observability would be to evaluate the determinant of  $\mathcal{O}(t)$  numerically. However, we can give more detailed necessary conditions.

**Theorem 4.5** (Necessary Conditions). *If the associated integer-order system (4.41) is completely observable, then*

1. the pair  $(C, A^{n_\alpha})$  is completely observable
2. the original system matrix is non-singular:  $\text{rank}(A) = n$ .

*Proof.* ( $\Rightarrow$  1) The full rank of the observability matrix, i.e.  $\text{rank}(\mathcal{O}(t)) = 2n$  implies  $\text{rank}(\mathcal{O}_1) = n$ . The column block  $\mathcal{O}_1$  is time invariant and can be rewritten to

$$\mathcal{O}_1 = \begin{pmatrix} \begin{pmatrix} C \\ C\tilde{A} \\ \vdots \\ C\tilde{A}^{n-1} \end{pmatrix} \\ \begin{pmatrix} C \\ C\tilde{A} \\ \vdots \\ C\tilde{A}^{n-1} \end{pmatrix} \tilde{A}^n \end{pmatrix} = \begin{pmatrix} \tilde{\mathcal{O}} \\ \tilde{\mathcal{O}}\tilde{A}^n \end{pmatrix}. \quad (4.45)$$

We see that the observability matrix of the pair  $(A^{n_\alpha}, C)$  occurs and is of full rank as the product  $\tilde{\mathcal{O}}\tilde{A}^n$  does not increase the rank. Hence the pair is observable.

( $\Rightarrow$  2) The rank of the memory function  $f(t)$  (see (4.6)) is determined by the system matrix  $A$

$$f(t) = t^{-1} \sum_{k=1}^{n_\alpha-1} \frac{A^{k-1} t^{\alpha k}}{\Gamma(\alpha k)} A = \tilde{f}(t)A. \quad (4.46)$$

Therefore, the second necessary condition is a result of the factorization of the second part

$$\mathcal{O}_2(t) = \underbrace{\begin{pmatrix} C & & & \\ C\tilde{A} & C & & \\ \vdots & \vdots & \ddots & \\ C\tilde{A}^{2n-1} & \dots & C\tilde{A} & C \end{pmatrix}}_{M \in \mathbb{R}^{2nq \times 2n^2}} \underbrace{\begin{pmatrix} 0 \\ \tilde{f}(t) \\ \dot{\tilde{f}}(t) \\ \vdots \\ \tilde{f}^{(2n-2)}(t) \end{pmatrix}}_{\tilde{F}(t) \in \mathbb{R}^{2n^2 \times n}} A.$$

With  $\text{rank}(\mathcal{O}(t)) = 2n$  we can conclude  $\text{rank}(\mathcal{O}_2(t)) = n$ , thus follows

$$n = \text{rank}(M\tilde{F}(t)A) \leq \min \left[ \text{rank}(M), \text{rank}(\tilde{F}(t)), \text{rank}(A) \right], \quad (4.47)$$

with  $\max(\text{rank}(A)) = n$  we conclude  $\text{rank}(A) = n$  which completes the proof.  $\square$

**Remark 4.6.** The memory function  $f(t)$  and all its derivatives converge to zero for large times  $t \rightarrow \infty$ , which leads to a numerically ill-conditioned observability matrix  $\mathcal{O}(t)$  for large  $t$

$$\text{rank}(\mathcal{O}(t)) \xrightarrow{t \rightarrow \infty} \text{rank}(\mathcal{O}_1) < 2n. \quad (4.48)$$

This is a consequence of the fractional-order operators and its memory. The effect of the initial conditions  $x_0$  on the actual state decreases over time.

**Remark 4.7.** The results of Theorem A.1 to check the observability of linear time varying systems are necessary and sufficient [90], hence we have to explain the case of the fractional-order system being observable but the time varying integer-order not. The reason for this discrepancy are the different system classes we are analyzing here. The theorem given in [90] can be applied to linear time-varying integer-order systems with an arbitrary initial state. The extended associated integer-order system, however, requires special initial conditions in the auxiliary state  $\xi$ . The observability analysis does not take these into account, hence the results of Theorem 4.5 are conservative.

**Remark 4.8.** The observability of the associated integer-order system is not required to estimate the state without an algebraic decay. If the fractional-order LTI system is completely observable we apply the idea of an impulsive observer [78] as shown in Section 4.3.3.

### 4.3.2 Time-Varying Integer-Order Observer

Supposing the associated integer-order system is completely observable, we can use a time-varying gain  $\bar{L}(t)$  to design an exponentially converging Luenberger observer. The time-varying observer in this case is given by

$$\begin{pmatrix} \dot{\hat{z}}(t) \\ \dot{\hat{\xi}}(t) \end{pmatrix} = \bar{A}(t) \begin{pmatrix} \hat{z}(t) \\ \hat{\xi}(t) \end{pmatrix} + \begin{pmatrix} \bar{B} \\ 0 \end{pmatrix} \bar{u}(t) - \bar{L}(t) [y(t) - \hat{y}(t)] \quad (4.49)$$

$$\hat{y}(t) = \bar{C} \begin{pmatrix} \hat{z}(t) \\ \hat{\xi}(t) \end{pmatrix} + \bar{D} \bar{u}(t). \quad (4.50)$$

The dynamics of the extended estimation error (including the initial state  $\xi$ ) with

$$\bar{e}(t) = \begin{pmatrix} z(t) \\ \xi(t) \end{pmatrix} - \begin{pmatrix} \hat{z}(t) \\ \hat{\xi}(t) \end{pmatrix} \quad (4.51)$$

are given by

$$\dot{\bar{e}}(t) = (\bar{A}(t) + \bar{L}(t)\bar{C}) \bar{e}(t). \quad (4.52)$$

As the matrix  $\bar{A}(t)$  as well as the corresponding observability matrix are unbounded at  $t = t_0$ , the observer has to start slightly afterwards at an initial time  $\hat{t}_0 > \varepsilon > 0$ .

The design of the time-varying gains  $L(t)$  is based on the Lyapunov transform  $V(t)$  which exists as the system is totally observable [90] such that  $\mathcal{O}(t)$  is non-singular on  $t \in [\hat{t}_0, t_F]$ . The state transformation is defined by [81]:

$$V^{-1}(t) = \begin{pmatrix} P_0(t) & P_1(t) & \cdots & P_{2n-1}(t) \end{pmatrix} \quad (4.53)$$

with

$$P_0(t) = O^{-1}(t)e_{2n}$$

$$P_k(t) = \bar{A}(t) (P_{k-1}(t)) + \frac{d}{dt}P_{k-1}(t).$$

Applying  $V(t)$  to the extended estimation error  $\epsilon(t) = V(t)\bar{e}(t)$  leads to the time-varying observable canonical form.

The choice of  $L(t)$  hence aims at the complete compensation of any time varying terms and ensuring asymptotic stability of the remaining time-invariant part:

$$\bar{L}(t) = - \sum_{k=0}^{2n-1} l_k P_k(t) \quad (4.54)$$

with  $l_k \in \mathbb{R}$  determining the Hurwitz polynomial

$$\lambda^{2n} + l_{2n-1}\lambda^{2n-1} \dots + l_1\lambda + l_0. \quad (4.55)$$

**Example 4.1.** To illustrate this concept we use a simulation study. We consider the following fractional-order LTI system:

$$\mathcal{D}^{\frac{1}{3}}x(t) = \begin{pmatrix} 0 & 1 \\ -1 & -2 \end{pmatrix} x(t) + \begin{pmatrix} -0.7 \\ 0.5 \end{pmatrix} u(t) \quad (4.56a)$$

$$y(t) = \begin{pmatrix} 0.5 & -2 \end{pmatrix} x(t) \quad (4.56b)$$

with  $x^\top(0) = \begin{pmatrix} 5 & -5 \end{pmatrix}$ . The system is asymptotically stable, with the eigenvalues at  $\lambda_{1,2} = -1$  and completely observable, as the observability matrix obeys

$$\text{rank}(\mathcal{O}) = \text{rank} \left( \begin{pmatrix} 0.5 & -2 \\ 2 & 4.5 \end{pmatrix} \right) = 2 = n.$$

The time-varying observability matrix of the extended integer-order system  $\mathcal{O}(t)$  is given by:

$$\mathcal{O}(t) = \begin{pmatrix} \frac{1}{2} & -2 & 0 & 0 \\ 7 & \frac{19}{2} & \frac{2t^{\alpha-1}}{\Gamma(\alpha)} - \frac{9t^{2\alpha-1}}{2\Gamma(2\alpha)} & \frac{9t^{\alpha-1}}{2\Gamma(\alpha)} - \frac{7t^{2\alpha-1}}{\Gamma(2\alpha)} \\ -\frac{29}{2} & -17 & o_{33}(t) & o_{34}(t) \\ 22 & \frac{49}{2} & o_{43}(t) & o_{44}(t) \end{pmatrix}$$

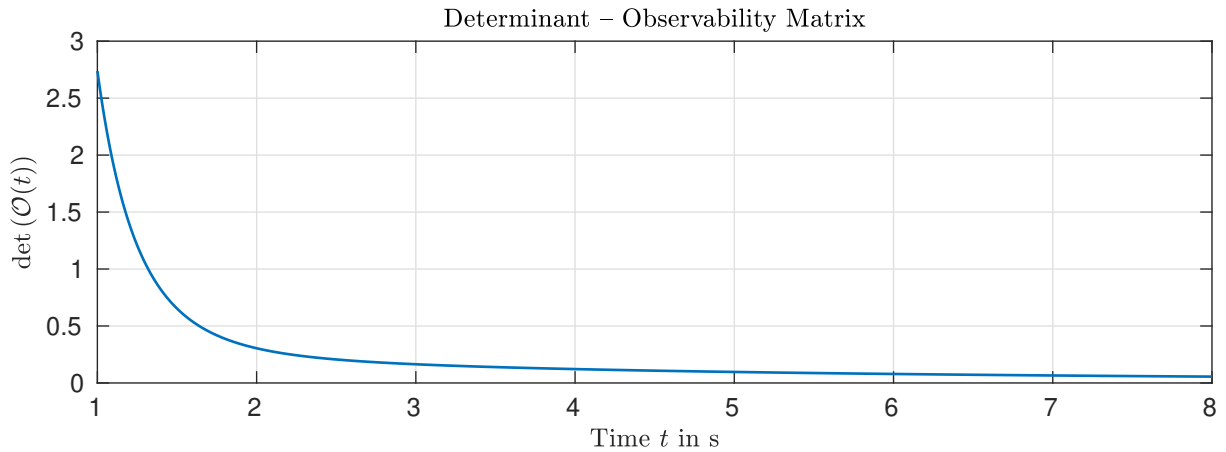


Figure 4.4: The determinant of the time-varying observability matrix tends to zero for large times.

with

$$\begin{aligned}
 o_{33}(t) &= \frac{12t^{2\alpha-1}}{\Gamma(2\alpha)} - \frac{19t^{\alpha-1}}{2\Gamma(\alpha)} - \frac{9(2\alpha-1)t^{2\alpha-2}}{2\Gamma(2\alpha)} + \frac{2(\alpha-1)t^{\alpha-2}}{\Gamma(\alpha)} \\
 o_{34}(t) &= \frac{29t^{2\alpha-1}}{2\Gamma(2\alpha)} - \frac{12t^{\alpha-1}}{\Gamma(\alpha)} - \frac{7(2\alpha-1)t^{2\alpha-2}}{\Gamma(2\alpha)} + \frac{9(\alpha-1)t^{\alpha-2}}{2\Gamma(\alpha)} \\
 o_{43}(t) &= \frac{17t^{\alpha-1}}{\Gamma(\alpha)} - \frac{39t^{2\alpha-1}}{2\Gamma(2\alpha)} + \frac{12(2\alpha-1)t^{2\alpha-2}}{\Gamma(2\alpha)} - \frac{19(\alpha-1)t^{\alpha-2}}{2\Gamma(\alpha)} + \\
 &\quad \frac{2(\alpha-1)(\alpha-2)t^{\alpha-3}}{\Gamma(\alpha)} - \frac{9(2\alpha-1)(2\alpha-2)t^{2\alpha-3}}{2\Gamma(2\alpha)} \\
 o_{44}(t) &= \frac{39t^{\alpha-1}}{2\Gamma(\alpha)} - \frac{22t^{2\alpha-1}}{\Gamma(2\alpha)} + \frac{29(2\alpha-1)t^{2\alpha-2}}{2\Gamma(2\alpha)} - \frac{12(\alpha-1)t^{\alpha-2}}{\Gamma(\alpha)} + \\
 &\quad \frac{9(\alpha-1)(\alpha-2)t^{\alpha-3}}{2\Gamma(\alpha)} - \frac{7(2\alpha-1)(2\alpha-2)t^{2\alpha-3}}{\Gamma(2\alpha)}
 \end{aligned}$$

For the chosen time interval from  $\hat{t}_0 = 1$  s to  $t_f = 10$  s the observability matrix of the associated integer-order system is regular. In Figure 4.4 the determinant is plotted. It is monotonically decreasing, which can lead to numerical errors towards the upper interval limit. The poles of the remaining time-invariant dynamics in the observer coordinates are set to  $\lambda = \{-3.99, -4.18, -3.61, -3.42\}$ . For comparison, a standard fractional-order observer with comparable poles at  $\lambda_{FO} = \{-3.99, -3.61\}$  is used. The results of the state estimates are depicted in Figure 4.5. The time-varying integer-order observer shows a huge peaking just after initialization. However, it converges exponentially and clearly leads to better estimates after  $t = 5$  s. The reason for this extreme peaking lies within the time-varying dynamics itself - in the observer coordinates, the overshooting of the estimation error is not that drastic. The peaking increases if the observer gains are increased or if the observer starts earlier, i.e.  $\hat{t}_0$  is reduced. Figure 4.6 shows the estimation of the initial state  $x_0$ . The observer is capable of estimating it with exponential convergence, as well, although the peaking phenomenon is also visible here.

The observer gains are shown in Figure 4.7. They increase over time, as the determinant of the observability matrix decays. The more time has passed, the more difficult it is to reconstruct the initial state based on measurements because the memory decays. For these reasons the observer is not very robust with respect to measurement noise and should only be applied on a closed time interval.

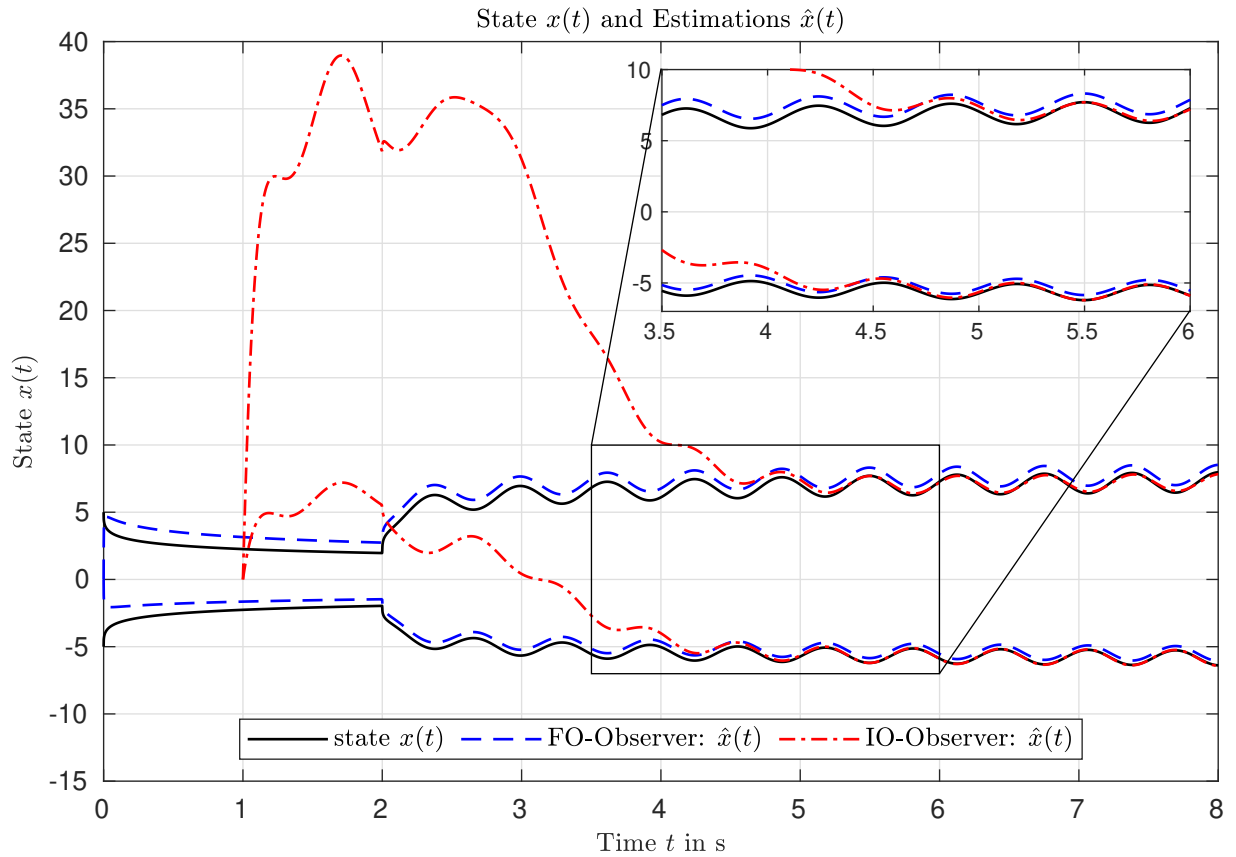


Figure 4.5: With the time-varying observer, the states are estimated exponentially. However, the initial peaking is large.

*Note that the absolute time  $t$  is a crucial parameter here. If the gains act with a time offset, the performance of the observer drops drastically, which results in a decay comparable to the original algebraic one.*

### 4.3.3 Impulsive-Observer Design and Implementation

Let us consider a fractional-order system with concentrated initial conditions as specified in equation (3.3). Instead of using a fractional-order Luenberger observer, we can also apply the concept of impulsive observers to the fractional-order case. Therefore, we consider two fractional-order observers with different gains  $L_1$  and  $L_2$

$$\mathcal{D}^\alpha \hat{x}_1(t) = (A + L_1 C) \hat{x}_1(t) + Bu(t) + L_1 y(t) \quad (4.57)$$

$$\mathcal{D}^\alpha \hat{x}_2(t) = (A + L_2 C) \hat{x}_2(t) + Bu(t) + L_2 y(t) \quad (4.58)$$

leading to the fractional-order dynamics of the estimation error  $e_i(t) = \hat{x}_i(t) - x(t)$  given by

$$\mathcal{D}^\alpha e_1(t) = (A + L_1 C) e_1(t) = F_1 e_1(t) \quad (4.59)$$

$$\mathcal{D}^\alpha e_2(t) = (A + L_2 C) e_2(t) = F_2 e_2(t). \quad (4.60)$$

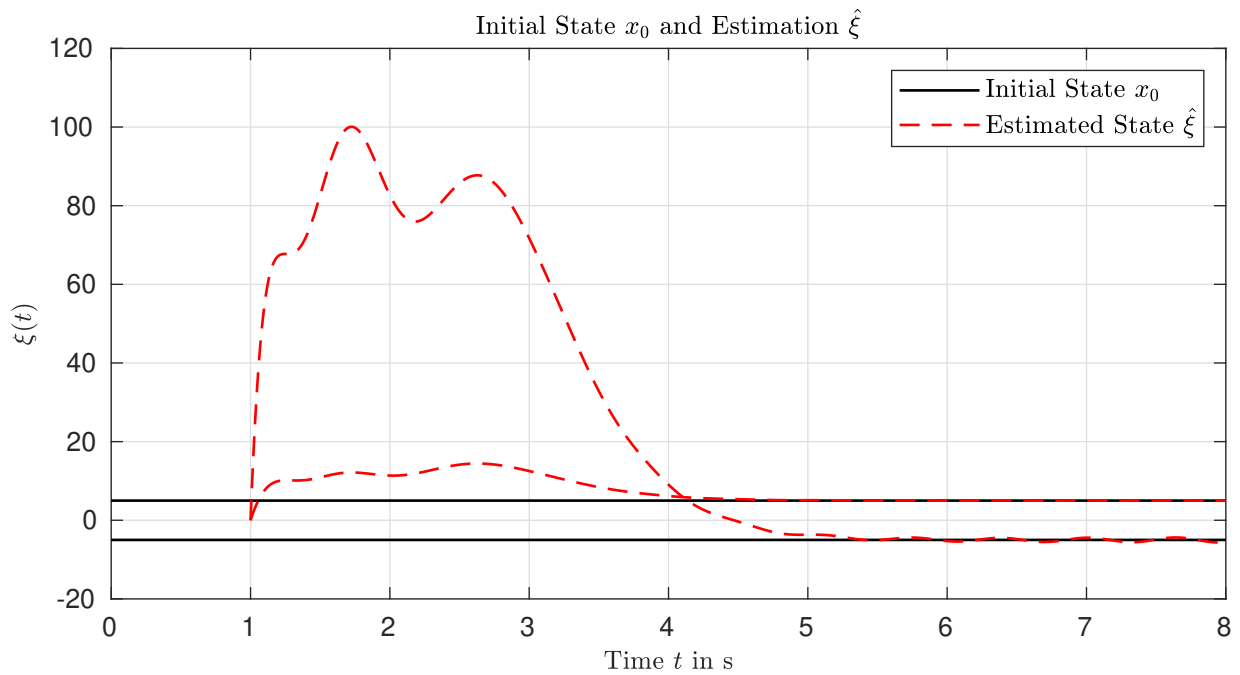


Figure 4.6: The initial states are also estimated correctly. The initial peaking also occurs in these additional states.

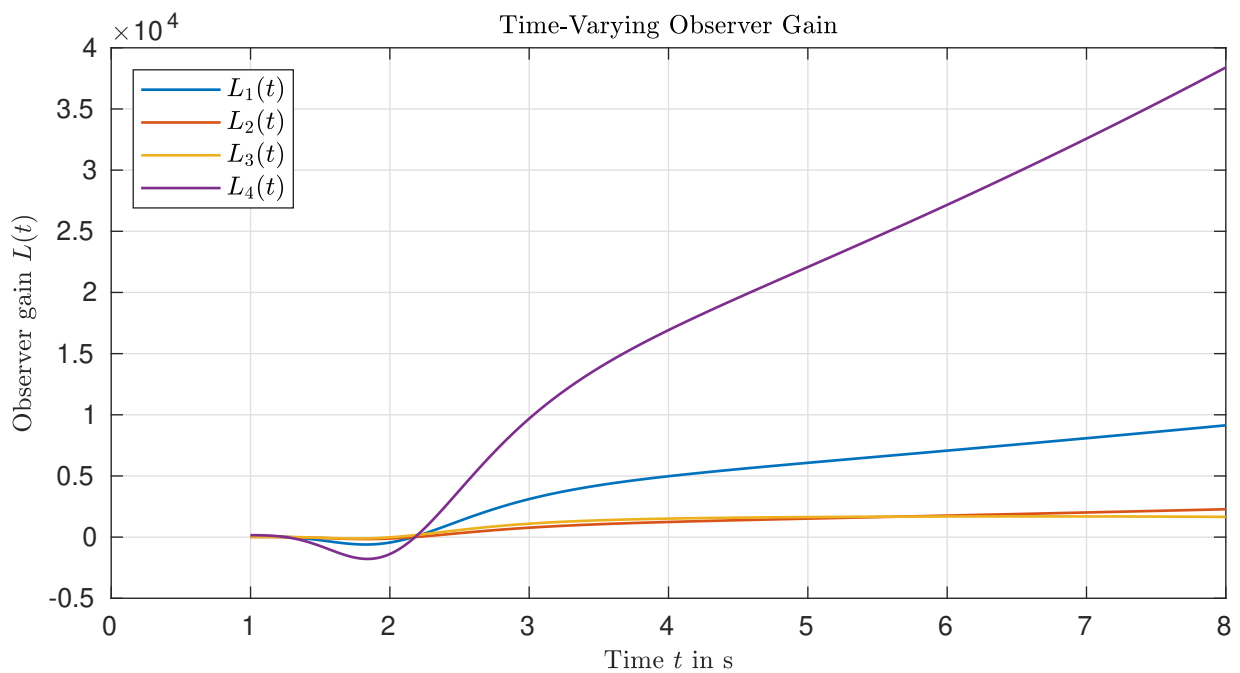


Figure 4.7: The observer gains  $L_i(t)$  increase with time, as the determinant of the observability matrix  $\det(\mathcal{O}(t))$  tends to zero.

The estimation error at the time  $\delta$  is given by the transition matrix and the initial error  $e_i(0)$ :

$$e_i(\delta) = \mathcal{E}_{\alpha,1}(F_i\delta^\alpha)e_i(0). \quad (4.61)$$

In this equation there are  $2n$  unknowns: the initial error  $e_i(0) \in \mathbb{R}^n$  and the actual error  $e_i(\delta) \in \mathbb{R}^n$ . The benefit of the second observer is clearly to add  $n$  equations, such that we can algebraically solve for the estimation error and the actual system state  $x(t)$  [78]. Going back to the original observer coordinates yields

$$\begin{pmatrix} \hat{x}_1(\delta) - x(\delta) \\ \hat{x}_2(\delta) - x(\delta) \end{pmatrix} = \begin{pmatrix} \mathcal{E}_{\alpha,1}(F_1\delta^\alpha) & 0 \\ 0 & \mathcal{E}_{\alpha,1}(F_2\delta^\alpha) \end{pmatrix} \begin{pmatrix} \hat{x}_1(0) - x(0) \\ \hat{x}_2(0) - x(0) \end{pmatrix}. \quad (4.62)$$

rearranging the matrix leads to

$$\underbrace{\begin{pmatrix} I & -\mathcal{E}_{\alpha,1}(F_1\delta^\alpha) \\ I & -\mathcal{E}_{\alpha,1}(F_2\delta^\alpha) \end{pmatrix}}_{\Omega} \begin{pmatrix} x(\delta) \\ x(0) \end{pmatrix} = \begin{pmatrix} \hat{x}_1(\delta) - \mathcal{E}_{\alpha,1}(F_1\delta^\alpha)\hat{x}_1(0) \\ \hat{x}_2(\delta) - \mathcal{E}_{\alpha,1}(F_2\delta^\alpha)\hat{x}_2(0) \end{pmatrix}. \quad (4.63)$$

Supposing the inverse exists, we can compute the initial state  $x(0)$  as well as the actual state  $x(\delta)$  by

$$\begin{pmatrix} x(\delta) \\ x(0) \end{pmatrix} = \Omega^{-1} \begin{pmatrix} \hat{x}_1(\delta) - \mathcal{E}_{\alpha,1}(F_1\delta^\alpha)\hat{x}_1(0) \\ \hat{x}_2(\delta) - \mathcal{E}_{\alpha,1}(F_2\delta^\alpha)\hat{x}_2(0) \end{pmatrix}. \quad (4.64)$$

For integer-order systems it is sufficient to reset the observer state at the time instant  $t = \delta$  such that the estimation error vanishes after the observer state reset. In the case of fractional-order systems this is not enough as it does not take the memory of the operator into account. One way to solve this issue would be to store the measurements of the in- and output for the first time interval  $t \in [t_0, \delta]$  and let the observer rerun this time period with the estimated initial state. This way the memory of the observer builds up correctly. The disadvantage of this approach is obvious - with a limited hardware we might only be able to reset the observer once within a small time interval  $\delta$ . Furthermore, we do not use the available information of the estimated state  $x(\delta)$ , as the rerun of the observer might include numerical errors.

The alternative would be to use the associated integer-order system if it exists, i.e.  $\alpha^{-1} = n_\alpha \in \mathbb{N}$ . Here, we do not have to restart any fractional-order integration, as only the inputs of the observer are given in terms of fractional-order derivatives and the corresponding memory is independent of the observer state. However, we have to make slight adjustments, as the direct usage of the associated integer-order system, i.e.

$$\dot{\hat{x}}_i(t) = A^{n_\alpha}\hat{x}_i(t) + f(t)\hat{x}_i(0) + \bar{B}\bar{u}(t) + \bar{L}_i\bar{e}_{y,i}(t) \quad (4.65)$$

with

$$\bar{L}_i = \begin{pmatrix} A^{n_\alpha-1}L_i \\ A^{n_\alpha-2}L_i \\ \vdots \\ L_i \end{pmatrix}, \quad \bar{e}_{y,i}(t) = \begin{pmatrix} e_{y,i}(t) \\ \mathcal{D}^\alpha e_{y,i}(t) \\ \vdots \\ \mathcal{D}^{(n_\alpha-1)\alpha} e_{y,i}(t) \end{pmatrix} \quad (4.66)$$

builds up a memory of the output error  $e_{y,i}(t) = C\hat{x}_i(t) - y(t)$  as the associated integer-order dynamics contain its fractional-order derivatives. Therefore, we set up the observer in a slightly different way

$$\dot{\hat{x}}_i(t) = A^{n_\alpha}\hat{x}_i(t) + f(t)\hat{x}_i(0) + \bar{B}\bar{u}(t) + L_i(C\hat{x}_i(t) - y(t)), \quad \hat{x}_i(0) = \hat{x}_{i,0}. \quad (4.67)$$



This leads to the disturbed integer-order error dynamics

$$\dot{e}_i(t) = (A^{n_\alpha} + L_i C)e_i(t) + f(t)e_i(0). \quad (4.68)$$

As shown in Theorem 4.4, the observability of the pair  $(C, A)$  differs from the pair  $(C, A^{n_\alpha})$ . Therefore, this implementation approach additionally requires the observability of the pair  $(C, A^{n_\alpha})$ . As the memory function  $f(t)$  is known we can derive the transition matrix of the initial estimation error:

$$e_i(\delta) = \left( \exp((A^{n_\alpha} + L_i C)\delta) + \int_0^\delta \exp((A^{n_\alpha} + L_i C)(\delta - \tau))f(\tau)d\tau \right) e_i(0) = \bar{\Phi}_i(\delta)e_i(0) \quad (4.69)$$

With the structure of  $f(t)$ , this transition matrix results in a sum of weighted fractional-order integrals of the matrix-exponential, which can be expressed in terms of Mittag-Leffer functions [74, p. 21]

$$\bar{\Phi}_i(\delta) = \sum_{k=0}^{n_\alpha-1} \delta^{\alpha k} \mathcal{E}_{1,1+\alpha k}(F_i \delta). \quad (4.70)$$

Due to the terms  $\delta^{\alpha k}$  the convergence of this observer is also algebraic. At the time instant  $t = \delta$  we can change the actual observer state as well as the initial guess of  $\hat{x}_i(0)$ . This leads to the following observer

$$\begin{pmatrix} \dot{\hat{x}}_i(t) \\ \dot{\hat{\xi}}_i(t) \end{pmatrix} = \begin{pmatrix} A^{n_\alpha} & f(t) \\ 0 & 0 \end{pmatrix} \begin{pmatrix} \hat{x}_i(t) \\ \hat{\xi}_i(t) \end{pmatrix} + \begin{pmatrix} \bar{B} \\ 0 \end{pmatrix} \bar{u}(t) + \begin{pmatrix} L_i \\ 0 \end{pmatrix} (C\hat{x}_i(t) - y(t)), \quad t \neq \delta, \quad (4.71)$$

$$\hat{\xi}_i(\delta) = \Omega^{-1} \begin{pmatrix} \bar{\Phi}_1(\delta)\hat{x}_1(0) - \hat{x}_1(\delta^-) \\ \bar{\Phi}_2(\delta)\hat{x}_2(0) - \hat{x}_2(\delta^-) \end{pmatrix}, \quad i = 1, 2 \quad (4.72)$$

with

$$\Omega = \begin{pmatrix} I & -\bar{\Phi}_1(\delta) \\ I & -\bar{\Phi}_2(\delta) \end{pmatrix}. \quad (4.73)$$

Note that this implementation can also be extended to a periodic reset of the observer states. As the system is time-varying we have to adopt the resetting matrix  $\Omega^{-1}$  for each time interval. This is one of the major differences compared to impulsive reconstruction of integer-order LTI systems. As the estimate of the initial state should not change, its values can be useful for fault diagnostics.

**Remark 4.9.** *The implementation of the observer still requires the state transformation (4.26) to avoid the online computation of the fractional-order derivatives of the input. However, with the observer initialization  $\hat{x}_i(0) = 0$  we can skip the time varying part with  $f(t)$ . For the impulsive restart of the observer at  $t = \delta$  this is not critical as  $f(\delta)$  is bounded.*

**Example 4.1** (continued). *We resume the previous example (4.56) and design the constant observer gains  $L_1$  and  $L_2$  such that the poles of both observers are located at  $\lambda_{1,i} \in \{-0.9, -1.2\}$  and  $\lambda_{2,i} \in \{-0.8, -1.1\}$ , respectively. In contrast to the previous approach, we do not have to extend the state and can choose eigenvalues closer to zero such that the initial peaking is reduced. Furthermore, we can start the observer at  $t = 0$ . The simulation results are shown in Figure 4.8. The pure fractional-order observer with the poles at  $\lambda_{FO} \in \{-3.99, -3.61\}$  converges faster in the first time interval. The integer-order*

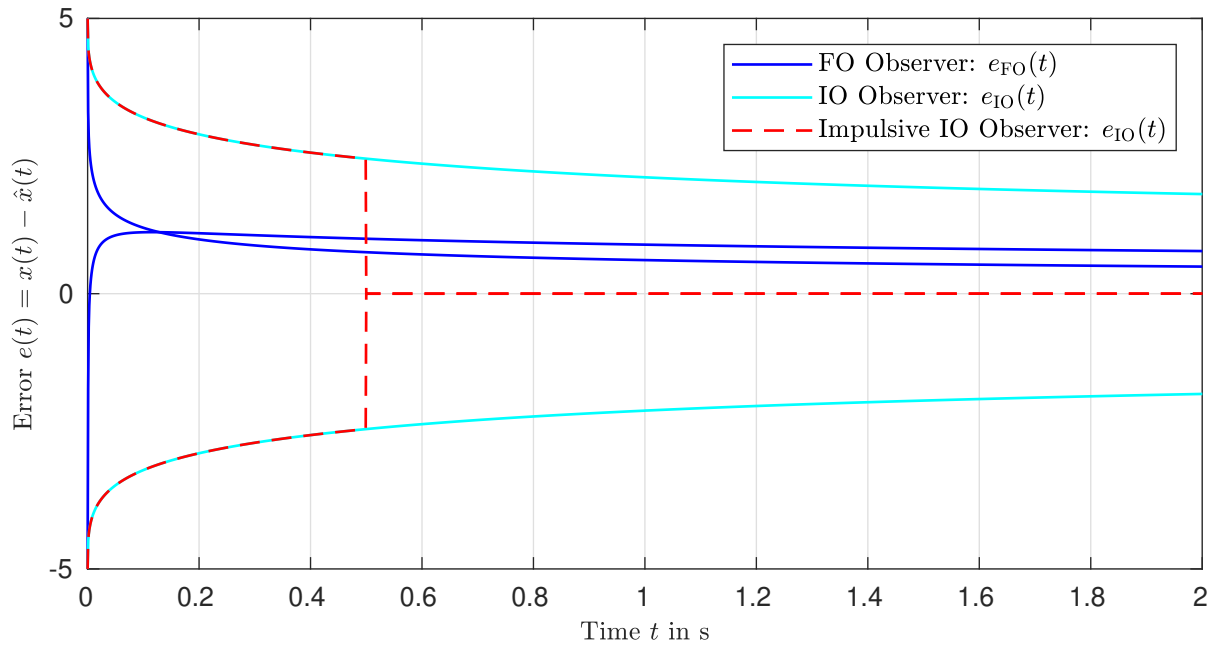


Figure 4.8: The impulsive observer can estimate the state in fixed time and with the lower observer gains the strong peaking is avoided.

approach with the impulsive reconstruction of the state estimates the correct state in fixed time. If we want to extend this approach to multiple resets, the matrix  $\Omega$  needs to be changed as  $\delta$  increases. For integer-order LTI systems (see [78]) this is not necessary as we can exchange  $x(0)$  with  $x((k-1)\delta)$  since the integer-order dynamics do not contain any additional memory.

#### 4.4 Associated Double-Order Systems

Considering the shape of the scalar Mittag-Leffler function as shown in Figure 3.1, there are two ways to increase the convergence of an observer to estimate the states of a physical fractional-order system. The standard approach would be to increase the gains, this, however, leads to an increased peaking in the transients and decreases the performance in the presence of measurement noise. The second approach is to change the order of derivation describing the error dynamics. In the previous Section 4.1, we changed the order such that the integer-order dynamics remain. This approach is limited to rational orders  $\alpha^{-1} \in \mathbb{N}$ .

In this section, we make use of similar techniques to change the order to  $\bar{\alpha} = 2\alpha$ . Exploiting the unknown input observer presented in Section 2.4 we can also accelerate the observation of input initialized fractional-order systems.

In order to design an observer for the system (3.3) with a new order of differentiation  $\bar{\alpha}$  closer to one, we introduce the concept of the associated double order system. Consider

$$\Sigma^2 : \quad \mathcal{D}^{2\alpha} \tilde{x}(t) = A^2 \tilde{x}(t) + \tilde{u}(t, u(\cdot), x_0) \quad (4.74)$$

with the initial state  $\tilde{x}(0) = \tilde{x}_0 \in \mathbb{R}^n$  and the extended input  $\tilde{u}$  depending on the initial state  $x_0$  and input  $u$  of (3.3).

**Definition 4.2** (Associated Double Order System [104]). System  $\Sigma^2$  is called associated double-order system to the fractional-order system  $\Sigma_{\text{FO}}$  in (3.3) if for every  $x_0$  and  $u(\cdot)$  there exists an extended input  $\tilde{u}(t, u(\cdot), x_0)$  such that

$$x(t) = \tilde{x}(t), \quad \forall t \geq 0. \quad (4.75)$$

**Theorem 4.6** (Associated Double Order System). For the system  $\Sigma_{\text{FO}}$  in (3.3) with  $\alpha \in (0, 1)$  the associated double-order system is given by

$$\mathcal{D}^{\tilde{\alpha}} \tilde{x}(t) = A^2 \tilde{x}(t) + \frac{Ax_0}{\Gamma(1-\alpha)} t^{-\alpha} + ABu(t) + B \left( \mathcal{D}^{\alpha} u(t) + \frac{u(0^+)}{\Gamma(1-\alpha)} t^{-\alpha} \right). \quad (4.76)$$

*Proof.* The construction of this associated system works similar to the one presented in Section 4.1. Multiplying the Laplace transform of (3.3a) with  $s^{\alpha}$  yields

$$\begin{aligned} s^{\alpha} X(s) - s^{\alpha-1} x(0) &= AX(s) + BU(s) && | \cdot s^{\alpha} \\ s^{2\alpha} X(s) - s^{2\alpha-1} x(0) &= As^{\alpha} X(s) + Bs^{\alpha} U(s) \end{aligned}$$

inserting the initial conditions of the state and input on the right side leads to fractional-order derivatives and a reduced memory function

$$\begin{aligned} s^{2\alpha} X(s) - s^{2\alpha-1} x(0) &= A(s^{\alpha} X(s) - s^{\alpha-1} x(0)) + As^{\alpha-1} x(0) + \\ &\quad B(s^{\alpha} U(s) - s^{\alpha-1} u(0)) + Bs^{\alpha-1} u(0) \\ \iff \mathcal{D}^{2\alpha} x(t) &= A\mathcal{D}^{\alpha} x(t) + \frac{A}{\Gamma(1-\alpha)} t^{-\alpha} x(0) + B\mathcal{D}^{\alpha} u(t) + \frac{B}{\Gamma(1-\alpha)} t^{-\alpha} u(0). \end{aligned}$$

Inserting the original dynamics (3.3) leads to the associated double-order system.  $\square$

Note that the order  $\alpha$  is not limited to be rational here. In this system with a higher order of differentiation, the memory of the original operator  $\mathcal{D}^{\alpha}$  is split into three parts.

1. The operator  $\mathcal{D}^{2\alpha}$  still contains infinite memory for  $\alpha \neq \frac{1}{2}$ . However, the amount of memory is reduced as the order is closer to one for  $\alpha \in \left(0, \frac{2}{3}\right)$  and the convolution kernel  $Y^+(t)$  included in the operator definition decays faster.
2. A second part of the memory is shifted to the input as the fractional-order derivative remembers the past of the input  $u(t)$  as well as a time-varying term weighing the initial input  $u(0)$ .
3. Finally, the main part of the memory is contained in the time-varying term weighing the initial conditions.

In the special case  $\alpha = \frac{1}{2}$  all memory is transferred to the right-hand side of the equation.

#### 4.4.1 Modification of the Unknown-Input Observer

We can now design an observer based on the double order system using the unknown input observer presented in section 3.4.3. The idea here is to reduce the influence of the shifted memory further. As the initial conditions are unknown, we cannot compensate the term  $\frac{Ax(0)}{\Gamma(1-\alpha)}t^{-\alpha}$ . However, a part of the memory is shifted to the input channel. Hence we consider this term as an unknown input. As the system matrix is changed to  $A^2$ , the existence conditions of Theorem 3.10 are adopted.

**Corollary 4.2** (UIO of Order  $2\alpha$  - Existence). *There exists an unknown input observer of the form (3.80) for the associated double-order system  $\Sigma^*$  in (4.76) if and only if the pair  $(C, \bar{A}_1)$  is detectable with*

$$\bar{A}_1 = \left( I - B \left( (CB)^\top CB \right)^{-1} (CB)^\top C \right) A^2 \quad (4.77)$$

and 
$$\text{rank}(CB) = \text{rank}(B). \quad (4.78)$$

Using the unknown input observer with the doubled order of differentiation  $\bar{\alpha} = 2\alpha$  and setting

$$Ed(t) = B \left( \mathcal{D}^\alpha u(t) + \frac{u(0^+)}{\Gamma(1-\alpha)} t^{-\alpha} \right) \quad (4.79)$$

leads to the error dynamics given by

$$\begin{aligned} \mathcal{D}^{2\alpha} e(t) = & \left( A^2 - HCA^2 - L_1C \right) e(t) + \left( F - (A^2 - HCA^2 - L_1C) \right) z(t) + \\ & \left( L_2 - (A^2 - HCA^2 - L_1C)H \right) y(t) + (T - (I - HC)) Bu(t) + \\ & (HC - I) \frac{Ax_0 t^{-\alpha}}{\Gamma(1-\alpha)} + (HC - I) B \left( \mathcal{D}^\alpha u(t) + \frac{u(0^+)}{\Gamma(1-\alpha)} t^{-\alpha} \right). \end{aligned} \quad (4.80)$$

If the conditions of Theorem 4.2 are satisfied, we can compute the required matrices as shown in Section 3.4.3 leading to

$$\mathcal{D}^{2\alpha} e(t) = Fe(t) + (HC - I) \frac{Ax_0}{\Gamma(1-\alpha)} t^{-\alpha}. \quad (4.81)$$

Note that for  $Ax_0 - \beta B = 0$  with  $\beta \in \mathbb{R}$  the estimation error convergence with the Mittag-Leffler function as the additional input is canceled by  $(HC - I)$ .

**Remark 4.10.** *The detectability of the pair  $(C, A_1)$  and  $(C, \bar{A}_1)$  may vary, as the system matrix is changed from  $A$  to  $A^2$ . The line of argumentation follows the proof of Theorem 4.4. As a result of these considerations, the existence of an unknown input observer for the original fractional-order system disturbed by  $Ed(t)$ , does not imply the existence of an unknown input observer with the doubled order of differentiation compensating the memory effect in the input channel  $B$ .*

**Remark 4.11.** *With this approach we cannot increase the differentiation order of the observer any further, e.g. by using an associated integer-order system. The additional restrictions on the system class*

would become conservative for the observer to work. Consider an associated system with  $\bar{\alpha} = 3\alpha$  given by

$$\begin{aligned} \mathcal{D}^{\bar{\alpha}}x(t) &= A^3x(t) + A^2Bu(t) + ABD^\alpha u(t) + BD^{2\alpha}u(t) \\ &\quad \left( \frac{At^{-\alpha}}{\Gamma(1-\alpha)} + \frac{t^{-2\alpha}}{\Gamma(1-2\alpha)} \right) (Ax_0 + Bu(0)) \end{aligned}$$

Now the derivatives  $\mathcal{D}^\alpha u(t)$  and  $\mathcal{D}^{2\alpha}u(t)$ , which cannot be computed online and are unbounded for  $u(\cdot) \in \mathcal{L}_{\text{loc}}^1$ , are considered as unknown inputs and the rank condition (4.78) from Theorem 4.2

$$\text{rank} \left( \begin{pmatrix} AB & B \end{pmatrix} \right) = \text{rank} \left( \begin{pmatrix} CAB & CB \end{pmatrix} \right) \quad (4.82)$$

is very restrictive, e.g. if the rank condition (4.82) holds the original system is either not observable ( $CA = \gamma_1 C$ ) or not controllable ( $AB = \gamma_2 B$ ). Hence this class of systems is less interesting from an engineering point of view.

#### 4.4.2 Input-initialized FO systems

Having defined an associated system to the side-initialized fractional-order system, we are now able to generalize this concept to improve the observer design for input-initialized systems (3.72).

**Theorem 4.7** (Input-Initialized Associated Double-Order System). *For the input-initialized system (3.72) with order of differentiation  $\alpha \in (0,1)$  and the limited history  $x(t)$  for  $t \in [a,0)$ , the associated double-order system with  $\bar{\alpha} = 2\alpha$  is*

$$\begin{aligned} {}_0\mathcal{D}_t^{\bar{\alpha}}x(t) &= A^2x(t) + ABu(t) - \Psi(x, \bar{\alpha}, 0, a, t) + \\ &\quad B \left( {}_a\mathcal{D}_t^\alpha u(t) + \frac{t^{-\alpha}}{\Gamma(1-\alpha)}u(0) + \frac{(t-a)^{-\alpha}}{\Gamma(1-\alpha)}u(a) \right). \end{aligned} \quad (4.83)$$

*Proof.* The proof uses the separation of the state  $x(t) = \bar{x}(t) + \underline{x}(t)$  as shown in Section 3.4.1. For each individual fractional-order differential equation the associated double order system is given by Theorem 4.6, i.e.

$${}_a\mathcal{D}^{2\alpha}\bar{x}(t) = A^2\bar{x}(t) + \frac{A\bar{x}(a)}{\Gamma(1-\alpha)}(t-a)^{-\alpha} + ABu(t) + B \left( {}_a\mathcal{D}^\alpha \bar{u}(t) + \frac{\bar{u}(a)}{\gamma(1-\alpha)}t^{-\alpha} \right) \quad (4.84)$$

$${}_0\mathcal{D}^{2\alpha}\underline{x}(t) = A^2\underline{x}(t) + \frac{A\underline{x}(0)}{\Gamma(1-\alpha)}t^{-\alpha} + ABu(t) + B \left( {}_a\mathcal{D}^\alpha \underline{u}(t) + \frac{\underline{u}(0)}{\gamma(1-\alpha)}t^{-\alpha} \right). \quad (4.85)$$

As the classical initial conditions are zero for each system  $\bar{x}(a) = 0 = \underline{x}(0)$  (see Equations (3.69) and (3.70)), these terms vanish.

$${}_a\mathcal{D}^{2\alpha}\bar{x}(t) = A^2\bar{x}(t) + ABu(t) + B \left( {}_a\mathcal{D}^\alpha \bar{u}(t) + \frac{\bar{u}(a)}{\gamma(1-\alpha)}t^{-\alpha} \right) \quad (4.86)$$

$${}_0\mathcal{D}^{2\alpha}\underline{x}(t) = A^2\underline{x}(t) + ABu(t) + B \left( {}_a\mathcal{D}^\alpha \underline{u}(t) + \frac{\underline{u}(0)}{\gamma(1-\alpha)}t^{-\alpha} \right) \quad (4.87)$$

The superposition of both states and the reformulation in terms of the  ${}_0\mathcal{D}^\alpha$  leads to the initialization function with the increased order

$$\begin{aligned}
{}_0\mathcal{D}^{2\alpha}x(t) &= {}_0\mathcal{D}^{2\alpha}\bar{x}(t) + {}_0\mathcal{D}^{2\alpha}\underline{x}(t) \\
&= ({}_0\mathcal{D}^{2\alpha}\bar{x}(t) - {}^C\Psi(\bar{x}, \alpha, 0, a, t)) + {}_0\mathcal{D}^{2\alpha}\underline{x}(t) \\
&= A^2\bar{x}(t) + ABu(t) + B \left( {}_a\mathcal{D}^\alpha\bar{u}(t) + \frac{\bar{u}(a)}{\Gamma(1-\alpha)}t^{-\alpha} \right) - {}^C\Psi(\bar{x}, \alpha, 0, a, t) + \\
&\quad A^2\underline{x}(t) + ABu(t) + B \left( {}_a\mathcal{D}^\alpha\underline{u}(t) + \frac{\underline{u}(0)}{\Gamma(1-\alpha)}t^{-\alpha} \right).
\end{aligned} \tag{4.88}$$

And with  ${}_a\mathcal{D}^\alpha u(t) = {}_0\mathcal{D}^\alpha \underline{u}(t)$  as  $\underline{u}(t)$  for  $t < 0$ ,  $u(t) = \bar{u}(t) + \underline{u}(t)$  and  ${}^C\Psi(\bar{x}, \alpha, 0, a, t) = {}^C\Psi(x, \alpha, 0, a, t)$  we have

$$\begin{aligned}
{}_0\mathcal{D}^{2\alpha}x(t) &= A^2x(t) + ABu(t) - {}^C\Psi(x, \alpha, 0, a, t) + \\
&\quad B \left( {}_a\mathcal{D}^\alpha u(t) + \frac{\bar{u}(a)}{\Gamma(1-\alpha)}t^{-\alpha} + \frac{\underline{u}(0)}{\Gamma(1-\alpha)}t^{-\alpha} \right).
\end{aligned} \tag{4.89}$$

□

Although all system history is built up via the input channel  $B$ , the initialization function acts on each line individually and the observer design leads to the error dynamics

$$\mathcal{D}^{2\alpha}e(t) = Fe(t) + (HC - I){}^C\Psi(x, 2\alpha, 0, a, t). \tag{4.90}$$

These dynamics converge as  ${}^C\Psi(\cdot)$  decays. Compared with the direct application of the unknown input observer this estimation error converges faster as the homogeneous dynamics and the initialization function itself decay faster. However, the channel of rejection is set by the input matrix  $B$ .

Only for  $\alpha = \frac{1}{2}$  the complete memory is shifted towards the input channel as the initialization function given by (2.93) is reduced to

$${}^C\Psi(x, 1, 0, a, t) = \frac{1}{\Gamma(1)} \int_a^0 \frac{\dot{x}(\tau)}{(t-\tau)^0} d\tau = \dot{x}(0) - \dot{x}(a). \tag{4.91}$$

As Caputo's operator only approaches a shifted integer-order derivative for  $\alpha \rightarrow 1$ , this nonzero initialization function still leads to integer-order dynamics

$$\begin{aligned}
\dot{x}(t) - \dot{x}(0) &= \dot{\underline{x}}(t) - \dot{\underline{x}}(0) + {}_a\mathcal{D}_t^1\bar{x}(t) - {}^C\Psi(x, 1, 0, a, t) \\
&= \dot{\underline{x}}(t) - \dot{\underline{x}}(0) + \dot{\bar{x}}(t) - \dot{\bar{x}}(a) - (\dot{\bar{x}}(0) - \dot{\bar{x}}(a)).
\end{aligned}$$

Cancelling the initial derivative  $\dot{x}(0) = \dot{\underline{x}}(0) + \dot{\bar{x}}(0)$  leads to:

$$\begin{aligned}
\dot{x}(t) &= \dot{\underline{x}}(t) + \dot{\bar{x}}(t) = A^2x(t) + ABu(t) + \\
&\quad B \left( {}_a\mathcal{D}_t^{\frac{1}{2}}u(t) + \frac{t^{-\frac{1}{2}}}{\Gamma(1-\frac{1}{2})}u(0^+) + \frac{(t-a)^{-\frac{1}{2}}}{\Gamma(1-\frac{1}{2})}u(a^+) \right).
\end{aligned}$$

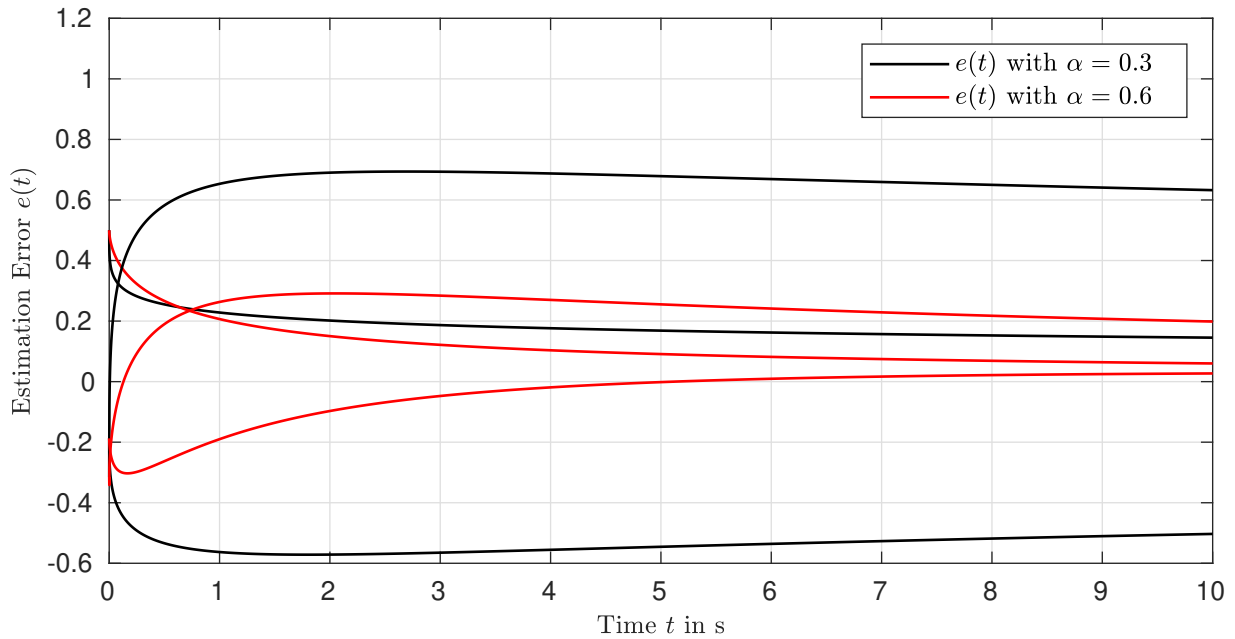


Figure 4.9: Estimation error of both unknown input observers for  $\alpha = 0.3$  and  $\alpha = 0.6$ .

Here, the complete memory is shifted to the input channel, hence the unknown input observer can estimate the state with undisturbed integer-order error dynamics, i.e.

$$\dot{e}(t) = Fe(t) \quad (4.92)$$

and the estimation error converges exponentially. Furthermore, the implementation does not require any fractional-order integrators and can be achieved memory efficiently.

**Example 3.2 (continued).** We circle back to the example used to illustrate the poor convergence of a Luenberger observer for the case of the initialization function slowing down the error dynamics. The eigenvalues of both unknown input observers are placed at  $\lambda_i \in \{-0.9, -1, -1.1\}$ . Furthermore, each observer is designed to reject disturbances in the input channel  $B$ . The results are plotted in Figure 4.9. With the identical initialization of each observer  $\hat{x}(0) = (0.5 \ 2 \ -1.5)^\top$ , we see that the observer with the lower order converges fastest for the first second as the unbounded derivative of the Mittag-Leffler function at  $t = 0$  is more prominent for smaller  $\alpha$ . The observer using the associated double-order system converges faster after that. However, the decay remains algebraic and the effect of the initialization function is still visible. As a second example we consider the case  $\alpha = \frac{1}{2}$ . The resulting error trajectories are depicted in Figure 4.10. As the associated double-order system is of integer order, the estimation error converges exponentially. This observer can be implemented with integer-order methods, such that the physical memory requirements are significantly reduced.

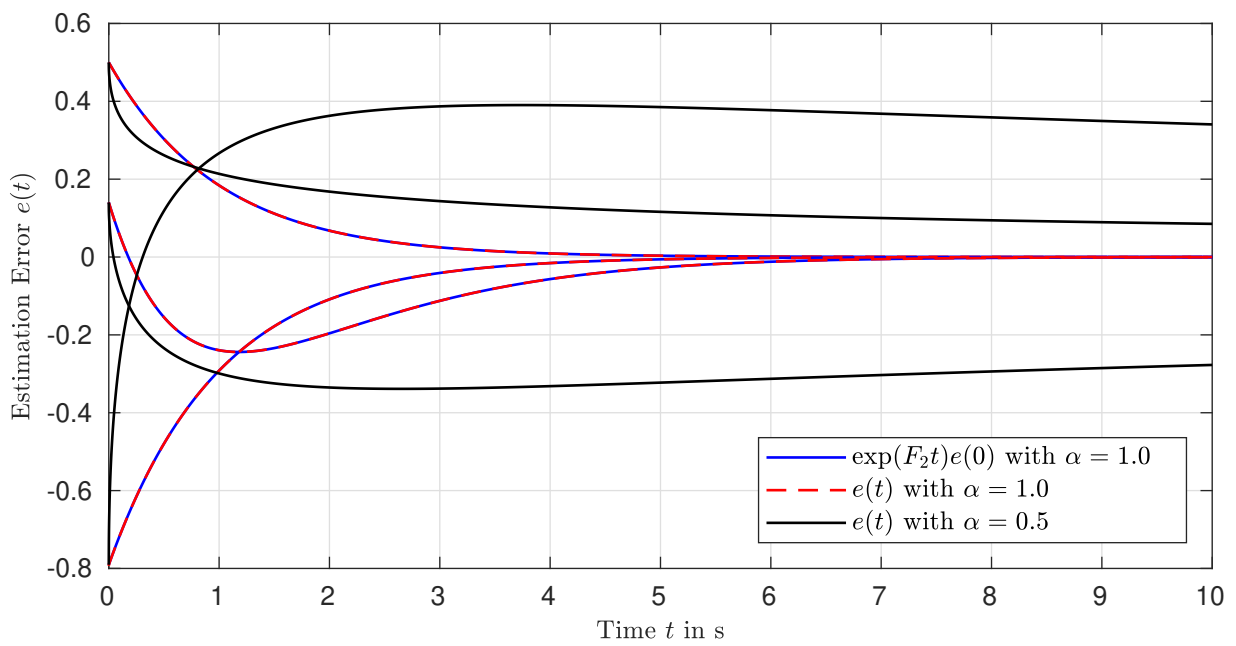


Figure 4.10: With  $\alpha = \frac{1}{2}$  the estimation error converges exponentially.



## 5 Associated Fractional-Order Systems

In this chapter, we are going to discuss the representation of integer-order systems with fractional-order derivatives. We will define the associated fractional-order system for an integer-order LTI system and present different state-space representations. In the following section, the properties of these associated systems are investigated. Finally, we will apply these fractional-order system representations to design a fractional-order observer and propose the fractional-order memory reset control concept.

### 5.1 Associated Fractional-Order System

We consider the integer-order LTI System of the form

$$\Sigma_{\text{IO}} : \begin{cases} \dot{x}(t) = Ax(t) + Bu(t) & (5.1a) \\ y(t) = Cx(t) & (5.1b) \end{cases}$$

with the state  $x(t) \in \mathbb{R}^n$ , input  $u(t) \in \mathbb{R}^p$ , output  $y(t) \in \mathbb{R}^q$ , initial conditions  $x(0) = x_0$ , and matrices of appropriate dimensions. As fractional-order operators do not show the semi-group property, we have to proceed with care. We want the composition rule to hold; for example with  $\alpha = \frac{1}{2}$  we would like to have

$$\mathcal{D}^\alpha (\mathcal{D}^\alpha f(t)) = \dot{f}(t). \quad (5.2)$$

Referring to [74, p. 74], this only holds under zero initial conditions which we have to include in our generalization approach.

**Definition 5.1** (Associated Fractional-Order System). *A system  $\Sigma^*$  with the order of differentiation  $\alpha^{-1} = \kappa \in \mathbb{N}$*

$$\Sigma^* : \quad \mathcal{D}^\alpha z(t) = \bar{A}z(t) + \bar{u}(u(\cdot), t, x_0) \quad (5.3)$$

*is called associated to an integer-order LTI-system  $\Sigma_{\text{IO}}$  of the form (5.1), if there exists a function  $\bar{u}(\cdot)$ , matrices  $\bar{A} \in \mathbb{R}^{\kappa n \times \kappa n}$ ,  $S \in \mathbb{R}^{n \times \kappa n}$  and an initial state  $z(0) = z_0$ , such that*

$$Sz(t) = x(t), \quad \forall t \geq 0. \quad (5.4)$$

We restrict ourselves to the case where the differentiation order is  $\alpha^{-1} = \kappa \in \mathbb{N}$ . However, we can extend this to the case  $\alpha < 1$  with  $\alpha \in \mathbb{Q}^+$  by applying the techniques presented to construct the associated-higher order systems (see Chapter 4.1). This, however, leads to a time-varying description, which is difficult to work with in the case of fractional-order derivatives due to the complexity of the Leibniz' rule (2.53).

### 5.1.1 Fractional-Order Integral Representation

A first approach to construct an associated fractional-order system can be derived by introducing fractional-order integrals of the original state  $x(t)$  to the extended state  $z(t)$

$$z(t) = \begin{pmatrix} z_1(t) \\ \vdots \\ z_{\kappa-1}(t) \\ z_k(t) \end{pmatrix} = \begin{pmatrix} \mathcal{I}^{(\kappa-1)\alpha} x(t) \\ \vdots \\ \mathcal{I}^\alpha x(t) \\ x(t) \end{pmatrix}. \quad (5.5)$$

The initialization of the fractional-order integrals is not restricted so far. With this state extension we can now define the integral representation of the associated fractional-order system.

**Theorem 5.1** (Integral Associated FO-LTI System). *The integral representation of a fractional-order system associated to the integer-order LTI system  $\Sigma_{\text{IO}}$  in (5.1a) is given by*

$$\mathcal{D}^\alpha z(t) = \underbrace{\begin{pmatrix} 0 & I & 0 & \cdots & 0 \\ 0 & 0 & I & \cdots & 0 \\ \vdots & \vdots & \vdots & \ddots & \vdots \\ 0 & 0 & 0 & \cdots & I \\ A & 0 & 0 & \cdots & 0 \end{pmatrix}}_{\bar{A} \in \mathbb{R}^{k\kappa \times k\kappa}} z(t) + \underbrace{\begin{pmatrix} 0 \\ 0 \\ \vdots \\ 0 \\ B \end{pmatrix}}_{\bar{B} \in \mathbb{R}^{k\kappa \times p}} \bar{u}(t) \quad (5.6)$$

with  $\alpha^{-1} = \kappa \in \mathbb{N}$  the new input

$$\bar{u}(t) = \mathcal{I}^{(\kappa-1)\alpha} u(t) = \mathcal{I}^{1-\alpha} u(t), \quad (5.7)$$

the extended initial conditions

$$z(0) = \begin{pmatrix} 0 \\ 0 \\ \vdots \\ 0 \\ x_0 \end{pmatrix} \quad (5.8)$$

and the selection matrix  $S$

$$S = \begin{pmatrix} 0 & 0 & \cdots & I \end{pmatrix}. \quad (5.9)$$

We apply Caputo's operator as the initial conditions of the original state are also a part of the extended initial state.

*Proof.* For the proof we use the Laplace transform for each block of  $n$  lines. The initial conditions vanish  $z_i(0) = 0$  for  $i = 1, 2, \dots, k-1$  and we have

$$\mathcal{L}\{\mathcal{D}^\alpha z_i(t)\} = s^\alpha Z_i(s) - s^{\alpha-1} z_i(0) = s^\alpha Z_i(s) = Z_{i+1}(s). \quad (5.10)$$

For the last  $n$  states we have

$$\mathcal{L}\{\mathcal{D}^\alpha z_k\} = s^\alpha Z_k(s) - s^{\alpha-1} z_k(0) = AZ_1(s) + Bs^{-(1-\alpha)} U(s). \quad (5.11)$$

Multiplying (5.11) with  $s^{1-\alpha}$  and inserting the initial state  $z_k(0) = x_0$ , one obtains the first order derivative

$$sZ_k(s) - x_0 = As^{1-\alpha}Z_1(s) + BU(s). \quad (5.12)$$

Finally, replacing  $s^{1-\alpha}Z_1(s)$  with  $Z_k(s)$  and applying equation 5.10 iteratively yields:

$$sZ_k(s) - x_0 = AZ_k(s) + BU(s). \quad (5.13)$$

In the time-domain we get the first-order differential equation for  $z_k$

$$\dot{z}_k(t) = Az_k(t) + Bu(t). \quad (5.14)$$

This equation equals the state equation (5.1a) of the original integer-order LTI system, hence the Matrix  $S$  selects the last  $n$  states of the extended state  $z$ .  $\square$

Note that the generalized system order combining the order of differentiation and the number of states of the system does not change as  $n = (\kappa n)\alpha = n$ .

### 5.1.2 Fractional-Order Derivative Representation

A second approach to construct an associated fractional-order system uses a more common state extension. The augmented state  $z(t)$  is now given by the original state  $x(t)$  and its fractional-order derivatives

$$z(t) = \begin{pmatrix} z_1(t) \\ z_2(t) \\ \vdots \\ z_\kappa(t) \end{pmatrix} = \begin{pmatrix} x(t) \\ \mathcal{D}^\alpha x(t) \\ \vdots \\ \mathcal{D}^{(\kappa-1)\alpha} x(t) \end{pmatrix}. \quad (5.15)$$

**Theorem 5.2** (Derivative Associated FO-LTI System). *A derivative representation of the fractional-order system associated to the integer-order LTI system  $\Sigma_{\text{IO}}$  in (5.1a) is given by*

$$\mathcal{D}^\alpha z(t) = \underbrace{\begin{pmatrix} 0 & I & 0 & \cdots & 0 \\ 0 & 0 & I & \cdots & 0 \\ \vdots & \vdots & \vdots & \ddots & \vdots \\ 0 & 0 & 0 & \cdots & I \\ A & 0 & 0 & \cdots & 0 \end{pmatrix}}_{\tilde{A} \in \mathbb{R}^{\kappa n \times \kappa n}} z(t) + \underbrace{\begin{pmatrix} 0 \\ 0 \\ \vdots \\ 0 \\ B \end{pmatrix}}_{\tilde{B} \in \mathbb{R}^{\kappa n \times p}} u(t) \quad (5.16)$$

with the extended initial conditions

$$z(0) = \begin{pmatrix} x_0 \\ 0 \\ \vdots \\ 0 \end{pmatrix} \quad (5.17)$$

and the selection matrix  $M$

$$S = \begin{pmatrix} I & 0 & \cdots & 0 \end{pmatrix}. \quad (5.18)$$

*Proof.* The proof consists of two parts. First, we have to show that the system (5.16) leads to the original integer-order dynamics. The second part is concerned with the interpretation of auxiliary states. We have to prove that the fractional-order derivative of the state  $x(t)$  is zero at the initial time. This is not obvious as the first-order derivative of the state depends on the input  $u(t)$ .

The first part uses the Laplace transform as shown previously. For  $i = 2, 3, \dots, \kappa - 1$ , the initial conditions vanish  $z_i(0) = 0$  and this yields

$$\mathcal{L}\{\mathcal{D}^\alpha z_i(t); s\} = s^\alpha Z_i(s) - s^{\alpha-1} z_i(0) = s^\alpha Z_i(s) = Z_{i+1}(s). \quad (5.19)$$

For the first  $n$  states we have

$$\mathcal{L}\{\mathcal{D}^\alpha z_1; s\} = s^\alpha Z_1(s) - s^{\alpha-1} z_1(0) = s^\alpha Z_1(s) - s^{\alpha-1} x_0 = Z_2(s). \quad (5.20)$$

The input appears in the last  $n$  states

$$\mathcal{L}\{\mathcal{D}^\alpha z_\kappa; s\} = s^\alpha Z_\kappa(s) - s^{\alpha-1} z_\kappa(0) = s^\alpha Z_\kappa(s) = AZ_1(s) + Bu(s). \quad (5.21)$$

Inserting equation (5.19) iteratively into (5.21) yields

$$s^{1-\alpha} Z_2(s) = AZ_1(s) + Bu(s), \quad (5.22)$$

where we can insert the equation (5.20) to construct the first-order derivative of the state  $z_1(t)$ , i.e.

$$sZ_1(s) - x_0 = AZ_1(s) + Bu(s). \quad (5.23)$$

As the matrix  $S$  selects the state  $z_1(t) = x(t)$  and equation (5.23) is the Laplace transform of the original integer-order system, the first part of the proof is finished.

The state trajectories of the original integer-order system satisfy the first order differential equation (5.1a), therefore,  $x(t)$  is differentiable  $x(t) \in \mathcal{C}^1([t_0, t_f])$  and its derivative is piecewise continuous  $\dot{x}(t) \in \mathcal{C}^0([t_0, t_f])$ . Following the definition of Caputo's derivative (2.43) for  $\alpha \in (0, 1)$  we can apply Theorem 2.1 to  $\dot{x}(t)$ , as Caputo's derivative is the fractional-order integral of  $\dot{x}(t)$ . This shows that the initial conditions of the fractional-order derivatives  $\mathcal{D}^\gamma x(t)$  of the state are always zero

$$\mathcal{D}^\gamma x(t)|_{t=0} = 0, \quad \gamma \in (0, 1), \quad (5.24)$$

at the initial time  $t = 0$ , as long as the initial state  $x(0)$  and input  $u(0)$  are bounded. This completes the proof.  $\square$

**Remark 5.1** (Different state-space representations). *Another representation of an associated fractional-order system can be derived by applying the same techniques used to derive the associated integer-order systems in Section 4.1. We demonstrate this for the homogeneous system*

$$\dot{x}(t) = Ax(t), \quad x(0) = x_0 \quad (5.25)$$

with  $\alpha = \frac{1}{2}$ . As the associated integer-order system in this case is defined by the square of the system matrix  $A$ , we should be able to construct a fractional-order system with a matrix  $M_A$  satisfying  $M_A^2 = A$ . The motivation of this approach is the possible difference of the observability properties of the pairs

$(C, A)$  and  $(C, M_A)$  as illustrated in Theorem 4.4. The ansatz of the associated fractional-order system also contains a weighting function  $f_A(t)$  of the initial state

$$\mathcal{D}^\alpha \tilde{x}(t) = M_A \tilde{x}(t) + f_A(t)x_0, \quad \alpha = \frac{1}{2}, \quad \tilde{x}(0) = x_0. \quad (5.26)$$

This system has only  $n$  states compared to the previously shown state extensions. We use the Laplace transform of (5.26)

$$s^\alpha \tilde{X}(s) - s^{\alpha-1}x_0 = M_A \tilde{X}(s) + F_A(s)x_0 \quad (5.27)$$

to determine  $f_A(t)$ . Multiplying the Laplace transform with  $s^{1-\alpha}$  yields

$$\begin{aligned} s\tilde{X}(s) - x_0 &= s^{1-\alpha}M_A\tilde{X}(s) + s^{1-\alpha}F_A(s)x_0 \\ \iff s\tilde{X}(s) - x_0 &= s^\alpha M_A\tilde{X}(s) + s^\alpha F_A(s)x_0 \\ \iff s\tilde{X}(s) - x_0 &= s^\alpha M_A\tilde{X}(s) + s^{1-\alpha}F_A(s)x_0 \\ \iff s\tilde{X}(s) - x_0 &= M_A \left( s^\alpha \tilde{X}(s) - s^{\alpha-1}x_0 \right) + M_A s^{\alpha-1}x_0 + s^{1-\alpha}F_A(s)x_0 \\ \iff s\tilde{X}(s) - x_0 &= M_A^2 \tilde{X}(s) + M_A F_A(s)x_0 + M_A s^{\alpha-1}x_0 + s^{1-\alpha}F_A(s)x_0 = A\tilde{X}(s). \end{aligned}$$

Finally, with  $\tilde{X}(s) = X(s)$ , the weighting function  $f_A(t)$  is given by

$$F_A(s) = -s^{\alpha-1}(Is^\alpha + M_A)^{-1}M_A, \quad (5.28)$$

which corresponds to the Mittag-Leffler-Function in the time domain

$$f_A(t) = -\mathcal{E}_{\alpha,1}(-M_A t^\alpha)M_A = -M_A \mathcal{E}_{\alpha,1}(-M_A t^\alpha). \quad (5.29)$$

The associated fractional-order system is of the same order and time-varying

$$\mathcal{D}^\alpha \tilde{x}(t) = M_A \tilde{x}(t) - M_A \mathcal{E}_{\alpha,1}(-M_A t^\alpha)x_0, \quad (5.30)$$

however, the Mittag-Leffler function is also generated by a fractional-order system

$$\mathcal{D}^\alpha \zeta(t) = -M_A \zeta(t), \quad \zeta(0) = x_0. \quad (5.31)$$

Combining both systems leads again to a system with  $n\alpha^{-1}$  states

$$\mathcal{D}^\alpha \begin{pmatrix} x(t) \\ \zeta(t) \end{pmatrix} = \begin{pmatrix} M_A & -M_A \\ 0 & -M_A \end{pmatrix} \begin{pmatrix} x(t) \\ \zeta(t) \end{pmatrix}, \quad \text{with:} \quad \begin{pmatrix} x(0) \\ \zeta(0) \end{pmatrix} = \begin{pmatrix} x_0 \\ x_0 \end{pmatrix}. \quad (5.32)$$

Hence this system representation is only a transformed state-space representation of either the derivative or the integral representation. The transformation matrix is given by

$$T = \begin{pmatrix} I & 0 \\ -M_A & M_A \end{pmatrix} \quad (5.33)$$

such that

$$\bar{A} = T \begin{pmatrix} M_A & -M_A \\ 0 & -M_A \end{pmatrix} T^{-1} = \begin{pmatrix} I & 0 \\ -M_A & M_A \end{pmatrix} \begin{pmatrix} M_A & -M_A \\ 0 & -M_A \end{pmatrix} \begin{pmatrix} I & 0 \\ -I & M_A^{-1} \end{pmatrix} = \begin{pmatrix} 0 & I \\ A & 0 \end{pmatrix}. \quad (5.34)$$

Obviously, this transformation requires the regularity of  $M_A$  and therefore  $\text{rank}(A) = n$ . The derivation of the associated system, however, did not require any assumptions on the system matrix. In this case, the fractional-order system matrices are dissimilar, as they show different Jordan forms. Consider the example

$$M_A = \begin{pmatrix} 0 & 1 \\ 0 & -2 \end{pmatrix}, \quad A = M_A^2 = \begin{pmatrix} 0 & -2 \\ 0 & 4 \end{pmatrix}, \quad (5.35)$$

which leads to two different Jordan canonical forms

$$J_1 = \begin{pmatrix} 0 & 0 & 0 & 0 \\ 0 & 0 & 0 & 0 \\ 0 & 0 & 2 & 0 \\ 0 & 0 & 0 & -2 \end{pmatrix} = T_1^{-1} \begin{pmatrix} 0 & 1 & 0 & -1 \\ 0 & -2 & 0 & 2 \\ 0 & 0 & 0 & -1 \\ 0 & 0 & 0 & 2 \end{pmatrix} T_1$$

$$J_2 = \begin{pmatrix} 0 & 1 & 0 & 0 \\ 0 & 0 & 0 & 0 \\ 0 & 0 & 2 & 0 \\ 0 & 0 & 0 & -2 \end{pmatrix} = T_2^{-1} \begin{pmatrix} 0 & 0 & 1 & 0 \\ 0 & 0 & 0 & 1 \\ 0 & -2 & 0 & 0 \\ 0 & 4 & 0 & 0 \end{pmatrix} T_2.$$

Only in the case of  $\text{rank}(A) < n$  this approach leads to an associated fractional-order system with a state-space that is independent of the previously shown representations (5.16) and (5.6). Note that the roots of the matrix  $A$  are not unique. A possible computation uses the Jordan canonical form. If  $A$  is diagonalizable the set of roots of the eigenvalues can be used and ordered arbitrarily. In the more general case, we have to compute a suitable decomposition of each Jordan block. Using the transformation matrices to change the coordinates back to the original state

$$M_A = A^\alpha = T J^\alpha T^{-1} \quad (5.36)$$

might introduce numerical errors. For these reasons, it is preferable to apply the integral or differential representation of the associated-fractional-order system.

**Associated Fractional-Order Systems with Riemann-Liouville Derivative** In the case of  $\text{rank}(A) = n$  it is also possible to construct an associated fractional-order system applying Riemann-Liouville's definition. However, we have to define the initial conditions differently compared with Caputo's approach.

**Theorem 5.3.** For the homogenous integer-order system  $\dot{x}(t) = Ax(t)$  with initial conditions  $x(0) = x_0 \in \mathbb{R}^n$  and  $\text{rank}(A) = n$  an associated Riemann-Liouville fractional-order system with  $\alpha^{-1} = \kappa \in \mathbb{N}$  is given by

$${}^R\mathcal{D}^\alpha z(t) = \underbrace{\begin{pmatrix} 0 & I & 0 & \cdots & 0 \\ 0 & 0 & I & \cdots & 0 \\ \vdots & \vdots & \vdots & \ddots & \vdots \\ 0 & 0 & 0 & \cdots & I \\ A & 0 & 0 & \cdots & 0 \end{pmatrix}}_{\tilde{A} \in \mathbb{R}^{\kappa n \times \kappa n}} z(t) \quad (5.37)$$

with the initial conditions

$$z(0) = \begin{pmatrix} 0 \\ \vdots \\ 0 \\ A^{-1}x_0 \\ 0 \end{pmatrix} \quad (5.38)$$

and the selection matrix  $M_R$

$$M_R = \begin{pmatrix} 0 & \cdots & 0 & I \end{pmatrix}. \quad (5.39)$$

*Proof.* The construction of the associated system using Riemann's operator is slightly different to the previous approaches. First, the original state of the integer-order system has to have zero initial conditions in the fractional-order domain. Hence we have to reconstruct the original integer-order dynamics in terms of the extended state  $z_\kappa(t)$  using the penultimate block of  $n$  equations. The Laplace transform of (5.37) for blocks of  $n$  equations including the initial conditions (5.38) reads

$$s^\alpha Z_1(s) - \bar{z}_1(0) = s^\alpha Z_1(s) \quad = Z_2(s) \quad (5.40)$$

$$\vdots$$

$$s^\alpha Z_{\kappa-1}(s) - \bar{z}_{\kappa-1}(0) = s^\alpha Z_{\kappa-1}(s) - A^{-1}x_0 \quad = Z_\kappa(s) \quad (5.41)$$

$$s^\alpha Z_\kappa(s) - \bar{z}_\kappa(0) = s^\alpha Z_\kappa(s) \quad = AZ_1(s). \quad (5.42)$$

Multiplying the first  $\kappa - 1$  block of equations with  $A$  and inserting the auxiliary states successively yields

$$s^{(\kappa-1)\alpha} AZ_1(s) - x_0 = AZ_\kappa(s), \quad (5.43)$$

and substituting  $AZ_1(s)$  with (5.42) yields the integer-order dynamics

$$s^{(\kappa-1)\alpha} s^\alpha Z_\kappa(s) - x_0 = sZ_\kappa(s) - x_0 = AZ_\kappa(s). \quad (5.44)$$

□

Due to the singularity in the auxiliary state  $z_{\kappa-1}(t)$ , the numerical evaluation of this associated system is difficult. Caputo's operator is better applicable if integer-order dynamics are involved.

**Nonlinear Systems** As the construction of the associated fractional-order system in the derivative representation does not exploit the linearity of the integer-order LTI system, we can extend this procedure to nonlinear systems, i.e.

$$\Sigma_{NL} : \quad \dot{x}(t) = f(x, t), \quad x(0) = x_0, \quad (5.45)$$

with the state  $x(t) \in \mathbb{R}^n$  and the function  $f(\cdot) : \mathbb{R}^n \times \mathbb{R} \rightarrow \mathbb{R}^n$  piecewise continuous in  $t$  and Lipschitz in  $x$ .

**Theorem 5.4.** A fractional-order system of the order  $\alpha^{-1} = \kappa \in \mathbb{N}$  is associated to the nonlinear integer-order system  $\Sigma_{\text{NL}}$  in (5.45) given by

$$\begin{aligned} \mathcal{D}^\alpha z_1(t) &= z_2(t) \\ \mathcal{D}^\alpha z_2(t) &= z_3(t) \\ &\vdots \\ \mathcal{D}^\alpha z_{\kappa-1}(t) &= z_\kappa(t) \\ \mathcal{D}^\alpha z_\kappa(t) &= f(z_1(t), t) \end{aligned} \tag{5.46}$$

$$\tag{5.47}$$

with the initial conditions

$$z(0) = \begin{pmatrix} x_0 \\ 0 \\ \vdots \\ 0 \end{pmatrix} \tag{5.48}$$

and the selection matrix  $S$

$$S = \begin{pmatrix} I & 0 & \cdots & 0 \end{pmatrix}, \tag{5.49}$$

such that  $x(t) = Sz(t) = z_1(t)$  for all  $t \geq 0$ .

This is a special case of Theorem 8.1 given in [20, p. 169].

*Proof.* As the state  $x(\cdot)$  is differentiable  $x(\cdot) \in \mathcal{C}^1([0, T])$  we can apply Theorem 2.1 to  $\dot{x}(\cdot) \in \mathcal{C}^0([0, T])$ , such that  $D^\gamma x(t)|_{t=0} = 0$  for  $\gamma \in (0, 1)$ . As the fractional-order derivatives of the state have zero initial conditions, the composition law holds and we have

$$\mathcal{D}^\alpha \left( \mathcal{D}^\alpha (\cdots \mathcal{D}^\alpha z_1(t)) \right) = \mathcal{D}^{\alpha+\alpha+\cdots+\alpha} z_1(t) = \mathcal{D}^1 z_1(t) = f(z_1(t), t). \tag{5.50}$$

□

Using the comparable assumptions, the same arguments can be used to represent fractional-order systems with a lower order [20, p. 169].

**Lemma 5.1.** Consider the fractional-order system defined by

$$\mathcal{D}^\alpha x(t) = f(x, t), \quad x(0) = x_0 \in \mathbb{R}^n, \quad \alpha \in (0, 1) \tag{5.51}$$

with  $x(\cdot) \in \mathcal{C}^1([0, t_1])$ , then the system

$$\begin{aligned} \mathcal{D}^\gamma z_1(t) &= z_2(t) \\ \mathcal{D}^\gamma z_2(t) &= z_3(t) \\ &\vdots \\ \mathcal{D}^\gamma z_{\kappa-1}(t) &= z_\kappa(t) \\ \mathcal{D}^\gamma z_\kappa(t) &= f(z_1(t), t) \end{aligned} \tag{5.52}$$



with  $\gamma = \frac{\alpha}{\kappa}$ ,  $\kappa \in \mathbb{N}$ , the initial conditions

$$z(0) = \begin{pmatrix} x_0 \\ 0 \\ \vdots \\ 0 \end{pmatrix} \quad (5.53)$$

and the selection matrix  $S$

$$S = \begin{pmatrix} I & 0 & \cdots & 0 \end{pmatrix}, \quad (5.54)$$

is associated to the fractional-order non-linear system (5.51) such that  $x(t) = Sz(t) = z_1(t)$  for all  $t \geq 0$ .

**Remark 5.2.** The same technique can also be applied to reduce the order of a fractional-order LTI system to achieve  $\gamma^{-1} \in \mathbb{N}$ . This is especially useful to bring the case of  $\alpha \in (1, 2)$  back to the usual case of  $\bar{\alpha} = \frac{\alpha}{2} \in (0, 1)$ , although this complicates the stability analysis as the region to place the poles changes from a convex to a non-convex one (see Figure 3.6).

## 5.2 Properties of Associated Fractional-Order Systems

In order to work with these associated fractional-order systems we have to investigate whether all relevant properties of the original integer-order system remain within the fractional-order framework. Hence we investigate stability, observability and controllability of the introduced representations (5.16) and (5.6).

As both representations have a similar system matrix despite the different state-spaces, we can assess the stability of either associated system by checking the eigenvalues of the extended system matrix  $\bar{A}$ .

**Theorem 5.5 (Eigenvalues).** Let  $\lambda_i$  denote some eigenvalue of  $A$ . Then  $\bar{\lambda}_i$  is an eigenvalue of  $\bar{A}$  if and only if

$$\bar{\lambda}_{i,l}^{\kappa} = \lambda_i \quad (5.55)$$

for  $i = 1, 2, \dots, n$  and  $l = 1, 2, \dots, \kappa$ .

*Proof.* We compute the characteristic polynomial of  $\bar{A}$  in terms of  $\lambda$  by splitting the matrix  $\Lambda = \bar{\lambda}I - \bar{A}$  into blocks:

$$\Lambda = \left( \begin{array}{c|cccc} \bar{\lambda}I & -I & 0 & \cdots & 0 \\ 0 & \bar{\lambda}I & -I & \cdots & 0 \\ \vdots & \vdots & \vdots & \ddots & \vdots \\ 0 & 0 & 0 & \cdots & -I \\ \hline -A & 0 & 0 & \cdots & \bar{\lambda}I \end{array} \right) = \left( \begin{array}{c|c} \Lambda_{11} & \Lambda_{12} \\ \Lambda_{21} & \Lambda_{22} \end{array} \right)$$

with  $\Lambda_{11} \in \mathbb{R}^{(\kappa-1)n \times n}$  and  $\Lambda_{22} \in \mathbb{R}^{n \times (\kappa-1)n}$ . As  $\Lambda_{12}$  is always regular we can use the decomposition

$$\Lambda = \begin{pmatrix} \Lambda_{12} & 0 \\ \Lambda_{22} & I \end{pmatrix} \begin{pmatrix} \Lambda_{12}^{-1} \Lambda_{11} & I \\ \Lambda_{21} - \Lambda_{22} \Lambda_{12}^{-1} \Lambda_{11} & 0 \end{pmatrix}. \quad (5.56)$$

Hence the characteristic polynomial may be written as

$$\det(\Lambda) = \det(\Lambda_{12}) \det\left(A + \Lambda_{22}\Lambda_{12}^{-1}\Lambda_{11}\right) \quad (5.57)$$

$$= (-1)^{n(\kappa-1)} \det\left(A + \bar{\lambda}^2 \begin{pmatrix} 0 & \cdots & 0 & 1 \end{pmatrix} \Lambda_{12}^{-1} \begin{pmatrix} I \\ 0 \\ \vdots \\ 0 \end{pmatrix}\right) \quad (5.58)$$

$$= (-1)^{n(\kappa-1)} \det(A - \bar{\lambda}^\kappa I). \quad (5.59)$$

Comparison with the characteristic polynomial of the IO system,  $\det(\lambda I - A) = 0$ , yields (5.55).  $\square$

**Remark 5.3.** Equation (5.55) is a means for comparing the eigenvalues of an integer-order system with a fractional-order system. We only have to consider the associated fractional-order system and can compare the eigenvalue location with respect to the same order of differentiation.

**Remark 5.4.** The relation of the eigenvalues can also be seen in the frequency domain. To illustrate this, we consider a first-order plant

$$G(s) = \frac{1}{s+1}. \quad (5.60)$$

Applying Equation 5.55 to  $\lambda = -a$  for  $\alpha_1 = \frac{1}{2}$  and  $\alpha_2 = \frac{1}{3}$  yields different fractional-order representations of the integer-order plant

$$G(s) = \frac{1}{(s^{\alpha_1} + j)(s^{\alpha_1} - j)} = \frac{1}{(s^{\alpha_2} + 1) \left(s^{\alpha_2} + \frac{1+j\sqrt{3}}{2}\right) \left(s^{\alpha_2} + \frac{1-j\sqrt{3}}{2}\right)}. \quad (5.61)$$

The integer-order pole is split into  $\kappa = \alpha^{-1}$  fractional-order poles. This can be applied to control non-minimum phase processes, as the stable fractional-order part of a non-minimum phase zero can be compensated. Rewriting  $G(s)$  in the pseudo polynomial form, shows the zero coefficients for the non-integer powers of  $s$

$$G(s) = \frac{1}{s^{2\alpha_1} + 0s^{\alpha_1} + 1} = \frac{1}{s^{3\alpha_2} + 0s^{2\alpha_2} + 0s^{\alpha_2} + 1}. \quad (5.62)$$

In the frequency domain, this split is quite obvious as the transfer function  $G(s)$  does not take the initial conditions into account.

**Theorem 5.6 (Stability).** The associated fractional-order system (5.16), respectively (5.6), is asymptotically stable if and only if this holds for the original integer-order LTI system  $\Sigma_{\text{IO}}$  from (5.1a).

*Proof.* With the stability condition of Theorem 3.3, i. e.  $|\arg(\lambda_i)| > \frac{\pi}{2}$ , it can be shown that the eigenvalues  $\bar{\lambda}_{i,l}$  are also located in the stable sector. We use (5.55) to determine the argument of the eigenvalue  $\bar{\lambda}_{i,l} = \sqrt[\kappa]{\lambda_i}$ , i.e.

$$\begin{aligned} \arg(\bar{\lambda}_{i,l}) &= \frac{\arg(\lambda_i) + 2\pi l}{\kappa} \\ \iff \kappa \arg(\bar{\lambda}_{i,l}) - 2\pi l &= \arg(\lambda_i), \quad l = 0, 1, \dots, \kappa - 1. \end{aligned} \quad (5.63)$$

and its absolute value limited to the range  $\arg(\cdot) \in [0, \pi]$ :

$$\kappa |\arg(\bar{\lambda}_{i,l})| \geq |\arg(\lambda_i)|. \quad (5.64)$$

Hence, if and only if the integer-order system is asymptotically stable, i.e.

$$|\arg(\lambda_i)| > \frac{\pi}{2} \iff |\arg(\bar{\lambda}_{i,l})| > \frac{\pi}{2\kappa} = \alpha \frac{\pi}{2} \quad (5.65)$$

the condition for asymptotic stability (3.42) is satisfied.

In the stable case with eigenvalues on the imaginary axis, we also have to show that the geometric multiplicity does not change. With the special structure of the matrix  $\bar{A}$ , its eigenvectors  $\bar{v}_i$  are completely determined by the eigenvectors  $v_i$  of the matrix  $A$ . For the non-zero eigenvalue  $\lambda_i \neq 0$  with geometric multiplicity  $l$  we have

$$\bar{v}_i = \begin{pmatrix} \lambda_i^{1-\kappa} v_{i,j} \\ \vdots \\ \lambda_i^{-1} v_{i,j} \\ v_{i,j} \end{pmatrix}, \quad \text{with: } Av_{i,l} = \lambda_i \quad (5.66)$$

for  $j = 1, \dots, l$ . And the eigenvectors  $\bar{v}_i$  are completely defined. In this case the geometric multiplicity of the corresponding fractional-order eigenvalues does not change.

Only in the case of  $\lambda_i = 0$  the geometric multiplicity is reduced. For the eigenvalue  $\lambda_i = 0$  with  $\text{multalg}(\lambda_i) = \text{multgeo}(\lambda_i)$  we have

$$\bar{v}_i = \begin{pmatrix} 0 \\ \vdots \\ 0 \\ v_{i,j} \end{pmatrix}, \quad \text{with: } Av_{i,l} = \lambda_i \quad (5.67)$$

for  $j = 1, \dots, l$ . The algebraic multiplicity is increased whereas the geometric multiplicity remains:

$$\text{multalg}(\bar{\lambda}_i) = \kappa \text{multalg}(\lambda_i), \quad \text{multgeo}(\bar{\lambda}_i) = \text{multgeo}(\lambda_i), \quad \bar{\lambda}_i = \lambda_i = 0. \quad (5.68)$$

In view of Theorem 3.3, this introduces unstable modes which do not occur in the integer-order system. These unstable modes, however, are not excited as the corresponding initial conditions are zero.  $\square$

### 5.2.1 Observability and Controllability

Let us first discuss the observability and controllability of the derivative representation of the associated fractional-order system. As the selection matrix  $S$  selects the first  $n$  states, the output equation is given by

$$y(t) = \begin{pmatrix} C & 0 & \dots & 0 \end{pmatrix} z(t) = \bar{C}z(t) \quad (5.69)$$

with the extended output matrix  $\bar{C} \in \mathbb{R}^{q \times \kappa n}$ .

**Theorem 5.7 (Observability).** *The associated fractional-order system in the derivative representation (5.16) is completely observable if and only if the original integer-order system (5.1) is completely observable.*

*Proof.* The proof of this theorem is straightforward. We compute the observability matrix of the extended system and output matrix pair  $(\bar{C}, \bar{A})$  using the Kronecker product  $\otimes$  leading to

$$\bar{\mathcal{O}} = \begin{pmatrix} C & \cdots & 0 \\ \vdots & \ddots & \vdots \\ 0 & \cdots & C \\ CA & \cdots & 0 \\ \vdots & \ddots & \vdots \\ 0 & \cdots & CA \\ \vdots & \vdots & \vdots \\ CA^{n-1} & \cdots & 0 \\ \vdots & \ddots & \vdots \\ 0 & \cdots & CA^{n-1} \end{pmatrix} = \begin{pmatrix} I_\kappa \otimes C \\ I_\kappa \otimes CA \\ \vdots \\ I_\kappa \otimes CA^{n-1} \end{pmatrix}. \quad (5.70)$$

Rearranging the lines of  $\bar{\mathcal{O}}$  we end up with

$$\text{rank } \bar{\mathcal{O}} = \text{rank} (\text{diag} (\mathcal{O}, \mathcal{O}, \dots, \mathcal{O})) = \kappa \text{rank}(\mathcal{O}). \quad (5.71)$$

Therefore, the associated fractional-order system is observable, i.e.  $\text{rank}(\bar{\mathcal{O}}) = \kappa n$ , if the original integer-order system is observable with  $\text{rank}(\mathcal{O}) = n$ .  $\square$

With this structure, we can also determine the dimension of the non-observable subspace. If  $\text{rank}(\mathcal{O}) = n_{\text{obs}} < n$  we have

$$\text{rank}(\bar{\mathcal{O}}) = \kappa n_{\text{obs}}. \quad (5.72)$$

This is a consequence of the construction of the extended state  $z(t)$ . If we cannot observe the state  $x_i(t)$ , we also cannot observe its fractional-order derivatives.

Following the same ideas we can assure, that the associated fractional-order system also inherits the controllability properties of the original integer-order system.

**Theorem 5.8 (Controllability).** *The associated fractional-order system (5.16) is completely controllable if and only if the original integer-order system (5.1) is completely controllable.*

*Proof.* The controllability matrix of the pair  $(\bar{A}, \bar{B})$  is given by

$$\bar{\mathcal{C}} = \begin{pmatrix} 0 & \cdots & B & 0 & \cdots & AB & \cdots & 0 & \cdots & A^{n-1}B \\ \vdots & \ddots & \vdots & \vdots & \ddots & \vdots & \cdots & \vdots & \ddots & \vdots \\ B & \cdots & 0 & AB & \cdots & 0 & \cdots & A^{n-1}B & \cdots & 0 \end{pmatrix} = \begin{pmatrix} \bar{I}_\kappa \otimes B \\ \bar{I}_\kappa \otimes AB \\ \vdots \\ \bar{I}_\kappa \otimes A^{n-1}B \end{pmatrix} \quad (5.73)$$

with the anti-diagonal matrix

$$\bar{I}_\kappa = \begin{pmatrix} 0 & \cdots & 1 \\ \vdots & \ddots & \vdots \\ 1 & \cdots & 0 \end{pmatrix} \in \mathbb{R}^{\kappa \times \kappa}. \quad (5.74)$$

The rearrangement of the columns lets us determine the rank

$$\text{rank } \bar{C} = \text{rank} (\text{diag} (C, C, \dots, C)) = \kappa \text{rank}(C). \quad (5.75)$$

In the case of the non-controllable state  $x_i(t)$ , the input can also not drive the fractional-order derivatives  $\mathcal{D}^{\alpha_j} x_i(t)$  with  $j = 1, \dots, \kappa - 1$  to zero.  $\square$

**Theorem 5.9** (Observability). *The associated fractional-order system in the integral representation (5.6) is completely observable if and only if the original integer-order system (5.16) satisfies  $\text{rank}(A) = n$  and is completely observable.*

*Proof.* In contrast to the derivative representation, this fractional-order system only conserves the observability properties of the original integer-order system if the system has no integrator, i.e.  $\text{rank}(A) \neq 0$ . The observability matrix of the pair  $(\bar{C}, \bar{A})$  is given by

$$\bar{\mathcal{O}} = \begin{pmatrix} & & \bar{C} \\ & I_\kappa \otimes & CA \\ & I_\kappa \otimes & CA^2 \\ & \vdots & \\ (I_{\kappa-1} \ 0) \otimes & & CA^n \end{pmatrix} \quad (5.76)$$

In this case rearranging the lines yields

$$\text{rank } \bar{\mathcal{O}} = \text{rank} (\text{diag} (\mathcal{O}A, \mathcal{O}A, \dots, \mathcal{O}A, \mathcal{O})) \quad (5.77)$$

$\bar{\mathcal{O}}$  has only full column rank if the integer-order system is completely observable, i.e.  $\text{rank}(\mathcal{O}) = n$  and  $\text{rank}(A) = n$ .

This additional requirement is not as restrictive as it seems. If  $\text{rank}(\mathcal{O}) = n$  and  $\text{rank}(A) < n$  all states of the non-observable subspace have the initial condition zero. Regarding the observer design, it is furthermore possible to include the fractional-order integral of the output. This changes the output matrix to

$$\bar{C}_{\text{new}} = (C \ * \ \cdots \ * \ C), \quad (5.78)$$

where each term denoted by  $*$  might also be exchanged with the matrix  $C$ .  $\square$

The controllability of the associated fractional-order system in the integral representation does only require the controllability of the original integer-order system.

**Theorem 5.10** (Controllability). *The associated fractional-order system in the integral representation (5.6) is completely controllable if and only if the original integer-order system (5.1) is completely controllable.*

*Proof.* To proof the controllability of the extended state with respect to the original input  $u(t)$ , we have to extend the state  $z(t)$  with the fractional-order integrals of the input. In the single input case this leads to

$$\mathcal{D}^\alpha \bar{z}(t) = \begin{pmatrix} \bar{A} & \bar{B} & 0 \\ 0 & 0 & I_{\kappa-2} \\ 0 & 0 & 0 \end{pmatrix} \begin{pmatrix} z(t) \\ \hat{u}_1(t) \\ \hat{u}_2(t) \end{pmatrix} + \begin{pmatrix} 0 \\ 0 \\ 1 \end{pmatrix} u(t), \quad (5.79)$$

introducing auxiliary states  $\hat{u}_2(t) \in \mathbb{R}^1$ ,  $\hat{u}_1(t) \in \mathbb{R}^{\kappa-2}$  with  $\hat{u}_1(0) = 0$  and  $\hat{u}_2(0) = 0$ . The second auxiliary state  $\hat{u}_2$  represents the fractional integral of order  $\alpha$  with respect to the original input:  $\hat{u}_2(t) = \mathcal{I}^\alpha u(t)$ . With the shifting part  $I_{\kappa-2}$  of the extended state matrix in (5.79) this fractional integration is performed  $\kappa - 2$  times such that the first element of  $\hat{u}_1$  resembles the input  $\bar{u}$  of (5.6):  $\hat{u}_{1,1}(t) = \mathcal{I}^{1-\alpha} u(t) = \bar{u}(t)$ . This state extension is also necessary to simulate the associated fractional-order system.  $\square$

**Remark 5.5** (Fractional-Order Paradox). *In view of the controllability analysis, let us consider the fractional-order pole placement control of scalar integer-order system*

$$\dot{x}(t) = ax + u, \quad x(0) = x_0. \quad (5.80)$$

Obviously, the derivative of the state is bounded if the state and the input is bounded.

Now, let us use the fractional-order control law

$$u(t) = -k_1 x(t) - k_2 \mathcal{D}^\alpha x(t), \quad \alpha = \frac{1}{2} \quad (5.81)$$

placing the closed loop eigenvalues on the negative real line, i.e.  $\lambda_1 \leq \lambda_2 < 0$ . With a bounded state and a bounded fractional-order derivative, this control law is also bounded. As both eigenvalues are negative and real, this control law clearly introduces fractional-order behavior, such that no hidden integer-order dynamics remain. With the extended fractional-order state-space, the closed loop dynamics read

$$\mathcal{D}^\alpha \begin{pmatrix} x(t) \\ \mathcal{D}^\alpha x(t) \end{pmatrix} = \begin{pmatrix} 0 & 1 \\ a - k_1 & -k_2 \end{pmatrix} \begin{pmatrix} x(t) \\ \mathcal{D}^\alpha x(t) \end{pmatrix}. \quad (5.82)$$

The solution to this fractional-order system is given in terms of the Mittag-Leffler function (3.5). The scalar Mittag-Leffler function, however, shows an unbounded derivative at  $t = 0$  which is a contradiction to the boundedness of the control law. To show how this paradox is resolved we have to derive the solution of (5.82) in detail using the Jordan canonical form. The transformation matrices are given by

$$T = \begin{pmatrix} \frac{\lambda_1 + k_2}{a - k_1} & \frac{\lambda_2 + k_2}{a - k_1} \\ 1 & 1 \end{pmatrix}, \quad T^{-1} = \frac{1}{\lambda_1 - \lambda_2} \begin{pmatrix} a - k_1 & -k_2 - \lambda_2 \\ -a + k_1 & -k_2 - \lambda_1 \end{pmatrix}. \quad (5.83)$$

This leads to the following solution of the fractional-order dynamics

$$\begin{pmatrix} x(t) \\ \mathcal{D}^\alpha x(t) \end{pmatrix} = T \begin{pmatrix} \mathcal{E}_{\alpha,1}(\lambda_1 t^\alpha) & 0 \\ 0 & \mathcal{E}_{\alpha,1}(\lambda_2 t^\alpha) \end{pmatrix} T^{-1} \begin{pmatrix} x_0 \\ 0 \end{pmatrix} \quad (5.84)$$

$$= T \begin{pmatrix} \mathcal{E}_{\alpha,1}(\lambda_1 t^\alpha) & 0 \\ 0 & \mathcal{E}_{\alpha,1}(\lambda_2 t^\alpha) \end{pmatrix} \frac{1}{\lambda_1 - \lambda_2} \begin{pmatrix} (a - k_1)x_0 \\ -(a - k_1)x_0 \end{pmatrix}. \quad (5.85)$$

The evolution of the original state then is given by

$$x(t) = \frac{x_0}{\lambda_1 - \lambda_2} \left( (\lambda_1 + k_2) \mathcal{E}_{\alpha,1}(\lambda_1 t^\alpha) - (\lambda_2 + k_2) \mathcal{E}_{\alpha,1}(\lambda_2 t^\alpha) \right) \quad (5.86)$$

with  $k_2 = -(\lambda_1 + \lambda_2)$  this leads to

$$x(t) = \frac{x_0}{\lambda_1 - \lambda_2} \left( \lambda_1 \mathcal{E}_{\alpha,1}(\lambda_2 t^\alpha) - \lambda_2 \mathcal{E}_{\alpha,1}(\lambda_1 t^\alpha) \right). \quad (5.87)$$

With this analytic solution we can now evaluate the derivative of  $x(t)$

$$\dot{x}(t) = \frac{x_0}{\lambda_1 - \lambda_2} \left( \lambda_1 \sum_{k=1}^{\infty} \frac{\lambda_2^k \alpha k t^{\alpha k - 1}}{\Gamma(\alpha k + 1)} - \lambda_2 \sum_{k=1}^{\infty} \frac{\lambda_1^k \alpha k t^{\alpha k - 1}}{\Gamma(\alpha k + 1)} \right) \quad (5.88)$$

For  $t = 0$  and  $\alpha = \frac{1}{2}$  only the first two summands of each Mittag-Leffler function are non-zero and we have

$$\dot{x}(0) = \frac{x_0}{\lambda_1 - \lambda_2} \left( \frac{\lambda_1 \lambda_2 t^{-\alpha}}{\Gamma(\alpha)} + \frac{\lambda_1 \lambda_2^2 t^0}{\Gamma(2\alpha)} - \frac{\lambda_1 \lambda_2 t^{-\alpha}}{\Gamma(\alpha)} - \frac{\lambda_1^2 \lambda_2 t^0}{\Gamma(2\alpha)} \right) \Big|_{t=0} \quad (5.89)$$

$$= \frac{x_0}{\lambda_1 - \lambda_2} \left( \frac{\lambda_1 \lambda_2 (\lambda_2 - \lambda_1)}{\Gamma(1)} \right) \quad (5.90)$$

$$= -\lambda_1 \lambda_2 x_0 = -k_1 x_0 + k_2 \cdot 0. \quad (5.91)$$

We see that the initial singularity in the derivative of each Mittag-Leffler function cancels such that the derivative of the state remains bounded as given by the bounded initial state and control law. This resolves the apparent paradox. Furthermore, we see that fractional-order control of integer-order systems does not accelerate the initial system response with an infinite derivative, however, it leads to the slow convergence for large times due to the algebraic decay.

### 5.3 Fractional-Order Observer for Integer-Order LTI System

With the fractional-order representation of the integer-order system we are now able to design an observer showing fractional-order error dynamics. The aim here is to increase the initial convergence, as the fractional-order dynamics can be designed such that they show an infinite derivative at the initial time. This acceleration at the beginning of the observation is suited to compensate the effect of unknown initial conditions.

We use the derivative representation of the associated fractional-order system (5.16) such that we can also include the case  $\text{rank}(A) < n$ . The fractional-order full-state observer of the Luenberger type is given by:

$$\mathcal{D}^\alpha \hat{z}(t) = \bar{A} \hat{z}(t) + \bar{B} u(t) + \bar{L}(y(t) - \bar{C} \hat{z}(t)) \quad (5.92a)$$

$$\hat{x}(t) = S \hat{z}(t), \quad (5.92b)$$

with  $\alpha^{-1} = \kappa \in \mathbb{N}$  and the observer gain  $\bar{L} \in \mathbb{R}^{\kappa n \times q}$ . With a reduced order  $\alpha$  the number of states of the associated system does increase. If the observer should only estimate the original state  $x(t)$  (and not any of its fractional-order derivatives), setting  $\alpha = \frac{1}{2}$  is sufficient to increase the initial convergence with a minimum of auxiliary states to keep the computational

costs low. With the extended state  $z(t)$  the measured output is given by  $y(t) = \bar{C}z(t)$ . The fractional-order dynamics of the extended estimation error  $e_z(t) = \hat{z}(t) - z(t)$  result in

$$\mathcal{D}^\alpha e_z(t) = (\bar{A} + \bar{L}\bar{C}) e_z(t), \quad e_z(0) = e_{z,0}. \quad (5.93)$$

The observer gain  $\bar{L}$  can be designed using standard algebraic methods [38] such that the poles of  $(\bar{A} + \bar{L}\bar{C})$  satisfy the asymptotic stability condition (3.41).

**Remark 5.6.** *If the observer is set up using the integral representation of the associated fractional-order system, it can be directly extended to a  $PI^\alpha$  observer [89] by modifying the output matrix  $\bar{C}$  to*

$$\tilde{C} = \begin{pmatrix} 0 & \cdots & 0 & 0 & C \\ 0 & \cdots & 0 & C & 0 \end{pmatrix} \quad (5.94)$$

such that a fractional-order integral of the measured output is included.

An integer-order Luenberger observer can set the eigenvalues  $\lambda$  of the matrix  $A + LC$  anywhere in the negative half plane  $\mathbb{C}^-$  to achieve an asymptotically stable estimation error. In view of the fractional-order domain, this observer gain  $L$  cannot place the corresponding fractional-order eigenvalues  $\bar{\lambda}$  arbitrarily close together. Due to (5.55) there is a minimum difference in the argument of the fractional-order eigenvalues

$$\bar{\lambda}_l = \sqrt[l]{\lambda_i} \quad \iff \quad \Delta \arg(\bar{\lambda}_l) \geq \frac{2\pi}{\kappa} \quad (5.95)$$

with  $l = 1, 2, \dots, \kappa$ . Hence, the integer-order observer cannot place the eigenvalue on the negative real axis in the fractional-order domain.

Thus, the fractional-order observer (5.92) has a higher degree of freedom. The eigenvalues can be placed arbitrarily in the fractional-order domain, especially negative real eigenvalues are possible. In order to generate real fractional-order dynamics, we have to exclude hidden integer-order dynamics, hence we require for some constant  $\lambda^*$

$$\bar{\lambda}_l \neq \sqrt[l]{\lambda^*}, \quad l = 1, 2, \dots, \kappa. \quad (5.96)$$

**Remark 5.7.** *Note that a part of the initial conditions is known as all auxiliary states  $\mathcal{D}^{i\alpha}x(t)$  are zero at  $t = 0$  as given by (5.17). With the observer initialization*

$$\hat{z}(0)^\top = \left( \hat{x}_0^\top \quad 0 \quad \cdots \quad 0 \right)^\top \quad (5.97)$$

the initial error  $e_z(0)$  reads

$$e_z(0)^\top = \left( \hat{e}_0^\top \quad 0 \quad \cdots \quad 0 \right)^\top. \quad (5.98)$$

Compared to the control paradox in discussed in Remark 5.5 the estimation error shows an unbounded derivative at  $t = 0$ . As the structure of the observer is slightly different, the concept of duality leads to wrong results. The observer is actually a fractional-order system (especially when the auxiliary states are not initialized with zero). Furthermore, the associated fractional-order system is somehow in a generalized block controllable canonical form and the observer gain sets the eigenvalues by influencing the first  $n$  columns.

All in all this observer achieves a fast convergence of the estimation error immediately after the initialization but shows a slow convergence for large times due to the algebraic decay of the Mittag-Leffler function [54].



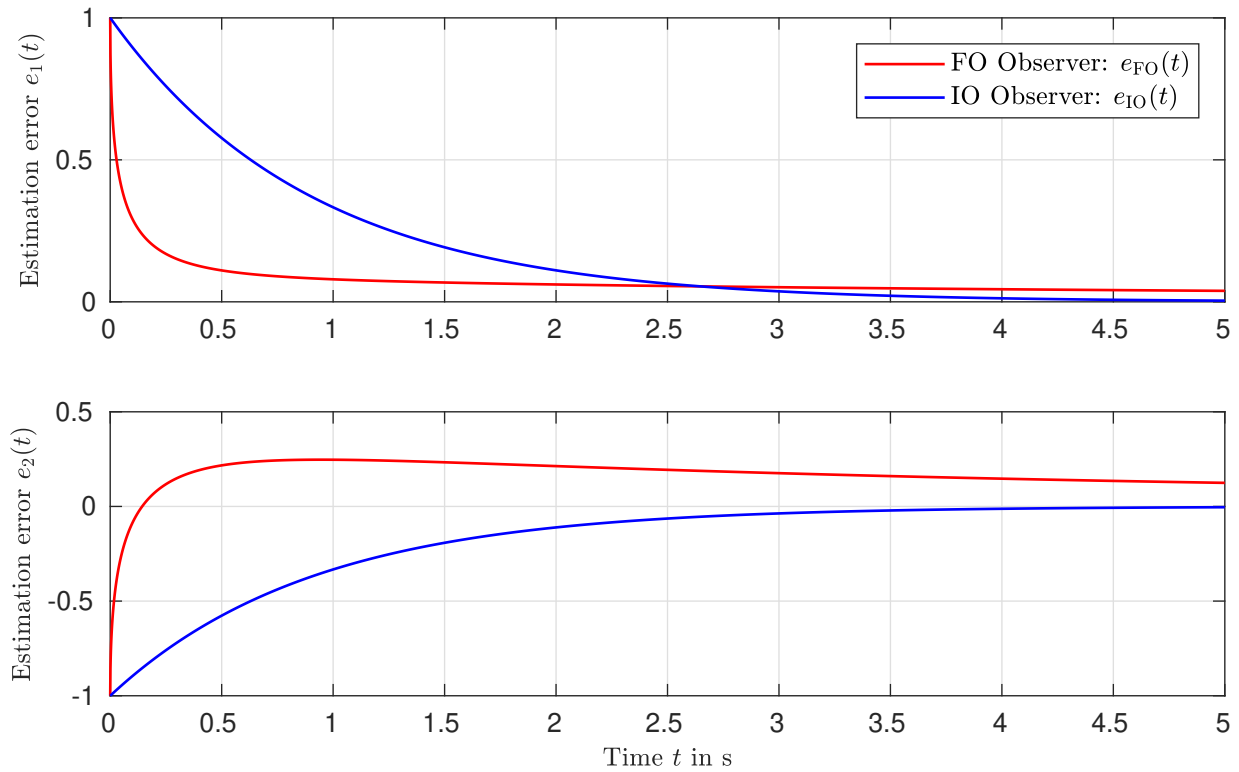


Figure 5.1: Estimation error of a fractional- and an integer-order Luenberger observer.

**Example 5.1.** Consider the academic example

$$\dot{x}(t) = \begin{pmatrix} 0 & 1 \\ 0 & -2 \end{pmatrix} x(t) + \begin{pmatrix} -1 \\ 0.5 \end{pmatrix} u(t), \quad x(0) = \begin{pmatrix} -1 \\ 1 \end{pmatrix}, \quad (5.99a)$$

$$y(t) = \begin{pmatrix} 1 & 0 \end{pmatrix} x(t). \quad (5.99b)$$

The fractional-order observer with  $\alpha = \frac{1}{2}$  is designed to place the eigenvalues of  $(\bar{A} + \bar{L}\bar{C})$  to  $\lambda_{\text{FO},i} \in \{-0.8, -0.9, -1.1, -1.2\}$ . For comparison, an integer-order observer with the eigenvalues  $\lambda_{\text{IO},i} \in \{-0.9, -1.1\}$  is used. We choose the absolute value of the eigenvalues to be close to one such that we can compare the eigenvalue location of both observers in the fractional-order domain without scaling the absolute value.

All observers are initialized with  $\hat{x}(0) = 0$ . To run the fractional-order observer, we resort to apply the fractional-order solver *FDE12.m* [21]. The results are shown in Figure 5.1. The initial benefit of the fractional-order observer is clearly visible as the convergence is driven by the infinite derivative at  $t = 0$ . For larger times  $t > 0.5$  s the algebraic decay degrades the performance drastically. So it is advisable to rely on an integer-order observer after  $t = 0.5$  s.

In view of the associated integer-order system presented in Chapter 4.1, the mechanism of how the fractional-order can accelerate the convergence is due to two terms. The first term weighs the initial estimation error  $e_z(0)$  with the memory function  $f(t)$  given in (4.6). This memory function induces the unbounded derivative to the state transitions. The second term

only occurs in the observer coordinates. In the integer-order representation of the fractional-order observer, the fractional-order derivatives of the output error  $e_y(t)$  accelerate the observer dynamics.

### 5.3.1 Fractional-Order Memory-Reset Luenberger Observer

As the integer-order system is time-invariant we can set the initial time of the observation arbitrarily. Hence the idea is to use the fast initial convergence multiple times. To achieve this, we have to reset the memory of the fractional-order operator at the time instants  $t_k = k\delta$  defining the observer dynamics

$${}_{\delta k}D^\alpha \hat{z}(t) = \bar{A}\hat{z}(t) + \bar{B}u(t) + \bar{L}(\bar{C}\hat{z}(t) - y(t)), \quad t \neq t_k \quad (5.100a)$$

$$\hat{x}(t) = S\hat{z}(t). \quad (5.100b)$$

This, however, is only a part of the reinitialization. As we change the initial time of the operator, we have to change the initial conditions of the associated fractional-order system. With the reinitialization of the observer states at the time instant  $t_k = \delta k$  given by

$$\hat{z}(t_k) = S^\top S\hat{z}(t_k^-) = \begin{pmatrix} \hat{x}(t_k^-) \\ 0 \\ \vdots \\ 0 \end{pmatrix}, \quad t = t_k, \quad (5.101)$$

the auxiliary states in the observer are reset to zero, the extended observer state is discontinuous and the complete error dynamics are given by a hybrid fractional-order system:

$${}_{k\delta}D^\alpha e_z(t) = (\bar{A} + \bar{L}\bar{C})e_z(t), \quad t \neq k\delta \quad (5.102)$$

$$e_z(t_k) = S^\top S e_z(t_k^-), \quad t = k\delta. \quad (5.103)$$

**Theorem 5.11.** *The estimation error dynamics defined by (5.102) are asymptotically stable if and only if*

$$|\lambda_i| < 1, \quad i = 1, 2, \dots, \kappa n, \quad (5.104)$$

where  $\lambda_i$  denotes the  $i$ th eigenvalue of the dynamic matrix  $\tilde{A}_d = S\mathcal{E}_{\alpha,1}((\bar{A} + \bar{L}\bar{C})\delta^\alpha)S^\top$ .

*Proof.* The periodic reset of the observer induces underlying discrete dynamics connecting the estimation error at the reset instants as described by the sequence

$$(e_z(\delta k)) = (e_z(0), e_z(\delta), e_z(2\delta), \dots). \quad (5.105)$$

The connection between two consecutive estimation errors is defined by the projection of the matrix Mittag-Leffler function

$$e_z((k+1)\delta) = S^\top S\mathcal{E}_{\alpha,1}((\bar{A} + \bar{L}\bar{C})\delta^\alpha)e_z(k\delta) = A_d e_z(k\delta). \quad (5.106)$$

Following the ideas presented in [108], we can assure the stability of the estimation error by investigating the eigenvalues of  $A_d$ . As the estimates of the auxiliary states are initialized

correctly at each reset instant, we can reduce the dimension of the analysis to the original error coordinates

$$e((k+1)\delta) = S\mathcal{E}_{\alpha,1}((\bar{A} + \bar{L}\bar{C})\delta^\alpha)S^\top e(k\delta) = \tilde{A}_d e(k\delta). \quad (5.107)$$

As the linear fractional-order time-invariant system has no finite escape time and the dynamics are bounded within a finite time interval, the stability analysis can be reduced to the reset instants  $e(k\delta)$ . Hence the location of the eigenvalues of  $\tilde{A}_d$  with respect to the unit circle determines the stability [81].  $\square$

**Corollary 5.1** (Exponential Convergence). *The fractional-order memory reset observer leads to an exponentially converging estimation error  $e_z(t)$ .*

As the induced discrete dynamics are exponentially stable, the exponential convergence of the estimation error is a direct consequence of Theorem 5.11.

**Corollary 5.2.** *Asymptotic stability of the hybrid fractional-order estimation error dynamics (5.102) neither requires nor needs the asymptotic stability of the non-reset estimation error dynamics (5.93).*

*Proof.* The stability of the memory reset estimation error dynamics is achieved regardless of the stability of the underlying non-reset fractional-order dynamics. This can be illustrated with the scalar system

$$\dot{y} = ay(t). \quad (5.108)$$

The extended fractional-order system for  $\alpha = \frac{1}{2}$  reads

$$\begin{aligned} \mathcal{D}^\alpha z(t) &= \begin{pmatrix} 0 & 1 \\ a & 0 \end{pmatrix} z(t) = \bar{A}z(t) \\ y(t) &= \begin{pmatrix} 1 & 0 \end{pmatrix} z(t) = \bar{C}z(t) \end{aligned}$$

with the gain  $\bar{L} = \begin{pmatrix} l_1 & l_2 \end{pmatrix}^\top$  the dynamics of the estimation error  $e_z(t)$  are given by

$$\mathcal{D}^\alpha e_z(t) = (\bar{A} + \bar{L}\bar{C})e_z(t) = \begin{pmatrix} l_1 & 1 \\ a + l_2 & 0 \end{pmatrix} e_z(t). \quad (5.109)$$

With the observer gain  $\bar{L}$  we can place the complex conjugate eigenvalues of  $(\bar{A} + \bar{L}\bar{C})$  in the stable domain. For the associated system with two states  $z(t) \in \mathbb{R}^2$  we have two possibilities to set the poles of  $(\bar{A} + \bar{L}\bar{C})$ . Either we chose two conjugate complex eigenvalues or two different real eigenvalues. For the reset period  $\delta = 0.01$  s we compute the projection of the Mittag-Leffler function and evaluate the eigenvalues of this discrete system matrix. The results are shown in Figure 5.2. The color of each eigenvalue indicates the absolute value of corresponding non-zero discrete eigenvalue  $\lambda_d$ . The green dots represent stable induced dynamics, whereas the red dots indicate unstable induced dynamics.

For the conjugate complex pole pairs close to the stability margin, the periodic reset of the system leads to an unstable behavior as one discrete eigenvalue has an absolute value larger than one. In the time domain we can interpret this phenomenon by considering the overshooting, which is generated by the complex pole pair with the low damping. If the reset takes place before the overshooting has declined, the same overshooting will occur in the subsequent time-interval increasing the norm of the state again. This results in instability.

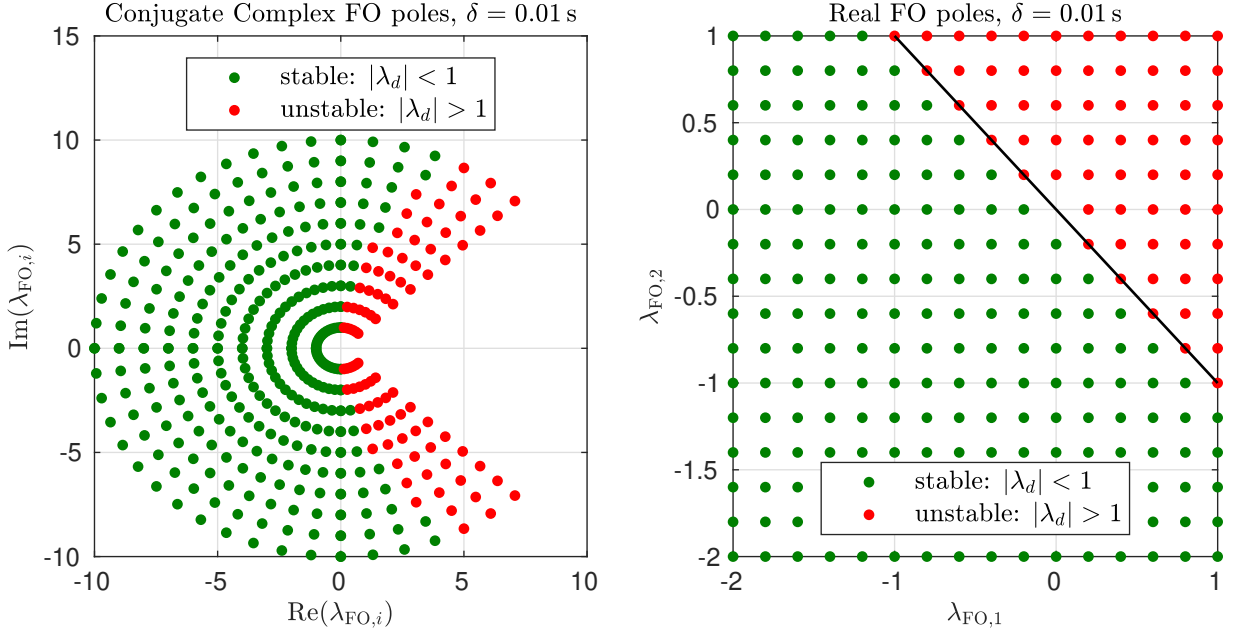


Figure 5.2: Poles of the induced discrete time system with respect to the original fractional-order pole locations.

Using the same example, we can show that the reset can stabilize unstable modes in the underlying non-reset dynamics. We set one eigenvalue of the fractional-order dynamics to be stable  $\lambda_{\text{FO},1} = -\gamma_1$  and the second one to be unstable  $\lambda_{\text{FO},2} = \gamma_2$  with  $\gamma_i > 0$ . The projection matrix  $M^T M$  cancels the unstable mode by shifting the corresponding unstable discrete eigenvalue to zero. Note that the stable pole somehow has to dominate the unstable mode  $\gamma_1 > \gamma_2$ , as illustrated in Figure 5.2 (right).

This is a known fact from integer-order reset systems. It can be used to improve reset controllers by introducing instability to the reset elements [69] to accelerate the dynamics.  $\square$

Finally, we discuss the effect of the reinitialization period  $\delta$  in detail. It is an additional design parameter to the fractional-order observer. We illustrate this discussion using the scalar system (5.108) from the previous considerations. First of all, we see that with a smaller  $\delta$  the stability region of the fractional-order poles is reduced if the poles are placed in the stable sector of the complex plane. This is shown in the left column of Figure 5.3. For the larger reset period  $\delta = 0.1$  s the large majority of the tested poles lead to stable discrete dynamics. For the real unstable poles, as illustrated in the right column of Figure 5.3, however, we see that more reset systems (with one positive real fractional-order pole) are stable if the reset period is larger. To show how the reinitialization period  $\delta$  influences the convergence rate of the system, we compare the continuous-time equivalent of the remaining discrete-time eigenvalue

$$\lambda_c = \frac{\ln(\lambda_d)}{\delta}, \lambda_d > 0. \quad (5.110)$$

If the remaining discrete dynamics only shows one stable but negative pole, we cannot interpret this in the continuous time domain. The results for three different reset periods are depicted in Figure 5.4. With a shorter reset time, the induced discrete time dynamics are

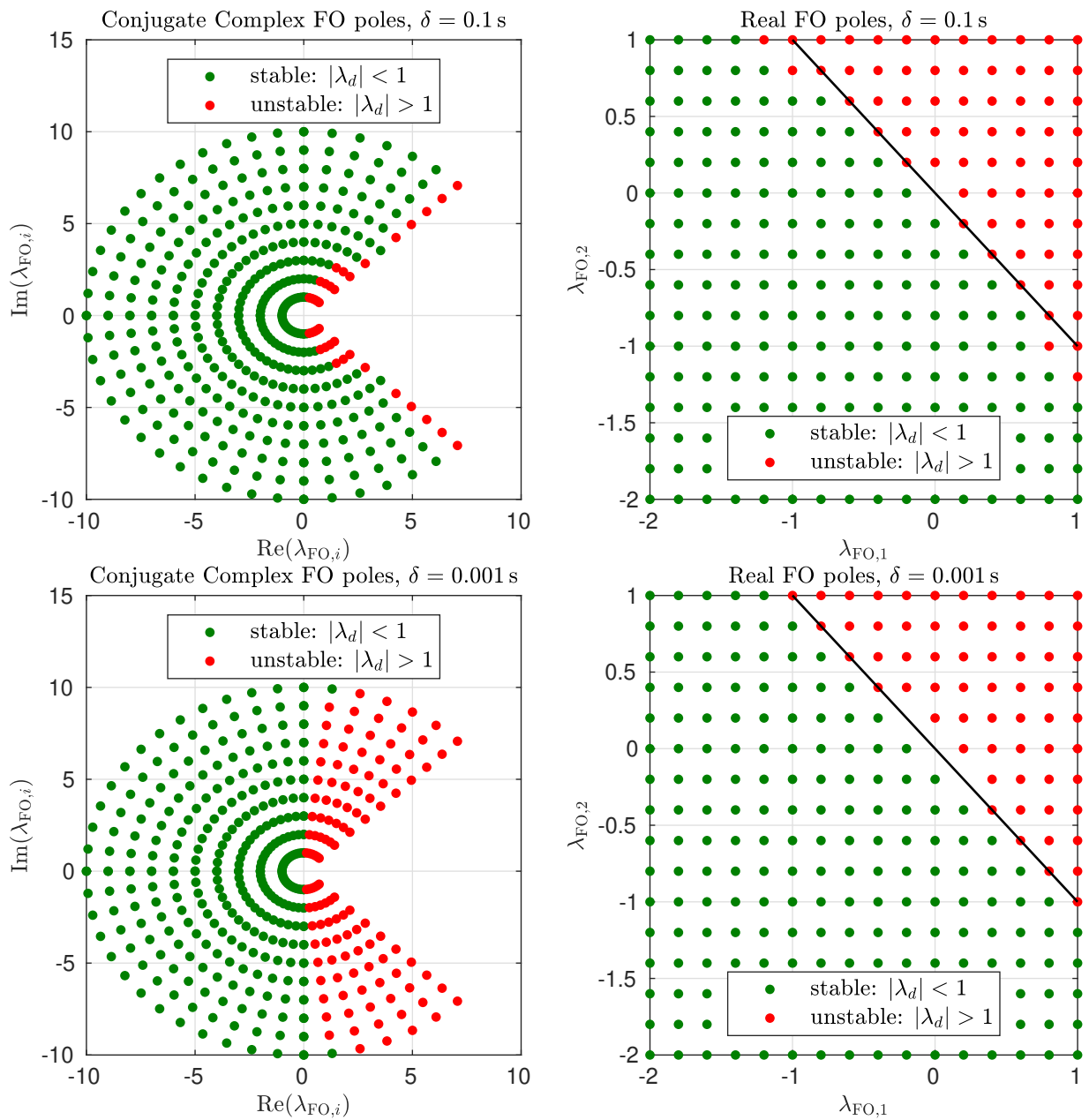


Figure 5.3: Poles of the induced discrete time system with respect to the original fractional-order pole locations for different reset periods  $\delta$ .

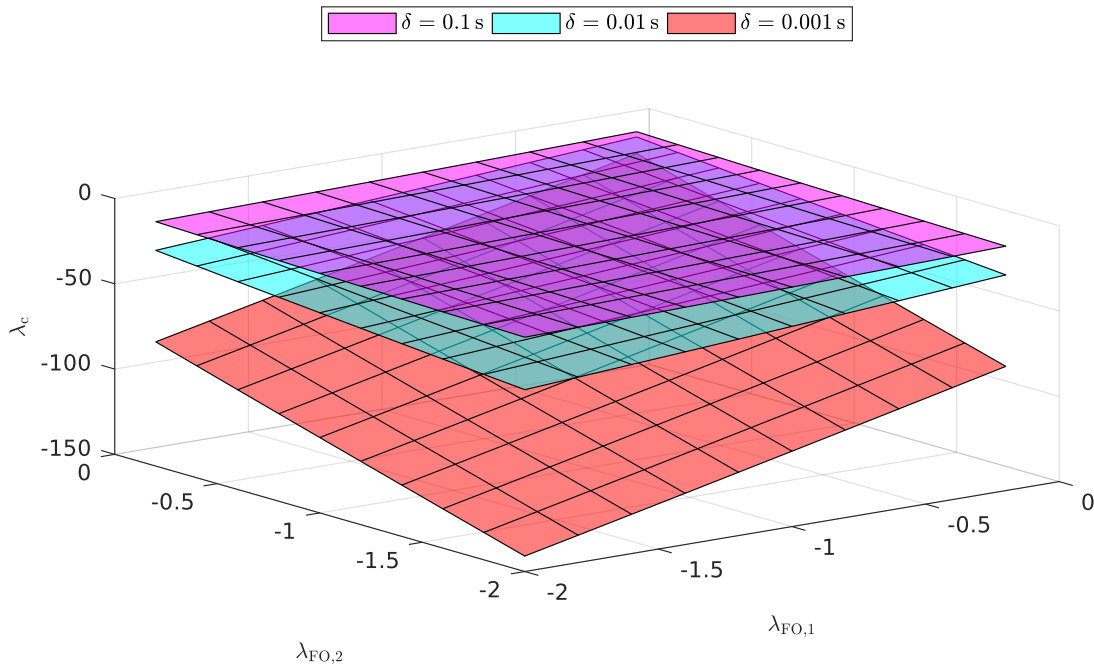


Figure 5.4: For shorter reset intervals, the exponential convergence rate given by  $\text{Re}(\lambda_c)$  is increased.

accelerated. Note that these higher exponential convergence rates can therefore be achieved without changing the observer gains.

**Example 5.1** (continued). Adding the memory reset with  $\delta = 0.2$  s to the fractional-order observer design for the example, (5.99) leads to the estimation error depicted in Figure 5.5. The reset leads to induced dynamics with the continuous eigenvalues located at  $\lambda_{c,1} = -8.85$  and  $\lambda_{c,2} = -0.65$ . To be comparable, the gains of the integer-order Luenberger observer are changed to achieve the identical eigenvalue location. The fractional-order observer still outperforms the integer-order approach in the initial time interval. For larger times, however, the retuned integer-order observer shows the same performance at the cost of increased observer gains

$$L_{\text{FO}} = \begin{pmatrix} -3.80 \\ 4.22 \\ -3.39 \\ 5.99 \end{pmatrix}, \quad L_{\text{IO},1} = \begin{pmatrix} -0.10 \\ -0.9 \end{pmatrix}, \quad L_{\text{IO},2} = \begin{pmatrix} -7.50 \\ 9.21 \end{pmatrix}. \quad (5.111)$$

As illustrated in Figure 5.6, the possible acceleration is limited. It shows the equivalent continuous eigenvalue of the induced dynamics defined by the fractional-order error dynamics in Example 5.1. Only the first eigenvalue  $\lambda_{c,1}$  tends to negative infinity for small  $\delta$ . This mode is connected to the measured output. The second eigenvalue approaches a minimum at  $\min(\lambda_{c,2}(\delta)) \approx -0.87$ . This still limits the convergence of the estimation error and a unified design of the pole location and reset period is required.

**Tuning Considerations** If not the strong initial convergence is required, we might shift the scope of the observer design towards robustness against measurement noise. This robustness

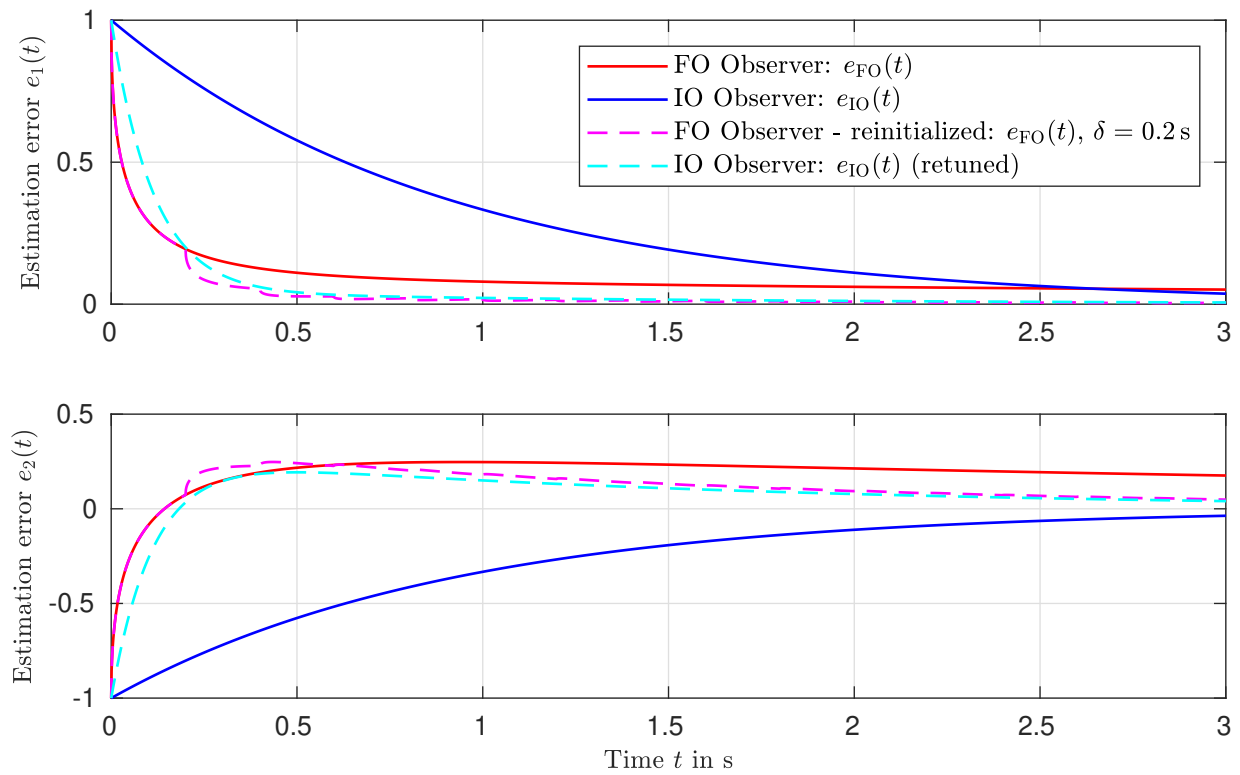


Figure 5.5: With the additional memory reset, the estimation error converges exponentially.

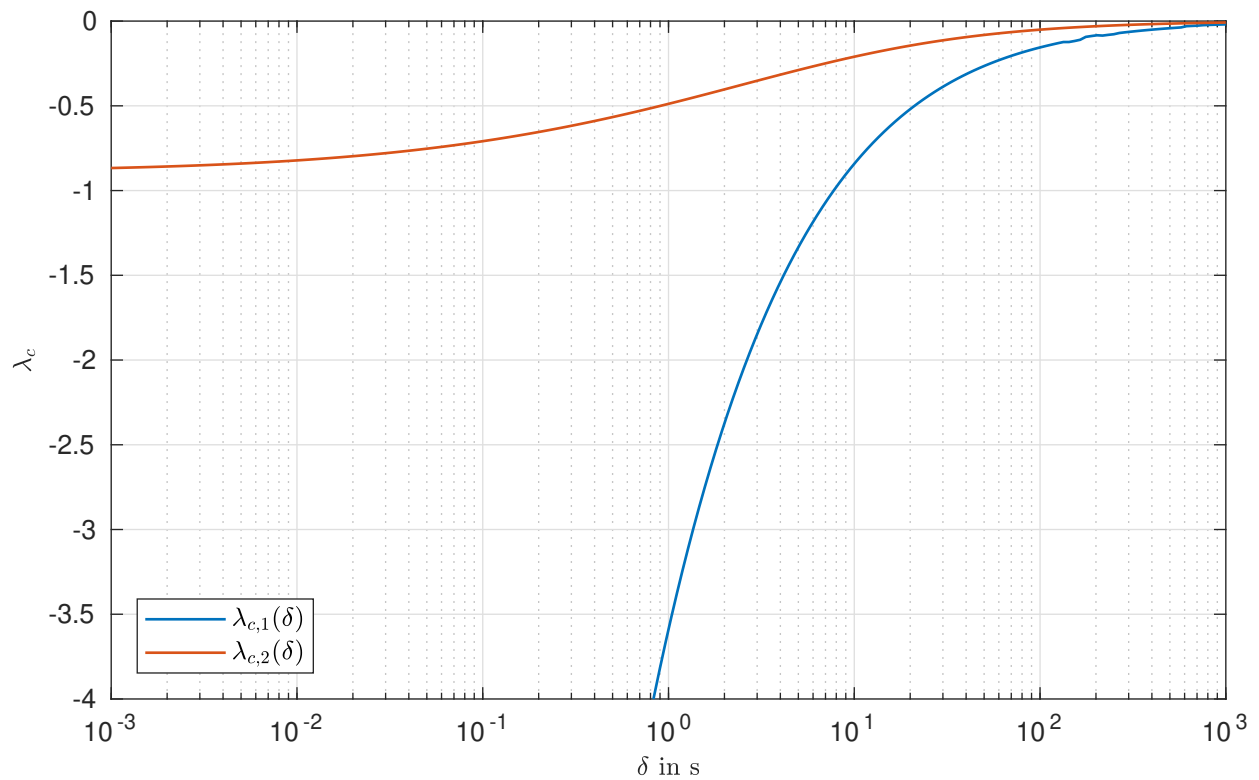


Figure 5.6: Continuous time eigenvalues  $\lambda_c$  of the induced dynamics for different reinitialization periods  $\delta$ .

can be achieved as we have more parameters compared to the integer-order case. In order to reduce the effect of the measurement noise on the state estimation, the objective is to reduce the gains, respectively  $\|\bar{L}\|$ , while maintaining a desired exponential convergence rate due to the reset period  $\delta$ .

However, we have to use non-linear optimization techniques to design the pole location and reset period of the reset observer. Due to the rank defect of the reset matrix  $S^\top S$ , we cannot invert the analysis procedure and desired discrete dynamics can be achieved by different sets of fractional-order poles and reset periods  $\delta$ .

**Example 5.1** (continued). *We continue with the integer-order example defined by (5.99) and illustrate how the fractional-order memory reset observer can handle measurement noise. For comparison, we use an integer-order observer which places the poles at the continuous counterparts of the induced dynamics.*

*Using the nonlinear optimization tool `fmincon` [8], the fractional-order memory reset observer was tuned by minimizing the euclidean norm of the observer gain, while guaranteeing exponential convergence with  $\max(\lambda_c) = -3.4$ . The optimization leads to an increased reset time  $\delta = 1.846$  s and fractional-order poles close to the imaginary axis  $\lambda_{\text{FO}} \in \{0.2323 \pm 1.5025j, -0.0598 \pm 1.5565j\}$  resulting in the induced continuous poles at  $\lambda_{\text{IO}} \in \{-3.8245 \pm 0.0016j\}$ . Clearly, the fractional-order observer shows smaller gains:*

$$L_{\text{FO}} = \begin{pmatrix} 0.3449 & 0.1608 & -2.6820 & -0.2439 \end{pmatrix}^\top, \quad L_{\text{IO},1} = \begin{pmatrix} -5.6491 & -3.3290 \end{pmatrix}^\top.$$

*The simulation results are depicted in Figure 5.7. Both observers are subjected to the same measurement disturbance  $d(t) = 2 \sin(100t)$ , such that the output equation is given by  $y(t) = Cx(t) + d(t)$ . As the fractional-order poles are not real, the initial convergence is no longer dominated by an unbounded derivative at the initial time. With the lower observer gains, the fractional-order observer achieves a better performance, especially in the unmeasured second state. This increased robustness is clearly visible in the frequency domain, regarding the amplitude response of the measurement disturbance  $\mathcal{L}\{d(t); s\} = D(s)$  affecting the estimation error  $\mathcal{L}\{e(t); s\} = E(s)$ , i.e.*

$$\begin{aligned} E_{\text{IO}}(s) &= (sI - (A + L_{\text{IO}}C))^{-1} L_{\text{IO}}D(s) \\ E_{\text{FO}}(s) &= \begin{pmatrix} I & 0 \end{pmatrix} (s^\alpha I - (\bar{A} + L_{\text{FO}}\bar{C}))^{-1} L_{\text{FO}}D(s). \end{aligned}$$

*The corresponding amplitude response is depicted in Figure 5.8 and we can see that the fractional-order observer damps the disturbance over a wide frequency range.*

*However, we can also observe, that the reset does increase the estimation error slightly after each reset. This is especially visible regarding the first error component. This is caused by the measurement disturbance. For slight modelling errors this effect might be worse.*

*Note that the observer design is still not optimal with respect to the measurement noise. However, this example illustrates the possible improvement one can achieve by introducing the additional degrees of freedom to the design.*

### 5.3.2 Reduced Order Impulsive Observer

As we have to reset the fractional-order observer dynamics to overcome the algebraic decay of the fractional-order estimation error dynamics, we can also extend the proposed observer by



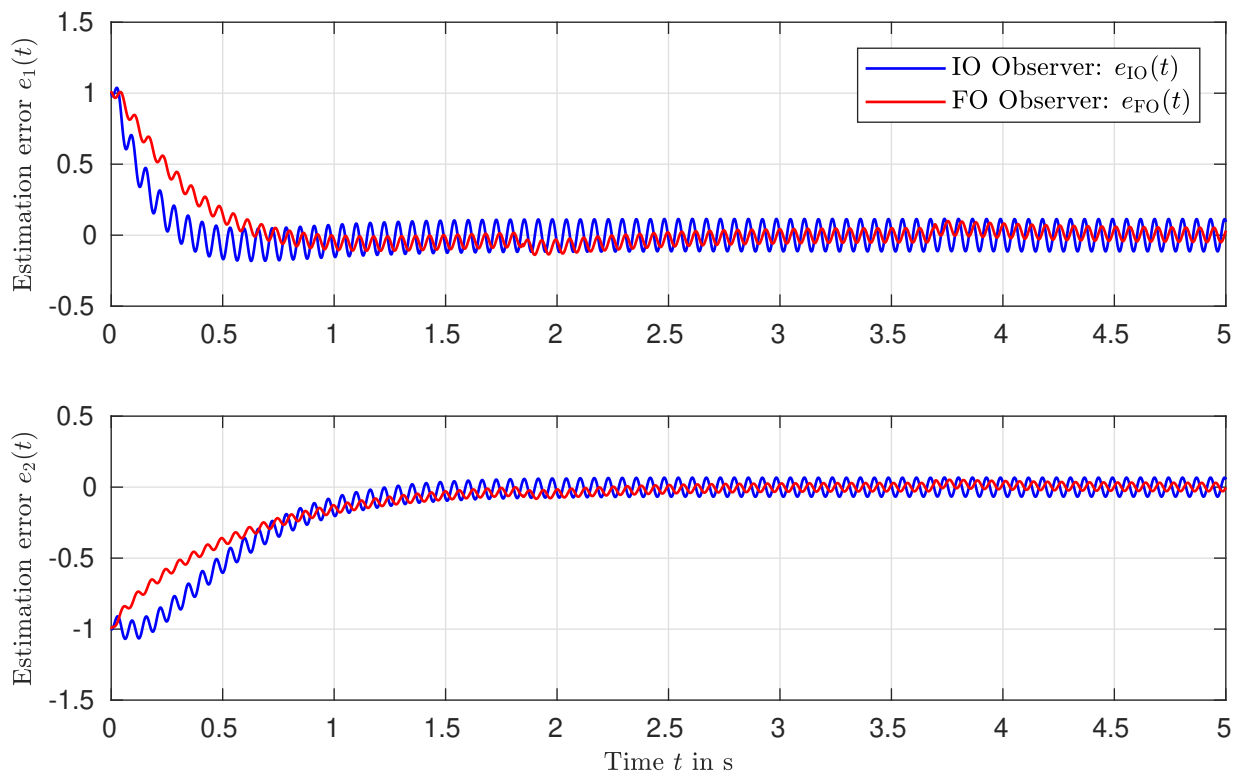


Figure 5.7: Simulation results of the redesigned observers subjected to measurement noise.

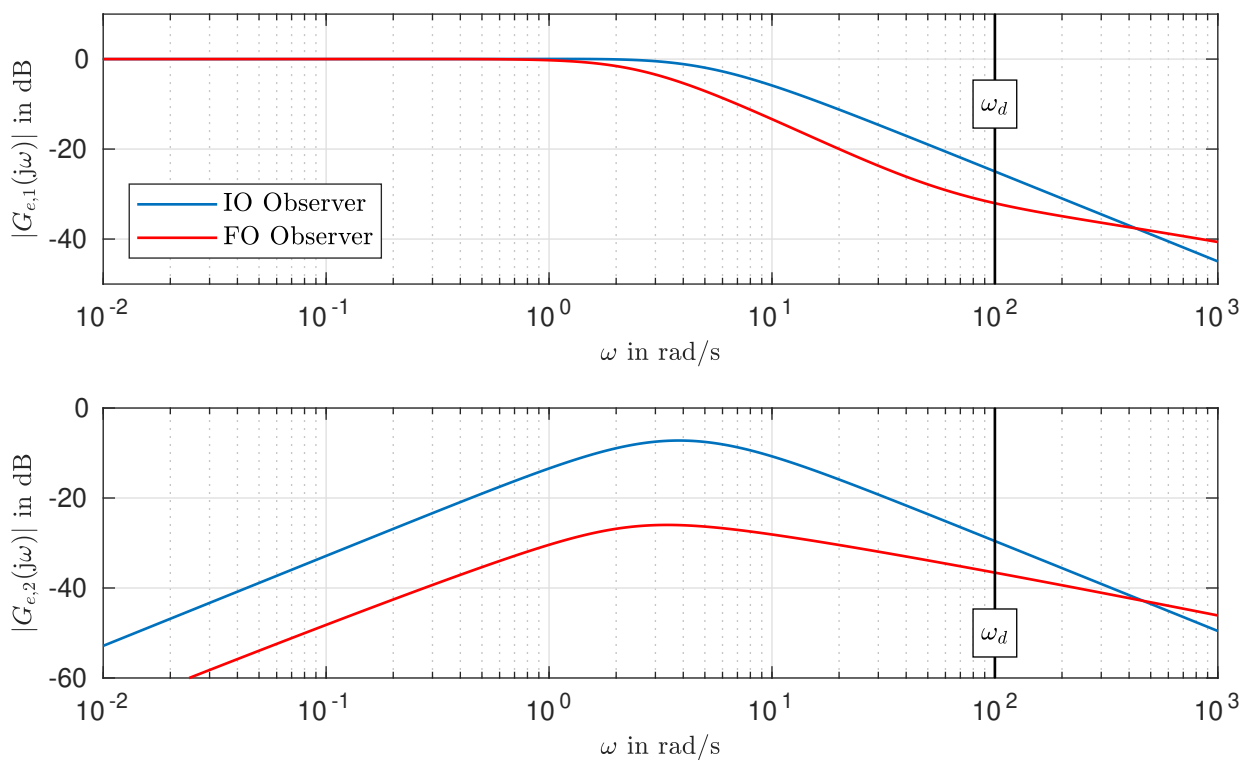


Figure 5.8: Frequency response of the measurement noise effecting the estimation error for the fractional- and integer-order observer approach.

an impulsive reconstruction of the state. This leads to fixed-time convergence of the estimation error.

As the system to be observed is of integer-order, the required second observer could also be an integer-order Luenberger observer

$$\dot{\hat{x}}_2(t) = (A + L_2C)\hat{x}(t) + Bu(t) - L_2y(t) = F_2\hat{x}(t) + Bu(t) - L_2y(t). \quad (5.112)$$

This reduces the numerical demand and we still make use of the fast initial convergence of the fractional-order observer within the first time interval before the algebraic decay decreases the convergence.

In order to keep the numerical effort small, we choose  $\alpha = \frac{1}{2}$  and only reconstruct the original system state  $x(\delta)$  and not the auxiliary fractional-order states. The estimation error  $e_1(\delta) = \hat{x}_1(\delta) - x(\delta)$  of the first observer is given by the projection of the Mittag-Leffler function

$$e_1(\delta) = Se_{z,1}(\delta) = S\mathcal{E}_{\alpha,1}(\bar{F}_1\delta^\alpha)e_{z,1}(0) = S\mathcal{E}_{\alpha,1}(\bar{F}_1\delta^\alpha)S^\top e_1(0). \quad (5.113)$$

The transition of each estimation error can be written as

$$\begin{pmatrix} \hat{x}_1(\delta) - x(\delta) \\ \hat{x}_2(\delta) - x(\delta) \end{pmatrix} = \begin{pmatrix} S\mathcal{E}_{\alpha,1}(\bar{F}_1\delta^\alpha)S^\top & 0 \\ 0 & \exp(F_2\delta) \end{pmatrix} \begin{pmatrix} \hat{x}_1(0) - x(0) \\ \hat{x}_2(0) - x(0) \end{pmatrix}. \quad (5.114)$$

Solving for the state  $x(\delta)$  and  $x(0)$ , we have to rearrange the terms again

$$\underbrace{\begin{pmatrix} I & -S\mathcal{E}_{\alpha,1}(\bar{F}_1\delta^\alpha)S^\top \\ I & -\exp(F_2\delta) \end{pmatrix}}_{\Omega} \begin{pmatrix} x(\delta) \\ x(0) \end{pmatrix} = \begin{pmatrix} \hat{x}_1(\delta) - S\mathcal{E}_{\alpha,1}(\bar{F}_1\delta^\alpha)S^\top \hat{x}_1(0) \\ \hat{x}_2(\delta) - \exp(F_2\delta)\hat{x}_2(0) \end{pmatrix}. \quad (5.115)$$

The difference to the fixed-time reconstruction of the fractional-order system in Section 4.3.3 is that we do not require the initial state of the system as all the memory is contained in the state itself. Hence, we can reduce the inversion of the matrix  $\Omega \in \mathbb{R}^{2n \times 2n}$  to the inversion of a smaller matrix  $\tilde{\Omega} \in \mathbb{R}^{n \times n}$ . We apply the Schur decomposition to  $\Omega$  with  $(\exp(F_2\delta))^{-1} = \exp(-F_2\delta)$

$$\Omega = \begin{pmatrix} I & 0 \\ -\exp(-F_2\delta) & I \end{pmatrix} \begin{pmatrix} I - S\mathcal{E}_{\alpha,1}(\bar{F}_1\delta^\alpha)S^\top \exp(-F_2\delta) & 0 \\ 0 & \exp(F_2\delta) \end{pmatrix} \begin{pmatrix} I & -\exp(-F_2\delta) \\ 0 & I \end{pmatrix}$$

and the state at the first reset instant is given by

$$x(\delta) = K \begin{pmatrix} \hat{x}_1(\delta) - S\mathcal{E}_{\alpha,1}(\bar{F}_1\delta^\alpha)S^\top \hat{x}_1(0) \\ \hat{x}_2(\delta) - \exp(F_2\delta)\hat{x}_2(0) \end{pmatrix}$$

with

$$K = \underbrace{\left( I - S\mathcal{E}_{\alpha,1}(\bar{F}_1\delta^\alpha)S^\top \exp(-F_2\delta) \right)}_{\tilde{\Omega}}^{-1} \begin{pmatrix} I & -S\mathcal{E}_{\alpha,1}(\bar{F}_1\delta^\alpha)S^\top \exp(-F_2\delta) \end{pmatrix}. \quad (5.116)$$

The structure of the reset matrix  $K$  is similar to the observer structure given in [78, p. 9]. Finally, the complete fractional-order impulsive observer is given by:

$${}_{k\delta}D^{\frac{1}{2}}\hat{z}_1(t) = (\bar{A} + \bar{L}_1\bar{C})z_1(t) + Bu(t) - \bar{L}_1y(t), \quad t \in [k\delta, (k+1)\delta) \quad (5.117a)$$

$$\hat{x}_2(t) = (A + L_2C)\hat{x}_2(t) + Bu(t) - L_2y(t) \quad t \in (k\delta, (k+1)\delta) \quad (5.117b)$$

$$\hat{x}_2(k\delta) = K \begin{pmatrix} \hat{x}_1(k\delta^-) - S\mathcal{E}_{\alpha,1}(\bar{F}_1(k\delta^-)^\alpha)S^\top \hat{x}_1((k-1)\delta) \\ \hat{x}_2(k\delta^-) - \exp(F_2k\delta^-)\hat{x}_2((k-1)\delta) \end{pmatrix} \quad t = k\delta \quad (5.117c)$$

$$\hat{z}_1(\delta) = \begin{pmatrix} \hat{x}_2(k\delta) \\ 0 \end{pmatrix} \quad t = k\delta \quad (5.117d)$$

In contrast to the impulsive reconstruction of fractional-order systems, we do not have to change the reset matrix  $K$  in each interval as the system under observation is time invariant.

**Theorem 5.12.** *An impulsive reconstruction of the state  $x(\delta)$  of system (5.1) applying by the observer (5.117) is possible if and only if the original integer-order system is completely observable.*

*Proof.* Following the approach leading to the observer (5.117) the critical point of the impulsive reconstruction is the existence of the reset matrix  $K$ . Hence, we have to show that the matrix  $\tilde{\Omega}$  is singular if the system (5.1) is not observable with  $\bar{n}_o$  non-observable states. In [78], this is proven for the impulsive reconstruction based on two integer-order observers. We have to modify this proof to include the fractional- and integer-order dynamics.

First, we rewrite  $\tilde{\Omega}$

$$\tilde{\Omega} = \left( \exp(F_2\delta) - S\mathcal{E}_{\alpha,1}(\bar{F}_1\delta^\alpha)S^\top \right) \exp(-F_2\delta). \quad (5.118)$$

We have to introduce the projection of the fractional-order representation of the integer-order transition  $\exp(F_2\delta)$  such that we can compare both Mittag-Leffler functions

$$\tilde{\Omega} = \left( S\mathcal{E}_{1,1}(\bar{F}_2\delta^\alpha)S^\top - S\mathcal{E}_{\alpha,1}(\bar{F}_1\delta^\alpha)S^\top \right) \exp(-F_2\delta) \quad (5.119)$$

with

$$\bar{F}_2 = \begin{pmatrix} 0 & I \\ F_2 & 0 \end{pmatrix} = \begin{pmatrix} 0 & I \\ A & 0 \end{pmatrix} + \begin{pmatrix} 0 \\ L_2 \end{pmatrix} \begin{pmatrix} C & 0 \end{pmatrix} = \bar{A} + \bar{L}_2\bar{C} \quad (5.120)$$

and we can factor out the projection matrices

$$\tilde{\Omega} = S \left( \mathcal{E}_{\alpha,1}(\bar{F}_2\delta^\alpha) - \mathcal{E}_{\alpha,1}(\bar{F}_1\delta^\alpha) \right) S^\top \exp(-F_2\delta). \quad (5.121)$$

Let us suppose that the system (5.1) is not observable. Then, the associated fractional-order system is also not observable and we separate the observable and non-observable states with the state-transformation  $\Theta$

$$\tilde{A} = \Theta^{-1}\bar{A}\Theta = \begin{pmatrix} \tilde{A}_{11} & 0 \\ \tilde{A}_{21} & \tilde{A}_{22} \end{pmatrix}, \quad \tilde{C}\Theta = \tilde{C} = \begin{pmatrix} \tilde{C}_1 & 0 \end{pmatrix}, \quad \Theta^{-1}\bar{L}_i = \tilde{L}_i = \begin{pmatrix} \tilde{L}_{1,i} & \tilde{L}_{2,i} \end{pmatrix} \quad (5.122)$$

with the transformation matrix

$$\Theta^{-1} = \begin{pmatrix} \tilde{O} \\ \tilde{O}_c \end{pmatrix} \in \mathbb{R}^{2n \times 2n}, \quad (5.123)$$

defined by  $\tilde{\mathcal{O}}$  containing  $2(n - \bar{n}_o)$  independent lines of the observability matrix  $\tilde{\mathcal{O}}$  and the complementary part  $\tilde{\mathcal{O}}_c$ . This results in

$$\begin{aligned}\mathcal{E}_{\alpha,1}(\bar{F}_i\delta^\alpha) &= \Theta\mathcal{E}_{\alpha,1}(\bar{F}_2\delta^\alpha)\Theta^{-1} \\ &= \Theta \begin{pmatrix} \mathcal{E}_{\alpha,1}(\tilde{A}_{11} - \tilde{L}_{1,i}\tilde{C}_1\delta^\alpha) & 0 \\ * & \mathcal{E}_{\alpha,1}(\tilde{A}_{22}\delta^\alpha) \end{pmatrix} \Theta^{-1},\end{aligned}\quad (5.124)$$

where the block  $*$  is not of particular interest. Despite the different transition matrices and observer gains building the impulsive observer, we can use the same transformation matrix here resulting in

$$\mathcal{E}_{\alpha,1}(\bar{F}_2\delta^\alpha) - \mathcal{E}_{\alpha,1}(\bar{F}_1\delta^\alpha) = \Theta \begin{pmatrix} \mathcal{E}_{\alpha,1}(\tilde{A}_{11} - \tilde{L}_{1,i}\tilde{C}_1\delta^\alpha) & 0 \\ * & 0 \end{pmatrix} \Theta^{-1}.\quad (5.125)$$

Hence, this matrix is not regular and of rank

$$\text{rank}(\mathcal{E}_{\alpha,1}(\bar{F}_2\delta^\alpha) - \mathcal{E}_{\alpha,1}(\bar{F}_1\delta^\alpha)) = 2(n - \bar{n}_o).\quad (5.126)$$

This might still be larger than the required rank  $n$ . However, the projection matrix  $S$  leads to an additional rank deficit as

$$\Theta^{-1}S^\top = \begin{pmatrix} C & 0 \\ 0 & C \\ AC & 0 \\ \vdots & \\ A^{\bar{n}_o}C & 0 \\ 0 & A^{\bar{n}_o}C \\ * & * \end{pmatrix} \begin{pmatrix} I \\ 0 \end{pmatrix} = \begin{pmatrix} C \\ 0 \\ AC \\ \vdots \\ A^{\bar{n}_o}C \\ 0 \\ * \end{pmatrix}\quad (5.127)$$

only has  $\text{rank}(\Theta^{-1}S^\top) \leq 2n - \bar{n}_o$ . These critical zero lines occur in the observable subspace, hence the rank of the product drops below  $n$  such that the reset gain  $K$  does not exist.  $\square$

Note that this proof also works for the associated fractional-order system given in Remark 5.1, despite the different initial value projection matrix.

**Example 5.1** (continued). *We extend the previously designed observer with an impulsive reconstruction. The results are shown in Figure 5.9. The fractional-order observer shows a better performance in the first time interval and is therefore suited to enhance the fixed-time state reconstruction.*

## 5.4 Fractional-Order Control

As shown in the previous section, there are certain measures to increase the convergence of fractional-order dynamics without pushing the gains too high. We want to exploit these concepts for the control of fractional- and integer-order systems.

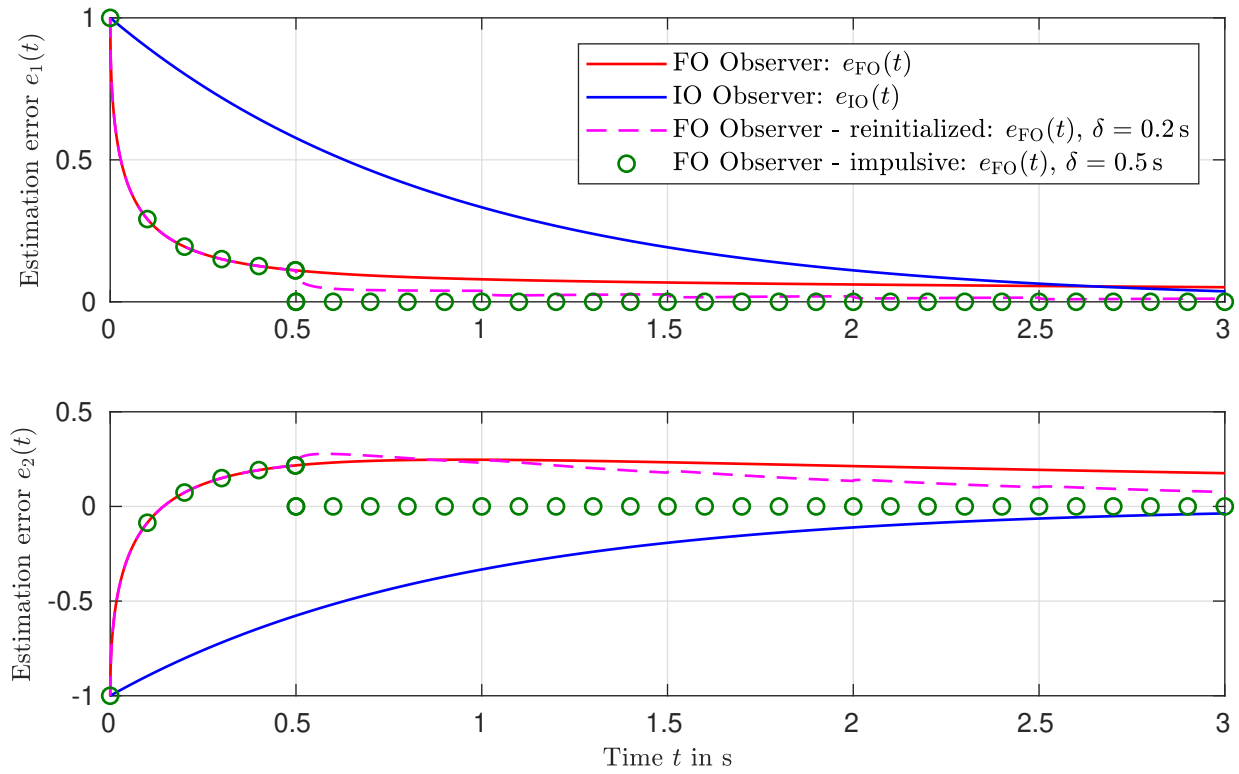


Figure 5.9: Estimation error extended by an impulsive state reconstruction at  $\delta = 0.5$  s.

#### 5.4.1 Inter-Order Pole-Placement and Prefilter

In this section, we want to control a fractional-order system such that it behaves like an integer-order system in the input-output dynamics. Note that the fractional-order process can also be obtained if we apply a fractional-order prefilter to an integer-order plant, e.g. to partially compensate non-minimum phase zeros. As this approach aims at the input-output dynamics, we rely on the frequency domain representation of the fractional-order process. We consider a SISO plant given by

$$G(s) = C(s^\alpha I - A)^{-1}B + D = \frac{A_G(s^\alpha)}{B_G(s^\alpha)}, \quad (5.128)$$

which corresponds to a state-space representation given in (3.3). The pseudo-polynomials  $A_G(s^\alpha)$  and  $B_G(s^\alpha)$  are given by (3.92). We use the standard compensator structure shown in Figure 5.10 and apply a controller of the same commensurate order  $\alpha$

$$C(s) = C_c(s^\alpha I - A_c)^{-1}B_c + D_c = \frac{P(s^\alpha)}{Q(s^\alpha)}, \quad (5.129)$$

where  $Q(s^\alpha)$  has a maximum order of  $\alpha n_c$ , with  $n_c$  being the number of controller states  $x_c(t) \in \mathbb{R}^{n_c}$  in the state-space representation of the controller (see (5.143)).

The transfer-function of the closed-loop without additional prefilter  $F(s)$  is given by

$$T(s) = \frac{Y(s)}{R(s)} = \frac{C(s)G(s)}{1 + C(s)G(s)}. \quad (5.130)$$

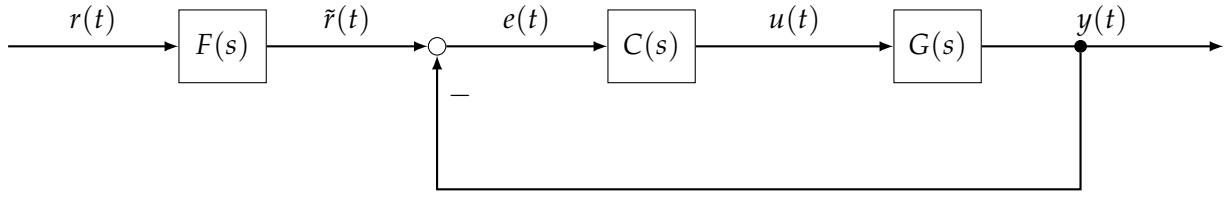


Figure 5.10: Controller structure including the prefilter  $F(s)$ .

The controller should achieve integer-order closed-loop dynamics. Hence the direct approach would be to specify  $T(s)$  and solve for the controller  $C(s)$ . This, however, is restricted to minimum phase processes. As the fractional-order control is especially suited for non-minimum phase processes [41] we have to use a different design approach.

If we use a pole placement approach, we can exploit the connection between integer- and fractional-order eigenvalues as given by (5.55). We rewrite the pseudo polynomials  $A_G(s^\alpha)$ ,  $B_G(s^\alpha)$ ,  $P(s^\alpha)$  and  $Q(s^\alpha)$  as polynomials in  $p = s^\alpha$ . The desired (integer-order) closed-loop denominator polynomial  $Q_T(p)$  defining the poles then reads

$$Q_T(p) = A(p)Q(p) + B(p)P(p). \quad (5.131)$$

The controller is then given by the solution of this Diophantine equation in  $p$ . For this problem we can use standard methods, e.g. algebraic methods based on Sylvester's matrix [37]. For the order of the pole-placement compensator  $n_c$ , there are generally two options [37]: With  $n_c = n + \nu$ , the controller is strictly proper. The controller order is increased by  $\nu$  which reflects the number of fractional-order integrators contained in the controller. The minimal order  $n_c = n + \nu - 1$  typically is bi-proper. Hence, there is a choice to adjust the order  $m = n + n_c$  of the desired denominator of the closed-loop transfer function,

$$Q_T(p) = c_m p^m + \dots + c_1 p + c_0. \quad (5.132)$$

As we want to achieve integer-order dynamics, we have to select the poles of  $Q_T(p)$  such that all the coefficients of non-integer power of  $s$  vanish. Hence we design integer-order poles  $\lambda_{IO}$  and build  $Q_T(p)$  with the corresponding set of fractional-order poles

$$\lambda_{IO,i} = \lambda_{FO,i,l}^{n_\alpha}, \quad (5.133)$$

with  $n_\alpha = \alpha^{-1} \in \mathbb{N}$ ,  $i = 1, 2, \dots, m\alpha$  and  $l = 1, 2, \dots, n_\alpha$ .

An important design specification here is that the order  $m$  has to match the order of differentiation  $\alpha$  such that

$$m\alpha = (n + n_c)\alpha \in \mathbb{N}. \quad (5.134)$$

If this condition is not satisfied, not all fractional-order pseudo poles can be shifted to their integer-order counterparts and some fractional-order dynamics will remain in the input-output behavior.

If the order of the process  $n$  and the commensurate order  $\alpha^{-1} \in \mathbb{N}$  do not match, the controller needs to fix a number of additional open-loop pseudo poles  $n_{\text{add}}$  in advance, i.e.

$$(n + 2n_{\text{add}} + n_c)\alpha \in \mathbb{N}. \quad (5.135)$$

Altogether there are three possibilities to match the orders.

1. We can choose a full ( $n_c = n + \nu$ ) or minimal ( $n_c = n + \nu - 1$ ) order compensation structure.
2. We can add  $n_{\text{add}}$  additional pseudo poles to the process or
3. we adjust the number of fractional-order integrator constraints  $\nu$  in the design process.

For controlling integer-order systems with  $\alpha = \frac{1}{2}$  with a minimal controller order (aiming for  $n_c = n$ ), we can choose  $\kappa = 1$  and  $n_{\text{add}} = 0$  resulting in  $n_c = 2n + 1 - 1$  and  $m = 4n$ . For the commensurate order  $\alpha = \frac{1}{3}$ , we might also choose  $\kappa = 0$  and  $n_{\text{add}} = 2$ .

Solving the pole-placement problem under these conditions leads to a closed-loop denominator of integer-order. The numerator of  $T(s)$  is still a pseudo polynomial and the remaining fractional-order pseudo zeros still slow down the input-response. Due to these fractional-order pseudo zeros the solution is still given in terms of Mittag-Leffler functions and therefore shows an algebraic decay.

At this point, we make use of the extended control structure and use the prefilter  $F(s)$  (see Fig. 5.10) to shape the reference, such that the effect of the fractional-order pseudo zeros is reduced. (see Fig. 5.11): We divide the numerator  $P_T(s)$  into a minimum and non-minimum phase part

$$P_T(s) = P_{Tb}(s^\alpha) P_{Tg}(s^\alpha) \quad (5.136)$$

with  $P_{Tb}(\lambda_i) = 0, |\arg(\lambda_i)| < \alpha\frac{\pi}{2}$  and  $P_{Tg}(\lambda_i) = 0, |\arg(\lambda_i)| \geq \alpha\frac{\pi}{2}$ . The minimum phase part  $P_{Tg}$  can be easily compensated while the components of  $P_{Tb}$  can only be moved to its integer-order non-minimum phase counterparts. Hence any non-minimum phase behavior of an integer-order process will remain in the input-output dynamics. However, the effect of the unstable pseudo zeros is reduced in the closed-loop.

To guarantee the causality of the filter  $F(s)$ , additional integer-order poles  $Q_{\text{add}}(s)$  are needed

$$F(s) = \frac{N_F(s)}{D_F(s)} = \frac{\bar{P}_{Tb}(s^\alpha)}{P_{Tg}(s^\alpha)Q_{\text{add}}(s)}. \quad (5.137)$$

Finally, the input response of the closed-loop decays exponentially since the control removes any FO memory effect:

$$\frac{Y(s)}{R(s)} = F(s)T(s) = \frac{P_{Tb}(s^\alpha)\bar{P}_{Tb}(s^\alpha)}{Q_T(s^\alpha)Q_{\text{add}}(s)}. \quad (5.138)$$

This performance, however, is only achieved for the reference response. Non-zero initial conditions and disturbances in the control loop are only compensated with an algebraic decay as the homogeneous system response as well as the disturbance rejection remain of fractional-order.

**Example 5.2.** We consider the non-minimum phase fractional-order system

$$G_{\text{FO}}(s) = \frac{-0.2s^\alpha + 1}{s + 2s^\alpha + 1}, \quad \alpha = \frac{1}{2} \quad (5.139)$$

and place the closed-loop poles to  $\lambda_{\text{IO}} = -2 \pm j$ . The resulting closed-loop is given by

$$T(s) = \frac{-1.06s^{3\alpha} + 4.89s^{2\alpha} + 0.94s^\alpha + 5}{s^{4\alpha} + 0s^{3\alpha} + 4s^{2\alpha} + 0s^\alpha + 5}. \quad (5.140)$$

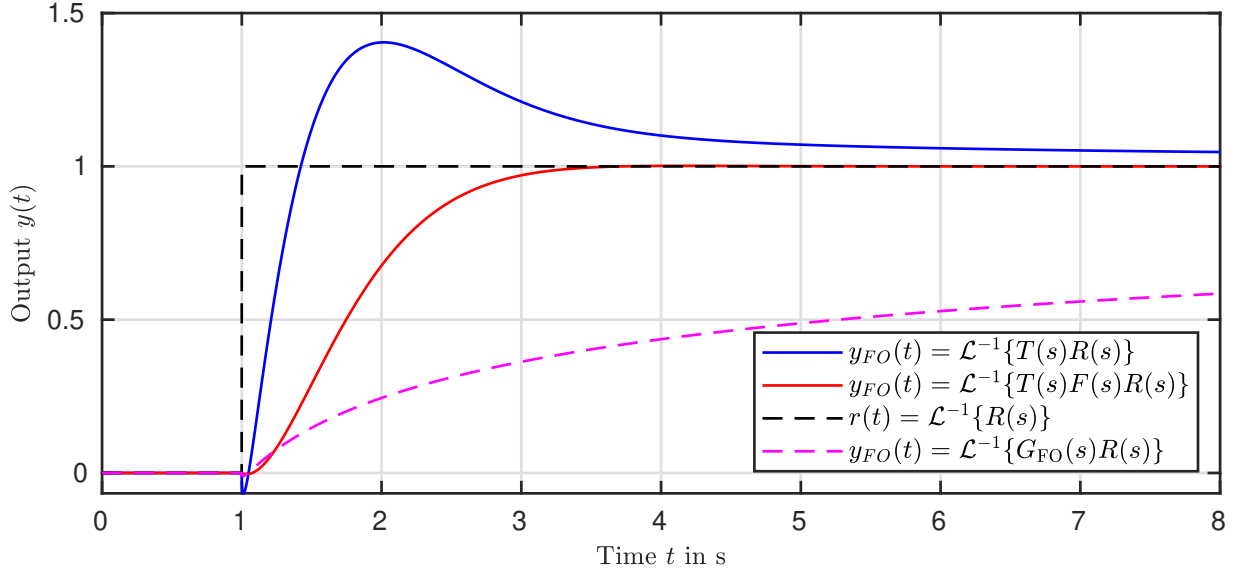


Figure 5.11: Step responses of the closed-loop system with integer-order assigned poles.

The numerator shows one non-minimum phase pseudo zero at  $s_0^\alpha = 5$  which cannot be compensated. Therefore, the filter is extended by an additional pseudo zero  $\bar{s}_0^\alpha = -5$  such that the filter  $F(s)$  is given by

$$F(s) = \frac{0.94737s^\alpha + 4.7368}{5s^{2\alpha} + 1.8421s^\alpha + 4.7368}. \quad (5.141)$$

Finally, all coefficients of fractional-order powers are removed and the closed-loop input-output response reads

$$F(s)T(s) = \frac{-0.2s + 5}{s^2 + 4s + 5}. \quad (5.142)$$

Fig. 5.11 shows the step responses of the fractional-order process  $G(s)$ , the closed-loop with designed integer-order poles  $T(s)$  and response of the extended structure  $F(s)T(s)$ . Although the filter introduces additional poles to the closed-loop response which slows down the system response, the benefit of the exponential converge is clearly visible. The filter also reduces the effect of the non-minimum phase zero.

**Remark 5.8.** Note that the compensation approach is only suited for systems of low order. It is numerically sensitive and an implementation of the filter  $F(s)$  and the controller  $C(s)$  relying on approximation does not lead to the desired dynamics.

In this compensator structure the pole placement approach is essential to be able to increase the controller gains without losing stability, such that the algebraic decay can already be dominated with the real part of the closed-loop eigenvalues, even if the remaining fractional-order pseudo zeros cannot be compensated.

#### 5.4.2 Fractional-Order Control of Integer-Order Systems

In this section we consider the control of the integer-order system as given by equation (5.1) and use the fractional-order controller given by

$$\Sigma_C : \begin{cases} {}_{t_0}D^\alpha x_c(t) = A_c x_c(t) + B_c u_c(t) & (5.143a) \\ u(t) = C_c x_c(t) + D_c u_c(t), & (5.143b) \end{cases}$$



with the controller (pseudo) state  $x_c(t) \in \mathbb{R}^{n_c}$ , and general input

$$u_c(t) = \begin{pmatrix} r(t) \\ y(t) \end{pmatrix} \quad (5.144)$$

combining the reference signal  $r(t)$  and output signal  $y(t)$ . With this input the controller matrices are partitioned as

$$B_c = \begin{pmatrix} B_{c,1} & B_{c,2} \end{pmatrix}, \quad D_c = \begin{pmatrix} D_{c,1} & D_{c,2} \end{pmatrix}. \quad (5.145)$$

This structure allows for observer based state-feedback as well as for output-feedback with  $B_{c,1} = -B_{c,2}$  and  $D_{c,1} = -D_{c,2}$ .

Note that for simplicity we restrict the commensurate order of differentiation to  $\alpha^{-1} = \kappa \in \mathbb{N}$ . The relaxation to  $\alpha \in \mathbb{Q}$  with  $\alpha < 1$  is straightforward by applying Lemma 5.1 first to split the rational order.

Using the derivative representation of the associated fractional-order system, we define the extended state  $\bar{z}(t) = \begin{pmatrix} z(t) & x_c(t) \end{pmatrix}$ . Now rephrase the closed-loop of the integer-order process (5.1) and the fractional-order controller (5.143) as

$${}_{t_0}\mathcal{D}^\alpha \bar{z}(t) = \begin{pmatrix} \bar{A} + \bar{B}D_{c,2}\bar{C} & \bar{B}C_c \\ B_{c,2}\bar{C} & A_c \end{pmatrix} \bar{z}(t) + \begin{pmatrix} \bar{B}D_{c,1} \\ B_{c,1} \end{pmatrix} r(t) = A_{cl}\bar{z}(t) + B_{cl}r(t). \quad (5.146)$$

As the solution of the fractional-order closed-loop is given in terms of the Mittag-Leffler function, the convergence of the control system is only algebraic. As the control effort  $u(t)$  is bounded, the physical system states do also not show an infinite derivative at  $t = t_0$  as illustrated previously (see Remark 5.5).

#### 5.4.2.1 Fractional-Order Memory Reset Control

Although the initial convergence is not as fast as in the observer case, we can still reset the memory of the closed loop to achieve exponential convergence. This is possible because the process is time-invariant and integer-order. The fractional-order controller introduces the memory to the closed-loop slowing down the system response. To delete this memory periodically, we have to change the initial time  $t_0$  of the operator  ${}_{t_0}\mathcal{D}^\alpha$  defining the controller dynamics (5.143). With the global initial time  $T_0 = 0$  the reset instants  $t_k$  are given by  $t_k = k\delta$  with the counter  $k \in \mathbb{N}_0$  starting from zero. This leads to the changed controller dynamics (5.143) given by

$$\Sigma'_K : \begin{cases} {}_{k\delta}\mathcal{D}^\alpha x_c(t) = A_c x_c(t) + B_c u_c(t), & t \neq k\delta & (5.147a) \\ x_c(k\delta) = x_c(k\delta^-), & t = k\delta & (5.147b) \\ u(t) = C_c x_c(t) + D_c u_c(t). & & (5.147c) \end{cases}$$

At this point, we do not require equation (5.147b) as the controller state  $x_c(t)$  is absolutely continuous only. Due to the restart, the controller states are not differentiable at the reset instants.

The change to a fractional-order operator  ${}_{k\delta}\mathcal{D}^\alpha$  with a time varying lower limit has to be taken into account in order to derive the closed-loop representation. We have to reset the auxiliary states of  $z$  to zero, as these initial conditions are required in the construction of the associated fractional-order system

$$z(\delta) = \begin{pmatrix} I_{n \times n} & 0 \\ 0 & 0 \end{pmatrix} z(\delta^-) = \begin{pmatrix} x(\delta^-) \\ 0 \end{pmatrix}. \quad (5.148)$$

Finally, the closed-loop dynamics read

$${}_{k\delta}\mathcal{D}^\alpha \bar{z}(t) = A_{cl}\bar{z}(t) + \bar{B}_{cl}r(t), \quad t \in (k\delta, (k+1)\delta) \quad (5.149a)$$

$$\bar{z}(k\delta^+) = M\bar{z}(k\delta^-), \quad t = k\delta, k \in \mathbb{N}_0 \quad (5.149b)$$

with matrices  $A_{cl}$  and  $B_{cl}$  as given in equation (5.146) and the new reset matrix  $M$  given by

$$M = \begin{pmatrix} I_{n \times n} & 0 & 0 \\ 0 & 0 & 0 \\ 0 & 0 & I_{n_c \times n_c} \end{pmatrix} \in \mathbb{R}^{(\kappa n + n_c) \times (\kappa n + n_c)}. \quad (5.150)$$

We can reset the auxiliary states here as they are only virtual in the fractional-order representation of the integer-order process using the operator  ${}_{k\delta}\mathcal{D}^\alpha$ . Although the controller states are continuous, the reset approach leads to a closed-loop which can be described by a hybrid fractional-order system. The auxiliary states jump at  $t = k\delta$ .

As in the observer case, the periodic reset induces discrete time dynamics which connect the extended state  $\bar{z}(k\delta)$  at the reset instants. These induced dynamics can be used to show the stability of the closed-loop system.

**Theorem 5.13.** *The origin of the closed-loop fractional-order memory reset control system (5.149) is asymptotically stable if and only if*

$$|\lambda_i| < 1, \quad (5.151)$$

where  $\lambda_i, i = 1, 2, \dots, \kappa n + n_c$ , denotes  $i$ -th eigenvalue of the induced discrete system matrix

$$A_d = M\mathcal{E}_{\alpha,1}(A_{cl}\delta^\alpha). \quad (5.152)$$

*Proof.* The discrete time dynamics describing the sequence

$$\left( \bar{z}(k\delta) \right) = (\bar{z}(0), \bar{z}(\delta), \bar{z}(2\delta), \dots) \quad (5.153)$$

are given by

$$\bar{z}((k+1)\delta) = M\mathcal{E}_{\alpha,1}(A_{cl}\delta^\alpha)\bar{z}(k\delta) = A_d\bar{z}(k\delta). \quad (5.154)$$

If the eigenvalues of the discrete system matrix  $A_d$  are located inside the unit circle, the dynamics are asymptotically stable [81].  $\square$

As the reset matrix  $M$  sets at least  $(\kappa - 1)n$  eigenvalues to zero, we can reduce the order of the discrete system matrix  $A_d$ . As all auxiliary states are zero at  $t = k\delta$ , the reduction of state leads to the reduced discrete dynamics

$$\begin{pmatrix} x((k+1)\delta) \\ x_c((k+1)\delta) \end{pmatrix} = \begin{pmatrix} I_{n \times n} & 0 & 0 \\ 0 & 0 & I_{n_c \times n_c} \end{pmatrix} \mathcal{E}_{\alpha,1}(A_{cl}\delta^\alpha) \begin{pmatrix} I_{n \times n} & 0 \\ 0 & 0 \\ 0 & I_{n_c \times n_c} \end{pmatrix} \begin{pmatrix} x(k\delta) \\ x_c(k\delta) \end{pmatrix}, \quad (5.155)$$

such that only the evolution of the system state  $x(k\delta)$  and the controller state  $x_c(k\delta)$  is involved.

**Remark 5.9.** *If the controller has the structure of an observer based state feedback, we can also reset the observer states. This also leads to discontinuous controller states  $x_c(t)$  and a discontinuous control law  $u(t)$ .*

**Remark 5.10 (Interpretation in the frequency domain).** *The periodical reset has a strong impact on the frequency response of the closed-loop. Within a single reset interval  $t \in [k\delta, (k+1)\delta)$  the frequency response is only determined by the design of the fractional-order controller leading to the following complementary sensitivity function*

$$T_{\text{design}}(s) = \begin{pmatrix} \bar{C} & 0 \end{pmatrix} (s^\alpha I - A_{\text{cl}})^{-1} B_{\text{cl}}. \quad (5.156)$$

*The effect of events occurring on the lower frequency band  $\omega \ll \frac{\pi}{\delta}$ , e.g. the change of a setpoint-value of the reference  $r(t)$ , is, however, dominated by the induced discrete-time dynamics (5.155).*

*In order to derive a frequency domain representation of this behavior, we assume constant reference signals within one reset interval, so that we can compute the input matrix  $B_d$  of the induced system using the forced part of the solution (3.5) and the properties of the Mittag-Leffler function given in [74, p. 21]*

$$B_d = \int_0^\delta (\delta - \tau)^{\alpha-1} \mathcal{E}_{\alpha,\alpha}(A_{\text{cl}}(\delta - \tau)^\alpha) B_{\text{cl}} d\tau = \delta^\alpha \mathcal{E}_{\alpha,\alpha+1}(F\delta^\alpha) B_{\text{cl}}. \quad (5.157)$$

*An approximation of the low-frequency dynamics is then obtained by the frequency responses of the discrete time system*

$$T_{\text{low}}(z) = \frac{Y(z)}{R(z)} \approx \begin{pmatrix} \bar{C} & 0 \end{pmatrix} (zI - A_d)^{-1} M B_d, \quad \omega \ll \frac{\pi}{\delta}. \quad (5.158)$$

*These low frequency dynamics can be interpreted quite well and simulations of the closed-loop in the time domain with sinusoidal inputs lead to a similar frequency response. However, this approximation cannot be used to calculate an open-loop frequency response for the low frequency range. The numerical results lack interpretability.*

*The effect of high-frequency reference signals is only visible within one reset interval, which can be characterized by  $T_{\text{design}}(s)$ . However, the signals are superimposed with the homogeneous solution of the fractional-order differential equation, which dominates the behavior for a long time due to the algebraic decay.*

*Note that the assumption of piecewise constant reference signals is less restrictive for smaller reinitialization periods and slower system dynamics.*

The insights the analysis in the frequency domain gives are best demonstrated by considering an example.

**Example 5.3.** *We use the fractional-order  $PI^\alpha$  controller  $C(s)$  given in [10] to control a normalized first-order plant  $G(s)$ :*

$$G(s) = \frac{1}{s+1} \quad (5.159)$$

$$C(s) = 1.3545 + \frac{9.7104}{s^\alpha}, \quad \alpha = \frac{1}{2}. \quad (5.160)$$

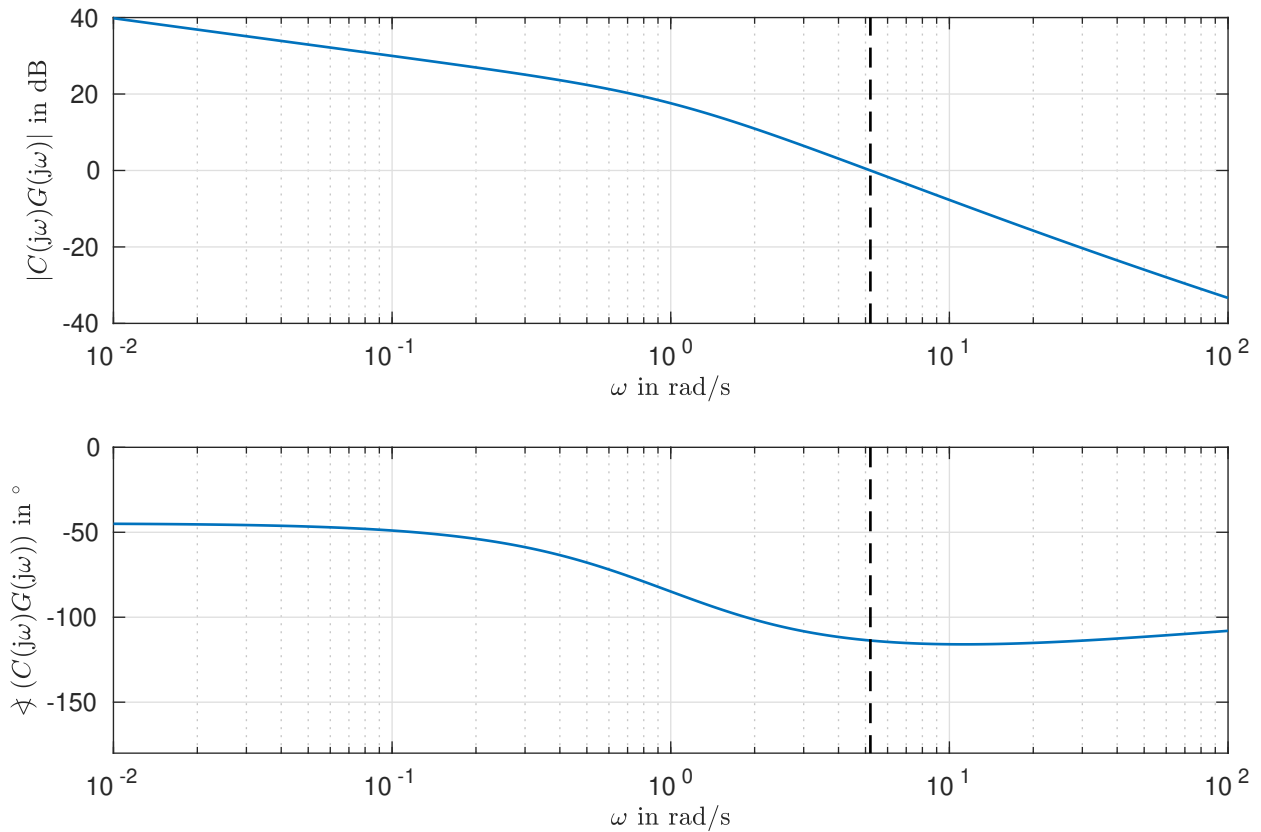


Figure 5.12: Frequency response of the open-loop  $L(j\omega) = C(j\omega)G(j\omega)$ .

This controller is designed to obtain a step-response with an overshoot of  $M_p < 20\%$ , a settling time of  $t_s < 3$  s and a vanishing steady-state error  $e_\infty = 0$ . The open loop  $L(s) = C(s)G(s)$  has a crossover frequency of  $\omega_c = 5.2 \frac{\text{rad}}{\text{s}}$ .

The bode plot of the open loop is depicted in Figure 5.12. It shows that the controller is tuned to have a flat phase around the crossover frequency. This iso-damping property [88, 13]

$$\left. \frac{d}{d\omega} \arg(C(j\omega)G(j\omega)) \right|_{\omega=\omega_s} = 0. \quad (5.161)$$

increases the robustness of the closed loop against gain variations of the process.

The step response is simulated using the `FDE12.m` routine [21] and shown in Figure 5.13. The convergence to the final value is slow even though the design specifications are met. For larger times, it appears like a (quasi) stationary steady-state error.

We use two different initialization intervals with  $\delta_1 = 2.0$  s and  $\delta_2 = 0.2$  s. With these time spans, we have  $\frac{\pi}{\delta_1} < \omega_c < \frac{\pi}{\delta_2}$ . In the first case, the resetting occurs at a lower frequency than the crossover frequency of the open loop. The dynamic properties which are achieved by the underlying baseline controller  $C(s)$  remain unchanged. The memory reset, however, leads to exponential convergence. This is clearly visible in the step response depicted in Figure 5.14. Note that the change of the step response is more significant if the reset instant occurs during the transient phase. In the second case with the shorter reset period  $\delta_2$ , the step response shows an increased overshooting (see Figure 5.13). This corresponds to a resonance peak in the frequency response of the induced discrete dynamics as depicted in Figure 5.14. However, this controller still achieves exponential convergence.

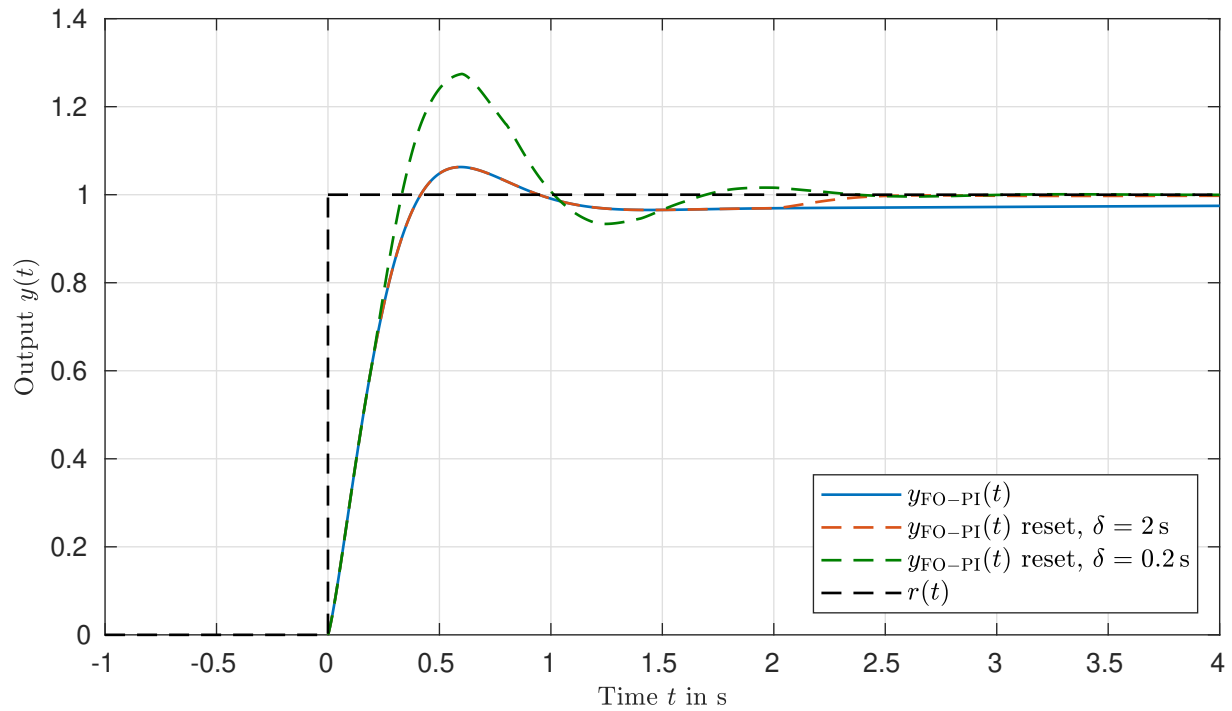


Figure 5.13: Closed-loop step responses for different reset periods  $\delta$ . For  $\delta = \infty$  the pure fractional-order controller acts without reset.

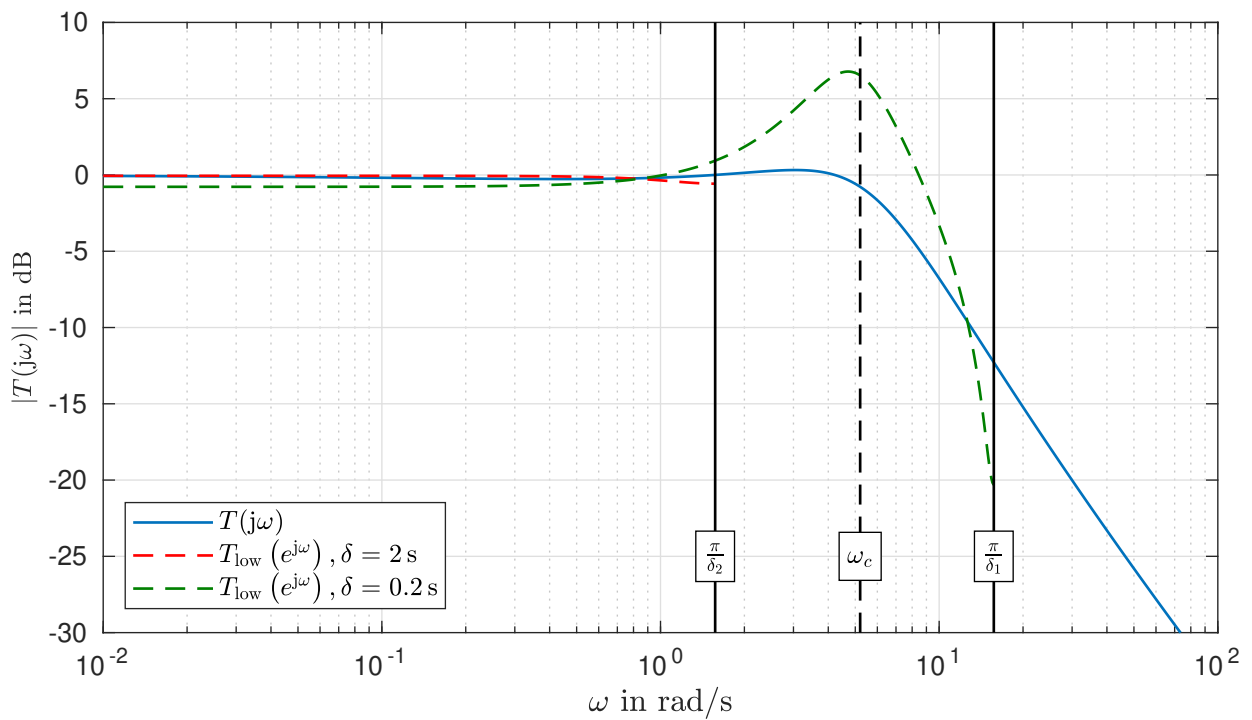


Figure 5.14: Amplitude response of the designed closed-loop  $T_{\text{design}}(j\omega)$  and the induced low frequency dynamics  $T_{\text{low}}(e^{j\omega})$ .

### 5.4.2.2 Hybrid Fractional-Order Control

Another approach to fractional-order reset control was developed in the various publications of HosseinNia et al. [30, 34, 36, 35, 32, 31, 33]. Therein the generalization of integer-order reset control systems is generalized towards fractional-order controllers and plants.

There are different approaches as to which time to choose to reset the controller. In classical approaches, like the Clegg integrator [107] a reset is triggered based on the zero-crossing of the tracking error. These approaches can be applied in order to avoid overshooting but are vulnerable to limit cycles [30].

The strategy of predetermined (periodic) reset instants is applied to accelerate the system response. Somehow, this approach is the control counterpart of the impulsive observers - in this case the controller is reset such that the control effort best fits the actual requirements based on the actual system output  $y(t)$  and the reference  $r(t)$ .

In order to be comparable with the memory reset scheme, the focus here is set to the periodic reset of the controller states. The fractional-order extension of the controller presented in [108] is given by [36]:

$${}_t D^\alpha x_c(t) = A_c x_c(t) + B_c e(t), \quad t \neq t_k \quad (5.162a)$$

$$x_c(t_k) = M_c x_c(t_k^-) + N_c r(t_k^-) + P_c e(t_k^-), \quad t = t_k \quad (5.162b)$$

$$u(t) = C_c x_c(t) + D_c e(t), \quad (5.162c)$$

with  $x_c(t) \in \mathbb{R}^{n_c}$  and constant reset period  $\delta = t_{k+1} - t_k, k = 0, 1, \dots$ . The controller consists of an underlying baseline controller defined by (5.162a) and (5.162c), i. e.  $C(s) = C_c(s^\alpha I - A_c)^{-1} B_c + D_c$ . The reset equation (5.162b) is an extension of the reset law presented in [30]. At each reset instant  $t_k$  the controller state is changed based on the actual reference  $r(t_k)$ , the tracking error  $e(t_k) = r(t_k) - y(t_k)$  and the controller state  $x_c(t_k)$ . This reset law requires only output measurement but an extension to the complete process state is straight forward.

With the controller order  $\alpha^{-1} \in \mathbb{N}$  we can derive the closed-loop representation using the associated fractional-order representation (5.16) of the integer-order process (5.1)

$${}_t D^\alpha \bar{z}(t) = \underbrace{\begin{pmatrix} \bar{A} - \bar{B} D_c \bar{C} & \bar{B} C_c \\ -\bar{B}_c \bar{C} & A_c \end{pmatrix}}_{=:A_{cl}} \bar{z}(t) + \underbrace{\begin{pmatrix} \bar{B} D_c \\ B_c \end{pmatrix}}_{=:B_{cl}} r(t), \quad t \neq t_k \quad (5.163a)$$

$$\bar{z}(t_k) = \begin{pmatrix} I_{n_k \times n_k} & 0 \\ -\bar{C} P_c & M_c \end{pmatrix} \bar{z}(t_k^-) + \begin{pmatrix} 0 \\ N_c + P_c \end{pmatrix} r(t_k^-), \quad t = t_k \quad (5.163b)$$

$$y(t) = \underbrace{(\bar{C} - \bar{D} D_c \bar{C} \quad \bar{D} C_c)}_{=:C_{cl}} \bar{z}(t) + \underbrace{(\bar{D} D_c)}_{=:D_{cl}} r(t). \quad (5.163c)$$

In contrast to the memory reset approach, the extended states of the process  $z(t)$  remain unchanged at the reset instant  $t_k$ . This is a result of the constant lower terminal of the chosen fractional-order operator  ${}_t D^\alpha$  as its memory is not deleted.

The included memory also complicates the stability analysis of the closed-loop. One can apply the so-called  $H_\beta$ -condition [34]. The fundamental idea here is motivated by linear integer-order hybrid systems. A common quadratic Lyapunov function is used to guarantee the stability

within one time interval and at the reset instant. The positive definite matrix  $P$  hence has to satisfy a continuous and a discrete Lyapunov inequality.

For fractional-order hybrid systems the linear matrix inequality (LMI) assuring the stability within one interval is replaced by an adopted LMI assuring the stability of the linear fractional-order continuous time dynamics [86]. These fractional-order LMI conditions are, however, not associated with a Lyapunov function.

Compared to the previous control approach, an exact representation of the induced dynamics is not as easy to find as it is time-varying due to the included memory. As the controller can be implemented with a higher order integer-order approximation, however, a pragmatic approach is to investigate the closed-loop dynamics obtained with the approximations (see Section 5.4.2.4).

### 5.4.2.3 Extended Fractional-Order Memory Reset Control

As the dynamics of the fractional-order memory reset controller are already reset, an extension to include the state reset suggests itself. Including the reset of the state allows for the reduction of the reset period  $\delta$  without decreasing the control performance as illustrated in Example 5.3. The combination of both approaches leads to the following controller:

$${}_{\delta k} \mathcal{D}^\alpha x_c(t) = A_c x_c(t) + B_c e(t), \quad t \in [k\delta, (k+1)\delta) \quad (5.164a)$$

$$x_c(t) = M_c x_c(t^-) + N_c r(t^-) + P_c e(t^-), \quad t = k\delta \quad (5.164b)$$

$$u(t) = C_c x_c(t) + D_c e(t), \quad (5.164c)$$

with the controller state  $x_c \in \mathbb{R}^{n_c}$ .

In contrast to the pure memory reset control, the reset law changes. The new update matrix  $\bar{M}$  not only resets the auxiliary states of associated fractional-order system to zero, it also changes the controller state  $x_c(t_k)$  itself

$$\bar{M} = \begin{pmatrix} I_{n \times n} & 0 & 0 \\ 0 & 0_{n(\kappa-1) \times n(\kappa-1)} & 0 \\ -P_c C & 0 & M_c \end{pmatrix}. \quad (5.165)$$

Furthermore, the new controller state  $x_c(t_k)$  is determined by the reference  $r(t_k)$  with the additional reset matrix  $\bar{P}$  given by

$$\bar{P} = \begin{pmatrix} 0 \\ 0 \\ N_c + P_c \end{pmatrix}. \quad (5.166)$$

As in the case of the pure memory reset control, we can reduce the stability analysis to the induced discrete time dynamics.

**Theorem 5.14 (Stability).** *The closed-loop of the integer-order system (5.25) and the extended fractional-order memory reset controller (5.164) are asymptotically stable if and only if*

$$|\lambda_i| < 1, \quad i = 1, 2, \dots, n\kappa + n_c, \quad (5.167)$$

where  $\lambda_i$  denotes the eigenvalues of the induced discrete system matrix  $A_d$  given by

$$A_d = \bar{M}\mathcal{E}_{1,\alpha}(A_{cl}\delta^\alpha). \quad (5.168)$$

The proof is a generalization of the plain memory reset approach and therefore omitted here. The reset based on the actual reference signal  $r(t_k)$  only changes the frequency domain interpretation due to an additional term in the induced discrete dynamics as the sequence of the combined state ( $\bar{z}(\delta k)$ ) is given by

$$\begin{aligned} \bar{z}(k\delta) &= \bar{M}\bar{z}(k\delta^-) + \bar{P}r(k\delta^-) \\ &= A_d\bar{z}((k-1)\delta) + \bar{P}r(k\delta) + \underbrace{\left( \bar{M} \int_0^\delta \frac{\mathcal{E}_{\alpha,\alpha}(A_{cl}(\delta-\tau)^\alpha)}{(\delta-\tau)^{1-\alpha}} B_{cl} d\tau \right)}_{B_d} r((k-1)\delta). \end{aligned} \quad (5.169)$$

for constant reference signals within one reset interval  $t \in [k\delta, (k+1)\delta)$ . In this difference equation, matrix  $\bar{P}$  represents a direct feed-through of the reference input  $r(\delta k)$  to the combined state  $\bar{z}(\delta k)$ . To remove the time shift in (5.169) we transform the controller state

$$\gamma(k\delta) = \bar{z}(k\delta) - \bar{P}r(k\delta) = \begin{pmatrix} z(k\delta) \\ x_c(k\delta) - Pr(k\delta) \end{pmatrix}. \quad (5.170)$$

With  $\begin{pmatrix} \bar{C} & 0 \end{pmatrix} \bar{P} = 0$  we have

$$\gamma((k+1)\delta) = A_d\gamma(k\delta) + (A_d\bar{P} + B_d) r(k\delta) \quad (5.171)$$

$$y(k\delta) = \begin{pmatrix} \bar{C} & 0 \end{pmatrix} \gamma(k\delta) + D_{cl}r(k\delta). \quad (5.172)$$

The interpretation of these discrete dynamics in the frequency domain for  $\omega \ll \frac{\pi}{\delta}$  is straight forward:

$$T_{low}(z) = \begin{pmatrix} \bar{C} & 0 \end{pmatrix} (zI - A_d)^{-1} (A_d\bar{P} + B_d) + D_{cl}. \quad (5.173)$$

**Remark 5.11.** Using a similar state transformation, it is also possible to extend the class of considered reference signals to piecewise linear signals, i.e.

$$r(t) = mt + r(k\delta) = \frac{r((k+1)\delta) - r(k\delta)}{\delta} t + r(k\delta), \quad t \in [k\delta, (k+1)\delta). \quad (5.174)$$

We see that the reference at the time instant  $t = (k+1)\delta$  is included and has to be removed in order to derive the first-order approximation of the low frequency dynamics. Inserting (5.174) into the solution of the fractional-order system (3.5) leads to

$$\begin{aligned} \tilde{B}_d &= \int_0^\delta (\delta-\tau)^{\alpha-1} \mathcal{E}_{\alpha,\alpha}(A_{cl}(\delta-\tau)^\alpha) B_{cl} \left( \frac{r((k+1)\delta) - r(k\delta)}{\delta} \tau + r(k\delta) \right) d\tau \\ &= \underbrace{\left( \delta^\alpha (\mathcal{E}_{\alpha,\alpha+1}(A_{cl}\delta^\alpha) + \mathcal{E}_{\alpha,\alpha+2}(A_{cl}\delta^\alpha)) B_{cl} \right)}_{\tilde{B}_1} r(k\delta) + \underbrace{\left( \delta^\alpha \mathcal{E}_{\alpha,\alpha+1}(A_{cl}\delta^\alpha) B_{cl} \right)}_{\tilde{B}_2} r(k+1)\delta. \end{aligned} \quad (5.175)$$



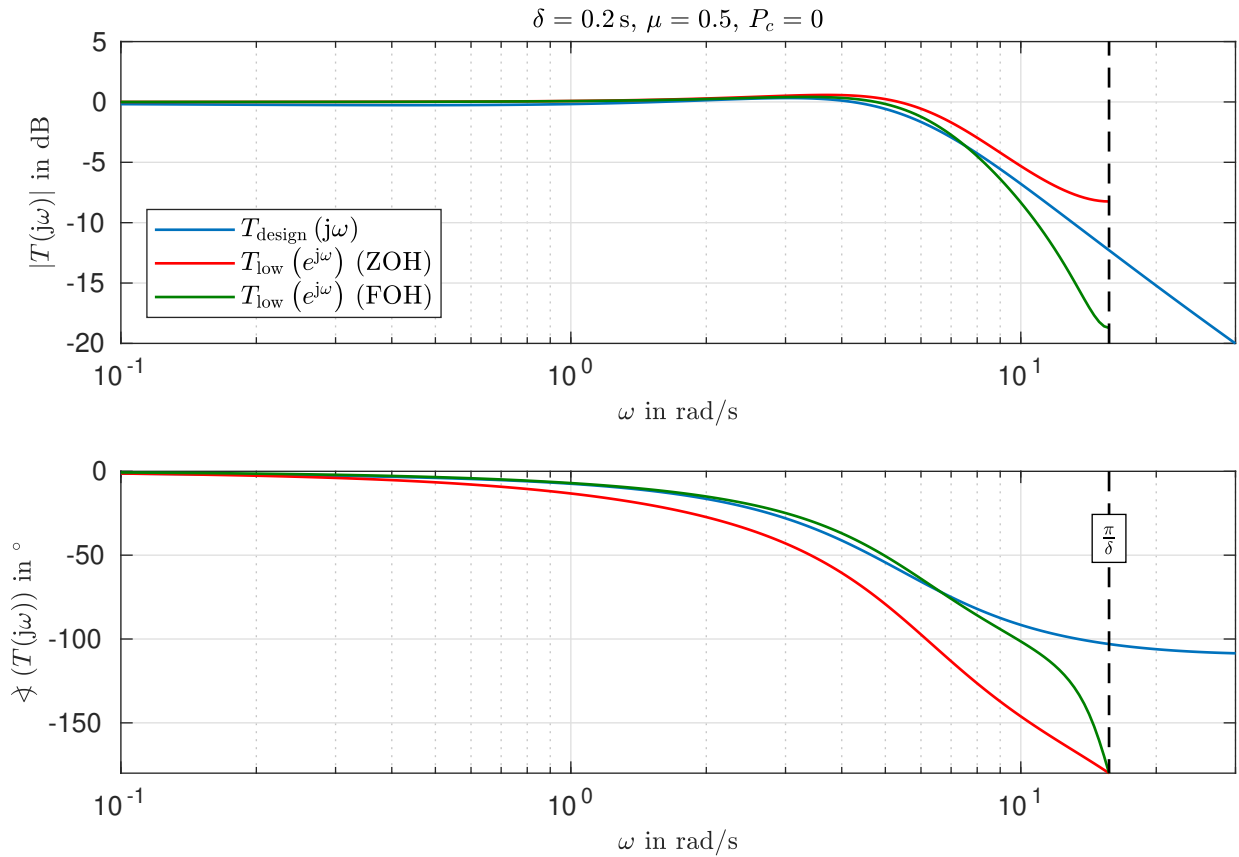


Figure 5.15: Comparison of the frequency response of the different approaches approximating the low frequency dynamics assuming constant reference signals (ZOH) or piecewise linear reference signals (FOH).

Finally, this new input matrix can be inserted into the reset equation:

$$\begin{aligned} \bar{z}(k\delta) &= \bar{M}\bar{z}(k\delta^-) + \bar{P}r(k\delta^-) \\ &= A_d\bar{z}((k-1)\delta) + \bar{M}\bar{B}_1r((k-1)\delta) + \bar{M}\bar{B}_2r(k\delta) + \bar{P}r(k\delta). \end{aligned} \quad (5.176)$$

Removing the time shift applying  $\tilde{\gamma}(k\delta) = \bar{z}(k\delta) - (\bar{M}\bar{B}_2 + \bar{P})r(k\delta)$ , similar to Equation (5.170), results in

$$\tilde{\gamma}((k+1)\delta) = A_d\tilde{\gamma}(k\delta) + \left( \bar{M}\bar{B}_1 + A_d(\bar{M}\bar{B}_2 + \bar{P}) \right) r(k\delta) \quad (5.177)$$

and the improved approximation in the frequency domain for the lower frequency range  $\omega \ll \frac{\pi}{\delta}$  is given by

$$\tilde{T}_{\text{low}}(z) = \begin{pmatrix} \bar{C} & 0 \end{pmatrix} (zI - A_d)^{-1} \left( \bar{M}\bar{B}_1 + A_d(\bar{M}\bar{B}_2 + \bar{P}) \right) + D_{cl} + \begin{pmatrix} \bar{C} & 0 \end{pmatrix} \bar{M}\bar{B}_2. \quad (5.178)$$

Figure 5.15 shows the comparison between different approximations of the low frequency dynamics continuing Example 5.3 with the reset parameters  $\mu = 0.5$  and  $P_c = 0$ . The approximation applying the first order hold of the reference shows a similar behavior as the previous approximation including the stationary gain of 0 dB and a peaking before  $\frac{\pi}{\delta}$ .

These dynamics can now be used to tune the reset matrices  $M_c$ ,  $N_c$  and  $P_c$ . As the general control structure is more suited to track piecewise constant references, we will use the zero order hold approximation of these lower frequency dynamics.

Besides the stability condition (5.167) the steady state tracking error has to be taken into account here. Assuming that the baseline controller is designed to achieve zero tracking error  $e(t \rightarrow \infty) = 0$ , the stationary control signal  $u_s$  is given by

$$u_s = K_{\text{DC}} r_s \quad \text{with} \quad K_{\text{DC}} = \frac{C(0)}{1 + C(0)G(0)}. \quad (5.179)$$

If the control system reaches such a stationary point, the next reset should not move the system states away. As  $e(t) = 0$  the control effort in (5.164c) only depends on the controller state  $u_s = C_c x_{c,s}$  and for the reset equation (5.164b) we hence require

$$x_{c,s} = M_c x_{c,s} + N_c r_s, \quad (5.180)$$

as we do not want to excite possible zero dynamics of the controller. Due to this condition, we cannot design each reset matrix independently. Following the ideas presented in [108], we reduce the design to the scalar variable  $\mu \in [0, 1]$  and set and choose the following reset matrices

$$M_c = \mu I \quad (5.181)$$

$$C_c N_c = (1 - \mu) K_{\text{DC}}. \quad (5.182)$$

We see that this choice satisfies (5.180) as follows

$$\begin{aligned} (1 - \mu) I x_{c,s} &= N_c x_{c,s} \\ \iff (1 - \mu) C_c x_{c,s} &= C_c N_c r_s \\ \iff (1 - \mu) u_s &= C_c N_c r_s \\ \iff (1 - \mu) K_{\text{DC}} r_s &= C_c N_c r_s. \end{aligned} \quad (5.183)$$

For  $\mu = 1$  the stationary behavior is only determined by the underlying baseline controller as the controller state remains unchanged at the reset instant. With this choice, the robustness of the baseline controller is maintained, as for example fractional-order integrator states are not reset and still account for modeling discrepancies. If also  $P_c = 0$ , we have again a pure memory reset control scheme. In the second extreme case with  $\mu = 0$ , the controller state is completely defined by the reference signal  $r(\delta k)$  and the DC gain  $K_{\text{DC}}$ . In this case it is crucial to know the exact process gains to maintain the stationary accuracy. The advantage of this setting is a fast closed-loop response. As the rank of the reset matrix  $\bar{M}$  is minimal, i.e.  $\text{rank}(\bar{M}) = n$ , all dynamics added by the controller are removed. To summarize this discussion, we have to set  $\mu$  close to one if the plant parameters are uncertain. To meet higher dynamic demands,  $\mu$  has to be chosen close to zero. Using time-varying reset matrices to achieve fast responses to reference jumps and also a certain amount of robustness should be investigated further. Also, an extension of the optimal reset presented in [108] for integer-order controllers is possible.

Finally, the remaining reset parameter  $P_c$  can be used to reduce the frequency peak induced by the memory reset for shortened reset periods.

**Example 5.3** (continued). *We extend the memory reset described previously with the presented controller state reset. In Figure 5.17 the effect of different values of  $\mu$  is illustrated. For  $\mu = 1$  the pure memory reset with the resonance peak is obtained. With the direct reset to the controller state, the resonance peak is reduced.*

*In Figure 5.18 the effect of the additional-tuning parameter  $P_c$  is illustrated. In combination with the parameter  $\mu$  we can adjust the low frequency dynamics further (even approaching the designed*

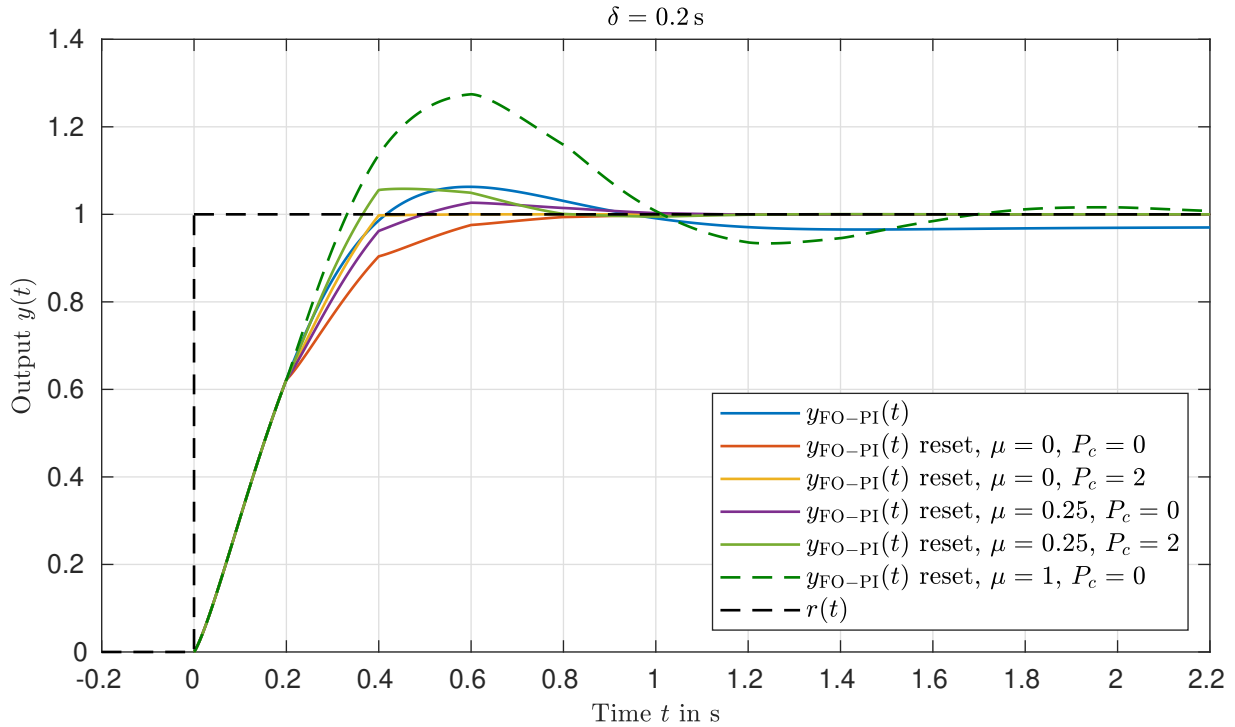


Figure 5.16: Step responses obtained with different reset strategies.

fractional-order dynamics). Note that the amplitude response is nearly constant over the frequency range.

In the time domain, the changed reset law leads to an improved step response as illustrated in Figure 5.16. However, for this reset period  $\delta = 0.2$  s we can only reduce the overshooting by setting  $\mu$  close to zero. This requires a good knowledge of the process as the integrator state in the controller is deleted periodically.

#### 5.4.2.4 Implementation Using Higher-Order Approximations

We conclude this chapter with a comment on the implementation of the different fractional-order reset controllers. This gives us additional insights as the approximation allows us to compare the memory and state reset in detail.

The realization of fractional-order controllers requires the implementation of fractional-order integrators. In order to keep the integration property for low frequencies, we have to split the approximation of the fractional order integrator

$$s^{-\alpha} = \frac{s^{1-\alpha}}{s} \approx \frac{H_{1-\alpha}(s)}{s}, \quad (5.184)$$

where  $H_{1-\alpha}(s)$  could be any higher-order approximation of the  $s^{1-\alpha}$ , e. g. an Oustaloup Filter, as given in equation (2.106). This approach splits the controller state  $x_c(t)$  from its memory as illustrated in Figure 5.19. The single integer-order integrator represents the actual controller state  $x_c(t)$  and the states defining  $H_{1-\alpha}(s)$  are an approximation of the memory. Figure 5.19 also illustrates already the different reset strategies. The additional advantage of this split is

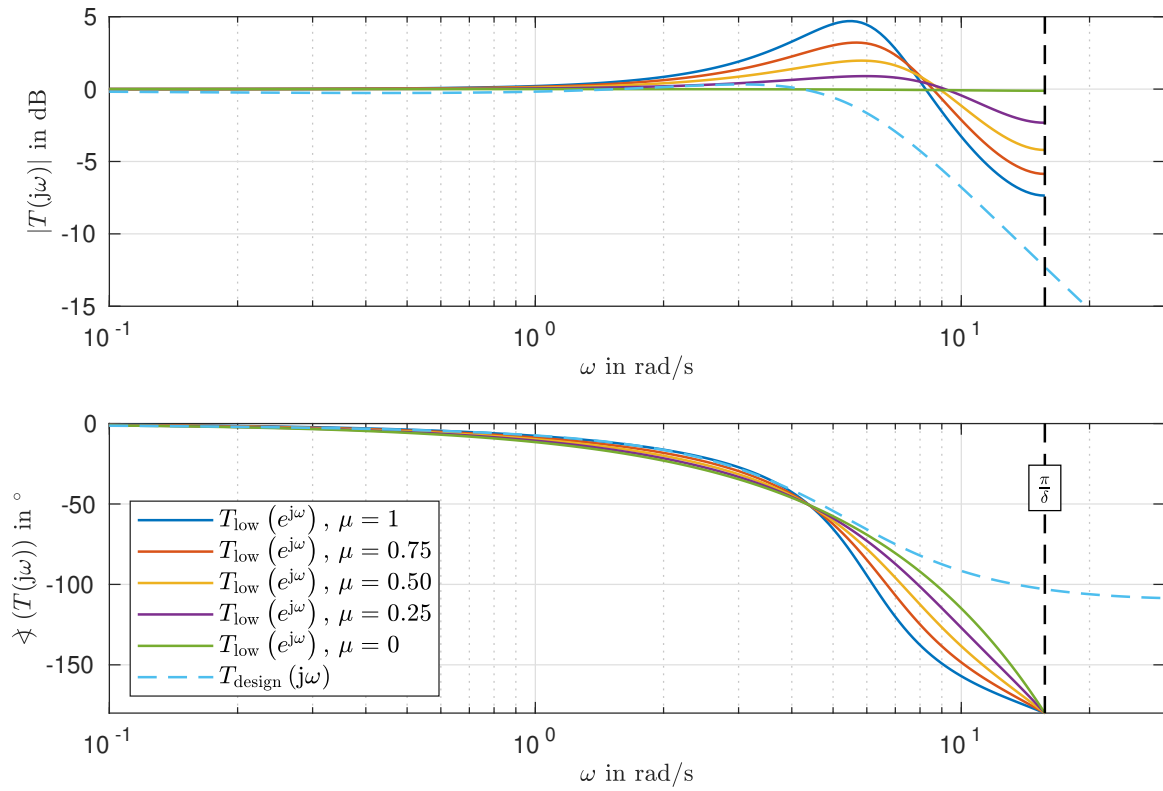


Figure 5.17: Frequency response of the approximated low frequency dynamics  $T_{low}(j\omega)$  for varying  $\mu$ .

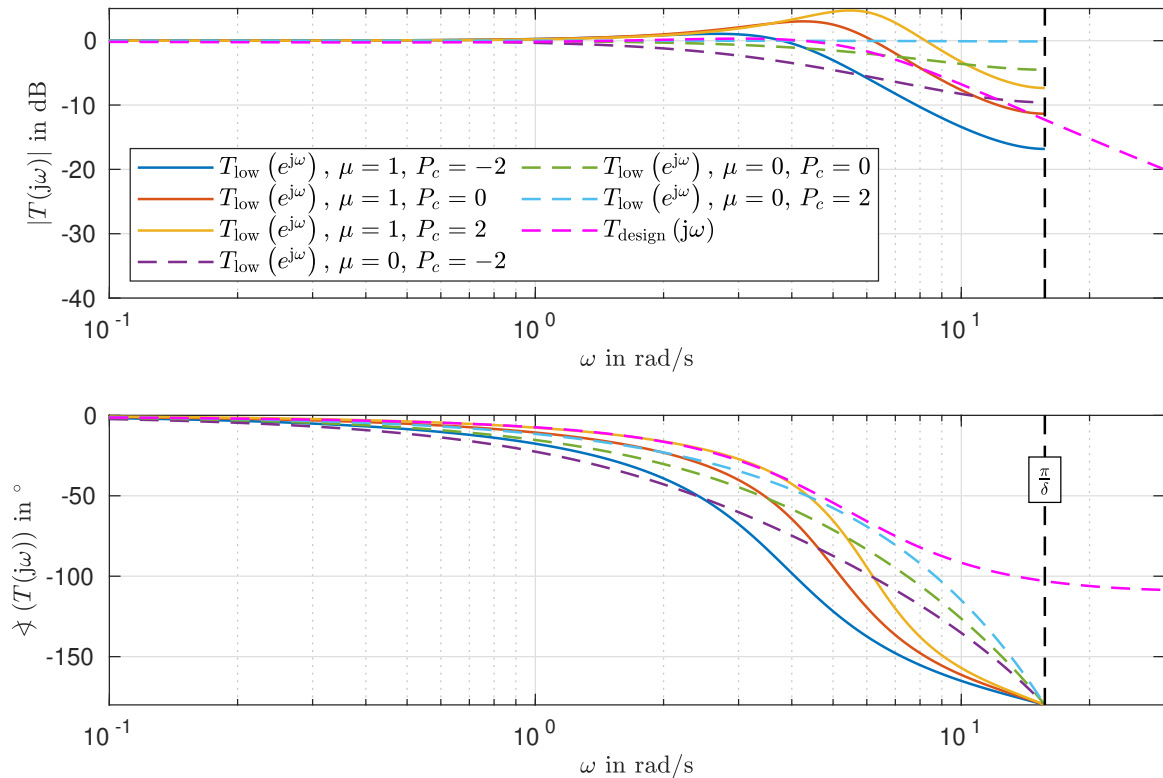


Figure 5.18: Frequency response of the approximated low frequency response  $T_{low}(j\omega)$  with changing reset parameter  $P_c$ .

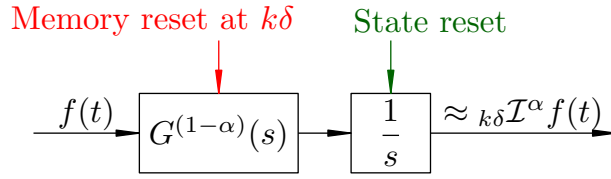


Figure 5.19: The approximation splits the pseudo state from its memory (see [30]).

the obtained relative degree of one, as the pure Oustaloup Filter, for example, is only proper. This is essential to avoid algebraic loops.

As each element of the controller state has its own memory, the implementation requires  $n_c$  additional systems

$$\tilde{G}(s) = \text{diag} \left( G^{(1-\alpha)}(s), \dots, G^{(1-\alpha)}(s) \right) = \tilde{C} \left( sI - \tilde{A} \right)^{-1} \tilde{B} + \tilde{D}.$$

With this approach, the implementation of the controller (5.162) reads

$$\begin{pmatrix} \dot{x}_c(t) \\ \dot{\tilde{x}}_c(t) \end{pmatrix} = \underbrace{\begin{pmatrix} \tilde{D}A_c & \tilde{C} \\ \tilde{B}A_c & \tilde{A} \end{pmatrix}}_{\tilde{A}_c} \begin{pmatrix} x_c(t) \\ \tilde{x}_c(t) \end{pmatrix} + \underbrace{\begin{pmatrix} \tilde{D}B_c \\ \tilde{B}B_c \end{pmatrix}}_{\tilde{B}_c} e(t) \quad (5.185a)$$

$$u(t) = \underbrace{\begin{pmatrix} C_c & 0 \end{pmatrix}}_{\tilde{C}_c} \begin{pmatrix} x_c(t) \\ \tilde{x}_c(t) \end{pmatrix} + D_c e(t) \quad (5.185b)$$

The closed-loop of the integer-order system (5.1) and this controller approximation is given by

$$\dot{\zeta}(t) = \underbrace{\begin{pmatrix} A - BD_cC & B\tilde{C}_c \\ -\tilde{B}_cC & \tilde{A}_c \end{pmatrix}}_{\tilde{A}_{cl}} \zeta(t) + \begin{pmatrix} BD_c \\ \tilde{B}_c \end{pmatrix} r(t)$$

$$y(t) = \begin{pmatrix} C - DD_cC & \tilde{C}_c \end{pmatrix} \zeta(t) + \begin{pmatrix} DD_c \end{pmatrix} r(t)$$

with the new extended state

$$\zeta^\top = \begin{pmatrix} x \\ x_c \\ \tilde{x}_c \end{pmatrix}. \quad (5.186)$$

Here, the closed-loop representation only contains the memory approximation of the controller and not the auxiliary states of the associated fractional-order system. The reset of the controller state at  $t = k\delta$  is given by

$$\zeta(k\delta) = \tilde{M}\zeta(k\delta^-). \quad (5.187)$$

The different reset strategies present themselves when comparing the individual reset matrices  $\tilde{M}$ . In case of a state reset the memory approximation of the controller state  $\tilde{x}_c$  remains unchanged, i. e.

$$\tilde{M}_{\text{state}} = \begin{pmatrix} I & 0 & 0 \\ -P_cC & M_c & 0 \\ 0 & 0 & I \end{pmatrix}, \quad (5.188)$$

whereas it is set to zero if the memory is reset as well

$$\tilde{M}_{\text{memory}} = \begin{pmatrix} I & 0 & 0 \\ 0 & I & 0 \\ 0 & 0 & 0 \end{pmatrix}, \quad \tilde{M}_{\text{extended}} = \begin{pmatrix} I & 0 & 0 \\ -P_c C & M_c & 0 \\ 0 & 0 & 0 \end{pmatrix}. \quad (5.189)$$

This approximation can also be applied to examine the stability of the pure state reset control approach and derive a frequency domain interpretation for the lower frequency range relying on the induced dynamics.

**Theorem 5.15.** *The approximation (5.185) of the fractional-order state reset controller (5.162) stabilizes the origin of the integer-order system (5.1) asymptotically if and only if*

$$|\lambda_i| < 1, \quad i = 1, 2, \dots, n + (N + 1), \quad (5.190)$$

where  $\lambda_i$  denotes the  $i$ -th eigenvalue of the induced system matrix

$$\tilde{A}_d = \tilde{M}_{\text{state}} \exp(\tilde{A}_{\text{cl}}\delta). \quad (5.191)$$

*Proof.* The induced dynamics including the approximation of the fractional-order controller are given by

$$\zeta((k+1)\delta) = \tilde{M}_{\text{state}} \exp(\tilde{A}_{\text{cl}}\delta) \zeta(k\delta) = \tilde{A}_d \zeta(k\delta) \quad (5.192)$$

and its stability can be assessed by evaluating the location of the eigenvalues with respect to the unit circle.

Note that  $\tilde{M}_{\text{state}}$  has full rank if  $\text{rank}(M_c) = n_c$  and the reset therefore shifts no eigenvalue of  $\tilde{A}_d$  to zero. A consequence of this is a reduced region of stability as unstable dynamics cannot be suppressed by the reset matrix any more.  $\square$

The low frequency behavior including the controller approximation is given by

$$\tilde{T}(z) = \tilde{C}_{\text{cl}} (zI - \tilde{A}_d)^{-1} \tilde{B}_d + DD_c \quad (5.193)$$

with

$$\tilde{B}_d = \tilde{M}_{\text{state}} \int_0^\delta \exp(\tilde{F}(t - \tau)) d\tau \begin{pmatrix} BD_c \\ \tilde{B}_c \end{pmatrix} + \tilde{A}_d \tilde{P}. \quad (5.194)$$

**Example 5.3 (continued).** *Finally, we also present the results for the pure state reset controller applied to the normalized first order plant. The parameters are set to  $\mu = 0$  and  $P_c = 2$ . The step response shown in Figure 5.21 shows the effect of the remaining memory. Although the transients change, we still see the relatively slow convergence, despite the correct stationary gain of the obtained frequency response  $T_{\text{low}}(j\omega)$  depicted in Figure 5.20. Here, the amplitude response is also very flat.*

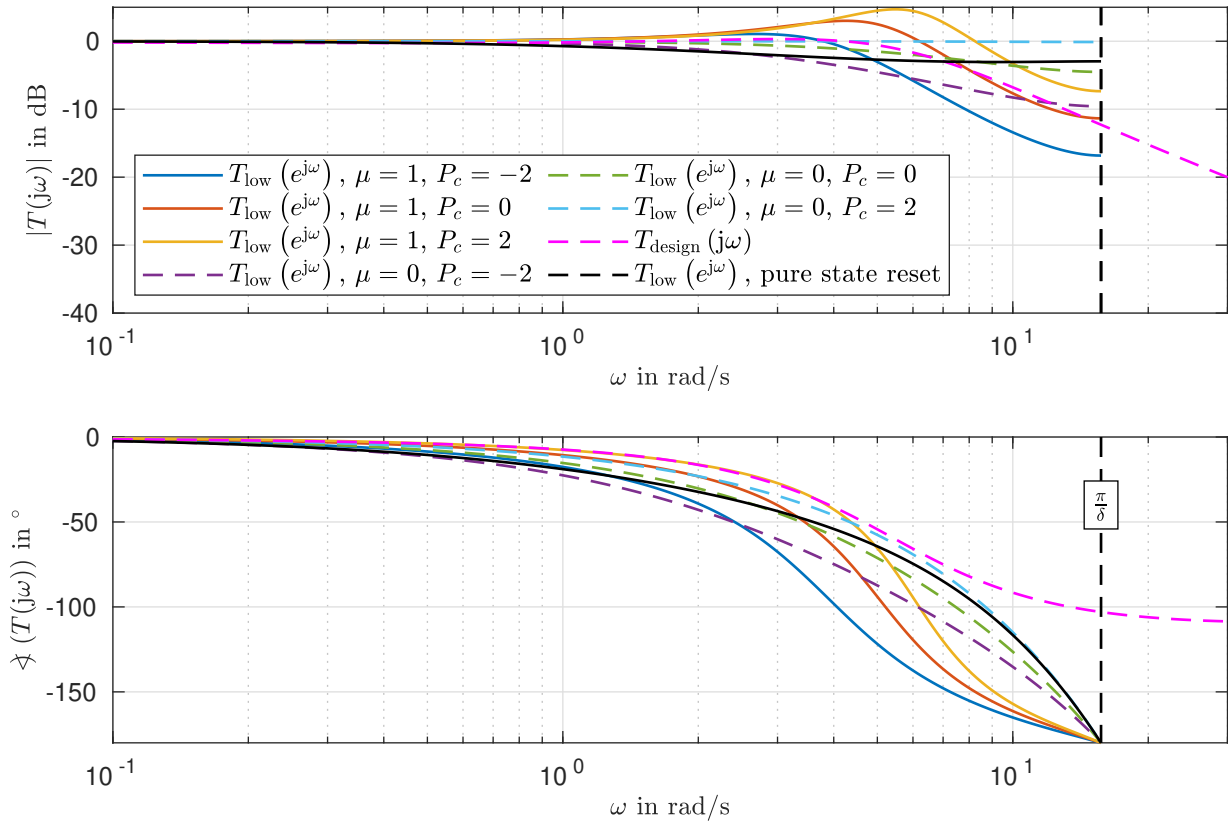


Figure 5.20: Frequency response of the approximated low frequency dynamics  $T_{\text{low}}(j\omega)$  including an approximation of the pure state reset control law.

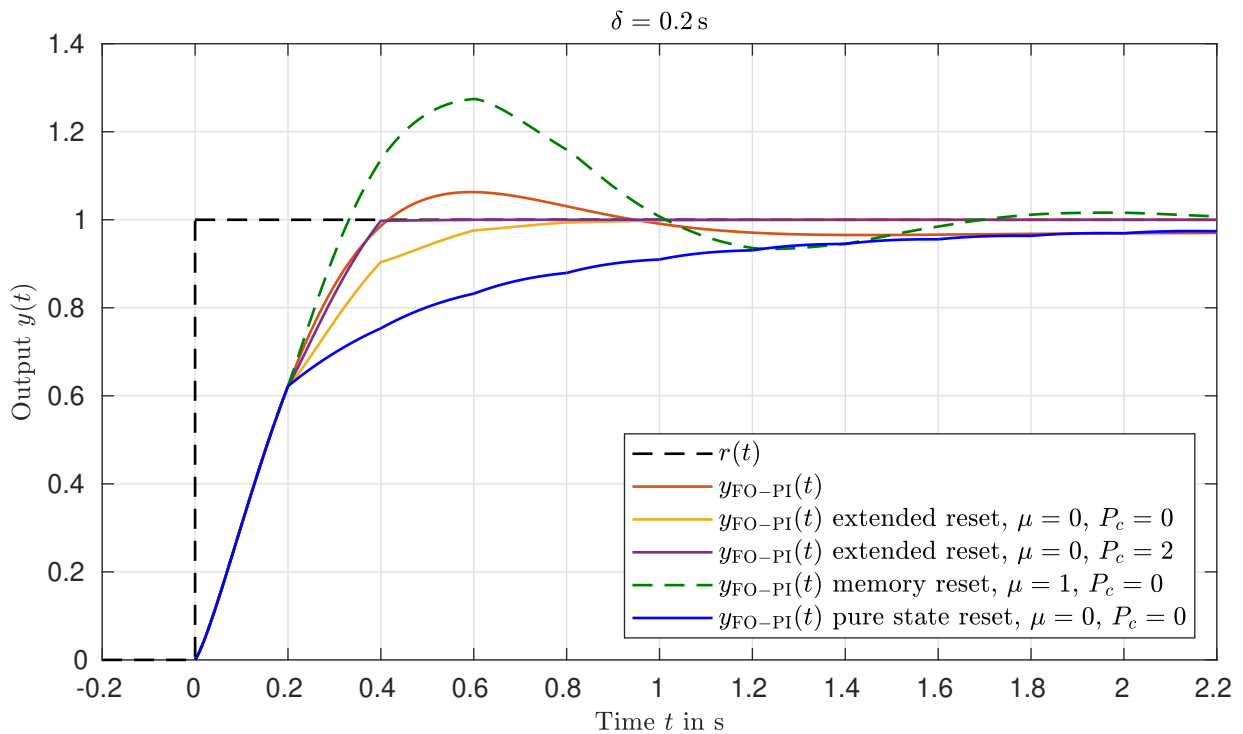


Figure 5.21: The step response obtained with the pure state reset controller converges slowly.





## 6 Experimental Results

The focus of the laboratory experiments is set on the application of fractional-order control on the one the hand and observer approaches to integer-order systems on the other hand as these systems are widely available and we can use existing laboratory testbenches. In our case we consider a DC motor driving a nearly balanced inertia and a magnetic brake as shown in Figure 6.1. The experimental setup is equipped with an encoder to measure the angular position of the driving shaft. Furthermore, an analogue tachometer exists such that the information of the angular velocity can also be used. However, the measurements are corrupted by noise and first experiments show an offset in the sensor, as the velocities do not coincide with the offline derived measurements of the position sensor. Therefore, we rely on the encoder for control and observation purposes only.

As the input is a normalized voltage, the system dynamics are theoretically of order three, as the system has two energy storages in addition to an integrator - the mass conserves kinetic energy and the motor coils store electromagnetic energy. With the state  $x(t) = (\varphi(t), \dot{\varphi}(t), i(t))^T$  the model results in

$$\dot{x}(t) = \begin{pmatrix} 0 & 1 & 0 \\ 0 & -\frac{\mu}{J} & \frac{K_m}{J} \\ 0 & -\frac{K_e}{L} & -\frac{R}{L} \end{pmatrix} x(t) + \begin{pmatrix} 0 \\ 0 \\ \frac{V}{L} \end{pmatrix} u(t) \quad (6.1)$$

with the total inertia  $J$ , the motor constants  $K_m$  and  $K_e$ , the electrical resistance  $R$ , the inductance  $L$ , the amplifier gain  $V$  and the coefficient  $\mu$  to describe viscous damping.

With a sampling time of  $T_s = 2$  ms, the identified step responses suggest that we can simplify the model to a second order plant, as the current dynamics are sufficiently fast. The final second order model with the state  $x(t) = (\varphi(t), \dot{\varphi}(t))^T$  contains the rotor position  $\varphi(t)$  and its

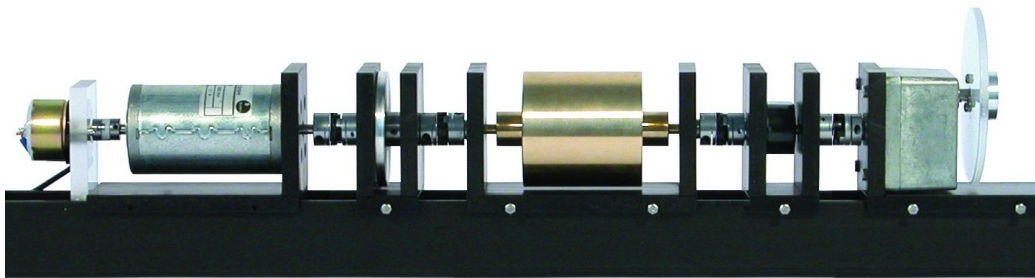


Figure 6.1: Testbench with DC motor and magnetic brake.

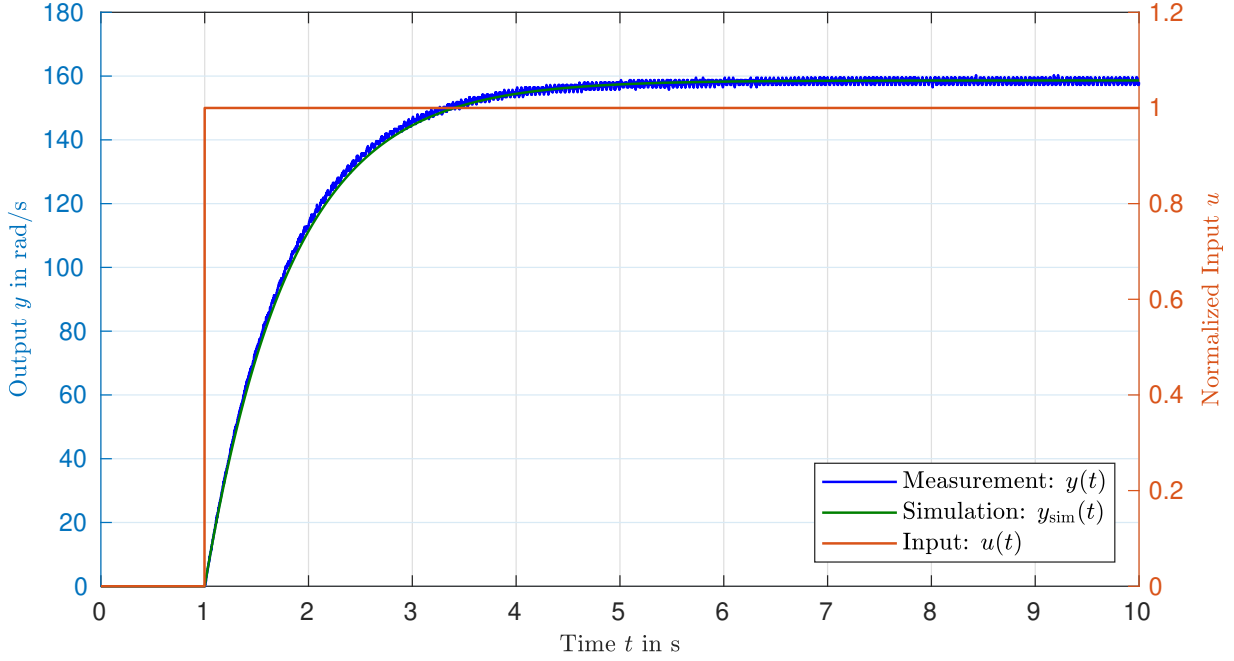


Figure 6.2: Step response for model validation.

angular velocity  $\dot{\varphi}(t)$  and is described by the following differential equation

$$\dot{x}(t) = \begin{pmatrix} 0 & 1 \\ 0 & -\tau^{-1} \end{pmatrix} x(t) + \begin{pmatrix} 0 \\ K \end{pmatrix} u(t), \quad \text{with} \quad \begin{matrix} \tau = 0.8261 \\ K = 158.64 \end{matrix}. \quad (6.2)$$

Figure 6.2 illustrates the accuracy of this simplified model.

## 6.1 Fractional-Order Memory Reset Observer

To test the fractional-order observer on the test setup, we rely on the implementation scheme shown in Figure 5.19. The state of the Oustaloup filter is reset to zero periodically and the integrators linked to the fractional-order derivatives of the state are also set to zero at  $t_k = \delta k$ . To excite various frequencies, a chirp signal is used as input and all observers are initialized with the same faulty initial conditions. We compare three different sets of eigenvalues

$$\begin{aligned} \lambda_{i,1} &\in \{-2.0, -2.1, -2.2, -2.3\}, \\ \lambda_{i,2} &\in \{-5.0, -5.1, -5.2, -5.3\}, \\ \lambda_{i,3} &= 3 \exp(j\varphi_i), \quad \varphi_i \in \left\{ \pm \frac{11}{20}\pi, \pm \frac{17}{20}\pi \right\} \end{aligned}$$

and the observation results for different reset instants  $\delta = 0.2 \text{ s}, 0.5 \text{ s}, 1.0 \text{ s}$  and  $\delta \rightarrow \infty$ , where the last reset interval is the non-reset version of the observer.

The results of the experiments for  $\delta = \infty$  are depicted in Figure 6.3. The fast initial response of the different observers is evident. With increased observer gains the convergence is accelerated at the cost of increased initial peaking. In Figure 6.4 the estimation error for the different

observer gains is plotted in detail. The distortion of the second estimation error signal  $e_2(t)$  is caused by the offline derived position measurement used to compute the error. Note that it does not converge to zero and is excited with the input even if initialized correctly with  $\hat{x}(0) = 0$ . This suggests that some nonlinear mechanical effects, e.g. an unbalanced mass, are not included in the model used to design the observer. For this reason, we also see that the memory reset version of the observer leads to additional peaks in the error signal each time the observer dynamics are reset. This is shown in Figure 6.5. This observation is similar to Example 5.1. For the set of real eigenvalues, the reset with the reduced reset interval  $\delta$  shows a slightly better initial convergence. The increased reset frequency, however, also increases the error after the initial transient has passed. As the system model is not fitting perfectly, the strong initial convergence sends the observer states in the wrong direction. This effect depends on the observer gains. In summary, the experiments show that the fractional-order approach works. The reset does not seem to be required. If the observer gains are sufficiently large, the algebraic convergence is sufficient and due to non-modelled dynamics, the reset introduces additional errors.

Future work might focus on the adaptation of the reset memory, such that these peaks are reduced and the observer can still be applied using a finite reset interval to keep the physical memory requirements low.

## 6.2 Extended Fractional-Order Reset Control

In this part we consider the velocity control of the DC motor via output feedback. As the velocity is not measured directly, we use the first order Euler discretization to derive the encoder signal online.

We apply a fractional-order  $PI^\alpha$  controller given by

$$C_{\text{FOPI}}(t) = K_p + \frac{K_i}{s^\alpha}. \quad (6.3)$$

This baseline controller is designed to achieve a crossover frequency  $\omega_c = 3 \frac{\text{rad}}{\text{s}}$  and a phase margin of  $\Phi_r = 60^\circ$ . The order of the integrator  $\alpha$  is set to  $\alpha = \frac{2}{3}$  such that a satisfying step response is obtained and the analysis of the closed-loop system only requires five states  $\bar{z}(t) \in \mathbb{R}^5$  with the commensurate order  $\bar{\alpha} = \frac{1}{3}$ .

The design equations

$$\begin{aligned} |C(j\omega)G(j\omega)|_{\omega=\omega_s} &= 1 \\ \pi + \angle(C(j\omega_s)G(j\omega_s)) &= \frac{\pi}{3} \end{aligned} \quad \text{with} \quad G(s) = \frac{K}{\tau s + 1}$$

are nonlinear and solved with the standard routine `lsqnonlin` resulting in  $K_p = 0.0024$  and  $K_i = 0.0312$ .

The implementation uses the method presented in [106] as we work on a finite time horizon. However, comparable results are obtained, if an Oustaloup filter of the order 19 with  $\omega \in [0.001 \frac{\text{rad}}{\text{s}}, 100 \frac{\text{rad}}{\text{s}}]$  is applied to approximate the fractional-order integration.

The resulting step responses and the required control effort  $u(t)$  are shown in Figure 6.6 and 6.7. To improve visibility, the graphics show a down-sampled and averaged output signal  $y(t)$ .

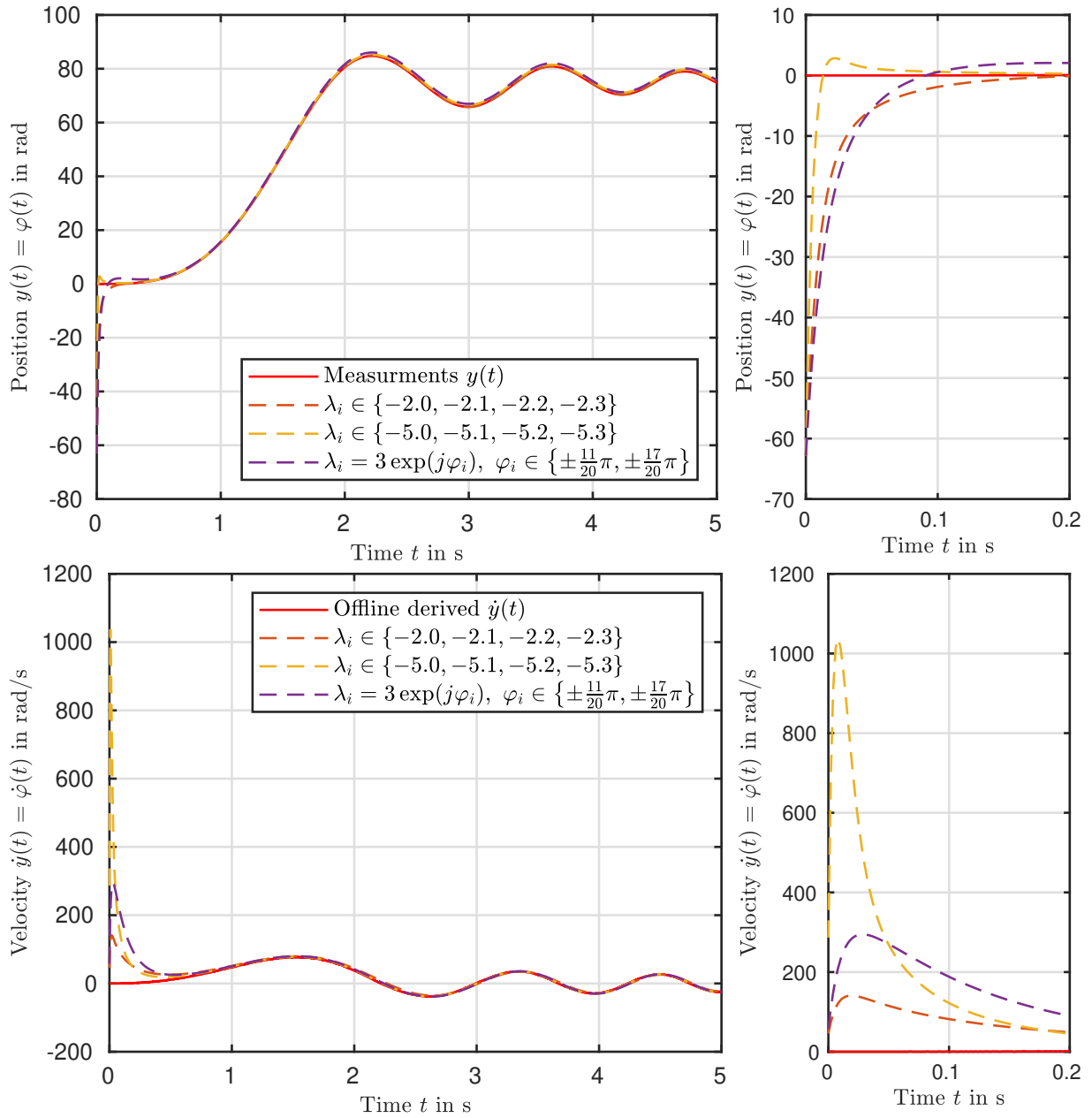


Figure 6.3: Transients of the state and estimates of different observers.

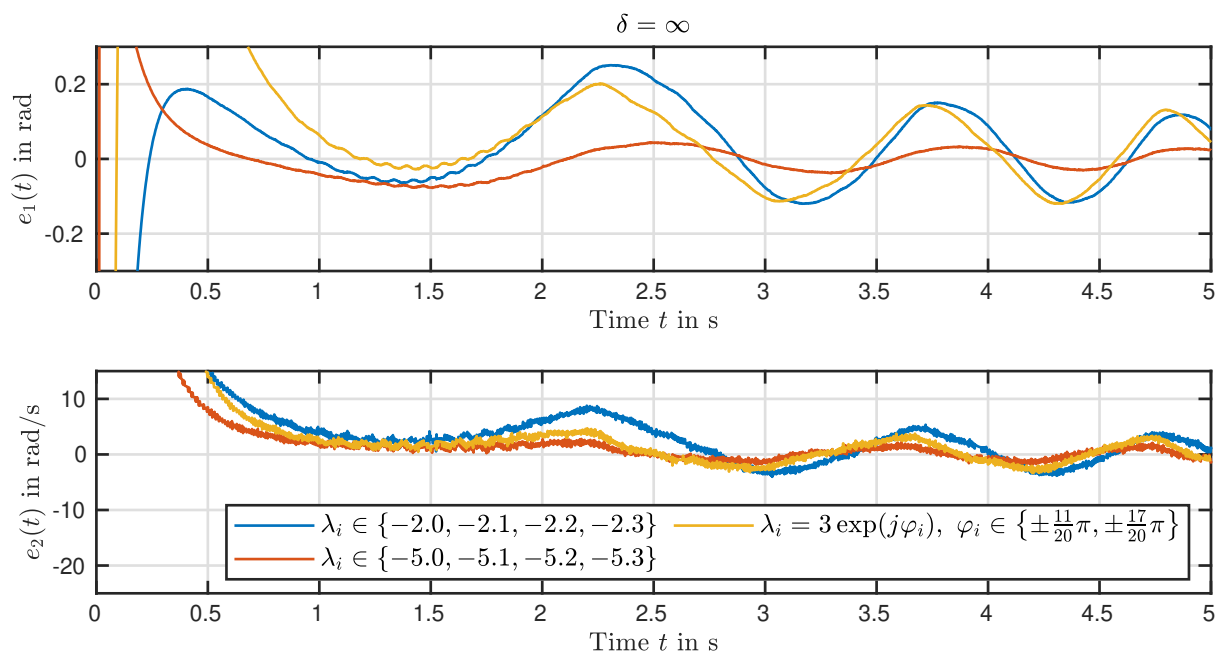


Figure 6.4: Comparison of the estimation error for different observer gains.

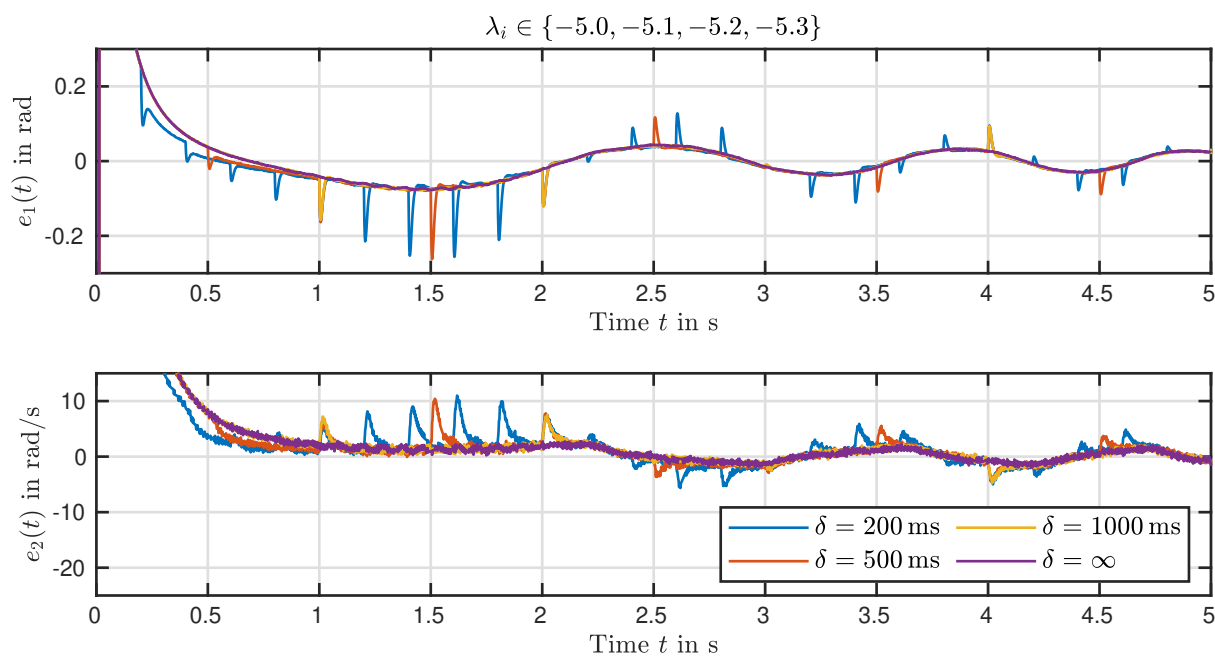


Figure 6.5: Comparison of the estimation error for different reset intervals.

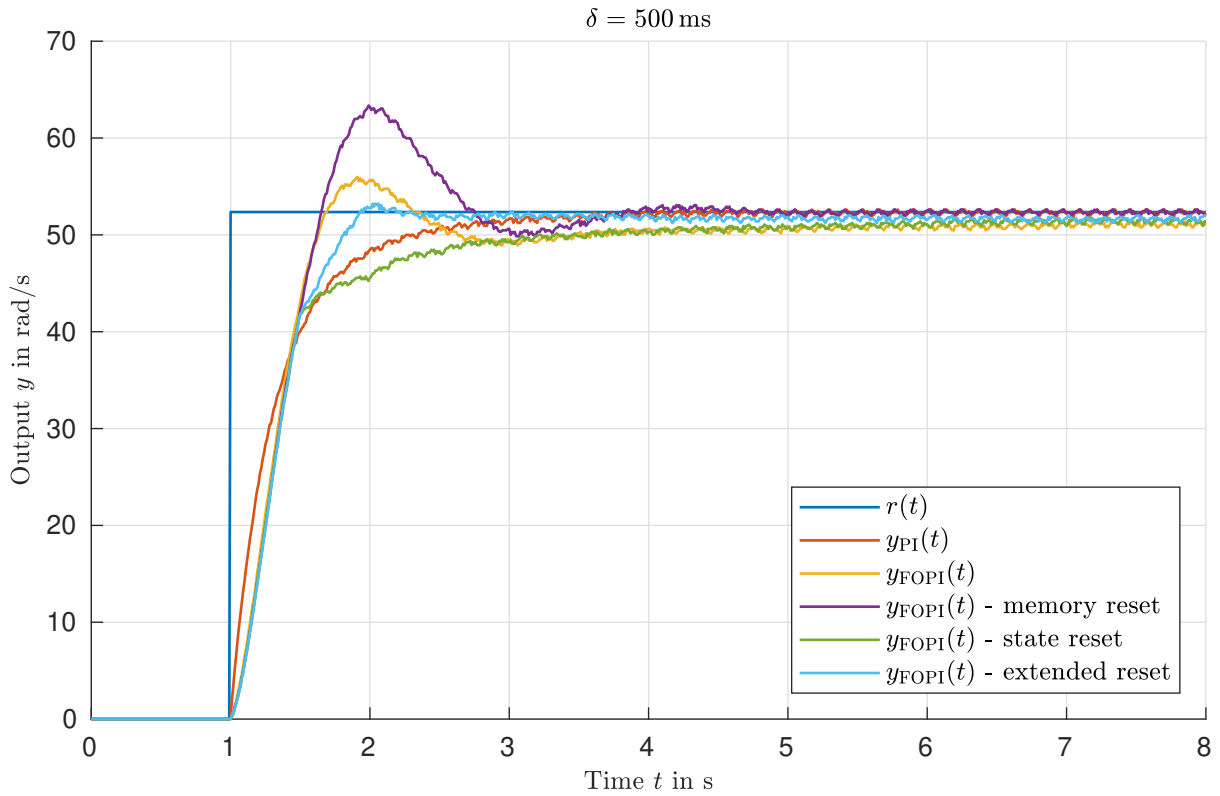


Figure 6.6: Step responses obtained with different controllers.

The ripples overlaying the steady state are caused by an imbalanced mass as the frequency of these ripples is corresponding to the rotational velocity. For different reference set points we can observe adjusted oscillations.

The pure fractional-order controller (yellow line) meets the design specifications and shows the expected slow convergence for large times  $t > 4$  s. With the memory reset with  $\delta = 0.5$  s we can increase the convergence such that the reference is tracked exponentially. However, as the reset frequency is higher than the crossover frequency  $\omega_c < \frac{\pi}{\delta} = 6.28 \frac{\text{rad}}{\text{s}}$ , the designed dynamics are degraded and overshooting occurs. For comparison, a PI controller is also tested (red line). The simulation of this controller leads to a different stationary control effort as illustrated in Figure 6.7 (black dashed line). Hence the process has a nonlinear stationary gain and reset matrices of each reset controller need to be adjusted. The final set of all parameters is given in Table 6.1.

The extended state reset controller (cyan line) reduces overshooting and also leads to a reduced control effort. The energy required to spin up the inertia,  $\int_0^t u(\tau) d\tau$ , is split up differently. Consequently, this controller can achieve faster convergence with a lower peak in the control signal.

Finally, the pure state reset controller given in [30] is examined. As the memory is not deleted, the output converges comparable to the initial fractional-order controller. However, the reset cancels the overshooting in the step response. The detailed results of all different experiments are listed in Table 6.2.

Table 6.1: Different tested controllers

Controller	$K_p$	$K_i$	$\alpha$	$N_c$	$P_c$	$M_c$	$\delta$
PI	$\frac{\tau\omega_s}{K} = 0.0157$	$\frac{\omega_s}{K} = 0.0190$	1	-	-	-	$\infty$
PI $^\alpha$	0.0024	0.0312	$\frac{2}{3}$	-	-	-	$\infty$
Memory Reset	0.0024	0.0312	$\frac{2}{3}$	0	0	1	0.5 s
State Reset	0.0024	0.0312	$\frac{2}{3}$	0.0073	0	0	0.5 s
Extended Reset	0.0024	0.0312	$\frac{2}{3}$	0.0073	0	0	0.5 s

Table 6.2: Evaluation of the different controllers with  $t_0 = 0$  and  $t_{\text{end}} = 8$  s.

Controller	$t_{90\%}$ in s	$u_{\text{max}}$	ISE	IAE	ITAE
PI	0.86	0.822	469.97	21.21	37.35
PI $^\alpha$	0.56	0.683	622.05	28.08	71.27
Memory Reset	0.59	0.676	685.48	32.11	74.35
State Reset	1.15	0.675	680.87	26.81	48.43
Extended Reset	0.69	0.681	643.34	22.37	42.74

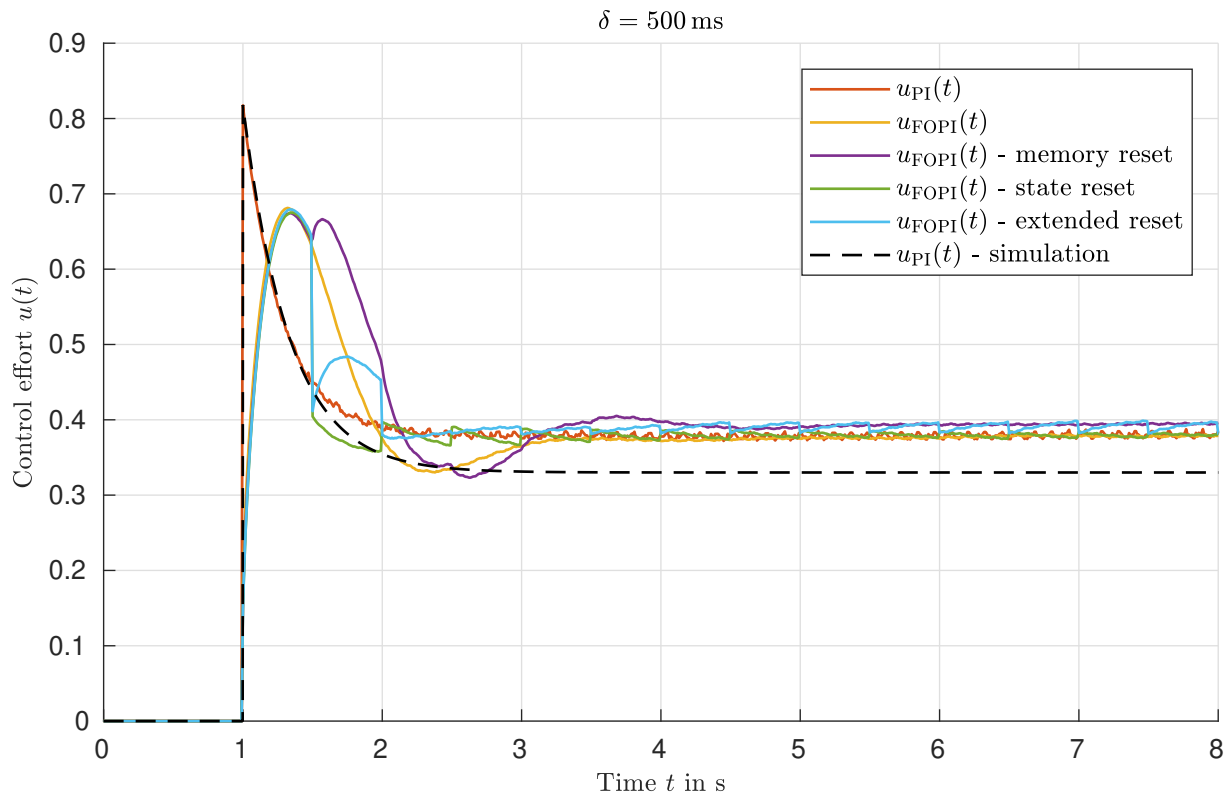


Figure 6.7: Control effort of the different control approaches in comparison with the simulation of the closed-loop.

Inspecting the control signal in Figure 6.7 in detail reveals that the stationary gain has also shifted between the individual experiments as both controllers which clearly achieve exponential tracking (PI and memory reset) require slightly different stationary control signals. As the state reset approaches are reset to a value in between those limits, the stationary performance is lacking. This shows that reset approaches are suitable to increase dynamics but also lead to reduced robustness with respect to unknown system parameters. An exception in this case would be the control of processes with an integrator as the stationary control signal has to be zero.



## 7 Conclusions

### 7.1 Summary

In this work, an equivalent representation of fractional- and integer-order linear time invariant systems is used and applied to implement fractional-order systems efficiently and to design both convergence improved observers and exponentially converging fractional-order controllers.

We start with the derivation of an associated integer-order system describing the state trajectories of a terminal initialized fractional-order system. This representation is then used to design a time-varying observer which leads to an exponentially converging estimation error. The drawback of this approach is a certain lag of robustness as the absolute time is an important parameter and the observer gains are increasing constantly. For this reason, we make use of the known transition matrices of the fractional-order system and derive an impulsive observer which is able to reconstruct the system state in a fixed predefined time.

However, the system class appears to be too restrictive. We hence shift the focus to the state estimation of input initialized fractional-order LTI systems. We derive an associated system with doubled order of differentiation. This system can be used to design an unknown input observer which is able to increase the convergence on the one hand and reduces the effect of the unknown past on the other hand.

The representation of the integer-order system in terms of fractional-order derivatives can be achieved by extending the state with fractional-order derivatives or integrals and properly initializing these with zero. For integer-order systems with a regular system matrix, all these associated fractional-order systems conserve the properties of the integer-order system: stability, controllability and observability.

These associated representations are then used for observer and controller design. In contrast to a standard observer of the Luenberger type, the estimation error achieved with a fractional-order observer converges only algebraically. For long time observations this is problematic as the unknown initial conditions still degrade the performance of the estimation. The algebraic convergence is a result of the memory of fractional-order derivatives and increased gains can only slightly reduce this effect. Within a short time interval just after the initialization of the observer, however, the convergence is faster than exponential as the estimation error shows unbounded derivatives at the initial time instant if the observer poles are placed on the negative real line. This is the major advantage of the fractional-order approach. Another drawback besides the poor convergence is the increased cost of implementation as the memory of the fractional-order derivatives has to be stored. To overcome both of these drawbacks, the memory of the fractional-order observer is reset which is possible due to the system being time invariant. The periodic reset induces discrete time dynamics linking the reset instant and defining the stability of the estimation error. A simulation example shows the potential of this observer: We can improve the response of the estimation error to measurement noise while guaranteeing a certain exponential convergence rate.

We apply the same ideas to a case of a fractional-order controller being used to control an integer-order process. With the periodically reset memory of the controller, the closed-loop is given by a hybrid fractional-order system which converges exponentially. We use the induced discrete time dynamics to derive a frequency domain representation of the closed-loop dynamics frequencies below the reset frequency. This representation can be used to design the reset period such that the desired dynamics of the underlying baseline controller remain the same. To reduce the reset period and by that the required physical memory for implementation further, we combine the memory reset of the fractional-order operator with a reset of the controller state. The additional reset parameters can be adjusted by inspecting the frequency response of the induced dynamics.

In addition to the various simulation studies illustrating the proposed methods throughout the thesis, we provide experimental results in the last chapter. A DC motor is used to demonstrate the applicability of the fractional-order observer and to illustrate the differences between the shown fractional-order reset control schemes.

## 7.2 Future Work

In this thesis, the potential of the fractional-order memory reset observer subjected to measurement noise is only illustrated in one example. A dedicated tuning method should be developed to benefit from the additional tuning parameters. As nonlinear optimization techniques have to be used, we have to define a suitable objective function. The application of the proposed methods to nonlinear integer-order processes are also promising.

The reset approaches could be extended such that an arbitrary memory is implanted in the controller. In this case various questions arise: How can we formulate a solution and how do we implement the controller itself?

Regarding the controller approaches, we have not discussed how to choose the reset matrices optimally. Furthermore, we can observe that the reset parameters of the extended fractional-order memory reset controller are critical to achieve zero stationary error. It should be extended by an online adaptation to increase the algorithm's robustness.

## A Miscellaneous

### A.1 Laplace Transforms

The Laplace transform of polynomials of an arbitrary order  $\alpha > -1$  can be derived with the substitution  $t = \frac{u}{s}$ ,  $\text{Re}\{s\} > 0$

$$\begin{aligned}\mathcal{L}\{t^\alpha; s\} &= \int_0^\infty t^\alpha e^{-st} dt \\ &= \int_0^\infty \frac{1}{s} \left(\frac{u}{s}\right)^\alpha e^{-u} du \\ &= \frac{1}{s^{\alpha+1}} \underbrace{\int_0^\infty u^\alpha e^{-u} du}_{\Gamma(\alpha+1)} \\ &= \frac{\Gamma(\alpha+1)}{s^{\alpha+1}}.\end{aligned}$$

### A.2 Linear-Time-Varying Integer-Order Systems - Observability

We consider the linear time-varying system of the form

$$\Sigma_{\text{TV}} : \begin{cases} \dot{x}(t) = A(t)x(t) + B(t)u(t), & x(t_0) = 0 & \text{(A.1a)} \\ y(t) = C(t)x(t), & & \text{(A.1b)} \end{cases}$$

with the state  $x(t) \in \mathbb{R}^n$ , the input  $u(t) \in \mathbb{R}^p$ , the output  $y(t) \in \mathbb{R}^q$  and matrices of appropriate dimensions, namely the system matrix  $A(t) \in \mathbb{R}^{n \times n}$ , the input matrix  $B(t) \in \mathbb{R}^{n \times p}$  and the output matrix  $C(t) \in \mathbb{R}^{q \times n}$ . We assume that the matrices  $A(t)$ ,  $B(t)$  and  $C(t)$  and their derivatives of the order  $n-2$ ,  $n-1$  and  $n-1$  are real-valued analytic functions [81, p. 23] defined for all  $t \in (-\infty, \infty)$ .

**Definition A.1** (Observability [90]). *1. The system  $\Sigma_{\text{TV}}$  is called completely observable on the interval  $t \in (t_0, t_1)$  if any initial state  $x(t_0) = x_0$  can be uniquely determined from the knowledge of the input  $u(t)$  and output  $y(t)$  on the interval  $t \in (t_0, t_1)$ .*

*2. The system  $\Sigma_{\text{TV}}$  is called totally observable (differentially observable) on the interval  $t \in (t_0, t_1)$ , if it is completely observable on every subinterval of  $(t_0, t_1)$ .*

The time-varying observability matrix is defined in [90].

$$\mathcal{O}(t) := \begin{pmatrix} S_0(t) \\ S_1(t) \\ \vdots \\ S_{n-1}(t) \end{pmatrix} \quad (\text{A.2})$$

with

$$\begin{aligned} S_0(t) &= C(t) \\ S_i(t) &= S_{i-1}(t)A(t) + \frac{d}{dt}S_{i-1}(t), \quad i = 1, 2, \dots, n-1 \end{aligned}$$

**Theorem A.1** (Observability of LTV-Systems [90]). *Linear time-varying system (A.1) is completely observable on the interval  $[t_0, t_1]$  if and only if*

$$\exists t_a \in [t_0, t_1] : \text{rank}(\mathcal{O}(t_a)) = n.$$

### A.3 Strong\* Detectability

We recall the concept related to unknown input observers for an integer-order system

$$\Sigma_{\text{IO}} : \begin{cases} \dot{x}(t) = Ax(t) + Bu(t) + Ed(t) & (\text{A.3a}) \\ y(t) = Cx(t) & (\text{A.3b}) \end{cases}$$

with state  $x(t) \in \mathbb{R}^n$ , output  $y(t) \in \mathbb{R}^q$ , known input  $u(t) \in \mathbb{R}^p$ , unknown input (disturbance)  $d(t) \in \mathbb{R}^r$  and matrices of appropriate dimensions. Without loss of generality we require  $\text{rank}(E) = r$  and  $\text{rank}(C) = q$  [11]. The decisive property for the existence of an unknown input observer is the so-called strong\* detectability:

**Definition A.2** (Strong\* Detectability (Integer Order) [27]). *System  $\Sigma_{\text{IO}}$  is strong\* detectable if*

$$\lim_{t \rightarrow \infty} y(t) = 0 \quad \Rightarrow \quad \lim_{t \rightarrow \infty} x(t) = 0. \quad (\text{A.4})$$

**Theorem A.2** (Strong\* Detectability Criterion (Integer Order) [64]). *System  $\Sigma_{\text{IO}}$  is strong\* detectable if and only if*

$$\text{rank}(CE) = \text{rank}(E) \quad (\text{A.5a})$$

$$(\text{A.5b})$$

and

$$\text{rank} \begin{pmatrix} sI - A & E \\ C & 0 \end{pmatrix} = n + q, \quad \forall s \in \mathbb{C}_0^+. \quad (\text{A.5c})$$

The first condition (A.5a) means that the disturbance may have the full influence on the first time-derivative of the output. The second condition can be interpreted as some minimum phase condition [64].

**Theorem A.3** (Existence of Unknown-Input Observer (Integer-Order) [64]). *There exists an unknown input observer for the system  $\Sigma_{\text{IO}}$  if and only if it is strong\* detectable.*

## Bibliography

- [1] O. P. Agrawal. A General Formulation and Solution Scheme for Fractional Optimal Control Problems. *Nonlinear Dynamics*, 38(1-4):323–337, 2004.
- [2] O. P. Agrawal. Fractional variational calculus and the transversality conditions. *Journal of Physics A: Mathematical and General*, 39(33):10375–10384, 2006.
- [3] B. Bandyopadhyay and S. Kamal. *Stabilization and Control of Fractional Order Systems: A Sliding Mode Approach*. Springer, 2014.
- [4] Z. Belkhatir and T. M. Laleg-Kirati. Parameters and Fractional Differentiation Orders Estimation for Linear Continuous-Time Non-Commensurate Fractional Order Systems. *Systems & Control Letters*, 115:26–33, 2018.
- [5] M. Bettayeb and S. Djennoune. A note on the controllability and the observability of fractional dynamical systems. *IFAC Proceedings Volumes*, 39(11):493–498, 2006.
- [6] Y. Boukal, M. Darouach, M. Zasadzinski, and N. E. Radhy.  $\mathcal{H}_\infty$  observer design for linear fractional-order systems in time and frequency domains. In *2014 European Control Conference (ECC)*, pages 2975–2980, 2014.
- [7] I. N. Bronstein, K. A. Semendjajew, G. Musiol, and H. Mühlig. *Taschenbuch der Mathematik*. Verlag Harri Deutsch, Frankfurt am Main, 7th edition, 2008.
- [8] R. H. Byrd, J. C. Gilbert, and J. Nocedal. A trust region method based on interior point techniques for nonlinear programming. *Mathematical Programming*, 89(1):149–185, 2000.
- [9] M. Caputo. Linear models of dissipation whose Q is almost frequency independent. *Annals of Geophysics*, 19:383–393, 1966.
- [10] F. J. Castillo-Garcia, A. San Millan-Rodriguez, V. Feliu-Batlle, and L. Sanchez-Rodriguez. Fractional-Order Control of First Order Plants with Guaranteed Time Specifications. *Journal of Applied Mathematics*, 2013.
- [11] J. Chen. *Robust residual generation for model-based fault diagnosis of dynamic systems*. PhD thesis, University of York, 1995.
- [12] L. Chen, N. Saikumar, and S. H. HosseinNia. Development of Robust Fractional Order Reset Control. *IEEE Transactions on Control Systems Technology*, 28(4):1404–1417, 2020.
- [13] Y.-Q. Chen, C. Hu, and K. L. Moore. Relay feedback tuning of robust PID controllers with iso-damping property. In *42nd IEEE Conference on Decision and Control*, pages 2180–2185, 2003.
- [14] Y.-Q. Chen, I. Petras, and D. Xue. Fractional order control - A tutorial. In *American Control Conference*, pages 1397–1411, 2009.
- [15] Y.-Q. Chen, B. M. Vinagre, and I. Podlubny. Fractional order disturbance observer for robust vibration suppression. *Nonlinear Dynamics*, 38(1-4):355–367, 2004.

- [16] S. Dadras and H. R. Momeni. A new fractional order observer design for fractional order nonlinear systems. In *ASME 2011 International Design Engineering Technical Conferences and Computers and Information in Engineering Conference*, pages 403–408, 2011.
- [17] S. Das. *Functional Fractional Calculus for System Identification and Controls*. Springer, 2007.
- [18] S. Das, S. Saha, A. Mukherjee, I. Pan, and A. Gupta. Adaptive Gain and Order Scheduling of Optimal Fractional Order  $PI^{\lambda}D^{\mu}$  Controllers with Radial Basis Function Neural-Network. In *International Conference on Process Automation, Control and Computing (PACC)*, pages 1–6, July 2011.
- [19] E. C. de Oliveira and J. A. Tenreiro Machado. A Review of Definitions for Fractional Derivatives and Integral. *Mathematical Problems in Engineering*, 2014:1–6, 2014.
- [20] K. Diethelm. *The Analysis of Fractional Differential Equations*. Springer, 2010.
- [21] K. Diethelm and A. D. Freed. The FracPECE subroutine for the numerical solution of differential equations of fractional order. In K. Kremer and V. Macho, editors, *Forschung und wissenschaftliches Rechnen 1998*, pages 57–71. Gesellschaft für wissenschaftliche Datenverarbeitung mbH Göttingen, 1999.
- [22] A. Erdelyi, W. Magnus, F. G. Tricomi, and F. Oberhettinger. Tables of integral transforms. *BATEMAN MANUSCRIPT PROJECT*, 1:402, 1954.
- [23] L. Fadiga, C. Farges, J. Sabatier, and M. Moze. On computation of  $\mathcal{H}_{\infty}$  norm for commensurate fractional order systems. In *2011 50th IEEE Conference on Decision and Control and European Control Conference*, pages 8231–8236, 2011.
- [24] V. Feliu-Batlle, R. Rivas-Pérez, F. J. Castillo-García, L. Sanchez-Rodríguez, and A. Linárez-Saez. Robust fractional order controller for irrigation main canal pools with time-varying dynamical parameters. *Computers and Electronics in Agriculture*, 76(2):205–217, 2011.
- [25] A. Freed, K. Diethelm, and Y. Luchko. Fractional-order Viscoelasticity (FOV): Constitutive Development Using the Fractional Calculus: First Annual Report. Technical report, Glenn Research Center, Cleveland, Ohio, 2002.
- [26] T. T. Hartley and C. F. Lorenzo. Dynamics and control of initialized fractional-order systems. *Nonlinear Dynamics*, 29(1-4):201–233, 2002.
- [27] M. L. J. Hautus. Strong detectability and observers. *Linear Algebra and its Applications*, 50:353–368, 1983.
- [28] M. Hinze, A. Schmidt, and R. I. Leine. Numerical solution of fractional-order ordinary differential equations using the reformulated infinite state representation. *Fractional Calculus and Applied Analysis*, 22(5):1321–1350, 2019.
- [29] M. Hinze, A. Schmidt, and R. I. Leine. Lyapunov Stability of a Fractionally Damped Oscillator with Linear (Anti-)Damping. *International Journal of Nonlinear Sciences and Numerical Simulation*, 21(5):425–442, 2020.
- [30] S. H. HosseinNia. *Fractional Hybrid Control Systems: Modeling, Analysis and Applications to Mobile Robotics and Mechatronics*. PhD thesis, Universidad de Extremadura, Spain, 2013.

- [31] S. H. HosseinNia, I. Tejado, D. Torres, B. M. Vinagre, and V. Feliu. A General Form for Reset Control Including Fractional Order Dynamics. In *IFAC World Congress*, pages 2028–2033, 2014.
- [32] S. H. HosseinNia, I. Tejado, and B. M. Vinagre. Basic properties and stability of fractional-order reset control systems. In *European Control Conference (ECC)*, pages 1687–1692, 2013.
- [33] S. H. HosseinNia, I. Tejado, and B. M. Vinagre. Fractional Order Hybrid Systems and their Stability. In *14th Int. Carpathian Control Conference (ICCC)*, pages 128–133, 2013.
- [34] S. H. HosseinNia, I. Tejado, and B. M. Vinagre. Fractional-Order Reset Control: Application to a Servomotor. *Mechatronics*, 23(7):781–788, 2013.
- [35] S. H. HosseinNia, I. Tejado, and B. M. Vinagre. Hybrid Systems and Control with Fractional Dynamics (I): Modeling and Analysis. In *International Conference on Fractional Differentiation and its Applications*, pages 239–244, 2014.
- [36] S. H. HosseinNia, I. Tejado, and B. M. Vinagre. Hybrid Systems and Control with Fractional Dynamics (II): Control. In *International Conference on Fractional Differentiation and its Applications*, pages 245–250, 2014.
- [37] J. P. How. Dynamic Output-Feedback Control Architectures Matter [Focus on Education]. *IEEE Control Systems Magazine*, 36(6):88–117, 2016.
- [38] J. Kautsky, N. Nichols, and P. van Dooren. Robust pole assignment in linear state feedback. *International Journal of Control*, 41(5):1129–1155, 1985.
- [39] A. A. Kesarkar and S. Narayanasamy. Asymptotic magnitude Bode plots of fractional-order transfer functions. *IEEE/CAA Journal of Automatica Sinica*, 6(4):1019–1026, 2019.
- [40] H. K. Khalil. *Nonlinear Systems*. Prentice Hall, 1996.
- [41] N. Khalili Zadeh Mahani, A. K. Sedigh, and F. M. Bayat. Performance evaluation of non-minimum phase linear control systems with fractional order partial pole-zero cancellation. In *Asian Control Conference (ASCC)*, pages 1–4, 2013.
- [42] R. Klages, G. Radons, and I. M. Sokolov. *Anomalous Transport: Foundations and Applications*. Wiley, 2008.
- [43] P. Lanusse, A. Oustaloup, and B. Mathieu. Third generation crone control. In *IEEE International Conference on Systems, Man and Cybernetics (SMC)*, pages 149–155, 1993.
- [44] P. Lanusse, J. Sabatier, and A. Oustaloup. Extension of pid to fractional orders controllers: a frequency-domain tutorial presentation. In *IFAC World Congress*, pages 7436–7442, 2014.
- [45] S.-C. Lee, Y. Li, Y.-Q. Chen, and H.-S. Ahn.  $\mathcal{H}_\infty$  and sliding mode observers for linear time-invariant fractional-order dynamic systems with initial memory effect. *Journal of Dynamic Systems, Measurement, and Control*, 136(5):051022:1–13, 2014.
- [46] C. P. Li and F. R. Zhang. A survey on the stability of fractional differential equations: Dedicated to Prof. Y.S. Chen on the Occasion of his 80th Birthday. *The European Physical Journal Special Topics*, 193(1):27–47, 2011.
- [47] Y. Li, Y.-Q. Chen, and I. Podlubny. Stability of fractional-order nonlinear dynamic systems: Lyapunov direct method and generalized Mittag-Leffler stability. *Computers & Mathematics with Applications*, 59(5):1810–1821, 2010.

- [48] Y. Li, Y.-Q. Chen, I. Podlubny, and Y. Cao. Mittag-leffler stability of fractional order nonlinear dynamic systems. *Automatica*, 45:1965–1969, 2009.
- [49] D.-Y. Liu, T. M. Laleg-Kirati, O. Gharu, and W. Perruquetti. Identification of Fractional Order Systems using Modulating Functions Method. In *American Control Conference (ACC)*, pages 1679–1684, 2013.
- [50] C. F. Lorenzo and T. T. Hartley. Initialized Fractional Calculus. *NASA Technical Report*, pages 3–18, 2000.
- [51] C. F. Lorenzo and T. T. Hartley. Initialization in fractional order systems. In *European Control Conference*, pages 1471–1476, 2001.
- [52] C. F. Lorenzo, T. T. Hartley, and J. L. Adams. Time-varying initialization and corrected laplace transform of the caputo derivative. *IFAC Workshop on Fractional Differentiation and Its Applications*, pages 161–166, 2013.
- [53] C. L. MacDonald, N. Bhattacharya, B. P. Sprouse, and G. A. Silva. Efficient computation of the Grünwald–Letnikov fractional diffusion derivative using adaptive time step memory. *Journal of Computational Physics*, 297:221–236, 2015.
- [54] F. Mainardi and R. Gorenflo. On Mittag-Leffler-type functions in fractional evolution processes. *Journal of Computational and Applied Mathematics*, 118(1–2):283–299, 2000.
- [55] D. Matignon. Stability results for fractional differential equations with applications to control processing. In *Multiconference on Computational Engineering in Systems Applications*, pages 963–968, 1996.
- [56] D. Matignon. Stability properties for generalized fractional differential systems. *ESAIM: Proceedings*, 5:145–158, 1998.
- [57] D. Matignon and B. d’Andréa-Novel. Some results on controllability and observability of finite-dimensional fractional differential systems. In *Multiconference on Computational Engineering in Systems Applications*, pages 952–956, 1996.
- [58] M. A. Matlob and Y. Jamali. The Concepts and Applications of Fractional Order Differential Calculus in Modelling of Viscoelastic Systems: A Primer. *Critical Reviews in Biomedical Engineering*, 47:pages 249–276, 2019.
- [59] F. C. Meral, T. J. Royston, and R. Magin. Fractional calculus in viscoelasticity: An experimental study. *Communications in Nonlinear Science and Numerical Simulation*, pages pages 939–945, 2010.
- [60] C. A. Monje, Y.-Q. Chen, B. M. Vinagre, D. Xue, and V. Feliu-Batlle. *Fractional-order Systems and Controls: Fundamentals and Applications*. Springer, 2010.
- [61] C. A. Monje, B. M. Vinagre, Y.-Q. Chen, V. Feliu, P. Lanusse, and J. Sabatier. Proposals for fractional  $PI^\lambda D^\mu$  tuning. *Proceedings of The First IFAC Symposium on Fractional Differentiation and its Applications (FDA04)*, 2004.
- [62] C. A. Monje, B. M. Vinagre, G. E. Santamaria, and I. Tejado. Auto-tuning of fractional order  $PI^\lambda D^\mu$  controllers using a PLC. In *IEEE Conference on Emerging Technologies and Factory Automation*, pages 10824–10829, Sept 2009.
- [63] M. J. Moran and H. N. Shapiro. *Fundamentals of engineering thermodynamics*. Wiley, Hoboken, NJ, 6. ed. edition, 2008.



- [64] J.A. Moreno. Existence of unknown input observers and feedback passivity for linear systems. In *Conference on Decision and Control*, pages 3366–3371, 2001.
- [65] M. Moze, J. Sabatier, and A. Oustaloup. LMI Tools for Stability Analysis of Fractional Systems. In *ASME 2005 International Design Engineering Technical Conferences and Computers and Information in Engineering Conference*, pages 1–9, 2005.
- [66] M. Moze, J. Sabatier, and A. Oustaloup. LMI Characterization of Fractional Systems Stability. In *J. Sabatier et al. (eds.): Advances in Fractional Calculus: Theoretical Developments and Applications in Physics and Engineering*, pages pages 419–434. Springer, 2007.
- [67] I. N’Doye, M. Darouach, H. Voos, and M. Zasadzinski. Design of unknown input fractional-order observers for fractional-order systems. *International Journal of Applied Mathematics and Computer Science*, pages 491–500, 2013.
- [68] I. N’Doye, H. Voos, M. Darouach, J. G. Schneider, and N. Knauf. An unknown input fractional-order observer design for fractional-order glucose-insulin system. In *Conference on Biomedical Engineering and Sciences*, pages 595–600, 2012.
- [69] D. Nešić, A. R. Teel, and L. Zaccarian. Stability and Performance of SISO Control Systems With First-Order Reset Elements. *IEEE Transactions on Automatic Control*, 56(11):2567–2582, 2011.
- [70] K. Oldham and J. Spanier. *The fractional calculus theory and applications of differentiation and integration to arbitrary order*. Dover, 1974.
- [71] A. Oustaloup and M. Bansard. First generation CRONE control. In *IEEE International Conference on Systems, Man and Cybernetics (SMC)*, volume 2, pages 130–135, 1993.
- [72] A. Oustaloup, B. Mathieu, and P. Lanusse. Second generation CRONE control. In *IEEE International Conference on Systems, Man and Cybernetics (SMC)*, pages 136–142, 1993.
- [73] A. Oustaloup and P. Melchior. The great principles of the CRONE control. In *Proceedings of IEEE Systems Man and Cybernetics Conference (SMC)*, pages 118–129 vol.2, Oct 1993.
- [74] I. Podlubny. *Fractional Differential Equations: An Introduction to Fractional Derivatives, Fractional Differential Equations, to Methods of Their Solution and Some of Their Applications*. Acad. Press, 1999.
- [75] I. Podlubny. Fractional-order systems and  $\pi^{\lambda}d^{\mu}$ -controllers. *IEEE Transactions on Automatic Control*, 44(1):208–214, 1999.
- [76] I. Podlubny. Geometric and Physical Interpretation of Fractional Integration and Fractional Differentiation. *Fractional Calculus and Applied Analysis*, 5(4):367–386, 2001.
- [77] D. Qian, C. Li, R. P. Agarwal, and P. J. Y. Wong. Stability analysis of fractional differential system with Riemann–Liouville derivative. *Mathematical and Computer Modelling*, 52(5-6):862–874, 2010.
- [78] T. Raff. *Impulsive Observers for Continuous Time Systems and Global Output Feedback Control*. VDI-Verlag, 2010.
- [79] H. F. Raynaud and A. Zergaiñoh. State-space representation for fractional order controllers. *Automatica*, 36(7):1017–1021, 2000.
- [80] S. Roman. The Formula of Fa’a di Bruno. *American Mathematical*, pages 805–809, 1980.

- [81] W. J. Rugh. *Linear System Theory*. Prentice-Hall, 1996.
- [82] J. Sabatier, O. P. Agrawal, Machado, and J. A. Tenreiro. *Advances in Fractional Calculus: Theoretical Developments and Applications in Physics and Engineering*. Springer, 2007.
- [83] J. Sabatier, C. Farges, M. Merveillaut, and L. Feneteau. On Observability and Pseudo State Estimation of Fractional Order Systems. *European Journal of Control*, pages 260–271, 2012.
- [84] J. Sabatier, C. Farges, and J.-C. Trigeassou. Fractional systems state space description: some wrong ideas and proposed solutions. *Journal of Vibration and Control*, 20(7):1076–1084, 2014.
- [85] J. Sabatier, M. Merveillaut, R. Malti, and A. Oustaloup. How to impose physically coherent initial conditions to a fractional system? *Communications in Nonlinear Science and Numerical Simulations*, 15(5):1318–1326, 2010.
- [86] J. Sabatier, M. Moze, and C. Farges. LMI stability conditions for fractional order systems. *Computers & Mathematics with Applications*, 59(5):1594–1609, 2010.
- [87] B. Saïdi, S. Najar, M. Amairi, and M.N. Abdelkrim. Design of a robust fractional pid controller for a second order plus dead time system. In *10th International Multi-Conference on Systems, Signals Devices (SSD)*, pages 1–6, 2013.
- [88] B. Saïdi, S. Najar, M. Amairi, and M.N. Abdelkrim. Design of a robust fractional PID controller for a second order plus dead time system. In *International Multi-Conference on Systems, Signals and Devices (SSD)*, pages 1–6, 2013.
- [89] B. Shafai and A. Oghbaee. Positive observer design for fractional order systems. In *World Automation Congress*, pages 531–536, 2014.
- [90] L. Silverman and H. Meadows. Controllability and Observability in Time-Variable Linear Systems. *SIAM Journal on Control*, 5(1):64–73, 1967.
- [91] W. Sumelka, T. Blaszczyk, and C. Liebold. Fractional Euler-Bernoulli beams: Theory, numerical study and experimental validation. *European Journal of Mechanics - A/Solids*, 54:243–251, 2015.
- [92] A. Tepljakov, E. Petlenkov, and J. Belikov. Fomcon: Fractional-order modeling and control toolbox for matlab. In *18th International Conference on Mixed Design of Integrated Circuits and Systems*, pages 684–689, 2011.
- [93] M. Thomassin and R. Malti. Subspace method for continuous-time fractional system identification. In *15th IFAC Symposium on System Identification*, pages 880 – 885, 2009.
- [94] J.-C. Trigeassou and N. Maamri. A new approach to the stability of linear fractional systems. In *6th International Multi-Conference on Systems, Signals and Devices*, pages 1–14, 2009.
- [95] J.-C. Trigeassou, N. Maamri, J. Sabatier, and A. Oustaloup. Transients of fractional-order integrator and derivatives. *Signal, Image and Video Processing*, 6(3):359–372, 2012.
- [96] H. Unbehauen. *Regelungstechnik II – Zustandsregelungen, digitale und nichtlineare Regelsysteme*, volume 2. Vieweg+Teubner Verlag, Wiesbaden, 9 edition, 2009.

- [97] D. Valério and J. S. da Costa. Identification of fractional models from frequency data. In *J. Sabatier et al. (eds.): Advances in Fractional Calculus: Theoretical Developments and Applications in Physics and Engineering*, pages pages 229–242. Springer, 2007.
- [98] D. Valério and J. S. da Costa. A review of tuning methods for fractional pids. In *4th IFAC Workshop on Fractional Differentiation and Its Applications*, volume 10, 2010.
- [99] D. Valério. Tuning of fractional controllers minimising  $\mathcal{H}_2$  and  $\mathcal{H}_\infty$  norms. *Acta Polytechnica Hungarica*, 3(4):55–70, 2006.
- [100] Y. Wei, Y. Chen, S. Cheng, and Y. Wang. Completeness on the stability criterion of fractional order lti systems. *Fractional Calculus and Applied Analysis*, 20(1):159–172, 2017.
- [101] C. Weise, R. Tavares, K. Wulff, M. Ruderman, and J. Reger. A Fractional-Order Control Approach to Ramp Tracking with Memory-Efficient Implementation. In *Advanced Motion Control*, pages 15–22, 2020.
- [102] C. Weise, K. Wulff, and J. Reger. Exponentially Converging Observer for a Class of FO-LTI Systems. In *Multi-Conference on Systems and Control*, pages 723–729, 2016.
- [103] C. Weise, K. Wulff, and J. Reger. Fractional-order observer for integer-order LTI systems. In *Asian Control Conference*, pages 2101–2106, 2017.
- [104] C. Weise, K. Wulff, and J. Reger. Observer with improved convergence for a class of initialized fo-lti systems. In *IEEE Conference on Control Technology and Applications (CCTA)*, pages 1570–1576, 2018.
- [105] C. Weise, K. Wulff, and J. Reger. Fractional-order memory reset control for integer-order LTI systems. In *Conference on Decision and Control*, pages 5710 – 5715, 2019.
- [106] C. Weise, K. Wulff, and J. Reger. Extended Fractional-Order Memory Reset Control for Integer-Order LTI Systems and Experimental Demonstration. In *IFAC World Congress*, pages 7773–7780, 2020.
- [107] L. Zaccarian, D. Nešić, and A. R. Teel. First order reset elements and the Clegg integrator revisited. In *American Control Conference*, pages 563–568, 2005.
- [108] J. Zheng, Y. Guo, M. Fu, Y. Wang, and L. Xie. Development of an extended reset controller and its experimental demonstration. *IET Control Theory Applications*, 2(10):866–874, 2008.



## List of Symbols

$\mathcal{D}^\alpha$	Caputos fractional-order derivative of order $\alpha$ with lower limit 0
$\mathcal{E}_{\alpha,\beta}(\cdot)$	two parameter Mittag-Leffler function
$\Gamma(\cdot)$	Euler's gamma function
$\mathcal{I}^\alpha$	Riemann-Liouville fractional-order integral of order $\alpha$ with lower limit 0
$\mathbb{N}_0$	$= \mathbb{N} \cup 0$ , the set of natural numbers including zero
$\mathbb{N}$	$= \{1, 2, 3, \dots\}$ , the set of natural numbers
$\mathbb{Q}$	rational numbers
$\mathbb{R}^+$	the set of positive real numbers
$\mathbb{R}$	the set of real numbers
$\mathbb{Z}$	$= \{0, \pm 1, \pm 2, \dots\}$ , the set of integer numbers
$\mathcal{C}^k([a, b])$	$= \{f : [a, b] \rightarrow \mathbb{R} \mid f \text{ has a continuous } k\text{-th derivative}\}$ , the set of functions with continuous $k$ -th derivative
$\mathcal{H}_\mu([a, b])$	$= \{f : [a, b] \rightarrow \mathbb{R} \mid \exists c > 0 \forall x, y \in [a, b];  f(x) - f(y)  \leq c  x - y ^\mu\}$ , the set of Hölder continuous functions
$\mathcal{L}^p([a, b])$	$= \{f : [a, b] \rightarrow \mathbb{R} \mid f \text{ is measurable on } [a, b] \text{ and } \int_a^b  f(x) ^p dx < \infty\}$
$\Psi(\cdot)$	Initialization function of the fractional-order integral
$I$	Identity matrix of order $n$ if not specified further
$IAE$	$= \int_{t_0}^{t_{\text{end}}}  e(\tau)  d\tau$ , integral absolute error
$ISE$	$= \int_{t_0}^{t_{\text{end}}} e^2(\tau) d\tau$ , integral square error
$ITAE$	$= \int_{t_0}^{t_{\text{end}}} \tau  e(\tau)  d\tau$ , integral time weighted absolute error
${}^C\Psi(\cdot)$	Initialization function of Caputo's derivative
${}^C_{t_0}\mathcal{D}^\alpha$	Caputos fractional-order derivative of order $\alpha$ with lower limit $t_0$
${}^R\mathcal{D}^\alpha$	Riemann-Liouville fractional-order derivative of order $\alpha$ with lower limit 0
${}^R\Psi(\cdot)$	Initialization function of Riemann-Liouville's derivative
${}^R_{t_0}\mathcal{D}^\alpha$	Riemann-Liouville fractional-order derivative of order $\alpha$ with lower limit $t_0$
${}_{t_0}\mathcal{D}^\alpha$	Caputos fractional-order derivative of order $\alpha$ with lower limit $t_0$
${}_{t_0}\mathcal{I}^\alpha$	Riemann-Liouville fractional-order integral of order $\alpha$ with lower limit $t_0$
FO	fractional-order
FOH	first order hold
IO	integer-order
LTI	linear time-invariant
LTV	linear time-varying
UIO	unknown input observer
ZOH	zero order hold



## List of Figures

1.1	Thermal conduction in an infinite one-dimensional media. . . . .	2
1.2	Sketch of the tautochrone / baristochrone problem. . . . .	3
2.1	Graphical illustration of the concepts of integration and differentiation. . . . .	7
2.2	Euler's gamma function for real arguments. . . . .	11
2.3	Three-dimensional representation of fractional-order integration. . . . .	13
2.4	Comparison of Caputo's and Riemann's fractional-order derivative of a third-order polynomial: $f(t) = \frac{5}{3}t^3 + \frac{5}{2}t^2 + \frac{15}{16}t + \frac{1}{3}$ . . . . .	16
2.5	The left and right fractional-order derivatives depend on the past and future of the function $f(t)$ [74, p. 89]. . . . .	19
2.6	The ignored history of the input function $u(t)$ has a huge influence on the system state. Neither Riemann's nor Caputo's operator give the exact solution if the history is ignored by starting at a later time instant ( $t_0 = 0$ ). Note that Riemann's response uses the wrong initial conditions here. . . . .	22
2.7	Comparison of the fractional-order integral starting at different initial conditions (see [51]). In the case $\alpha \in (0, 1)$ , the initialization function $\Psi(\cdot)$ decays to zero. . . . .	25
2.8	The initialization function corresponding to Caputo's operator only decays for $\alpha \in (0, 1)$ . This is caused by the order of operations defining the operator, the fractional-order integral causes an increasing initialization function for $\alpha > 1$ . . . . .	27
2.9	Initialization function and its bounds for the Riemann-Liouville derivative. . . . .	28
2.10	The coefficients of the discretized Grünwald-Letnikov operator represent the operator's memory. For $\alpha > 0$ these weights decay relatively fast towards past time instants. . . . .	30
2.11	The coefficients of the discretized Grünwald-Letnikov operator represent the operator's memory. For $\alpha < 0$ these weights decay slowly towards the past time instants compared to the differentiation case with $\alpha > 0$ . . . . .	30
2.12	Frequency response of the discrete approximation of the Grünwald-Letnikov derivative for different memory lengths $L$ . . . . .	32
2.13	Oustaloup filters of different order to approximate the semi-derivative. . . . .	32
3.1	The scalar Mittag-Leffler functions show different decays depending on the order $\alpha$ . . . . .	37
3.2	Inverses of different scalar pseudo-transitions $\Phi_\alpha(t, t_0)$ . Only for $\alpha = 1$ the inverse is given by swapping the time arguments. . . . .	38
3.3	Due to the memory of the operator, the interconnection of two pseudo transitions leads to different results than a single transition to the final time $t$ . The reason here is that the second transition is computed based on the memory-free initial-conditions at $t = t_1$ . . . . .	39
3.4	Illustration of the possible location of the argument $z$ of the Mittag-Leffler function. Lemma 3.1 leads to the yellow colored sector and Lemma 3.2 is represented by the purple colored area. The angle defining $\mu$ may vary according to $\alpha\frac{\pi}{2} < \mu < \min\{\pi, \alpha\pi\}$ . . . . .	40

3.5	Comparison of an integer-order system with two fractional-order systems defined by different operators. . . . .	41
3.6	For $\alpha \in (0,1)$ the region of stability is a non-convex set. . . . .	48
3.7	Superposing the known and unknown states. . . . .	53
3.8	Simulation results of a Luenberger-observer applied to an initialized fractional-order system. . . . .	54
3.9	Estimation error of an unknown input observer and a fractional-order observer without additional compensation of the unknown history. . . . .	57
3.10	Frequency responses of the explicit and implicit fractional-order lead-lag compensator . . . . .	60
4.1	Comparison of the numerical solutions applying the associated integer-order system. Due to the unstable homogeneous dynamics, the integer-order solution deviates. . . . .	63
4.2	Comparison of the numerical solutions applying the associated integer-order system. As the matrix $A^3$ is Hurwitz, the simulation of the integer-order system leads to the correct (stable) solution. . . . .	64
4.3	Reduced stability domains for Theorem 4.2 (colored in blue). . . . .	64
4.4	The determinant of the time-varying observability matrix tends to zero for large times. . . . .	73
4.5	With the time-varying observer, the states are estimated exponentially. However, the initial peaking is large. . . . .	74
4.6	The initial states are also estimated correctly. The initial peaking also occurs in these additional states. . . . .	75
4.7	The observer gains $L_i(t)$ increase with time, as the determinant of the observability matrix $\det(\mathcal{O}(t))$ tends to zero. . . . .	75
4.8	The impulsive observer can estimate the state in fixed time and with the lower observer gains the strong peaking is avoided. . . . .	78
4.9	Estimation error of both unknown input observers for $\alpha = 0.3$ and $\alpha = 0.6$ . . . . .	83
4.10	With $\alpha = \frac{1}{2}$ the estimation error converges exponentially. . . . .	84
5.1	Estimation error of a fractional- and an integer-order Luenberger observer. . . . .	101
5.2	Poles of the induced discrete time system with respect to the original fractional-order pole locations. . . . .	104
5.3	Poles of the induced discrete time system with respect to the original fractional-order pole locations for different reset periods $\delta$ . . . . .	105
5.4	For shorter reset intervals, the exponential convergence rate given by $\text{Re}(\lambda_c)$ is increased. . . . .	106
5.5	With the additional memory reset, the estimation error converges exponentially. . . . .	107
5.6	Continuous time eigenvalues $\lambda_c$ of the induced dynamics for different reinitialization periods $\delta$ . . . . .	107
5.7	Simulation results of the redesigned observers subjected to measurement noise. . . . .	109
5.8	Frequency response of the measurement noise effecting the estimation error for the fractional- and integer-order observer approach. . . . .	109
5.9	Estimation error extended by an impulsive state reconstruction at $\delta = 0.5$ s. . . . .	113
5.10	Controller structure including the prefilter $F(s)$ . . . . .	114
5.11	Step responses of the closed-loop system with integer-order assigned poles. . . . .	116
5.12	Frequency response of the open-loop $L(j\omega) = C(j\omega)G(j\omega)$ . . . . .	120



5.13	Closed-loop step responses for different reset periods $\delta$ . For $\delta = \infty$ the pure fractional-order controller acts without reset. . . . .	121
5.14	Amplitude response of the designed closed-loop $T_{\text{design}}(j\omega)$ and the induced low frequency dynamics $T_{\text{low}}(e^{j\omega})$ . . . . .	121
5.15	Comparison of the frequency response of the different approaches approximating the low frequency dynamics assuming constant reference signals (ZOH) or piecewise linear reference signals (FOH). . . . .	125
5.16	Step responses obtained with different reset strategies. . . . .	127
5.17	Frequency response of the approximated low frequency dynamics $T_{\text{low}}(j\omega)$ for varying $\mu$ . . . . .	128
5.18	Frequency response of the approximated low frequency response $T_{\text{low}}(j\omega)$ with changing reset parameter $P_c$ . . . . .	128
5.19	The approximation splits the pseudo state from its memory (see [30]). . . . .	129
5.20	Frequency response of the approximated low frequency dynamics $T_{\text{low}}(j\omega)$ including an approximation of the pure state reset control law. . . . .	131
5.21	The step response obtained with the pure state reset controller converges slowly. . . . .	131
6.1	Testbench with DC motor and magnetic brake. . . . .	133
6.2	Step response for model validation. . . . .	134
6.3	Transients of the state and estimates of different observers. . . . .	136
6.4	Comparison of the estimation error for different observer gains. . . . .	137
6.5	Comparison of the estimation error for different reset intervals. . . . .	137
6.6	Step responses obtained with different controllers. . . . .	138
6.7	Control effort of the different control approaches in comparison with the simulation of the closed-loop. . . . .	140

